

MUD AND DEBRIS FLOWS RISK ASSESSMENT- BASIC FUNDAMENTALS



Research Group

Applied Environmental Studies Group (GEAA)

Conservation Bioprospecting and Sustainable Development Group (COBIDES)



Sello Editorial

Universidad Nacional
Abierta y a Distancia

MUD AND DEBRIS FLOWS RISK ASSESSMENT- BASIC FUNDAMENTALS

Authors:

Jessica Paola Páez Pedraza

Denisse Viviana Cortés Castillo

UNIVERSIDAD NACIONAL ABIERTA Y A DISTANCIA – UNAD

Jaime Alberto Leal Afanador

Chancellor

Constanza Abadía García

Vice-Chancellor for Academic and Research

Leonardo Yunda Perlaza

Vice-Chancellor for Educational Media and Learning Mediation

Edgar Guillermo Rodríguez Díaz

Vice-Chancellor for Applicants, Students, and Alumni Services

Leonardo Evemeleth Sánchez Torres

Vice-Chancellor for Interinstitutional and International Relations

Julialba Ángel Osorio

Vice-Chancellor for Social Inclusion, Regional Development, and Community Outreach

Jordano Salamanca Bastidas

Dean, School of Agricultural, Livestock, and Environmental Sciences

Juan Sebastián Chiriví Salomón

National Director, Research Management System (RMS)

Martín Gómez Orduz

Director, UNAD University Press

Mud and debris flows risk assessment- basic fundamentals

Authors:

Jessica Paola Páez Pedraza
Denisse Viviana Cortés Castillo

Research Group:

Applied Environmental Studies Group (GEAA)
Conservation Bioprospecting and Sustainable Development Group (COBIDES)

363.34
P127

Páez Pedraza, Jessica Paola
Basic Rationale of Torrential Flood Risk Assessment / Jessica Paola Páez Pedraza, Denisse Viviana Cortés Castillo -- [1.a. ed.]. Bogotá: UNAD Publishing House/2024. (Research groups: Applied Environmental Studies Group (GEAA in Spanish-) – Conservation, Bioprospecting and Sustainable Development Group (COBI-DES in Spanish-). (School of Agricultural, Livestock, and Environmental Sciences -ECAPMA in Spanish-)

e-ISBN: 978-628-7786-19-6

1. Risk assessment 2. Mass movement 3. Disaster prevention 4. Environmental threats I. Páez Pedraza, Jessica Paola II. Cortés Castillo, Denisse Viviana

e-ISBN: 978-628-7786-19-6

School of Agricultural, Livestock and Environmental Sciences

©Publisher
UNAD University Press
National Open and Distance University
Calle 14 sur No. 14-23
Bogota, D.C.
November 2024

Translation: Smart translators

Cover Design: Shadya López

Layout: Paola Andrea D´Luyz Monsalve
Hipertexto - Netizen

How to cite this Book: Páez-Pedraza, J. & Cortés Castillo, D. (2024). *Mud and debris flows risk assessment- basic fundamentals*. UNAD University Press. DOI: <https://doi.org/10.22490/UNAD.9786287786196>

This work is licensed under a Creative Commons – Attribution – Non-Commercial – No Derivatives 4.0 International https://co.creativecommons.org/?page_id=13.



CONTENT

Book's review	13
Authors' review	14
Presentation	15
Acknowledgments	17
Introduction	18
Chapter 1	
GENERALITIES	21
1.1 The mud and debris flows	21
1.2 Triggering mechanisms of mud and debris flows	25
1.3 Types of flows	26
1.4 Types of fluids and rheology	41
1.5 Risk analysis	51
Chapter 2	
AGEOSPATIAL ANALYSIS OF SUSCEPTIBILITY AND THREAT BY TORRENTIAL FLOODS	57
2.1 Inventory of historical events	60
2.2 Physiographical characterization of the basin	72
2.3 Climate characterization of the basin	100
2.4 Methodologies for susceptibility analysis	105
2.5 Methodologies for the analysis of trigger factors and probability of occurrence	133
2.6 Threat analysis	146

Chapter 3

MODELING SUSCEPTIBILITY AND THREAT DUE TO TORRENTIAL FLOODS

149

3.1	Hydrological rainfall– runoff modeling	159
3.2	Modeling example hydrological – La Negra creek, Útica, Cundinamarca	188
3.3	Modeling of triggering mechanisms – landslides generated by rains	203
3.4	Modeling of triggering mechanisms – dam break	216
3.5	Modeling of trigger mechanisms –in-channel processes	223
3.6	Modeling of triggering mechanisms- incorporation of washing load	224
3.7	Example modeling of triggering mechanisms – La Negra creek, Útica, Cundinamarca	237
3.8	Example generation of liquid hydrograms and solids– La Negra creek, Útica, Cundinamarca	259
3.9	Hydraulic modeling of flood propagation and rheology calibration	263
3.10	Example hydraulic modeling – La Negra creek, Útica, Cundinamarca	271
3.11	Generation of the threat map	281

Chapter 4

Analysis of vulnerability and risk

285

4.1	Vulnerability analysis	287
4.2	Risk analysis	304

References

306

INDEX OF FIGURES

Figure 1. Comparison of the Taruca River flood valley before and after the mud and debris flows of 2017	19
Figure 2. Representation of a sludge flow (screen view, cross section, waves, lobe, trunk)	28
Figure 3. Comparison of a sludge flow and a non-viscous flow	29
Figure 4. Lateral deposits formed in sludge flows due to elevation in curves	29
Figure 5. Hyperconcentrated flow scheme	30
Figure 6. Debris flow representation	32
Figure 7. Flotation of large blocks in debris flows	32
Figure 8. Phase diagram of debris flows and landslides	34
Figure 9. Classification of flows and landslides according to the solid fraction and the type of material	35
Figure 10. Classification of landslides and flows according to speed and sediment concentration	37
Figure 11. Representation of the speed profile of a fluid	41
Figure 12. Types of Newtonian and non-Newtonian fluids	43
Figure 13. General mental map for risk assessment due to mud and debris flows	54
Figure 14. Steps to follow for geospatial analysis of susceptibility and threat from mud and debris flows	59
Figure 15. Sources de información para inventario de eventos históricos	60
Figure 16. Lateral deposits formed in sludge flows due to elevation in curves	62
Figure 17. Active erosion and mass removal processes in the upper Quebrada Liboriana basin, Salgar, Antioquia	64
Figure 18. Deposits and migration of the La Liboriana creek channel, Salgar, Antioquia	65
Figure 19. Deposits in the form of lateral bars in the curves and widening of the channel in La Liboriana creek, Salgar, Antioquia	66
Figure 20. Active erosion and mass removal processes in the upper La Negra creek basin, Útica, Cundinamarca	67
Figure 21. Widening of the La Negra creek channel, Útica, Cundinamarca	68
Figure 22. Lateral deposits and migration of the La Negra creek channel, Útica, Cundinamarca	68
Figure 23. Active erosion and mass removal processes of the Sangoyaco River and Taruca Creek, Mocoa – Putumayo	69
Figure 24. Widening of the Sangoyaco River channel, Mocoa – Putumayo	69
Figure 25. Sangoyaco River deposits and migration of the Mocoa River channel, Mocoa – Putumayo	70
Figure 26. Infographic basic steps to develop social cartography	71
Figure 27. Order of currents Horton–Strahler method	90
Figure 28. Multivariate analysis methodology scheme with Saaty analytical hierarchies	105

Figure 29. Example of a hierarchy level for variable analysis	111
Figure 30. Example of two levels of hierarchy for variable analysis	112
Figure 31. Comparison of sigmoid and hyperbolic tangent functions	114
Figure 32. Comparison of different normalizations for positive values of variables	116
Figure 33. Classification tree structure	125
Figure 34. Methodology for construction of classification trees for mud and debris flows	126
Figure 35. Example homogeneity/purity of a node	127
Figure 36. Example of selecting the partition point of a node	129
Figure 37. Logistic regression	132
Figure 38. Methodologies for the analysis of conditioning factors	134
Figure 39. Methodology to determine empirical thresholds of rainfall triggering landslides	136
Figure 40. Example identification of thresholds of precipitation triggering landslides	137
Figure 41. Methodology to determine empirical thresholds of rain triggering mud and debris flows	139
Figure 42. Example of thresholds of rain triggering mud and debris flows	140
Figure 43. Methodology for determining the threat of landslides due to an increase in the water table	142
Figure 44. Flowchart symbology explanation	151
Figure 45. Steps to follow for modeling susceptibility and threat from mud and debris flows torrenciales	152
Figure 46. Steps to follow for modeling susceptibility and threat from mud and debris flows	153
Figure 47. General flowchart modeling susceptibility and threat from mud and debris flows – Hydrological modeling	154
Figure 48. General flowchart modeling susceptibility and threat from mud and debris flows – Modeling of triggering mechanisms	155
Figure 49. General flow diagram modeling susceptibility and threat from mud and debris flows – Generation of mud and debris flows hydrographs	156
Figure 50. General flow diagram modeling susceptibility and threat from mud and debris flows – Hydraulic modeling of flood propagation and rheology calibration	157
Figure 51. Classification of hydrological/hydraulic models	160
Figure 52. Rainfall–runoff modeling flowchart	162
Figure 53. Graphic Representation of runoff generation methods	163
Figure 54. TOPMODEL soil water balance diagram	164
Figure 55. SMA model tank diagram	171
Figure 56. TETIS model tank diagram	178
Figure 57. Main drainages of La Negra stream	190
Figure 58. La Negra creek sub-basins	191
Figure 59. Thiessen polygons Black River subbasins	193
Figure 60. Precipitation and evaporation La Negra creek basin (April 8, 1987 – December 31, 1989)	196

Figure 61. Estimated flows for La Negra creek calibration (April 8, 1987 - December 31, 1989)	197
Figure 62. La Negra creek humidity topographic index	199
Figure 63. Fit to the objective function for each TOPMODEL parameter	201
Figure 64. Regional sensitivity of TOPMODEL parameters	202
Figure 65. Modeling of triggering mechanisms - landslides generated by rain	205
Figure 66. Flowchart modeling triggering mechanisms–dam break	218
Figure 67. Geological map of La Negra creek basin	241
Figure 68. Landslide inventory map of the La Negra creek basin	244
Figure 69. Stability map for medium humidity conditions of the La Negra creek basin	247
Figure 70. Stability map for humidity conditions preceding the mud and debris flows event of November 17, 1988, La Negra stream basin	248
Figure 71. Geometry for calculating the depth of dams	252
Figure 72. Location of possible reservoirs generated in the La Papaya stream	253
Figure 73. La Papaya creek dam failure hydrograph	258
Figure 74. La Papaya stream dam break hydrograph traveled to the mouth with La Negra stream	259
Figure 75. Triangular hydrograph of the SCS	260
Figure 76. Landslides that potentially contribute sediment to the flow	262
Figure 77. Synthetic hydrographs of water and mud and debris flows sub-basins of La Negra creek	263
Figure 78. Flowchart for hydraulic modeling and rheology calibration	266
Figure 79. Flowchart for hydraulic modeling and rheology calibration	267
Figure 80. Hydrograph traveled until the end of section 1	272
Figure 81. Hydrograph of mud and debris flows to be traveled in section 2	273
Figure 82. Comparison of simulated depths for each rheological model at t = 2 hours	277
Figure 83. Comparison of simulated depths for each rheological model at t = 3 hours	278
Figure 84. Comparison of simulated depths for each rheological model at t = 3 hours	279
Figure 85. Comparison of simulated velocities for each rheological model at t = 3 hours	280
Figure 86. POMCAS methodology based on index and indicator models	288
Figure 87. Dimensions and indicators for vulnerability analysis	291
Figure 88. Vulnerability assessment in the Salgar case	293
Figure 89. Análisis de vulnerabilidad en centros urbanos – PREDES	295
Figure 90. Retrospective analysis of floods that occurred	297
Figure 91. Vulnerability assessment for POMCAS	298
Figure 92. Vulnerability indicators in the CONARE jurisdiction	299
Figure 93. Factors and components of vulnerability	301
Figure 94. Elements of vulnerability in organizations	302
Figure 95. Vulnerability analysis for urban sector	303

TABLES INDEX

Table 1. Definitions of mud and debris flows	23
Table 2. Names of mud and debris flows in different countries	25
Table 3. Classification of mudflows according to O'Brien and Julien	36
Table 4. Classification of flows according to sediment type and channel slope	38
Table 5. Classification of flows according to type of material and moisture content	39
Table 6. Landslide speed scale proposed by Cruden and Varnes	40
Table 7. Rheological model recommendation for each type of fluid	51
Table 8. Legend Corine Land Cover for susceptibility analysis due to movements, mass and mud and debris flows	73
Table 9. Surface geological units (UGS)	76
Table 10. Subunits indicative of mass removal processes and mud and debris flows type processes	78
Table 11. Classification of fluvial forms associated with floods and mud and debris flows	84
Table 12. Relief according to the average slope	88
Table 13. Description by compactness index ranges K_c	91
Table 14. Range Description Form Factor K_f	91
Table 15. Description elongation ratio ranges	92
Table 16. Relationships to categorize the morphometric index	96
Table 17. Categories morphometric index of torrentiality	97
Table 18. Variability Index Categories	99
Table 19. Classification of the vulnerability index to torrential events (IVET)	99
Table 20. Relationship of physiographic variables with the generation of mud and debris flows	106
Table 21. Saaty Paired Comparison Scale	117
Table 22. Ejemplo comparación pareada variables fisiográficas	118
Table 23. Example calculation of variable weights	119
Table 24. Example lamda calculation	120
Table 25. Example calculation of lamda max	120
Table 26. RI based on matrix order	121
Table 27. Thresholds for consistency ratio	122
Table 28. Example classification of historical events for threat analysis	135
Table 29. Threat categorization according to the FS	145

Table 30. TOPMODEL parameters	167
Table 31. Comparison of hydrological models	185
Table 32. Evaporimeter tank coefficient type A	194
Table 33. TOPMODEL parameter calibration ranges	200
Table 34. Results November 17, 1988 for the top 5 simulations	202
Table 35. Stability classification in the SHALSTAB model	208
Table 36. Susceptibility classification with SHALSTAB model	209
Table 37. Infinite slope model stability classification	212
Table 38. Structure and permeability indices by texture	227
Table 39. USLE K factor in ton/ha	228
Table 40. NN factor	229
Table 41. LS factor for different slopes and slope lengths	230
Table 42. Vegetation cover factor C_3	234
Table 43. Factor C by type of crop	234
Table 44. Factor t type of Tillage	235
Table 45. P factor for crops at level	236
Table 46. P factor for strip crops	236
Table 47. P factor for different agricultural practices	237
Table 48. Characterization geological units of La Negra creek basin	239
Table 49. SINMAP calibrated parameters	242
Table 50. SINMAP model stability classification	245
Table 51. Area-volume relationships for each geological unit	250
Table 52. Description BREACH parameters	254
Table 53. Reservoir area and width vs height	257
Table 54. Comparison of hydraulic models for mud and debris flows	270
Table 55. Results of calibration of rheological parameters	274
Table 56. Measured vs simulated depths in the floodplain	275
Table 57. RSME for selected rheological models	276
Table 58. Intensity and threat categorization matrix for mud and debris flows	282
Table 59. Categorías del índice de vulnerabilidad en la metodología empleada en POMCAS	289
Table 60. Vulnerability ranges in the dimension-based methodology	292
Table 61. Proposed classification of risk	304

BOOK'S REVIEW

Mud and debris flows are sudden and highly destructive natural phenomena that have generated great economic, human and infrastructure losses in our country, which is why adequate territorial planning and risk management in to face of these events must be established as a priority.

This book, the result of the research project ECAPMAPIE012019 entitled "Proposition of a comprehensive methodology for the evaluation of the threat caused by mud and debris flows at the basin scale in Colombia", aims to provide theoretical and methodological guidelines from the understanding of the characteristics of these natural phenomena, the analysis geospatial analysis and water resource modeling to adequately address risk management due to mud and debris flows.

AUTHORS' REVIEW

Jessica Paola Páez Pedraza

Environmental Engineer from the Universidad de los Andes, Master in Civil Engineering Sustainable Management of Water Resources and Hydroinformatics from the Universidad de los Andes.

Teacher and researcher at the School of Agricultural, Livestock and Environmental Sciences of the National Open and Distance University (UNAD).

Research areas: management and risk assessment due to mud and debris flows and floods, ecohydrology, hydrometeorology, climate change, river hydraulics and sedimentology, water quality.

Consulting engineer: hydrological and hydraulic modeling in Water Resources Management Plans and stream regulation.

Denisse Viviana Cortés Castillo

Graduate in Biology from the National Pedagogical University, Master and Doctor in Biological Sciences with emphasis in Biodiversity and Conservation from the National University of Colombia.

Associate researcher at the National University of Colombia (2012-2016). Teacher and researcher at the School of Agricultural, Livestock and Environmental Sciences of the National Open and Distance University (UNAD).

Leader of the Applied Environmental Studies Group (GEAA).

Research areas: biodiversity and conservation, dendrology and botany, risk from mud and debris flows, ecohydrology, climate change, water quality from bioindicators.

Consulting engineer: water quality studies based on environmental bioindicators.

PRESENTATION

Mud and debris flows are one of the most important natural disasters in our country due to the high susceptibility of the territory due to its relief characteristics and the establishment of populations in reservoir areas or flood valleys, which is why the evaluation of the Risk is a fundamental tool for territorial planning and for effective protection of human lives and economic and social infrastructure. However, despite the high frequency and destructive power of these events, it is a natural phenomenon little studied in our country and in the world; It was only until very few years ago that risk studies began to be developed taking this component into account.

That is why at the National Open and Distance University (UNAD) we began the development of the research project ECAPMAPIE012019 entitled "Proposal of a comprehensive methodology for the evaluation of the threat from mud and debris flows at the basin scale in Colombia", in the search to consolidate a robust conceptual and methodological heritage for the analysis and modeling of mud and debris flows events; this book is the product of said research project.

The text aims to present basic theoretical and methodological foundations for the analysis of susceptibility, threat, vulnerability, and risk due to mud and debris flows, supported by the exhaustive bibliographic review of more than 100 studies of various kinds (Plans for the Ordination and Management of Hydrographic Basins [POMCAS] , risk studies, scientific articles, postgraduate theses, technical guides, among others) related to the analysis and modeling of these phenomena, added to some recommendations from the authors' experience in the comprehensive management of water resources from academia and the consulting.

ACKNOWLEDGMENTS

We especially thank the National Open and Distance University (UNAD) for allowing us to develop the research project of which this book is part and for the support throughout the process of the research groups Group of Applied Environmental Studies (GEAA) and Conservation Group, Bioprospecting and Sustainable Development (COBIDES).

We thank professor Mario Díaz-Granados Ortiz of the Department of Civil and Environmental Engineering of the Universidad de los Andes, for his valuable teachings both professionally and personally and for having inspired us to be upright professionals and work hard every day for the sustainable management of water resources in our country.

Finally, we thank the National University of Colombia and the Colombian Geological Service for the information from the Quebrada La Negra basin, which was used for the development of the example case study.

INTRODUCTION

Mud and debris flows in our country have generated thousands of losses of human lives, victims and damage to both infrastructure and crops. It is enough to name some of the greatest tragedies such as Armero in 1985, which left more than 25,000 fatalities (Noticias Caracol, 2018), the mud and debris flows in the Tapartó river, Antioquia, in 1993, which left 120 dead, or some of the most recent ones such as the La Liboriana creek, in the municipality of Salgar, which left 80 dead and 120 missing (Those affected by avalanche in Salgar are growing, 2015) or the Mocoa tragedy that destroyed a large part of the urban area of the municipality and left at least 200 dead. It is against this backdrop that risk management must be a priority in our country, supported by adequate territorial planning.

This book aims to provide theoretical and methodological guidelines that allow the generation of decision-making tools for territorial planning and adequate risk management in the most susceptible basins, in order to prevent these natural phenomena from continuing to take human lives in the future. and continue to generate irreparable damage.

“Tragedies caused by mud and debris flows can be avoided if there is adequate territorial planning supported by rigorous risk assessment and zoning.”

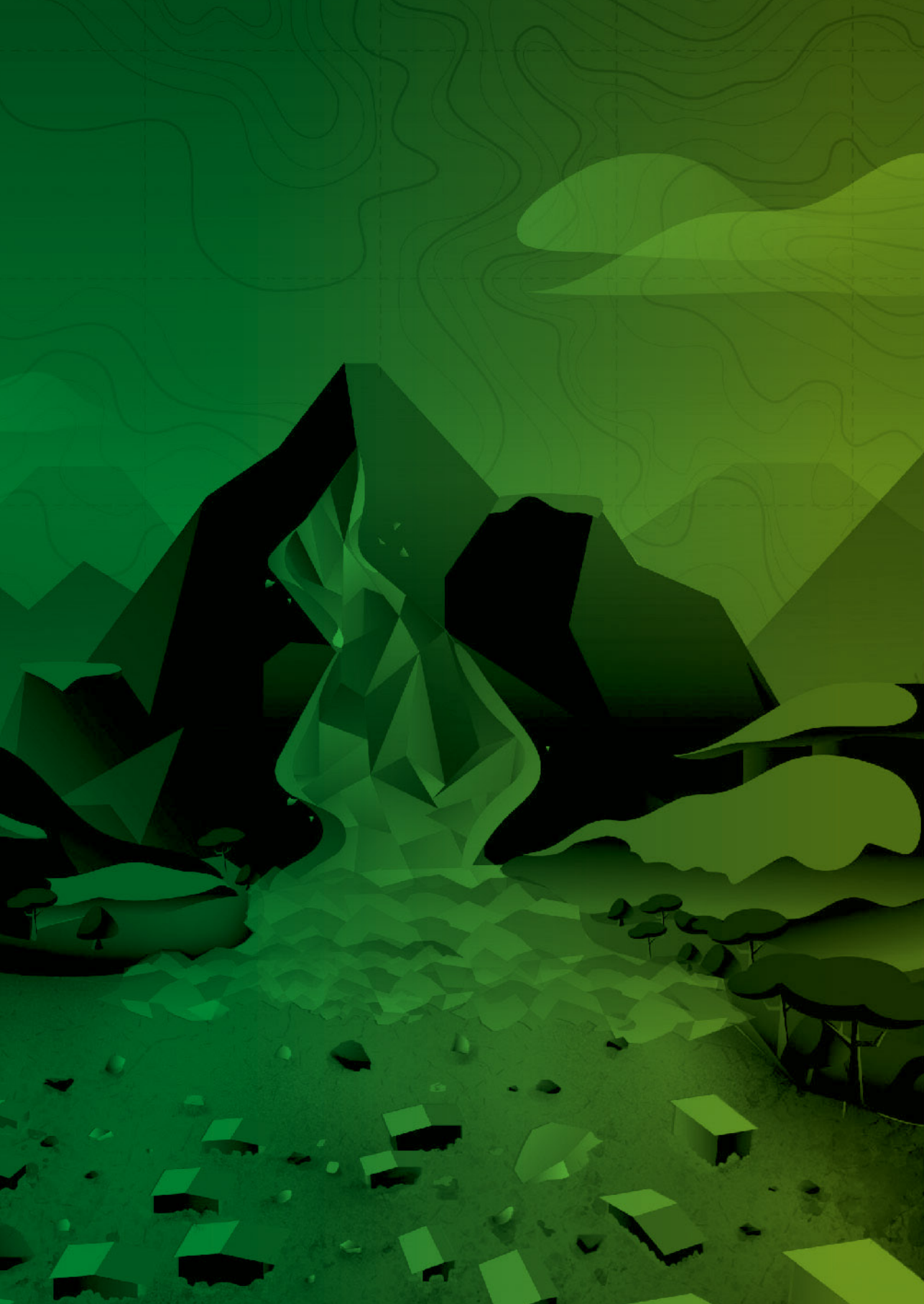
Jessica Paola Páez Pedraza
Denisse Viviana Cortés Castillo

Figure 1. Comparison of the Taruca River flood valley before and after the mud and debris flows of 2017



Note: a) Taruca ravine flood valley, Mocoa– Putumayo in 2001, there were few buildings on the banks of the creek. b) Taruca ravine flood valley in 2013 completely urbanized (non-formalized neighborhoods).c) Quebrada Taruca overflows and deposits large sediments in the torrential flood of 2017, generating one of the greatest tragedies due to mud and debris flows in Colombia.

Source: Google Earth.



GENERALITIES

1.1 THE MUD AND DEBRIS FLOWS

Within risk management, the analysis of events associated with mud and debris flows is of utmost importance because they are highly destructive and unpredictable natural phenomena. However, the study of this type of phenomena becomes difficult due to the complex nature of the flow, which makes it susceptible to confusion in its definition and modeling. Below are different definitions of this natural phenomenon, as well as some of its synonyms or names in some countries.

Table 1. *Definitions of mud and debris flows*

Definition	Author
An avalanche is a mass movement that moves suddenly along the slopes of a mountain, dragging a large amount of rock material, vegetation and debris. They can range from a small surface flow to a gigantic destructive mass.	Institute of Hydrology, Meteorology and Environmental Studies (IDEAM, 2015).
A mud and debris flows is a violent flow of water in a basin, sometimes reported as rising (sudden, rapid), or as a torrent. It is applied when in the reports – it appears as 'avalanche', when the flood transports tree trunks or abundant fine sediments to even blocks of rock. They can be generated by rain, by the breaking of dams or by abundant landslides of a basin.	Disaster Inventory System Desinventar (Velazques y Rosales 1999, 117)
A mud and debris flows is a very fast to extremely fast flow of saturated, non-plastic debris (plasticity index less than 5%), which occurs mainly confined along a channel or channel with a steep slope. It is one of the most dangerous mass movements due to its characteristics of sudden occurrence, high speeds and long travel distances.	National Committee for Risk Knowledge (2017, p. 39).

Definición	Autor
Mud and debris flows are sudden floods resulting from heavy rainfall that cause rapid increases in the water level of high-slope rivers and streams. These floods can be accompanied by sediment flow according to the conditions of the basin. Due to their characteristics, they can cause great damage to infrastructure and loss of human life (adapted from Standards Group for Mass Movements [GEMMA], 2007).	District Institute for Risk Management and Climate Change (IDIGER, 2016).
Mud and debris flows correspond to sudden floods in mountain channels, with peak discharges of great magnitude, produced by severe storms generally of limited extent in area.	Institute of Hydrology, Meteorology and Environmental Studies (IDEAM, 2013).
An avalanche refers to a large mass of matter that falls off a slope, precipitating it.	Royal Academy of the Spanish Language (RAE, 2020).

Source: own elaboration.

In accordance with the definitions in Table 1, throughout this document the definition of the DesInventar disaster inventory system will be used, since it takes into account the most important characteristics of these phenomena: they are sudden and fast, they can carry high amounts of sediment, can drag logs and have multiple triggering causes, among the most frequent being landslides due to intense rain.

Additionally, mud and debris flows have different names depending on the country, so those presented in table 2 can be taken as synonyms.

Table 2. *Names of mud and debris flows in different countries*

Denomination	Country
Avalanches	Colombia
Huaycos	Peru
Floods	Bolivia
Lahars	Indonesia
Debris or debris flows	Spain

Source: Suárez (2009).

1.2 TRIGGERING MECHANISMS OF MUD AND DEBRIS FLOWS

For a mud and debris flows event to be triggered, some geological and hydrological characteristics must be met, including intense rains, sufficient availability and contribution of sediments by the basin, and a shallow relief (Hsu et al., 2010). However, there are multiple triggering mechanisms for a mud and debris flows, which in many cases act together; the most important ones are described below.

1.2.1 LANDSLIDES DUE TO HEAVY RAINS

The most frequent trigger mechanism for mud and debris flows is the generation of multiple landslides due to intense rains. These can be produced by a single large rainfall or by periods of prolonged rain after periods of drought, which causes soil saturation. and the detachment of this, which together with the sudden increase in water generates a flow with high sediment content.

On the other hand, large landslides can also be generated that can begin to flow in the channel reaching high speeds, the flow increases its concentration of sediments as it drags the materials it finds in its pathway, generating a scour process both bottom and lateral (Suárez, 2001).

The most frequent trigger mechanism for mud and debris flows is the generation of multiple landslides due to intense rains.

1.2.2 WATER DAMING

This mechanism acts in combination with others; it is generated when a landslide produces an accumulation of water for several days and a natural dam is generated, acting as a small reservoir. This dam breaks suddenly with intense rain and the mud and debris flows is generated (Suárez, 2001).

1.2.3 PROCESSES IN CHANNEL

In areas of very high slope, during a very heavy rain event, a large amount of bed material can be transported, above the normal bottom transport (sediment concentration greater than 20% by volume), therefore, the processes in channel. They refer to these erosive processes that generate scour of the channel and transport of a large amount of material (Bateman and Medina, 2019).

1.2.4 EARTHQUAKES

Again this mechanism is related to the generation of landslides, the occurrence of a seismic event of great magnitude and shallow depth of focus in conjunction with a rainy period can generate widespread landslides and in turn the detonation of a mud and debris flows (Suárez, 2001).

1.2.5 MELTING OF SNOWCAPE AND PYROCLASSIC FLOWS

Volcanoes are highly susceptible to the generation of mud and debris flows, mainly due to their high slope and inclined layer structure, which is why, during a volcanic eruption, when pyroclastic flows are deposited on the slopes, they can generate additional flows down the slopes activated by rains. Additionally, snowy volcanoes can more easily generate these events because the eruptions melt the snow generating mud flows, this is the case of the event that occurred in Armero, Colombia, in 1985 (Suárez, 2001).

1.3 TYPES OF FLOWS

Depending on the characteristics of the mud and debris flows, different types of flows may occur, which in turn present different behaviors, it should be noted that mud and debris flows must be clearly differentiated from floods, since these can contain

between 20 to 90% sediment concentration by volume, which makes their behavior very different from a flood.

The main difference between the flows is due to their sediment concentration and the type of sediment (gravel, sand, silt and clay). According to this, in basins with high silt and clay content, mud flows are generated, while basins with coarser materials such as sand and gravel tend to generate debris or hyperconcentrated sediment flows (Suárez, 2009).

1.3.1 MUD FLOWS

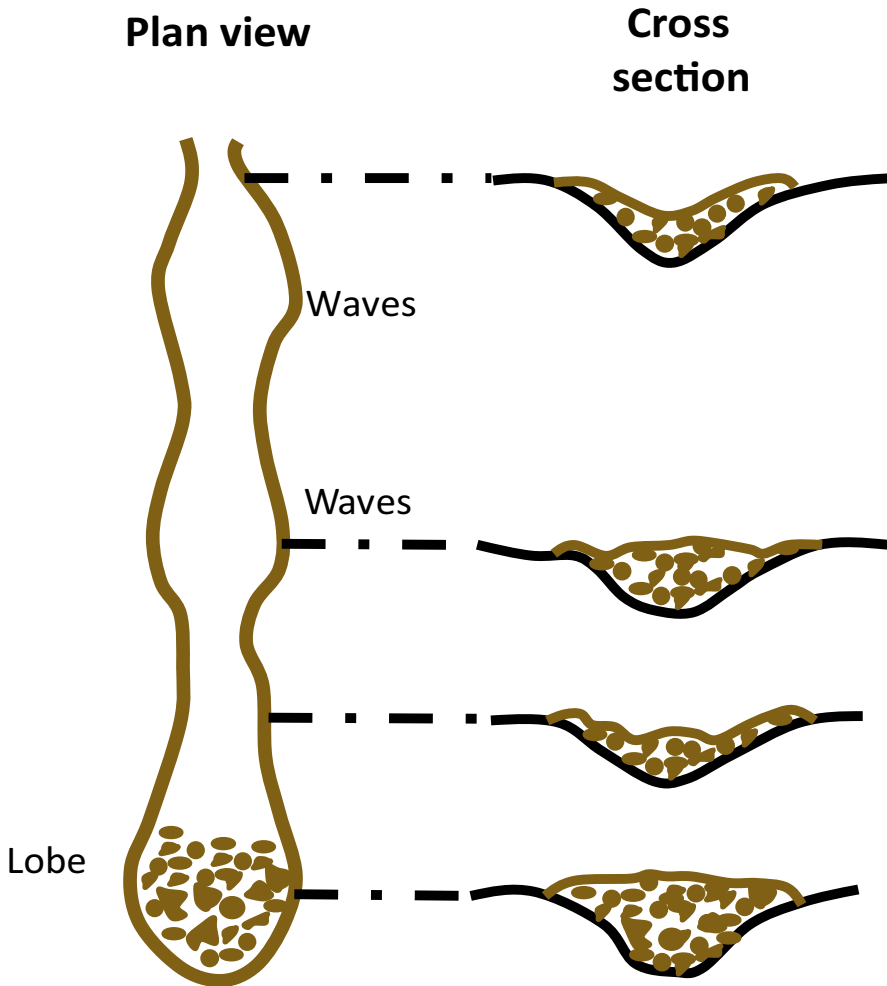
Mud flows are generated in basins with high availability of silt and clay type sediments, however, these flows can also transport large blocks of rock, because as the concentration of sediments increases, they flocculate rapidly and the viscosity increases forming cohesion in the mixture.

Sludge flows are characterized by having intermittent pulses, from 10 to hundreds of them. As more sediment adheres, the flow becomes more viscous and slower. Due to the viscosity of the flow, these tend to rise in curves to heights greater than 10 meters and generally the flow is higher, wider and steeper at the front, generating a trunk.

When the flow accumulates, elongated lateral deposits form next to the main channel, parallel to the flow, which may be tongue-shaped. During sedimentation, no classification of sediments occurs, but rather the flow moves as a single mass (Suárez, 2009).

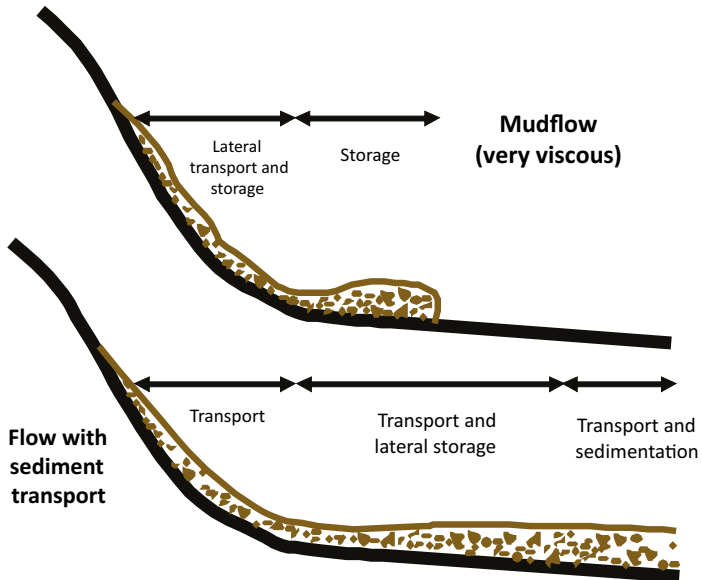
Sludge flows are generated in basins with high availability of silt and clay type sediments, however, these flows can also transport large blocks of rock

Figure 2. Representation of a sludge flow (screen view, cross section, waves, lobe, trunk)



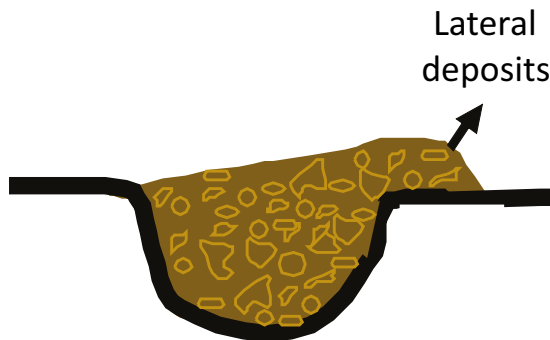
Source: adapted from Johnson and Rodine (1984).

Figure 3. Comparison of a sludge flow and a non-viscous flow



Source: adapted from Johnson and Rodine (1984).

Figure 4. Lateral deposits formed in sludge flows due to elevation in curves



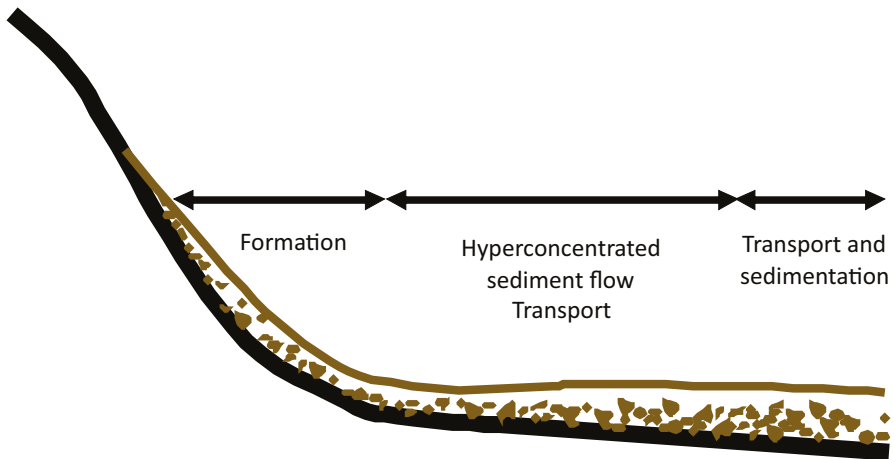
Source: adapted from Johnson and Rodine (1984).

1.3.2 HYPERCONCENTRATED SEDIMENT FLOWS

Hyperconcentrated sediment flows can have sediment concentrations greater than 5% and less than 60% by volume; Unlike mud flows, these are not viscous due mainly to the granulometry of the sediments, which is much coarser and is composed of sand, gravel, stones and blocks, which generates little cohesion in the water-sediment mixture, forming a weak turbulent flow (Suárez, 2009).

In hyperconcentrated sediment flows the particles move partially as background load and partially suspended; and because they possess a certain degree of plasticity they create deformation patterns along the current. When the particles settle, first the coarsest ones and then the finer ones, a classified deposit of particles is formed (Suárez, 2001). A granular hyperconcentrated flow is schematically presented in Figure 5.

Figure 5. *Hyperconcentrated flow scheme*



Source: adapted from Suárez (2001).

1.3.3 DEBRIS OR DEBRIS FLOWS

When the sediment concentration in a flow increases above 60% by volume, it becomes a debris flow (debris flow) and the water-sediment mixture becomes a paste similar to wet concrete; This mixture is capable of sustaining gravel-sized particles in suspension at low speeds or even in static conditions. However, if the channel in which the debris flow occurs is very steep, the flow can reach high speeds and transport large blocks in suspension (Suárez, 2009).

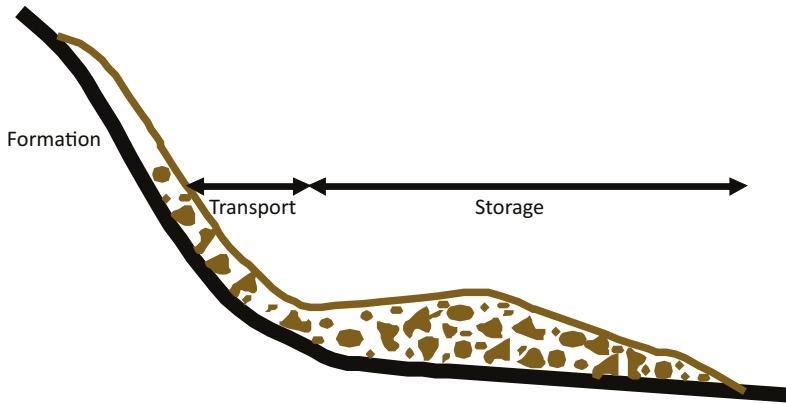
In debris flows, sediments control the flow and can be related to a “turbulent grain” flow; the movement is produced by the transfer of momentum when moving particles or blocks collide. In turn, when this particle collision is generated, there is an internal shear stress and the flow can behave like a dilatant non-Newtonian fluid.

The deposit of the flow occurs when there is a decrease in the slope, an increase in the width of the channel or the presence of obstacles that increase the resistance of the flow and decrease its speed. As the materials are deposited, types of dams are formed that raise the flow, as shown in Figure 6, which further promotes the deposition process.

When the change in channel width or slope is very strong, the speed decreases drastically and most of the solid material is deposited, forming fans or bars of large blocks. The largest particles are deposited first, while the fine particles try to travel a greater distance before sedimentation occurs (Suárez, 2001).

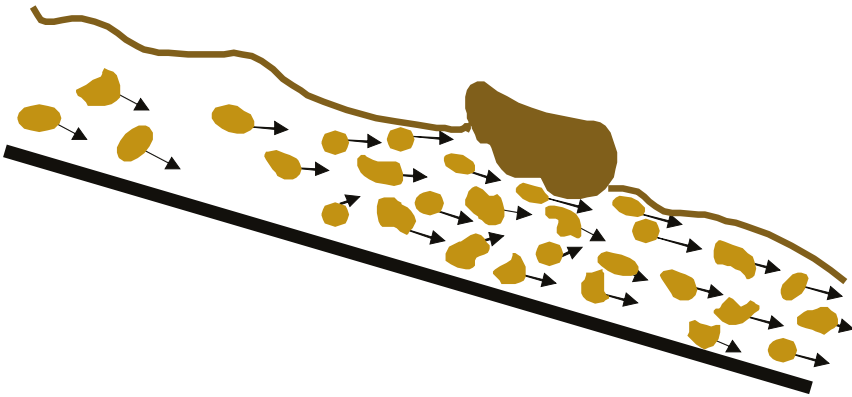
When the change in channel width or slope is very strong, the speed decreases drastically and most of the solid material is deposited, forming fans or big bar blocks

Figure 6. *Debris flow representation*



Source: adapted from Suárez (2009).

Figure 7. *Flotation of large blocks in debris flows*



Note: The block travels at a slower speed than the rest of the flow

Source: adapted from Suárez (2009).

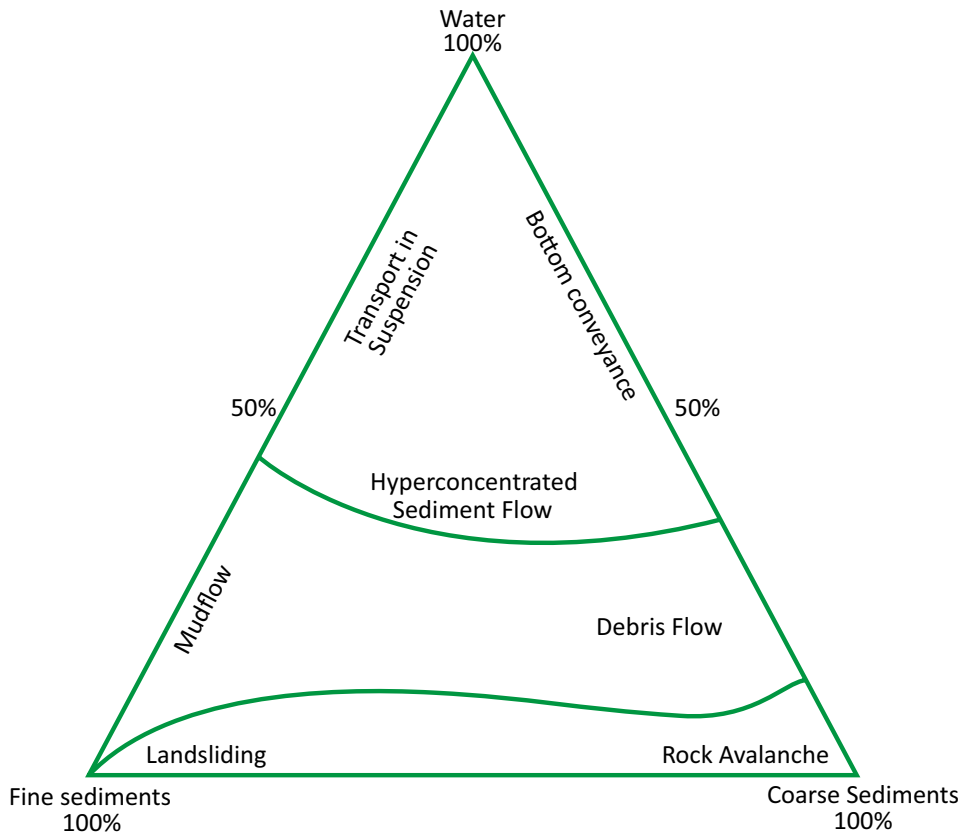
1.3.4 CLASSIFICATION OF FLOWS BY TYPE AND CONCENTRATION OF SEDIMENT

As indicated above, each type of flow has different characteristics, which is why when carrying out a risk assessment for these events it is important to have an initial notion of what type of flow can occur in the study area, since this will influence its behavior and the possible damage caused.

The type of flow depends not only on the sediment concentration, but also on the type of sediment. A greater amount of fine sediments with concentrations greater than 20% may generate a sludge flow, while if the predominant type of sediment is gravel or sand, a hyperconcentrated flow or a debris flow may be generated; The higher the concentration of sediments, the more it will resemble a debris flow, while for concentrations greater than 70 – 80% by volume we could already be talking about rock avalanches or landslides.

There are several tools such as diagrams and tables that allow an approach to the type of flow, taking into account the concentration and type of sediments. Among them are the phase diagrams which are similar to a textural triangle, in which one of the vertices shows the water content and in the other two the type of sediment, whether fine or coarse. Some of these diagrams take into account mud flows, while others only hyperconcentrated and debris flows.

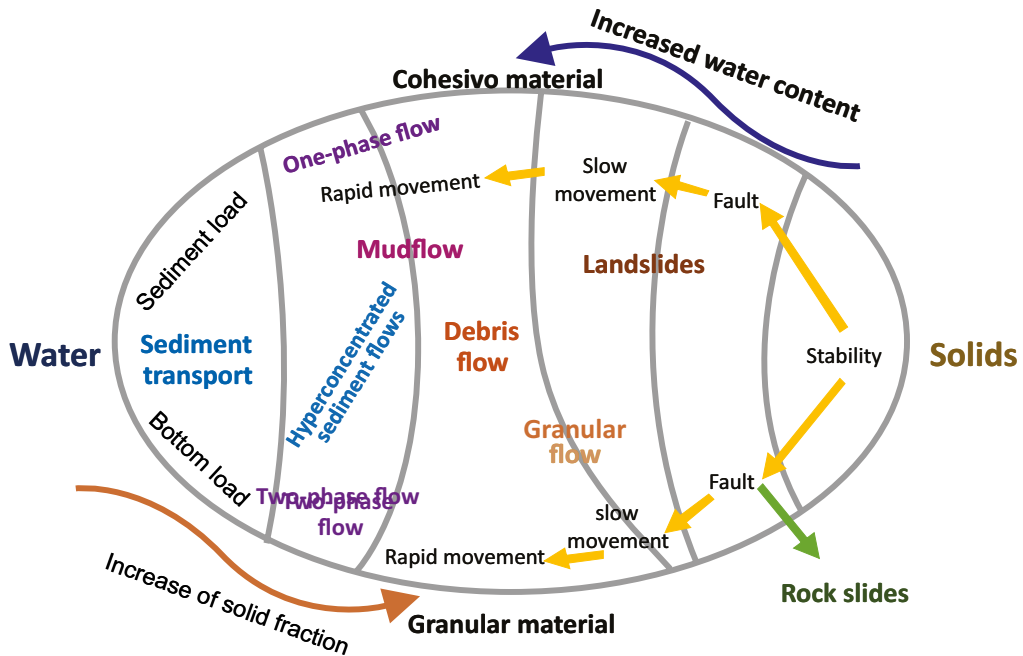
Figure 8 shows the phase diagram of Rickenmann (2016), who modified it based on the original by Phillips and Davis (1991). This diagram shows that for concentrations greater than 50 - 60% there is a debris or sludge flow, while for lower concentrations it can behave either as water with sediment transport or as a hyperconcentrated flow. Likewise, the Cousot and Meunier (1996) diagram is presented in figure 9, which classifies the flows according to the type of material, whether granular or cohesive, and the amount of water and sediment, as well as the speed of the flow.

Figure 8. Phase diagram of debris flows and landslides

Source: adapted from Rickenmann (2016).

This diagram shows that for concentrations greater than 50 – 60% there is a debris or sludge flow, while for lower concentrations can behave either as water with sediment transport or as a hyperconcentrated flow.

Figure 9. Classification of flows and landslides according to the solid fraction and the type of material



Source: adapted from Coussot and Meunier (1996).

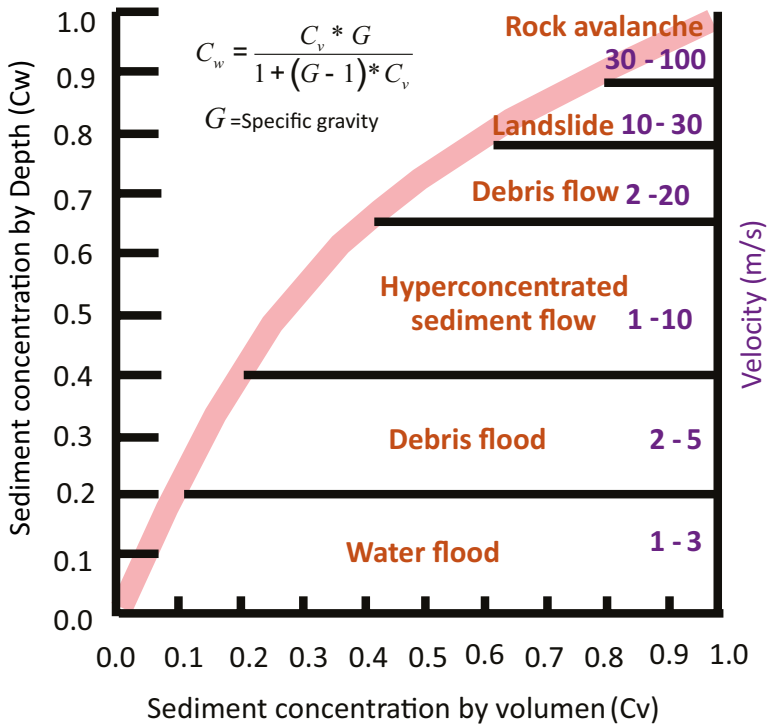
On the other hand, O'Brien and Julien (1997) studied sludge flows and found some relevant characteristics of these according to the concentration of sediments (mostly fine) as presented in table 3. However, in the 2000 O'Brien, developer of the FLO-2D model, one of the first hydraulic models that allows modeling mud and debris flows, modified this classification in such a way that the type of flow depended directly on the concentration of sediments in volume and in weight, classification also modified by Suárez (2009) in such a way that hyperconcentrated sediment flows and debris flows were included, as seen in figure 10. Suárez (2009) also presents a classification which additionally takes into account the slope of the channel, as seen in table 4.

Table 3. *Classification of mudflows according to O'Brien and Julien*

Flow type	Concentration of sediments		Characteristics
	In volume	In weight	
Glide	0.65 – 0.80	0.83 – 0.91	Does not flow, fails by block sliding.
	0.55 – 0.65	0.76 – 0.83	Failure by sliding of blocks with internal deformation during the slide; slow creep before failure.
Sludge flow	0.48 – 0.55	0.72 – 0.76	Slow sludge flow with sustained creep; plastic deformation under its own weight; cohesive, does not flow on a flat surface.
	0.45 – 0.48	0.69 – 0.72	Flow on flat surface, cohesive flow.
Mud flood	0.40 – 0.48	0.65 – 0.69	The flow is easily mixed, during deformation it shows characteristics of a fluid, it extends on a horizontal surface but the surface of the fluid maintains a certain inclination; settlement of large particles; with the appearance of waves that dissipate quickly.
	0.35 – 0.40	0.59 – 0.65	Marked gravel settlement, almost total spread on horizontal surface; two fluid phases appear on the liquid surface, waves travel on the surface.
	0.3 – 0.35	0.54 – 0.59	Separation of water at surface, waves travel easily, most gravel and sand has settled and moves as bed load.
	0.2 – 0.30	0.54 – 0.41	Action other than the wave, fluid surface, all particles rest on the bed under static conditions.
Flooding	<0.20	<0.41	Conventional flooding with suspended load and bottom drag.

Source: O'Brien and Julien (1997).

Figure 10. Classification of landslides and flows according to speed and sediment concentration



Source: adapted from Suárez (2009).

There are several tools such as diagrams and tables that allow an approach to the type of flow, taking into account the concentration and type of sediment.

Table 4. Classification of flows according to sediment type and channel slope

		Channel slope (%)				
Characteristics sediments	Concentration sediments (Kg/m ³)	>100	100 – 50	50 – 20	20 – 10	10 – 5
More than 20% of the total weight of the sediments are fine particles	<90	Hyperconcentrated flow			Mud flow	
	>90	Mud flow				
	<300	Hyperconcentrated flow				
Less than 20% of the total weight of the sediments They are particles fine	300 – 600	Turbulent flow of debris- (debris flow)		Hyperconcentrated flow		
	They are particles	Turbulent debris flow (debris flow)				
	fine	Laminar debris flow				

Source: Suárez (2009).

Finally, Hungr et al. (2001) present a classification according to the type of material, the moisture content and the speed scale for landslides proposed by Cruden and Varnes (1996), as seen in table 5.

It should be clarified that these tools are only approximations that allow us to know the type of flow that will occur in a channel based on a deep knowledge of the geology of the basin and channel materials; however, if possible, historical events should be studied. to determine with greater certainty the type of flow and likewise the choice of the most appropriate rheology to describe its behavior.

Table 5. *Classification of flows according to type of material and moisture content*

Material	Moisture content	Special condition	Speed	Denomination
Slime Sand, gravel, and debris	Dry, wet, and saturated	No excess of interstitial pressure. Imitated volume	Several	Non-liquefiable sand flow
Slime, sand, debris, and weak rock (high porosity)	Saturated on the breaking surface	Liquefiable material. Constant moisture content	Extremely fast	Sliding flow or sand fluidization
Sensitive clay	At or above the liquid limit	On-site liquefaction. Constant moisture	Extremely fast	Sliding flow or clay fluidization
Peat	Saturated	Excess of interstitial pressure	Slow to very fast	Peat flow
Clay or soil	Close to the plastic limit	Slow movement. Rigid flow without cutting deformation	Less than fast	Soil flow
Debris	Saturated	Increased moisture content	Extremely fast	Debris flow
Mud	At or above the liquid limit	Debris flow of fine grains	Greater than very fast	Mud flow
Debris	Presence of free water	Discharge of the same order of flood or rise	Extremely fast	Debris torrent

Material	Moisture content	Special condition	Speed	Denomination
Debris	Partially or fully saturated	Non-consolidated channel. Relatively superficial, steep slope	Extremely fast	Debris avalanche
Fragmented rock	Mainly dry	Intact rock at the origin	Extremely fast	Rock avalanche

Source: Hungr et al. (2001).

Table 6. *Landslide speed scale proposed by Cruden and Varnes*

Description	Speed
Extremely fast	>5 m/s
Very fast	0.05 – 5m/s
Quick	0.05m/s – 1.8m/h
Moderate	1.8 m/h – 13 m/month
Slow	13 m/month – 1.6 m/year
Very slow	1.6 m/year – 16 mm/year
Extremely slow	<16 mm/year

Source: Cruden and Varnes (1996).

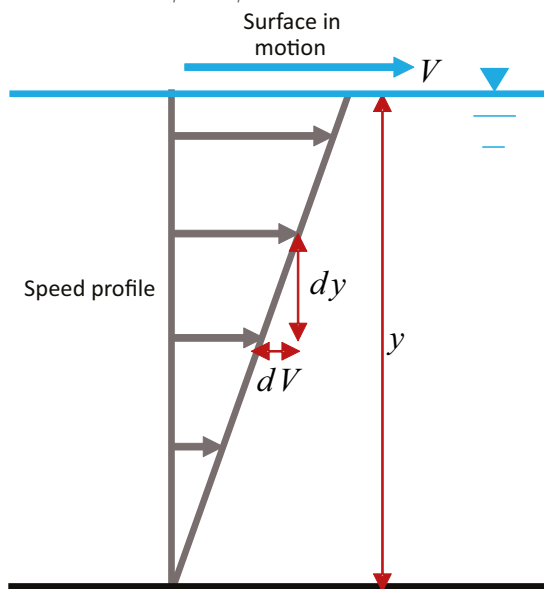
1.4 TYPES OF FLUIDS AND RHEOLOGY

Rheology refers to the branch of physics that studies the viscosity, plasticity and elasticity of matter. Rheological models allow us to describe the behavior of fluids. The most used is Newton's law of viscosity, in which the force exerted to deform the fluid or shear stress depends linearly on the rate of deformation; this is the model used for water. However, there are other types of fluids that do not follow this law, these are called non-Newtonian fluids, for which their behavior is described using additional components of the shear stress.

Shear stress can be defined as the force required to slide a layer of unit area of one substance or fluid over another, which is why it is a force per unit area. When this force is exerted, the fluid generates resistance. This resistance to the movement of a fluid or deformation speed is called viscosity. The proportionality between the deformation of the fluid and the applied shear stress is called dynamic or absolute viscosity and is represented by the letter μ for Newtonian fluids, for which it maintains a constant value and η for non-Newtonian fluids for which it is a variable value (Mott, 2015).

In a fluid in contact with a surface, the shear stress will decrease as it gets closer to the surface, so the speed of the surface will be greater than that of the bottom, since less resistance is being exerted, as shown. see in figure 11.

Figure 11. Representation of the speed profile of a fluid



Source: own elaboration.

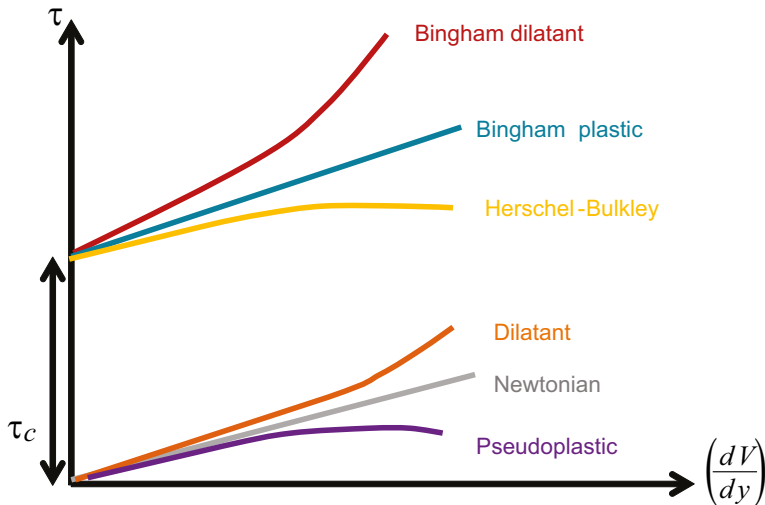
In some cases, mud and debris flows can be modeled with Newton's law of viscosity, that is, as if only water with sediment transport were treated; However, when there are high concentrations of sediments, it is most advisable to model these flows as non-Newtonian fluids, since, depending on the amount and type of sediment, the flow can become a viscous fluid in which there are more particles in constant flow. shock than water.

Although there is no clear limit between what we could call viscous fluids and non-viscous fluids, in general it can be said that fluids that have a lower viscosity than water correspond to mobile fluids, while those that have a higher viscosity are called viscous fluids. In accordance with the above, for the purposes of this document, viscous fluids will be called those that have a viscosity higher than that of water due to their high content of fine sediments and behave as a single mass, that is, they are of one phase, while that those fluids that have a moderate or low concentration of fine sediments and a viscosity similar to that of water, present two water-sediment phases and correspond to non-viscous fluids.

However, it is worth clarifying that this can be very variable and there are no clear limits that determine the transition point between viscous and non-viscous fluids, especially when talking about hyperconcentrated sediment flows, which is why it is important that when choosing the rheology one takes into account the Several fluid models are taken into account and the one that best suits the particular conditions of the basin is selected.

The non-Newtonian fluid models most used for modeling mud and debris flows are the Bingham type, pseudoplastic fluids and dilatant fluids. Bingham type fluids are viscous and require a minimum shear stress to initiate their fluidity, while pseudoplastic fluids are those that flow more easily the greater the shear stress, on the contrary, the dilatant fluids flow more difficult the greater the shear stress. shear stress. Figure 12 shows the behavior of the different types of fluids depending on the applied shear stress.

Figure 12. *Types of Newtonian and non-Newtonian fluids*



Source: own elaboration.

1.4.1 NEWTONIAN FLUIDS

Newtonian fluids, as their name indicates, follow Newton's law of viscosity, so there is a linear relationship between viscosity and shear stress. For these fluids, viscosity is constant and is the model used for water flows.

$$\tau = \mu \left(\frac{dv}{dy} \right)$$

Where:

τ = Shear stress

μ = Dynamic viscosity

v = Speed

y = Depth

Hyperconcentrated sediment flows can also be modeled as Newtonian fluids, however, due to the high concentration of sediments and collisions between particles, there is greater dissipation of potential energy (Suárez, 2009), therefore, if this model is used for the mud and debris flows, the Manning coefficient must be increased to values much higher than those commonly used, that pseudo-Manning can range between 0.08 – 0.14. In China, the following relationship is used to calculate the of pseudo-Manning, where h corresponds to the depth of the flow:

$$n = 0,035 * h^{0,34}$$

1.4.2 NON-NEWTONIAN FLUIDS

Non-Newtonian fluids can be represented by adding five shear stress components. The stresses included in the equation depend on the type of fluid, whether turbulent, pseudoplastic, Bingham or dilatant, as shown below

$$\tau = \tau_o + \tau_{mc} + \tau_v + \tau_t + \tau_d$$

Where:

τ_c = yield shear stress

τ_o = Cohesive yield strenght

τ_{mc} = Mohr–Coulomb stress

τ_v = Viscous shear stress

τ_t = Turbulent shear

τ_d = Dispersive shear stress

$$\tau = \tau_c + \eta \left(\frac{dv}{dy} \right) + C \left(\frac{dv}{dy} \right)^2$$

$$\tau_c = \tau_o + \tau_{mc}$$

$$\tau_t + \tau_d = C \left(\frac{dv}{dy} \right)^2$$

C = Dispersive turbulent coefficient

η = Apparent dynamic viscosity

1.4.2.1 Bingham Model

Bingham fluids are of the viscous type and behave like a solid until a minimum shear stress or yield shear stress is exceeded. From that moment on, the relationship between deformation and shear stress can be linear as in Newtonian fluids or similar to pseudoplastic or dilatant fluids. In these fluids, Van der Waals forces produce a mutual attraction between particles that immobilizes them until a minimum shear stress is produced. Additionally, these fluids can flow on flat surfaces, while non-viscous fluids can flow only with the existence of a slope. The Bingham model was introduced by Bingham and Green (1919) and the equation that describes it is the following.

$$\tau = \tau_o + \mu \left(\frac{dv}{dy} \right)$$

1.4.2.2 Herschel Bulkley Model

The Herschel and Bulkley (1962) model is very similar to the Bingham model and also requires a minimum shear stress to start flowing, in the latter is replaced by dynamic viscosity and $n=1$. This model can be used to represent sludge under a wide range of particle sizes.

$$\tau = \tau_o + k \left(\frac{dv}{dy} \right)^n$$

k = Consistency factor

n = Flow rate

The coefficient allows to represent the viscosity or thickening of the fluid, while indicates the degree to which the fluid is thinning or thickening, these are parameters that must be calibrated.

1.4.2.3 Dilatant fluid models

In dilatant fluids, the viscosity becomes greater as the shear stress increases, until it reaches a point where it takes on a constant value, that is, there is greater resistance to flow for greater shear stresses (Ibarrola, 2015), the equation that describes the general model of dilatant fluids is the following.

$$\tau = \mu \left(\frac{dv}{dy} \right) + C \left(\frac{dv}{dy} \right)^2$$

According to Takahashi (1991), the debris flow is composed of a liquid and a solid phase, for which he derived conservation equations of momentum for each phase and added the equations of the two phases, the collision stresses between particles and the stresses in the interstitial flow, due to turbulence and viscosity, to generate their dilatant flow model (Suárez, 2009).

1.4.2.4 O'Brien quadratic model

On the other hand, there is the quadratic model of O'Brien and Julien (1985), this model includes all the shear stress components, and the viscosity and yield shear stress parameters depend on the sediment concentration, it is similar to the Bingham model but with a dilating behavior.

$$\tau = \tau_c + \mu \left(\frac{dv}{dy} \right) + C \left(\frac{dv}{dy} \right)^2$$

$$\mu = \alpha_1 * e^{\beta_1 c}$$

$$\tau_c = \tau_o + \tau_{mc}$$

$$\tau_c = \alpha_2 * e^{\beta_2 [c]}$$

$$C = \rho_m l_m + f(\rho_m, c) d_s^2$$

Where:

$\alpha_1, \alpha_2, \beta_1, \beta_2$ = Coefficients that depend on the type of sediment

c = Sediment concentration

ρ_m = Density of the mixture

l_m = Mixing length

d_s = Average diameter of sediments

1.4.2.5 Bagnold model

(Bangold, 1954) developed a dilatant fluid model in which he differentiates three types of flows that depend on the diameter, density and concentration of the sediments: a

macroviscous regime, a transitional regime, and an inertial granular regime, which can be determined by the Bagnold number, as follows:

$$B_a = \frac{\lambda^2 * \rho_s * c^2 \left(\frac{dv}{dy} \right)}{\mu}$$

$$\lambda = \frac{1}{\left(\frac{C_0}{C} \right)^{\frac{1}{3}} - 1}$$

Where:

c = Particle diameter

C = Volume concentration of solids (must be less than $0.9 * C_0$)

C_0 = Maximum possible concentration (in spherical particles 0.74 and in granular materials 0.65)

$\frac{dv}{dy}$ = Warp speed

μ = Dynamic viscosity

ρ_s = Density of solid particles

Therefore, we have an equation that describes the shear stress as a function of the fluid deformation for each regime as follows:

$$B_a < 40 \rightarrow \text{Macroviscous regime}$$

$$40 \leq B_a \leq 450 \rightarrow \text{Transition regime}$$

$$B_a > 40 \rightarrow \text{Inertial granular regime}$$

Macroviscous regime:

$$\tau = a_v * \lambda^2 * \mu \left(\frac{dV}{dy} \right) * \text{sen}(\alpha_1)$$

$$a_v = 3,75; \alpha_1 \cong 37^\circ$$

Inertial granular regime:

$$\tau = a_i * \rho_s * \lambda^2 * c^2 \left(\frac{dV}{dy} \right)^2 * \text{sen}(\alpha_1)$$

$$a_i = 0,042 \text{ for } \lambda < 14; a_i = 0,24 \text{ for } 14 < \lambda < 17; a_i \cong 17^\circ$$

Where:

a_i, a_1 = Experimental constant

α_1 = Dynamic friction angle (different from internal friction angle)

1.4.2.6 Takahashi model

Takahashi's model (1978) is based on Bagnold's, but introducing modifications in the parameter a_i . In addition, an equation is incorporated that allows calculating the value of α_1 , which is a function of the sediment concentration and is valid for concentrations greater than 30%, this is the most used model in Japan

Inertial granular regime:

$$\tau = a_i * \rho_s * \lambda^2 * c^2 \left(\frac{dV}{dy} \right)^2 * \text{sen}(\alpha_1)$$

$$\tan(\alpha_1) = \left(\frac{C_0}{C} \right)^{\frac{1}{3}} \tan(\phi)$$

ϕ = Angle of internal friction of the flow

$$0,35 \leq a_i \leq 0,5$$

1.4.2.7 Mohr–Coulomb model

The Mohr – Coulomb model was proposed by Johnson (1970) based on the Coulomb model, which is used for ground movement, and combining it with a modification of the Bingham model.

In this model, the shear stress depends on a minimum stress or yield shear stress (C) and the angle of internal friction of the material. For soils, the angle of internal friction is related to the angle of repose or maximum possible angle for which a material will remain at rest without sliding. However, in the case of mud and debris flows, this angle corresponds to the angle of the terrain at which the flow begins to slow down and settle.

In this model, the yield shear stress depends on the cohesion of the particles, defined as the adhesion between particles produced by intragranular forces.

$$\tau = C + \sigma_n \tan \phi$$

$$\tau_{mc} = C$$

Where:

C = Cohesion

σ_n = Normal effort

ϕ = Internal friction angle

In 1970 Johanson proposed that the total shear stress should be defined as a combination of the Coulomb stress and the viscous stress, resulting in the Mohr-Coulomb viscous model:

$$\tau = C + \sigma_n \tan \phi + \mu \left(\frac{dv}{dy} \right)$$

1.4.2.8 Voellmy model

This model was developed by Voellmy (1955) for snow avalanches and Körner (1976) implemented it for rock avalanches. It takes into account the coefficient of friction (C_z), the flow density and the angle of internal friction (ϕ)

$$\tau = g\rho \left(h \cos(\theta) \tan(\phi) + \left(\frac{V}{C_z} \right)^2 \right)$$

1.4.2.9 Pseudoplastic fluid

In pseudoplastic fluids, the viscosity measured by the slope of the deformation curve decreases with the increase in shear stress until reaching a constant asymptotic value (Ibarrola, 2015); The higher the shear speed, the lower the viscosity and the lower the shear speed, the higher the viscosity. Taking the above into account, a pseudoplastic fluid flows more easily the greater the shear stress. This type of fluid model is not commonly used in flood modeling.

$$\tau = \mu \left(\frac{dv}{dy} \right) - C \left(\frac{dv}{dy} \right)^2$$

1.4.3 Selection of the rheological model according to the type of flow

As indicated in previous sections, the behavior of each type of flow is different according to the concentration and type of sediment, which is why it is important to properly choose the appropriate rheological model to describe the behavior of the flow. In accordance with the above, it is worth clarifying that there are specific rheological models for viscous flows, such as the Bingham models and those that take into account a yield shear stress, and models for non-viscous turbulent flows such as those of Takahashi or Voellmy.

Thus, in general we could say that sludge flows correspond to viscous fluids, while debris flows are non-viscous turbulent fluids; However, when the sediment concentration is greater than 85 – 90%, the debris flow becomes laminar and can have a viscous behavior.

In the middle of the two previously mentioned flows, there are hyperconcentrated granular flows, which can be viscous or non-viscous depending on the concentration of fine sediments. When these types of flows are not viscous, they can be described with the traditional Manning model. However, for these cases a value of Manning much higher than the traditional value for water flows, in such a way that the dissipation of energy due to the collision between the particles is taken into account. In accordance with the above, Table 7 presents the recommended rheological models for each type of flow.

Table 7. *Rheological model recommendation for each type of fluid*

Flow type	Recommended rheological model
Sludge flow (viscous)	Bingham / Herschel Bulkley / O'Brien
Granular (viscous) hyperconcentrated flow	Bingham/ O'Brien
Granular hyperconcentrated flow (non-viscous)	Manning/ Bagnold / Voellmy
Turbulent debris flow (non-viscous)	Bagnold /Takahashi /Mohr – Coulomb /Voellmy
Laminar debris flow (viscous)	Bingham/ O'Brien

Source: modified from Chien and Wan (1999) and Takahashi (1991).

1.5 RISK ANALYSIS

In accordance with Law 1523 of 2012, risk analysis:

involves consideration of the causes and sources of risk, its consequences, and the probability that those consequences may occur. It is the model through which the threat and vulnerability of the exposed elements are related, in order to determine the possible social, economic and environmental effects and their probabilities. The value of potential damages and losses is estimated and compared with established safety criteria, with the purpose of defining the types of intervention and scope of risk reduction and preparation for response and recovery.

Therefore, the risk analysis includes determining the threat and vulnerability of the exposed elements; In the case of mud and debris flows, the threat would be the probability of an event occurring and its magnitude, while the vulnerability would take into account the fragility of the communities exposed to this possible threat.

1.5.1 THREAT

According to Law 1523 of 2012, the threat is constituted as a latent danger that a physical event of natural origin, or accidentally caused or induced by human action, occurs with sufficient severity to cause loss of life, injuries or other health impacts, as well as damage and loss to property, infrastructure, livelihoods, service delivery and environmental resources.

The threat must be described in terms of the magnitude or intensity and the frequency of occurrence. For mud and debris flows, the magnitude can be expressed qualitatively (recommended on a regional scale) in terms of high, medium or low or quantitatively (recommended on a local scale) as a measure of the size of the event (flooded area, flow volume, flooding depth) and intensity (speed), while a return period can be assigned for frequency (Colombian Geological Service [SGC], 2017).

1.5.2 SUSCEPTIBILITY

The definition of susceptibility can be taken in two ways depending on which variable is being analyzed. On the one hand, when the vulnerability analysis is carried out, it generally refers to the susceptibility due to exposure. In this sense, susceptibility refers to the fragility of the exposed element. On the other hand, when the threat analysis is carried out we refer to the susceptibility of the territory as its conditions that may or may not be conducive to the generation of a threatening event. For the purposes of this document we will only refer to susceptibility for the threat analysis and fragility for the vulnerability analysis.

According to the above, susceptibility is determined solely under the analysis of intrinsic or conditioning factors of the terrain, in addition to climatic factors of the study area that may contribute to the increase or decrease of the threat. For the analysis of mud and debris flows, susceptibility corresponds to physical aspects of the basin such as geology, geomorphology, slopes, and vegetation cover that will be determining factors when determining if a basin has a tendency to present mud and debris flows events and what would be its intensity, likewise its probability of occurrence can be described by means of the conditioning factors such as rain and the return period associated with the thresholds that trigger the events.

1.5.3 VULNERABILITY

According to Law 1523 of 2012, vulnerability refers to:

physical, economic, social, environmental or institutional fragility that a community has to be affected or suffer adverse effects in the event that a dangerous physical event occurs. It corresponds to the predisposition to suffer loss or damage to human beings and their livelihoods, as well as their physical, social, economic and support systems that may be affected by dangerous physical events.

Vulnerability can be understood as the combination of the fragility of the affected territory or community with the exposure of the threatened elements

$$\text{Vulnerability} = \text{Fragility} * \text{Exposure}$$

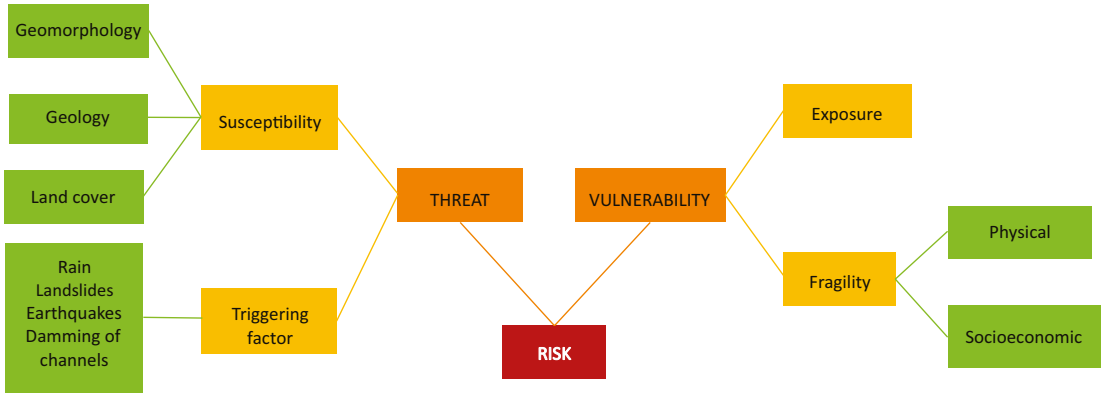
1.5.4 DISASTER RISK

According to Law 1523 of 2012:

corresponds to the potential damages or losses that may occur due to dangerous physical events of natural, socio-natural, technological, bio-sanitary or unintentional human origin, in a specific period of time and that are determined by the vulnerability of the exposed elements; Therefore, disaster risk is derived from the combination of hazard and vulnerability.

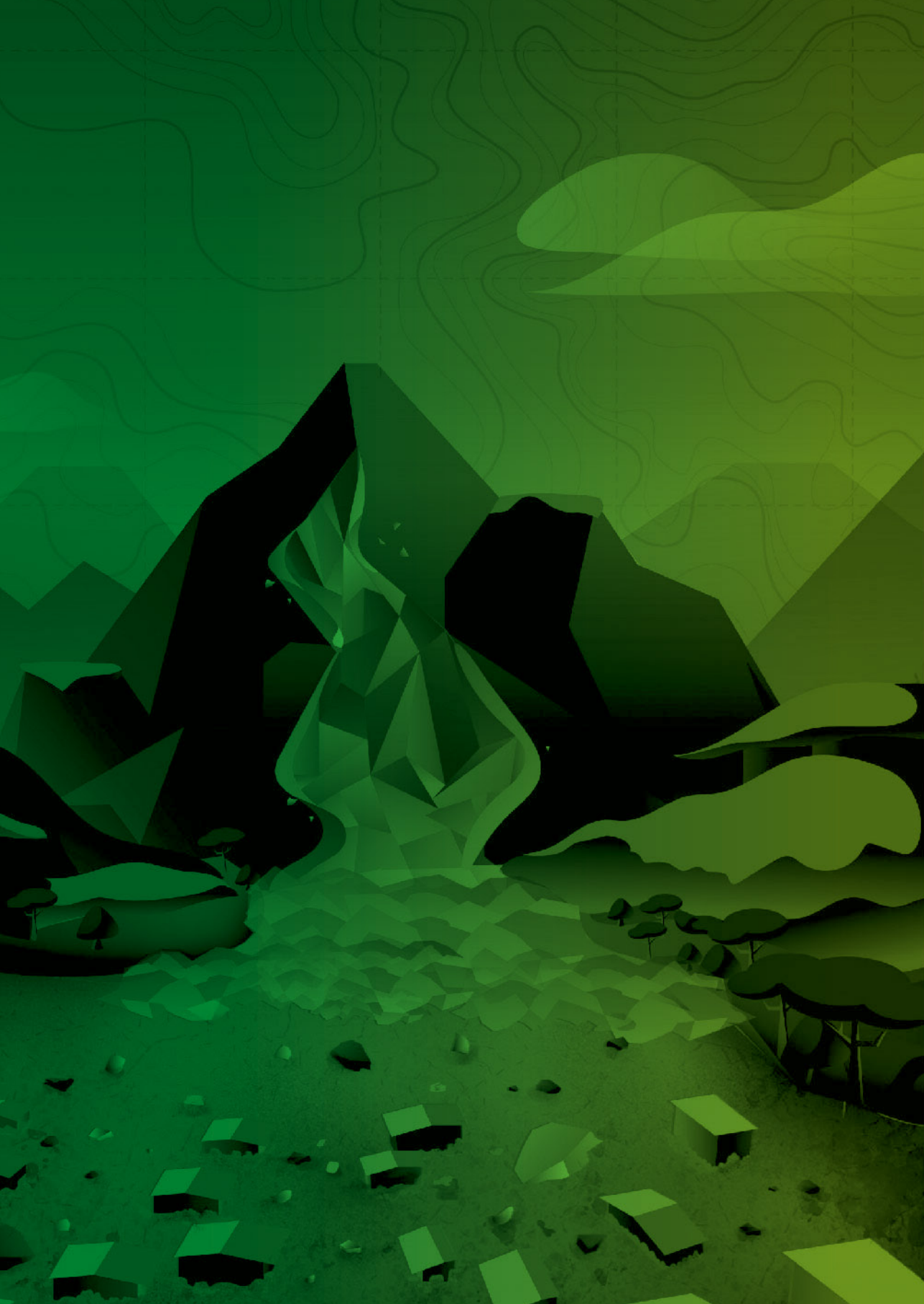
$$\text{Risk} = \text{Threat} * \text{Vulnerability}$$

Figure 13. General mental map for risk assessment due to mud and debris flows



Source: own elaboration.

The definition of susceptibility can be taken from two ways according to which variable is being analyzed, on the one hand when the analysis is carried out vulnerability generally refers to the susceptibility due to exposure, in this sense susceptibility refers to the fragility of the exposed element



**GEOSPATIAL ANALYSIS OF
SUSCEPTIBILITY AND THREAT
FROM TORRENTIAL FLOODS**

The analysis of mud and debris flows can have several approaches, among them is geospatial analysis which is a less detailed analysis that can be used for large areas, for example, in rural soil or in very large basins. Likewise, this analysis can be a preliminary step before modeling, since geospatial analysis allows prioritizing basins for the development of detailed modeling, and many inputs from this analysis are useful for a more complete analysis. Figure 14 presents the step by step to develop the geospatial analysis.

Figure 14. Steps to follow for geospatial analysis of susceptibility and threat from mud and debris flows

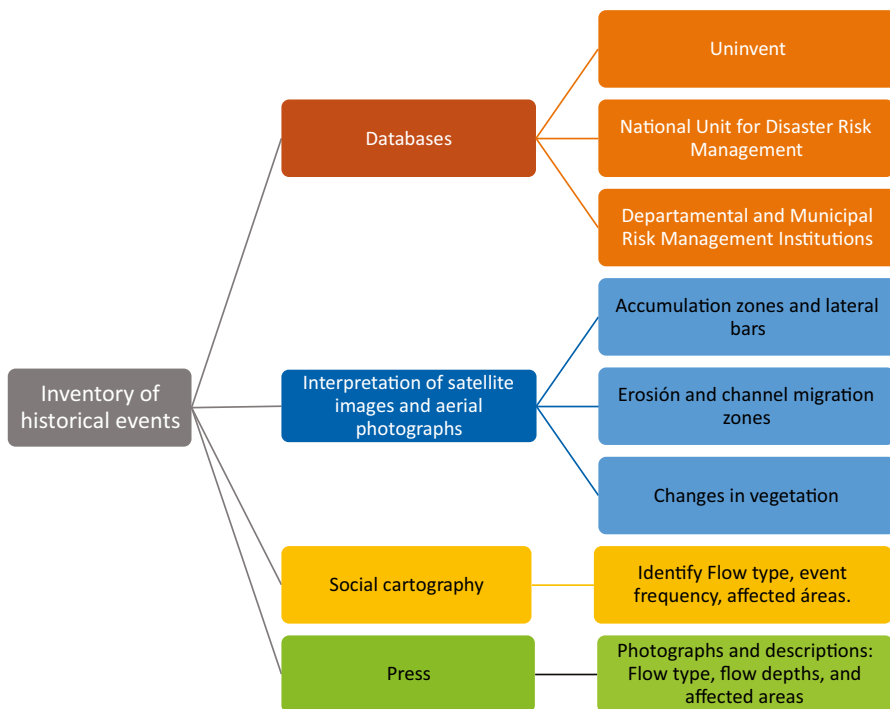
1	Inventory of Historical Events <ul style="list-style-type: none"> • The inventory of historical events must be carried out from unofficial databases, • It must be complemented and corroborated with other sources of information
2	Physiographic characterization of the basin <ul style="list-style-type: none"> • Characterization of relevant physiographic variables such as geology, geomorphology, vegetation cover, among others. • Some morphometric parameters may indicate greater intrinsic fragility of the basin to generate flood events, as well as mass removal processes.
3	Climatic characterization of the basin <ul style="list-style-type: none"> • Analysis of precipitation regime, as well as maximum and minimum events. • Analysis of other climatic variables.
4	Susceptibility analysis <ul style="list-style-type: none"> • Select a methodology to evaluate susceptibility. Mostly taking into account physiographic and morphometric parameters. • Some methodologies include parameter weighting methods and others take into account an analysis of historical events in relation to these
5	Analysis of conditioning factors and threat assessment <p>Depending on the methodology selected for susceptibility analysis, the threat can be estimated as a combination of susceptibility with one or more of the following aspects:</p> <ul style="list-style-type: none"> • Inventory of historical events • Precipitation thresholds that trigger mass removal events

Source: own elaboration.

2.1 INVENTORY OF HISTORICAL EVENTS

The inventory of historical events is a fundamental process for evaluating the risk of mud and debris flows, since it allows us to have an idea of the frequency of occurrence of the events, prioritize the basins that have had historical events of great magnitude and calibrate the basic analyzes or regional and detailed simulation hydraulic models. Figure 15 presents the main sources of information for the analysis of historical events.

Figure 15. *Sources de información para inventario de eventos históricos*



Source: own elaboration.

2.1.1 DATABASES

The primary source of information on historical events corresponds to disaster or emergency response databases. There is the DesInventar tool which is constituted as “a conceptual and methodological development on disasters of all magnitudes and on diversity of environments: local, national and regional” (OSSO Research Group and

LA RED, 2009, p. 4), this is a disaster inventory information collection system, where information on the characteristics and effects of different types of disasters is recorded (Research Group OSSO and LA RED, 2009). The sources of information for the events recorded in DesInventar are of diverse nature, the main ones being the National Unit for Disaster Risk Management, the Regional Autonomous Corporations, the institutions for departmental and municipal disaster risk management and the press.

It is worth clarifying that DesInventar has records of “mud and debris flows” type events, however, the review should not remain exclusively in the databases of this type of events, since in reviews carried out by the authors it is observed that in some cases in the emergency care database of the National Unit for Disaster Risk Management an event is reported as sudden flooding and in DesInventar this same event is reported as “flood” and in other cases as “mud and debris flows.”

Additionally, it is observed that in some cases events such as “flood” have been reported, however, due to the characteristics of the basin or information from other sources it is likely that it was a “mud and debris flows” event, this happens because when the sediment concentration is not high enough to cause a debris flow, the people making the reports or the community in general may confuse the event with a rapid flood.

In accordance with the above, when collecting information from databases it is important to also carefully review the events reported as floods or flash floods since they may actually be mud and debris flows. If possible, the information should be corroborated with other sources and complemented with social cartography and review of photographs of the event.

2.1.2 INTERPRETATION OF SATELLITE IMAGES AND AERIAL PHOTOGRAPHS

The interpretation of satellite images or aerial photographs is carried out in order to identify indicators of mud and debris flows events; it additionally has the following purposes:

- Give an initial idea of what channels can produce mud and debris flows events
- Identify mud and debris flows events that have not been recorded in the databases
- Identify areas that tend to generate erosion processes and mass removal

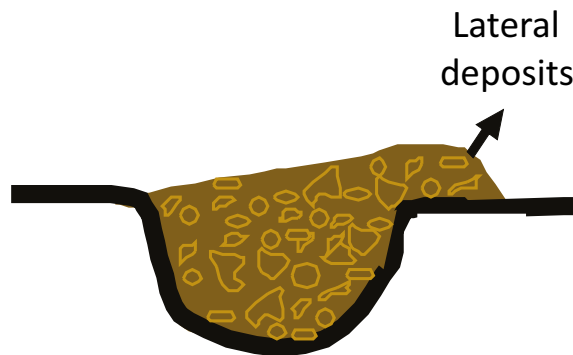
- Identify storage areas
- Give an idea of the magnitude of mud and debris flows events

What to look for in aerial photographs and satellite images?

Mud and debris flows events leave marks that can be easily distinguished through aerial photographs. These marks are related to scars from erosive processes and areas of sediment accumulation, especially when it comes to basins with thick materials. Below are the variables that are indicators of mud and debris flows events:

- Deposits or accumulation areas.
- Deep erosion zones: indicators of landslides or processes in-channel.
- Lateral bars: due to the elevation of the flow in the curves, lateral bars of deposited material are formed as seen in figure 16.
- Changes and damage to vegetation: the passage of coarse sediments can damage surrounding vegetation.
- Widening or migration of the main channel: indicates erosion and sedimentation processes within the channel itself.

Figure 16. *Lateral deposits formed in sludge flows due to elevation in curves*



Source: adapted from Johnson and Rodine (1984).

It is necessary to mention that it is easier to find these indicators in basins where hyperconcentrated flow or debris flow type events occur, since through the satellite image it is possible to observe thick sediments, however, in the case of mud flows it may be difficult to distinguish when an event occurs through aerial photographs, with the exception of erosion zones or landslide marks that can be more easily visualized.

How to photo-interpret satellite images and aerial photographs?

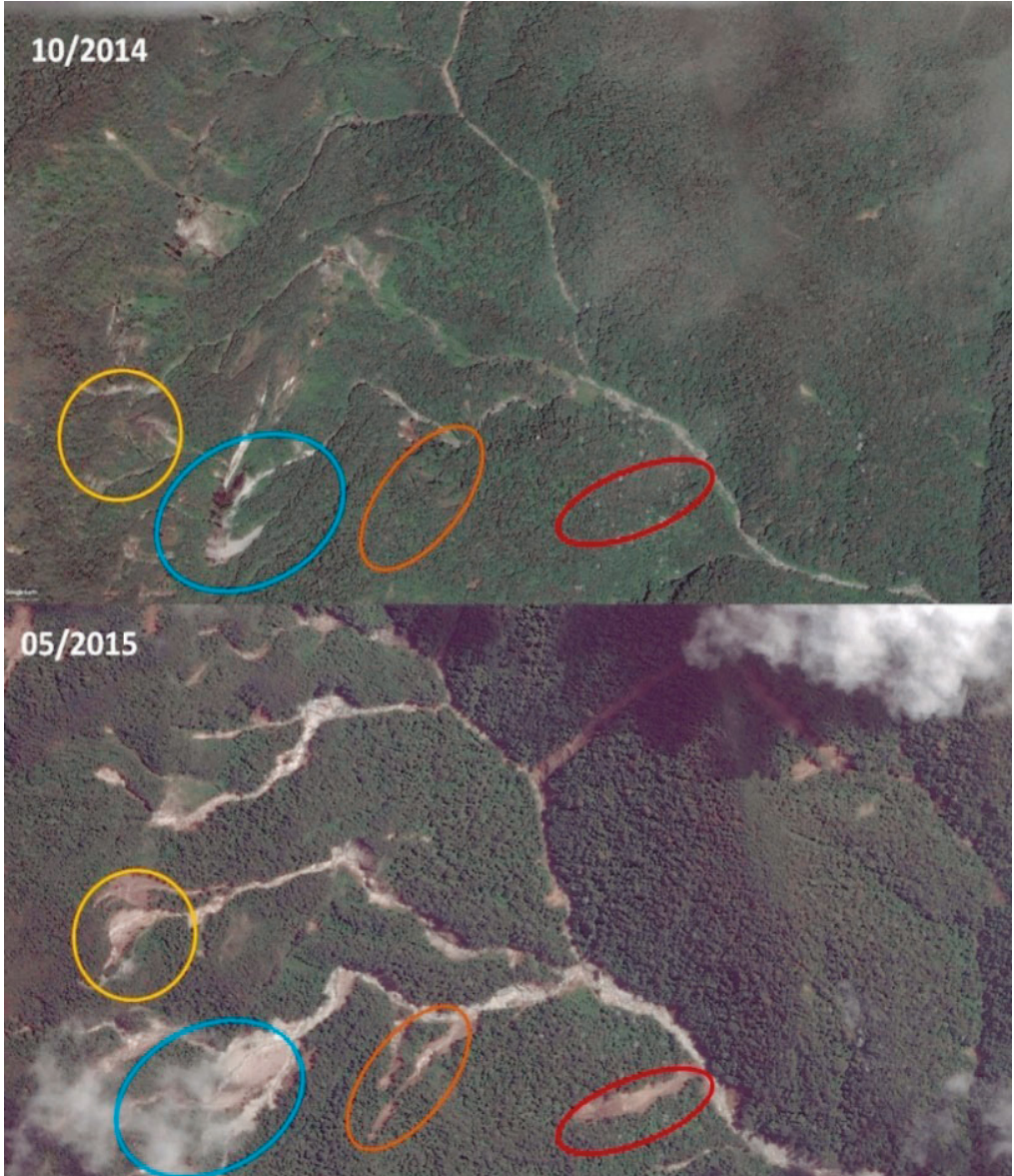
- **Simple observation of digital images:** A simple observation can be made from satellite images or with tools such as *Google Earth*. They can also be compared with cartography and contour lines or montages of photographs on three-dimensional models of the terrain to better visualize the relief.
- **Interpretation of aerial photographs using a stereoscope:** For this analysis, two images of the same area taken from different angles or positions are used. The photographs are arranged separately and are observed at the same time through a stereoscope, in this way a three-dimensional view of the relief is obtained. Normally, this analysis is carried out with printed photographs of flights, however, there is already the possibility of acquiring images from some remote sensors that can be analyzed stereoscopically.

Below are 3 examples of simple observation with Google Earth looking for indicators of mud and debris flows events.

- **Example 1: La Liboriana creek – Salgar, Antioquia**

The first example corresponds to the La Liboriana stream in the municipality of Salgar, Antioquia, the most recent event that was generated in that channel was on May 18, 2015 and the basin probably tends to generate hyperconcentrated flow type events.

Figure 17. Active erosion and mass removal processes in the upper Quebrada Liboriana basin, Salgar, Antioquia



Source: Google Earth.

Figure 18. *Deposits and migration of the La Liboriana creek channel, Salgar, Antioquia*



Source: Google Earth.

Figure 19. Deposits in the form of lateral bars in the curves and widening of the channel in La Liboriana creek, Salgar, Antioquia



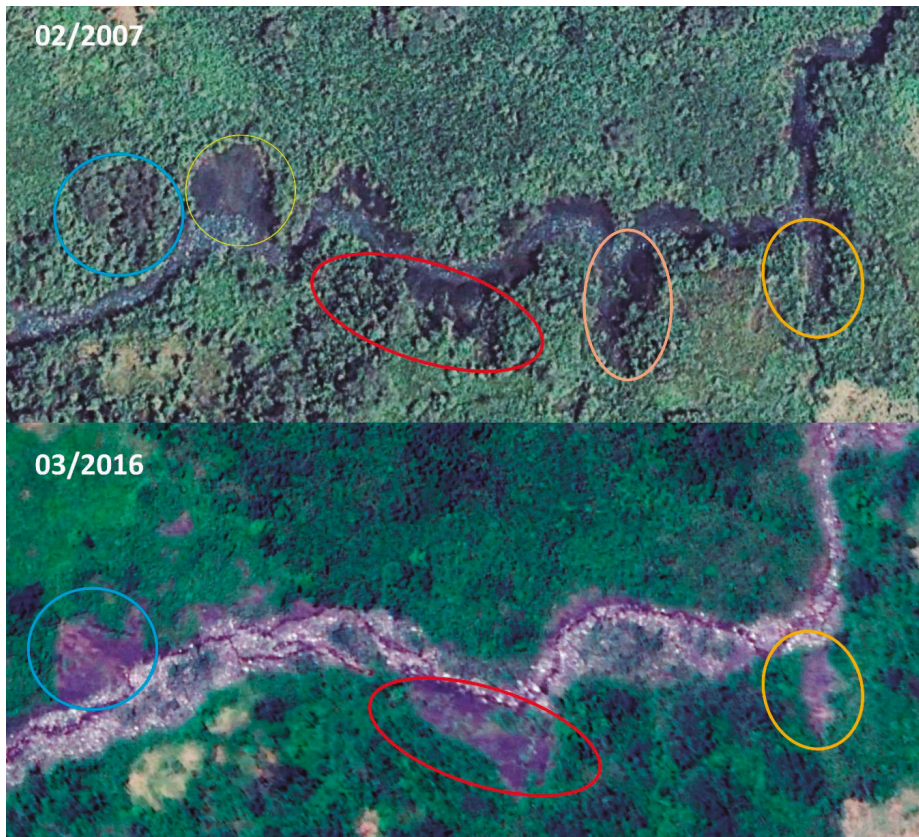
Source: Google Earth.

- **Example 2: La Negra creek - Útica, Cundinamarca**

The second example corresponds to the La Negra stream in the municipality of Útica, Cundinamarca, the most recent event that was generated in this channel was on April 18, 2011. In this basin, sludge flow type events are generated in which the Most of the sediments are fine, silt and clay types, however, they can transport suspended rocks.

In the images, a clear difference is observed in the parent material of the basin, which corresponds to sedimentary rocks with silt-clay textures in contrast to examples 1 and 3 that correspond to sandstones and gravels.

Figure 20. Active erosion and mass removal processes in the upper La Negra creek basin, Útica, Cundinamarca



Source: Google Earth.

Mud and debris flows events leave marks that can be easily distinguished through aerial photographs, these marks are related with scars from erosive processes and areas of sediment accumulation

Figure 21. *Widening of the La Negra creek channel, Útica, Cundinamarca*



Source: Google Earth.

Figure 22. *Lateral deposits and migration of the La Negra creek channel, Útica, Cundinamarca*

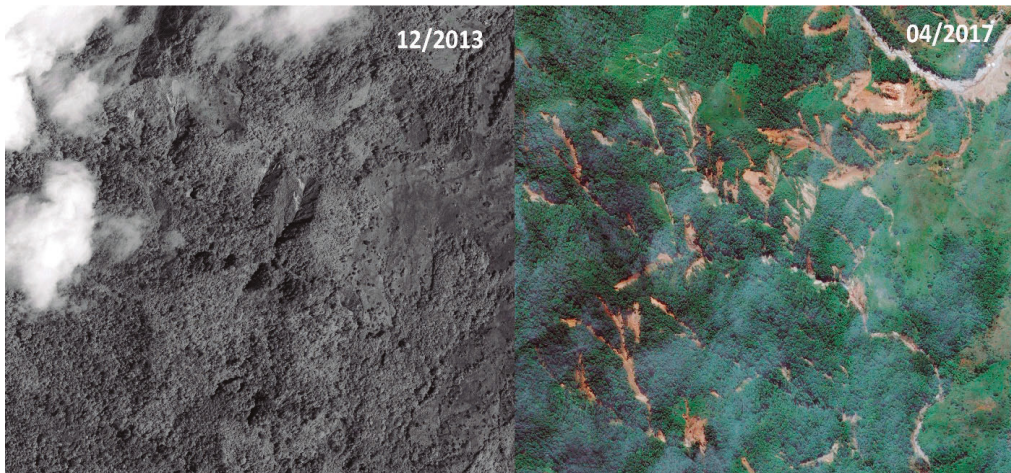


Source: Google Earth.

- **Example 3: Taruca creek, Sangoyaco river - Mocoa, Putumayo**

The third example corresponds to the Taruca stream and the Sangoyaco River in the municipality of Mocoa, Putumayo, the most recent event that was generated in these channels was on March 31, 2017. In this basin, debris flow type events are generated, in which mostly large rocks and thick sediments are transported.

Figure 23. *Active erosion and mass removal processes of the Sangoyaco River and Taruca Creek, Mocoa – Putumayo*



Source: Google Earth.

Figure 24. *Widening of the Sangoyaco River channel, Mocoa – Putumayo*



Source: Google Earth.

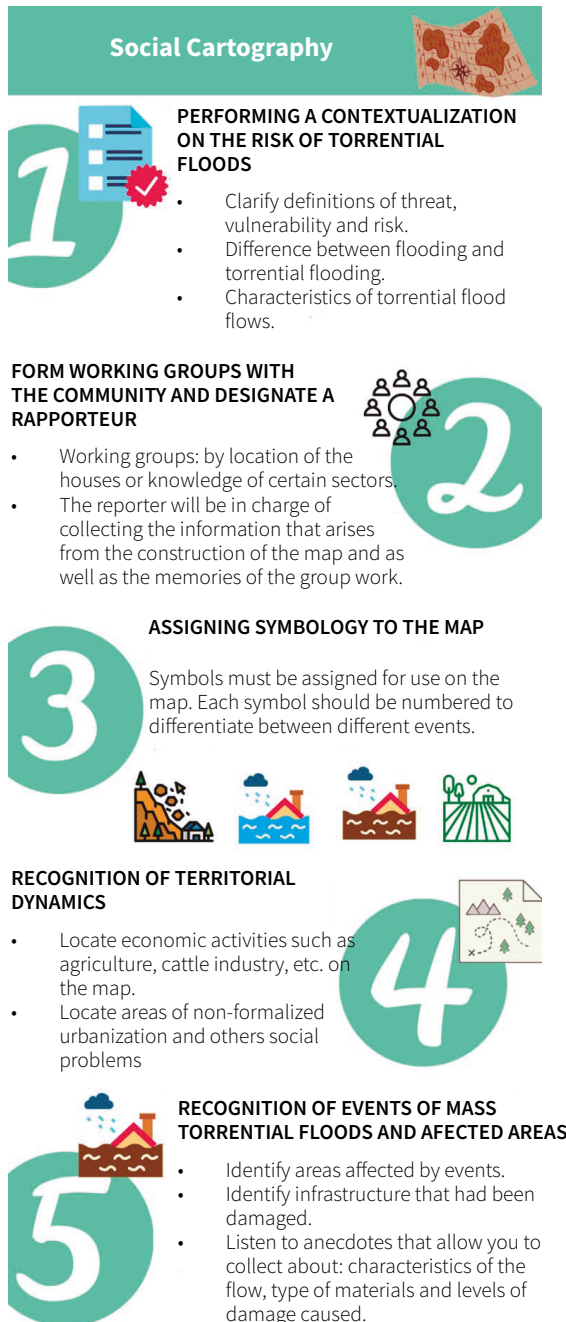
Figure 25. *Sangoyaco River deposits and migration of the Mocoa River channel, Mocoa – Putumayo*



Source: Google Earth.

2.1.3 SOCIAL MAPPING

Social cartography is a participatory research method, in which reality is constructed based on people's experiences, taking into account their socio-cultural context; It is a participatory territorial planning process, in which the inhabitants themselves rethink the territory from the map they make. The method consists of generating work groups with the communities in such a way that they identify on a map the areas affected by mud and debris flows and other events, as well as the characteristics and frequency of historical events. It is important, when carrying out this exercise, to clarify very well to the community the differences between a mud and debris flows and a flood, as well as their characteristics, so that the events are more easily identified. Figure 26 presents an infographic with the basic steps to carry out a social mapping exercise.

Figure 26. Infographic basic steps to develop social cartography

Source: own elaboration.

2.2 PHYSIOGRAPHICAL CHARACTERIZATION OF THE BASIN

2.2.1 LAND COVER

Changes in land cover can be conditions for the generation of mass removal processes that contribute sediments or generate damming in high mountain channels and that in turn trigger mud and debris flows. Land cover acts on the stability of slopes from two points of view: firstly, due to mechanical effects, due to the rooting and anchoring of the soil to more stable underlying strata and the control of water and wind erosion; and, secondly, due to the hydrological effect, due to rain interception, infiltration capacity, moisture retention in the soil and evapotranspiration (SGC, 2017).

Land cover maps are developed using the Corine Land Cover methodology, which corresponds to a methodology that identifies the earth's surface from the interpretation of remote sensing images. This methodology was adapted for Colombia by IDEAM (2010) and covers five large categories: artificialized lands, agricultural territories, forests and semi-natural areas, humid areas and water surfaces, which in turn are subdivided into several categories from level 2 to level 5 (SGC, 2017).

In line with the above, Table 8 presents the land cover categories that are used by the Colombian Geological Service (SGC) for the analysis of susceptibility due to mass movements and that can also be used for the analysis due to mud and debris flows. However, according to the level of detail and scale being worked on, the adaptation of the Corine methodology can be used IDEAM Land Cover (2010) to analyze the land cover of the study basin.

Table 8. Legend Corine Land Cover for susceptibility analysis due to movements, mass and mud and debris flows

Level 1	Level 2	Level 3	
1. Artificialized territories	1.1	Urbanized areas	
	1.2	Industrial or commercial areas and communication networks	
	1.3	Mining extraction areas and waste dumps	
2. Agricultural territories	2.1	Transitional crops	
	2.2	Permanent crops	
	2.3	Pastures	
	2.4	Heterogeneous agricultural areas	
3. Forests and semi-natural areas	3.1	3.1.1	Natural
		3.1.2	Seminatural
		3.1.3	Forest plantation
	3.2	3.2.1	Grassland
		3.2.2	Bush
		3.2.3	Secondary or transition vegetation
	3.3	3.3.1	Rock outcrops
		3.3.2	Bare lands and degraded
		3.3.3	Burned areas

Level 1	Level 2	Level 3
4. Wet areas	4.1 Continental humid areas	
5. Water surfaces	5.1 Natural continental waters	
	5.2 Artificial continental waters	
	5.3 Maritime waters	

Source: SGC (2017).

2.2.2 GEOLOGY

Geology is also a conditioning factor for the generation of mass movements that in turn trigger mud and debris flows. Likewise, depending on the lithology of the basin and the channel bed, sludge, hyperconcentrated or debris type flows will be generated; Therefore, the characterization of the geology is a fundamental element for the analysis of the threat caused by mud and debris flows.

The geological maps used for the analysis of the threat from mud and debris flows must include engineering aspects, which show information on the distribution and physical and mechanical properties of the soil, rocks and groundwater, among them they differentiate materials between soils and rocks, define soil thicknesses and structural characteristics of the rock and characterize the mechanical properties of the soils (SGC, 2016).

To prepare the geology map, materials must initially be classified according to their origin in surface geological units (UGS); UGS refer to the material exposed on the surface of the ground and that preserves the same origin, physical and geomechanical characteristics up to a few tens of meters below the surface.

Rocks are classified according to their mineralogical composition, degree of weathering, hardness, and resistance index; while soils are classified by their origin, mineralogical composition, genetic classification, structure, gradation, color, shape, particle composition, degree of weathering, consistency, moisture retention, relative density, compactness, among others (SGC, 2017). Table 9 presents the superficial geological units according to the modification made by the SGC (2017) for the units proposed by Hermelin (1985).

Once the initial classification is made by the origin of the UGS, the map must be complemented by including the lithological and stratigraphic characteristics, as well as the basic geomechanical characteristics. The criteria that must be included in the geological maps to be used are the following::

- **Genesis:** classification according to origin (table 9).
- **Lithology:** mineralogical composition (texture).
- **Engineering properties:** hardness, strength, consistency, humidity condition, relative density and compactness.
- **Geomechanical properties:** quality indices of the rock massif, geological resistance index.
- **Degree of weathering:** qualitative description of weathering and discontinuities (residual, decomposed soil, weathered rock, fine saprolite, etc.).
- **Structural features:** faults, joints, folds and fractures.

Geological maps used for threat analysis from mud and debris flows must include engineering aspects, which show information about the distribution and physical properties and mechanics of soil, rocks, and underground water

Table 9. *Surface geological units (UGS)*

Material type	Origin of the UGS		UGS Type
Rock	Unaltered rock		Hard rock intermediate rock soft rock
Floor	Rock derivatives <i>on site</i>		Residual soil: coarse saprolite and fine saprolite
	Transported soil	Deposits volcanic primary	Pyroclastic flows, pyroclastic surge and pyroclastic falls
		Depósitos volcánicos secundarios	Lahar and debris avalanche
		Alluvial deposits	Recent floods and active channel Floodplain Alluvial fans or cones Alluvial terraces Fluviotorrential deposits
		Lake and paludal deposits	Fluviolacustrine soils Paludal soils

Material type	Origin of the UGS		UGS Type
Floor	Transported soil	Coastal deposits	Deltas, bars and beaches
		Wind deposits	Dunes and dunes Loess
		Glacial deposits	Moraines and tillites Fluvioglacial soils
		Gravity tanks and hillside	Colluvial Talus, debris earring Mud, soil and debris flows
		Anthropic deposits	Garbage landfills Rubble fills Mixed fillings

Source: SGC (2017).

2.2.3 GEOMORPHOLOGY

Geomorphological analysis is one of the fundamental tools for evaluating susceptibility to mud and debris flows, since these events tend to occur in steep basins with certain characteristics such as high slopes or flattened shapes, among others. Different aspects must be analyzed, such as morphogenesis, morphodynamics, both of the basin in terms of mass movements, and of the channel in terms of fluvial dynamic processes and finally morphometry, which through quantitative indices allows describing the land forms.

2.2.3.1 Morphogenesis

Morphogenesis corresponds to the origin of geofoms and in turn indicates endogenetic and exogenetic processes that gave rise to them. According to the above, a geofom map must be generated that includes morphogenesis and the geomorphological subunit or geofoms for the entire study basin. According to the *Methodological guide for threat zoning due to mass movements at a scale of 1:25,000* (SGC, 2017) Table 10 shows the geofoms that are indicative of mass movements and generation of mud and debris flows.

Table 10. *Subunits indicative of mass removal processes and mud and debris flows type processes*

Morphogenesis	Geomorphological subunit	Indicative
Morphostructural	Structural hill	Fall-type mass movements
	Structural hill	
	Fault Line Escarpment	
	Structural plateau escarpment	
	Triangular facet	
	Counterslope	
	Homoclinal mountain range counterslope slope	
	Counterslope slope of anticline mountain range	
	Counterslope slope of syncline mountain range	

Morphogenesis	Geomorphological subunit	Indicative
Morphostructural	Slope Counterslope Slope	Fall-type mass movements
	Backbone Counterslope Slope	
	Structural plateau	
	Homoclinal mountain range structural slope	
	Structural slope of anticline mountain range	
	Structural syncline mountain slope	
	Structural slope slope	
	Structural backbone slope	
	Iron	
	Structural bar saw	
Volcanic	Lava flow escarpment	Fall-type mass movements
	Volcanic slope	Sediment contribution areas in mud and debris flows
	Laharic cone	
	Terraced Laharic Flow Escarpment	
	Terraced pyroclastic flow scarp	
	Terraced lahar flow	

Morphogenesis	Geomorphological subunit	Indicative
Volcanic	Terraced pyroclastic flow	Sediment contribution areas in mud and debris flows
	Lahar flow lobe	
	Pyroclastic flow lobe	
Denudational	Debris flow cone	Fall-type mass movements
	Talus cone	
	Remnant or relict hill	
	Major erosion scarp	
	Minor erosion scarp	Flow or mud and debris flows type processes
	Faceted scarp	
	Undifferentiated flow cone or lobe	
Fluvial	Debris avalanche lobe and cone	Fall-type mass movements
	Rock Avalanche Lobe and Cone	
	River fan escarpment	Sediment contribution areas in mud and debris flows
	Erosion terrace escarpment	
	Albardones or natural dike	
	Fluvial	Shore complex
Confined floodplain		
Plane or flood plain		

Morphogenesis	Geomorphological subunit	Indicative
Fluvial	Accumulation terrace	Sediment contribution areas in mud and debris flows
	Accumulation terrace escarpment	
	Subcrescent accumulation terrace	
	Old accumulation terrace	
	Flood plane	
	Alluvial fan	Flow or mud and debris flows type processes
	Ancient alluvial fan	
	Subcrescent alluvial fan	
	Current alluvial fan	
	Incised alluvial fan	
	Undifferentiated coalescent alluvial fans	
	Dejection cone	
Coastal marine	Cliff	Fall-type mass movements
Glacial	Counterslope slope of glaciated homoclinal mountain range	Fall-type mass movements
	Counterslope slope of glaciated anticline mountain range	
	Counterslope slope of glaciated syncline mountain range	

Morphogenesis	Geomorphological subunit	Indicative
Glacial	Counterslope slope of glaciated structural slope	Fall-type mass movements
	Counterslope slope of glaciated spine	
	Structural slope of glaciated homoclinal mountain range	
	Structural slope of glaciated anticline mountain range	
	Glaciated structural slope slope	
	Structural Glaciated Backbone Slope	
	Gelifraction cone and lobe	Sediment contribution areas in mud and debris flows
Glaciofluvial cones		
Glaciated volcanic flow		
Karst	Karst escarpment	Fall-type mass movements
Anthropogenic	Quarries	Fall-type mass movementsS
	Mining exploitation	

Source: SGC (2017).

2.2.3.2 Basin morphodynamics

Morphodynamics studies the processes that affect geofoms and corresponds to exogenous dynamics related to wind, water, snow and gravity. Morphodynamics allows identifying the evolution of denudational processes such as erosion and mass removal processes; Likewise, it allows these movements to be classified. The general classification of mass removal movements is presented below:

- Falls.
- Overturns
- Rotational slides.
- Translational landslides.

- Reptation.
- Lateral spread.

On the other hand, erosion is a process of continuous and selective loss of materials caused by natural agents such as water, melting glaciers and anthropic forces. Erosive processes can be classified according to the following:

- Lamellar erosion
- Erosion in furrows.
- Canyons.
- Gullies.
- Undermining.
- Bad lands.
- Terraces.
- Wind erosion.
- Glacial erosion.
- Karst erosion.
- Marine erosion.

2.2.3.3 River morphodynamics and morpho evolution

On the other hand, the morphodynamics and morphoevolution of the channels can be described, which generates shapes and patterns, some of them are indicative of scour, flooding and flood processes. Table 11 shows the fluvial forms associated with floods and mud and debris flows according to Díez-Herrero et al. (2008).

Table 11. *Classification of fluvial forms associated with floods and mud and debris flows*

Flat	Mesoform	Microform or action		
Pattern	Straight channels	Channels for rectification		
	Meandriform canals	Intertwined channels		
		Arches of meander monitored by	Extension	
			Rotation	
			Translation	
		Arches of meander abandoned by	Shortening	
			Constriction	
			Avulsion channels	
Intertwined channels	High entanglement channels			
Anastomosing canals	High anastomosing channels			
Profile	Uniform	Flat beds		
		Rapid		
		Steps		
	Irregular	Wells	Wells and fords	
			Wells at the foot of the waterfall	
			Stepped wells	

Flat	Mesoform	Microform or action	
Cross section erosive forms	Macroforms (>Dc)	Internal or interior channels	
		Canyons	
		Widening of scarps on shore banks	
	Mesoforms >(m)	Polished and polished surfaces	Polished surfaces
			Faceted blocks
		Bout excavations	Semilunars
			Giant kettles
		Reinforced surfaces	
	Microforms (<m)	Grooves	
		Microfacets	
		Transverse shapes	
		Flute brands	
		Boot cavities	
		Microstreaks	
		Micro Kettles	
		Erosive scarps	

Flat	Mesoform	Microform or action		
Depositional forms	Microforms (<dm)	Curls		
		Linear tank	Adhering slime lines	
			Floating bands	
		Desiccation cracks		
	Mesoforms (>dm) and macroforms (<Dm)	Bars and banks	Lateral	Longitudinal
				Meandering
			Means and diagonals	Longitudinal
				Transverse
		Obstacle	Semilunars	
			Natural dikes	Linear
		Digitized		
		Dunes and mega curls	Straight crest	
			Wavy crest	
		Mantles and sheets		
	Lobes, spills and cords	Fanned		
		Elongated		
	Fans and cones	Confluence of tributaries		
Mouth				

Source: Díez-Herrero et al. (2008).

2.2.3.4 Morphometry

Morphometry is the part of geomorphology that quantitatively analyzes the surface, in terms of discrete and continuous features of the landforms (SGC, 2017). The relief, due to its arrangement and orientation, can generate meteorological situations that favor intense or abundant rainfall, as is the case of basins bordered by mountainous areas that generate orographic effects; these basins tend to more easily generate mud and debris flows events. On the other hand, the layout of the basin, such as its elongation and direction, can enhance this precipitation (Díez-Herrero et al., 2008).

Additionally, the geomorphology of the basin in terms of its slope, elongation, compactness, among others, influences the transformation of rainfall into runoff, the concentration time and therefore the flow hydrographs, in such a way that for each rainy conditions, one basin may behave differently from another and may or may not produce mud and debris flows events (Díez-Herrero et al., 2008). Below, the most relevant morphometric parameters are presented when analyzing the susceptibility of a basin to mud and debris flows.

2.2.4 DRAINAGE AREA

The drainage area corresponds to the horizontal projection of the area that collects the runoff that reaches a channel. The drainage area is delimited according to the following criteria (Ruiz and Torres, 2008).

- The watershed must cut the contour lines perpendicularly.
- The watershed must pass through the points of highest topographic level.
- The watershed cuts the contour lines on their convex side.
- The watershed can never cut a drainage, except at the point of exit from the basin.

2.2.5 MAXIMUM, AVERAGE, AND MINIMAL ELEVATION

The maximum elevation corresponds to the highest elevation of the basin, which is usually found near the watershed, the average elevation corresponds to the average elevation of the entire basin in masl, while the minimum elevation corresponds to the lowest elevation of the basin, which is usually found near the mouth or confluence with another channel or outlet of the basin.

2.2.6 AVERAGE SLOPE OF THE BASIN

The average slope of the basin corresponds to the variation in the inclination of the land with respect to the horizontal; this determines the behavior of water movement and its erosion capacity. Additionally, the average slope of the terrain directly includes the concentration time and the formation time of floods and floods. The basins can be classified according to the slope from flat to very steep relief according to what is presented in table 12.

Table 12. *Relief according to the average slope*

Average slope (%)	Relief
0 – 3	Flat
3 – 7	Mild
7 – 12	Moderately rugged
12 -20	Hilly
20 – 35	Heavily crashed
35 – 50	Very heavily rugged
50 – 75	Steep
>75	Very steep

Source: Pérez (1979).

2.2.7 AVERAGE SLOPE OF THE WATERWAY

The average slope of the main channel can be calculated with different equations, one of the most used is presented here, corresponding to the Taylor method, in which the weighted average slope is calculated according to the slope and length of several sections.

$$S_o = \left(\frac{L}{\sum_{i=1}^n \frac{L_i}{\sqrt{S_i}}} \right)^2$$

S_o = Average slope (m/n)

L = Total length of the channel (m)

L_i = Section length (m)

S_i = Slope of the section (m)

2.2.8 STREAM LENGTH AND MAXIMUM STREAM LENGTH ROUTE

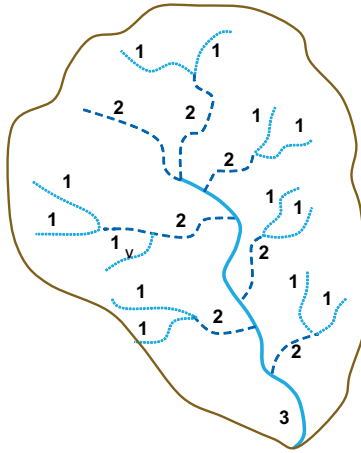
The length of the stream corresponds to the length of the main channel, while the maximum length of the path corresponds to the maximum length that a drop of water travels until it reaches the mouth or outlet of the basin, that is, the longest possible length of route, this is used to calculate the concentration time.

2.2.9 CURRENT ORDER

The current order indicates the degree of structure of a drainage network; the higher the order of the current, the more structured and defined it will be. This parameter could also indicate the presence of structural controls and a greater possibility of erosion or a more eroded basin that would also indicate greater age.

One of the most used methods is the Horton – Strahler method, which indicates that the smallest current that does not have tributaries is of order n and as a current of order n converges with another of order not of order $n+1$, the resulting current will be of order $n+1$, as seen in figure 27.

Figure 27. *Order of currents Horton–Strahler method*



Source: own elaboration.

2.2.10 DRAINAGE DENSITY

Drainage density corresponds to the total length of the channels in a basin and its drainage area.

$$D = \frac{L_T}{A_\Omega}$$

L_T = Current length

A_Ω = Area of the boundary of order Ω (Km²)

2.2.11 COMPACTNESS INDEX

The compactness index or Gravelius index is a dimensionless parameter that relates the perimeter of the basin to the perimeter of a circle of equal area to that of the basin. This parameter describes the geometry of the drainage area and is closely related to the concentration time. This parameter takes a value of 1 for exactly circular basins and the smaller the volume, the greater the tendency to concentrate large amounts of water or in shorter times. For this parameter, three categories are defined, presented in table 13.

$$K_c = \frac{\text{Perímetro}}{2\pi * \left(\frac{\text{Área}}{\pi}\right)^{\frac{1}{2}}}$$

Table 13. Description by compactness index ranges K_c

K Rank _c	Description
1 – 1,25	Shape almost round to oval – round
1,25 – 1,5	Oval – oblong shape
>1,5	Shape oval – oblong to rectangular – oblong

Source: own elaboration.

2.2.12 HORTON FORM FACTOR

This factor indicates how elongated a basin is and relates the drainage area to the square of the maximum run length. This parameter measures the tendency of the basin towards very intense rapid and slow floods or slow and sustained floods.

$$K_f = \frac{A}{L^2}$$

A = Basin area (Km^2)

L = Maximum travel length (Km)

Table 14. Range Description Form Factor K_f

Range K_f	Shape	Susceptibility to floods torrential
<1	Elongated basin	Low

Range K_f	Shape	Susceptibility to floods torrential
=1	Square basin	Average
>1	Flattened basin	High

Source: own elaboration.

2.2.13 ELONGATION RATIO

The elongation ratio is the relationship between the diameter of a circle that has the same surface or drainage area of the basin and the maximum path length. This relationship indicates whether the basin is completely flat or has areas of pronounced relief.

$$Re = \frac{1.128\sqrt{A}}{L}$$

A = Basin area (Km^2)

L = Maximum travel length (Km)

Table 15. *Description elongation ratio ranges*

R Ranke _e	Description
0.8 - 1	Completely flat
≤0.8	Parts of pronounced relief

Source: own elaboration.

2.2.14 MELTON INDEX

The Melton index corresponds to the relationship between the maximum difference in heights in the basin and the area of the basin, it is also called ruggedness number and is a way to represent the average slope of the basin. A basin tends to be torrential if the Melton index is greater than 0.5 (Melton, 1965).

$$\text{Melton index} = \frac{H_{\text{máx}} - H_{\text{mín}}}{\sqrt{A}}$$

2.2.15 TORRENCIALITY COEFFICIENT

This coefficient corresponds to the relationship between the number of channels of order one and the area of the basin, the greater the number of channels and the smaller the area, the greater the torrentiality of the basin, because the water travels short distances until it heads to the currents. main and the download speed is greater (Romero and López, 1978).

$$Ct = \frac{N_t}{A}$$

A = Basin area (Km^2)

N_t = Number of streams of order one

2.2.16 LEMNISCATA RADIO

The lemniscate radius is a proportion that indicates how close the shape of the basin is to that of a lemniscate, which according to Chorley (1957) is the ideal shape of a basin, the graphical Representation of this curve generates a similar figure. to the infinity symbol. This radius is another way to represent the average slope of the basin.

$$\text{Lemniscate radius} = \frac{L_b^2 * \pi}{4 A}$$

Where:

L_b = Basin length

A = Basin area (Km^2)

2.2.17 CONCENTRATION TIME

The concentration time corresponds to the time in which the entire basin is contributing runoff simultaneously, that is, the time it takes for the furthest drop to reach the basin outlet. This generally depends on the maximum length of the route and the slope; it is expected that the maximum flow rates will occur at this time. Below are some of the equations used for the calculation of concentration time.

Temez equation:

$$T_c = 0.3 \left(\frac{L}{S_o^{0.25}} \right)^{0.75}$$

Kirpich equation:

$$T_c = 0.066 \left(\frac{L}{S_o^{0.5}} \right)^{0.77}$$

Giandioti equation:

$$T_c = \frac{4\sqrt{A} + 1.5L}{25.3\sqrt{L S_o}}$$

Ven T Chow equation:

$$T_c = 0.8773 \left(\frac{L_c^{1.5}}{\sqrt{C_m - C_b}} \right)^{0.64}$$

Where:

T_c = Concentration time (**hrs**)

L = Maximum travel length (**Km**)

S_o = Average slope (**m/m**)

A = Basin area (**Km²**)

L_c = Length of the main channel (**m**)

C_m = Maximum elevation of the main channel (**msnm**)

C_b = Minimum elevation of the main channel (**msnm**)

2.2.18 VULNERABILITY INDEX TO TORRENTIAL EVENTS (IVET)

The vulnerability index to torrential events (IVET) is an index generated by the IDEAM, which relates the morphometric index of torrentiality and the flow variability index and actually corresponds to a susceptibility index of the basin (see definitions in the numeral 1.5.2 of this document).

The morphometric index of torrentiality is constructed as a relationship between the compactness index, the average slope of the basin and the drainage density, which indicate the way in which the runoff is concentrated, as well as the speed with which the water and the Sediments leave the basin after a rain event (Rivas et al., 2009).

To determine this index, a value from 1 to 5 is assigned to each evaluated parameter (drainage density, average slope of the basin and compactness coefficient) and subsequently the values for each parameter are crossed and the category of the morphometric index of torrentiality is determined. , which is qualitative from very low to very high. Table 16 shows the categories for each parameter evaluated and Table 17 shows the categories for assigning the morphometric index of torrentiality.

The vulnerability index to torrential events (IVET) is an index generated by IDEAM, which relates the morphometric index of torrentiality and the flow variability index.

Table 16. Relationships to categorize the morphometric index

Morphometric index	Scale	Basin area (km ²)	Categorie				
			1	2	3	4	5
Drainage density (km/km ²)	1:10000	<15	<1.5	1.51 – 2.0	2.01 – 2.50	2.51 – 3.00	>3.0
	1:25000	16 – 50	<1.2	1.21 – 1.80	1.81 – 2.00	2.01 – 2.50	>2.5
	1:100000	>50	<1.0	1.01 – 1.50	1.51 – 2.00	2.01 – 2.50	>2.5
	Category name		Low	Moderate	Moderate high	High	Very high
Elevation average of the basin (%)	1:10000	<15	<20	21 – 35	36 – 50	51 – 75	> 75
	1:100000	>50	<15	16 – 30	30 – 45	46 – 65	>65
	Category name		Accident-given	Strong	very strong	Steep	Very steep
Coefficient of compactness			<1 625	1,376 – 1,500	1,251 – 1,375	1,126 – 1,250	1.00 – 1,125
Category name		Oval-oblong to rectangular-oblong		Oval-round to oval-oblong		Almost round to oval-round	

Source: Rivas et al. (2009).

Table 17. *Categories morphometric index of torrentiality*

		Average basin slope						
		1	2	3	4	5		
Drainage density	1	111	121	131	141	151	1	Shape coefficient
		112	122	132	142	152	2	
		113	123	133	143	153	3	
		114	124	134	144	154	4	
		115	125	135	145	155	5	
	2	211	221	231	241	251	1	
		212	222	232	242	252	2	
		213	223	233	243	253	3	
		214	224	234	244	254	4	
		215	225	235	245	255	5	
	3	311	321	331	341	351	1	
		312	322	332	342	352	2	
		313	323	333	343	353	3	
		314	324	334	344	354	4	
		315	325	335	345	355	5	
	4	411	421	431	441	451	1	
		412	422	432	442	452	2	

		Average basin slope										
		1	2	3	4	5						
Drainage density		413	423	433	443	453	3	Shape coefficient				
		414	424	434	444	454	4					
		415	425	435	445	455	5					
	5	511	521	531	541	551	1					
		512	522	532	542	552	2					
		513	523	533	543	553	3					
		514	524	534	544	554	4					
		515	525	535	545	555	5					
		Very low		Low		Moderate			High		Very high	

Source: Rivas et al. (2009).

On the other hand, the variability index represents the behavior of the flows, determining that a torrential basin is one that presents greater variability or difference between the minimum and maximum flows (IDEAM, 2013). This index is obtained from the flow duration curve and can be expressed as follows:

$$Variability\ index = \frac{Log(Q_i) - Log(Q_f)}{Log(X_i) - Log(X_f)}$$

Q_i and Q_f correspond to the maximum and minimum flows and X_i y X_f to the percentages of respective exceedance taken from the flow duration curve. The categories of the variability index are presented in table 18, while the categories of the vulnerability index to torrential events (IVET) are presented in table 19.

Table 18. *Variability Index Categories*

Variability index	Category
<10	Very low
10,1 – 37	Low
37,1 – 47	Average
47,1 – 55	High
>55	Very high

Source: IDEAM (2013).

Table 19. *Classification of the vulnerability index to torrential events (IVET)*

Variability index	Morphometric index of torrentiality				
	Very low	Low	Average	High	Very high
Very low	Very low	Very low	Average	High	High
Low	Low	Average	Average	High	Very high
Average	Low	Average	High	High	Very high
High	Average	Average	High	Very high	Very high
Very high	Average	High	High	Very high	Very high

Source: IDEAM (2013).

The IVET can be used as an initial step to determine the susceptibility of an extensive basin and select areas with high or very high values to carry out a slightly more detailed analysis; or it can be used as a variable within the multivariate analysis of physiographic variables.

2.3 CLIMATE CHARACTERIZATION OF THE BASIN

The statistical analyzes of the hydroclimatological information allow, on the one hand, to have a baseline of the hydrological behavior of the study basin and, on the other hand, to develop mathematical models that assist in the planning and management of water resources, as well as models that allow determining conditioning factors. of mud and debris flows.

The climate characterization must include a description of the spatial and temporal variability of the climate variables, as well as the analysis of box and whisker plots (box-whisker), which allow identifying anomalous values, as well as the percentiles between which the climatic variables move.

The main source of climate information corresponds to ground stations from IDEAM and environmental corporations, which contain series of continuous records at a monthly, daily and hourly level. However, in some cases in the study area there is not enough information from hydrometeorological stations, so information from remote sensors can be used; It must be clarified that this information must be handled very carefully since the level of resolution and precision will never be the same as that of ground stations.

The fundamental climatic variables that must be analyzed as part of the risk assessment for mud and debris flows correspond to::

- Precipitation: temporal and spatial distribution, homogeneity and maximum precipitation in 24 hours.
- Temperature: temporal and spatial distribution.
- Wind speed: temporal distribution and wind rose.
- Relative humidity: temporal and spatial distribution.
- Potential evapotranspiration: temporal and spatial distribution.
- Real evapotranspiration: temporal and spatial distribution.
- Solar radiation: spatial and temporal distribution.

Some of the remote sensors that contain weather information are the following:

- **Giovanni:** temperature, evaporation, evapotranspiration, radiation, precipitation and daily wind speed <https://giovanni.gsfc.nasa.gov/giovanni/>
- **National Centers for Environmental Prediction (NCEP):** temperature, precipitation, wind speed, relative humidity and daily solar radiation https://lp-daac.usgs.gov/product_search/, <https://earthexplorer.usgs.gov/>
- **MODIS:** potential evapotranspiration every 8 days and radiation https://lp-daac.usgs.gov/product_search/, <https://earthexplorer.usgs.gov/>
- **ERA5 – Copernicus:** temperature, wind speed, radiation, evaporation and monthly precipitation, <https://cds.climate.copernicus.eu/cdsapp#!/dataset/reanalysis-era5-single-levels-monthly-means?tab=form>

2.3.1 PRECIPITATION

Precipitation is the most important climatic variable, since it is one of the main triggers of landslides and mud and debris flows. It is important to carry out the following precipitation analyzes:

- Temporal distribution analysis: with this analysis, the hydrological regime is determined, whether bimodal or unimodal, as well as the dry and wet months. This behavior in the precipitation regime is related to the displacement of the intertropical confluence zone (ITCZ), this is an area of the atmosphere where the trade winds from the north and south of the planet converge, it is characterized by having low pressures and masses. ascending air. This strip passes through Colombia twice a year, the first time in April and May and the second time in September and October, causing the two rainy periods in the bimodal regimes.
- Analysis of spatial distribution: this analysis is carried out through isohyets, which illustrate lines of equal precipitation, this allows preliminary determination of homogeneous areas.
- Analysis of homogeneity between stations: this analysis is carried out to
- determine hydrologically homogeneous zones, which present similar behavior.
- Initially, a simple mass curve analysis is carried out in which the total accumulated precipitation of a station is graphed against time. With this analysis, the consistency of the data can be identified throughout the recording period and thus establish whether the station was moved or if there were significant changes in the hydrological regime.

- Subsequently, a preliminary analysis of homogeneity between stations can be carried out taking into account the following:

$$\text{If} \rightarrow 90\% * P_{\text{Station A}} < P_{\text{Station B}} < 110\% * P_{\text{Station A}}$$

→ Station A and Station B are hydrologically homogeneous

Finally, a double mass analysis must be carried out to confirm which stations are effectively homogeneous with others. To do this, the accumulated precipitation of station A is plotted against the accumulated precipitation of station B. If there are more than two stations, the plot is plotted. on the ordinates the station to be analyzed and on the abscissa the average of the other stations. If the graph presents a linear behavior, it indicates that the stations are hydrologically homogeneous with each other.

- Box and whisker diagrams: this analysis allows the mean and median of the precipitation data to be identified. Additionally, the 25% and 75% percentiles are plotted (boxes), as well as the standard deviation (whiskers) and it is possible to identify *outliers* or anomalous data that may correspond to poorly measured data or extreme events
- Analysis of maximum precipitation in 24 hours and generation of IDF curves:
- to carry out the analysis of maximum precipitation in 24 hours, a frequency analysis must be carried out and the values adjusted to a probability distribution, some of the most used are Weibull, Gamma, Gumbel, Lognormal. Most of the time the data fit well to two or more probability distributions, in these cases you can choose one or you can weight the results by giving greater weight to the one with a lower standard deviation, like this:

$$P_{\text{ponderada}} = \frac{\sum_{i=1}^n P_i * \frac{1}{\sigma_i}}{\sum_{i=1}^n \frac{1}{\sigma_i}}$$

Where:

P_i = Precipitation for the distribution-adjusted return period t

σ_i = Standard deviation associated with P_i

Once the adjustment to the probability distributions is made, maximum rainfall in 24 hours associated with different return periods can be determined, which are the fundamental input for the construction of the IDF curves. These curves are made for each station by adjusting an equation like the one presented below, where the

constants of the equation are found through logarithmic regressions and assuming rainfall distribution coefficients over the 24 hours (Campos, 1978). There are also coefficients determined in studies for different areas of the country

$$I \left(\frac{mm}{hr} \right) = K \frac{T^m}{t^n}$$

Where:

I = Intensity for different durations (mm/h)

T = Return period (years)

t = Duration (minutes)

K, m, n = Constants for each season

2.3.1 POTENTIAL EVAPOTRANSPIRATION

Potential evapotranspiration can be calculated in several ways, the most recommended is the Penman–Monteith equation, although the Food and Agriculture Organization of the United Nations (FAO) made a modification that includes aerodynamic and surface resistance equations. This equation uses as input data the average wind speed, daily hours of sunshine (for radiation calculation), average air temperature and relative humidity, as presented below:

$$ET_o = \frac{0,408 \Delta (R_n - G) + \gamma \frac{900}{T + 273} u_2 (e_s - e_a)}{\Delta + \gamma(1 + 0,34 u_2)}$$

Where:

ET_o = Reference potential evapotranspiration

R_n = Net surface radiation

T = Mean air temperature

u_2 = Average wind speed

e_s = Saturation vapor pressure

e_a = Actual steam pressure

Δ = Vapor pressure curve slope

γ = Psychometric constant

Other equations used are those of Thornthwaite, Christiansen, Linacre, Turc and Hargreaves (Gómez-Blanco and Cadena, 2017).

2.3.3 ACTUAL EVAPOTRANSPIRATION

Potential evapotranspiration corresponds to the maximum value that evapotranspiration can take for reference conditions; however, this considers unlimited availability of water (precipitation), which is not met in dry periods. Due to the above, actual evapotranspiration is not always equal to potential, which is why it is necessary to calculate actual evapotranspiration to obtain a more realistic value in accordance with the limited water availability.

The calculation of real evapotranspiration for the study area was carried out following the Budyko (1974) equation. This equation is used to transform potential evapotranspiration into actual evapotranspiration, taking into account annual ETP and precipitation data over a given area.

$$ETR \left(\frac{mm}{año} \right) = \sqrt{ETP * P * \tanh\left(\frac{P}{ETP}\right) * \left[1 - \cosh\left(\frac{ETP}{P}\right) + \sinh\left(\frac{ETP}{P}\right) \right]}$$

The formulation of the Budyko equation is based on a mass balance considering that an increase in precipitation generates an increase in runoff, while, with a decrease in precipitation, the flow tends to a limit value. Likewise, the final equation considers that in dry conditions $R/p \rightarrow 0$ o $ETR/p \rightarrow \infty$; On the other hand, in humid conditions $ETR \rightarrow ETP$ when $R/p \rightarrow 0$.

2.4 METHODOLOGIES FOR

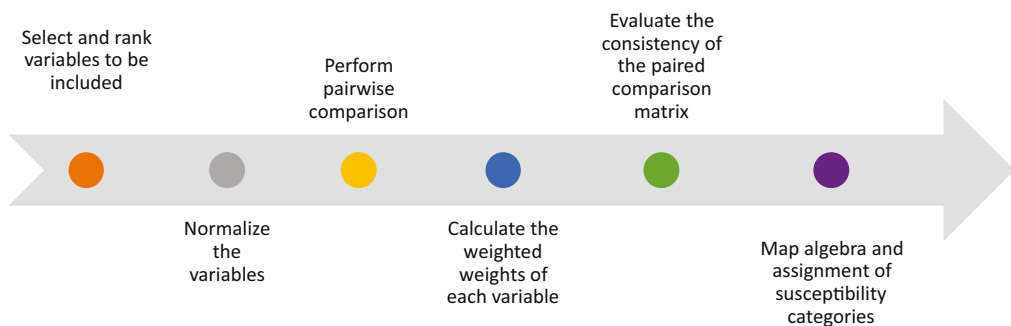
SUSCEPTIBILITY ANALYSIS

2.4.1 MULTIVARIATE ANALYSIS OF PHYSIOGRAPHICAL VARIABLES

The multivariate analysis is based on the method of analytical hierarchies proposed by Saaty (1980), in which weighted weights are assigned to each of the variables, taking into account that not all the variables to be analyzed have the same importance in the susceptibility to mud and debris flows.

The method of analytical hierarchies or AHP allows us to assign weights to variables that are normally ranked and which usually come into conflict. It is recommended, to avoid excessive comparisons, not to take more than 7 different variables. If it is necessary to take more than 7, these can be ranked, at several levels, thereby making a comparison within each level. Once the ranking of the variables is defined, a direct pairwise comparison is carried out between the variables, to determine which of them is more important (Yepes, 2018). Figure 28 presents the general scheme for the development of this methodology.

Figure 28. *Multivariate analysis methodology scheme with Saaty analytical hierarchies*



Source: own elaboration.

2.4.1.1 Selection and ranking of variables to include

The first step is the selection of the variables that will be taken into account in the analysis. The relationship of each of the variables described in section 2.2 with the generation of mud and debris flows (AT) is presented. The evaluator must choose the variables that he considers most relevant or can try several scenarios of selected variables and compare the result.

Table 20. *Relationship of physiographic variables with the generation of mud and debris flows*

Variable	Relationship with generation of mud and debris flows	Variable type	Relationship type
Land Cover	Mechanical effects: The coverage generates rooting and anchoring to the soil; without it, processes of erosion, scour and mass movements can be promoted, which in turn trigger mud and debris flows events.		Qualitative
	Hydrological effects: bare soil or soil with little vegetation cover can alter infiltration and evapotranspiration, which implies greater volumes of runoff contributed to the channel in short periods of time.		

Mud and debris flows are normally generated in very steep areas of slopes and hills.

Variable		Relationship with generation of mud and debris flows	Variable type	Relationship type
Geology		The hardness and weathering of rocks are conditioning factors for the generation of mass movements. Depending on the lithology, different types of mud and debris flows can be generated.	Qualitative/Quantitative	
Geomorphology	Morphogenesis	<p>Mud and debris flows are normally generated in very steep areas of slopes, hills and hills.</p> <p>Additionally, some geoforms may be prone to the generation of damming in the channel that triggers mud and debris flows. Table 10 shows the geoforms indicative of mud and debris flows and mass removal processes.</p>	Qualitative	

Some erosive and depositional patterns and forms of the channels are indicative of generation of mud and debris flows

Variable		Relationship with generation of mud and debris flows	Variable type	Relationship type
Morphometry	Morphodinamica basin	Landslides and erosion of the basin are the main conditioning factors for the generation of mud and debris flows. If mass removal events usually occur in the basin, it can be highly prone to generating mud and debris flows.	Qualitative	The greater the susceptibility to removal events in mass, greater susceptibility at - AT
	River Morphodynamics	Some erosive and depositional patterns and shapes of the channels are indicative of the generation of mud and debris flows (see table 11).	Qualitative	
	Mean basin slope	The slope of the basin indicates whether the relief is steep; mud and debris flows tend to be generated in steep basins with high slopes.	Quantitative	The higher the value greater susceptibility to AT

Some erosive and depositional patterns and forms of the channels are indicative of generation of mud and debris flows

Variable		Relationship with generation of mud and debris flows	Variable type	Relationship type
Morphometry	Slope me-channel day	The slope of the channel will determine the speed with which the flow will move; mud and debris flows tend to occur in channels with relatively high slopes	Quantitative	The older higher value susceptibility to AT
	Composition index peace	The compactness index indicates the shape of the basin, round and flatter basins have shorter concentration times, which implies that the water will leave the basin more quickly, generating events of high volumes of runoff in short periods of time.		
	For-factor Horton's ma	The shape factor indicates whether the basin is flattened, elongated or square; a flattened basin has a greater susceptibility to generating mud and debris flows.		

The compactness index indicates the shape of the basin, round and flatter basins have shorter concentration times

Variable		Relation with the generation of torrential floods	Type of variable	Type of relation
Morphometry	Elongation ratio	A low elongation ratio indicates basins with pronounced relief, these basins may have greater susceptibility to generate torrential flood processes.	Quantitative	The lower the value, the greater the susceptibility to AT
	Melton index	A basin is called torrential if its Melton index is greater than 0.5, it is an indirect measure of the slope of the basin.	Quantitative	The higher the value, the greater the susceptibility to AT
	Torrentiality coefficient	The torrential coefficient indicates the ratio between the number of first-order channels and the area of the basin, the greater this number, the greater its torrentiality since the water travels short distances to the outlet, so its concentration time is shorter.	Quantitative	The higher the value, the greater the susceptibility to AT
	Lemniscate radius	It is a proportion that indicates how close the basin is to the shape of a lemniscate, the higher this value is, the narrower the lemniscate, which implies a more elongated basin.	Quantitative	The lower the value, the greater the susceptibility to AT

Variable		Relationship with generation of mud and debris flows	Variable type	Relationship type
Morphometry	Vulnetability index to torrential events (IVET)	This index directly indicates the ranges for which susceptibility is from very low to very high.	Quantitative	The higher the value greater susceptibility to mud and debris flows

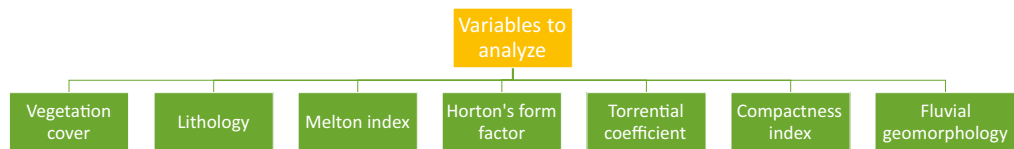
Note: Other variables may be included such as current order, drainage pattern, proximity to currents, USLE erosion, among others, according to what the evaluator considers necessary.

Source: own elaboration.

The analysis can be carried out using one, two or more levels of hierarchy of the variables, that is, if two levels of hierarchy are used, the variables can be grouped, while if a single level is used, all the variables must be taken separately. . An example with one level of hierarchy is presented in Figure 29 and an example with two levels of hierarchy is presented in Figure 30.

If two hierarchical levels are used, the weighted weights must be estimated for each secondary level subgroup and the weighted weights are subsequently estimated for the entire set of variables at the higher level.

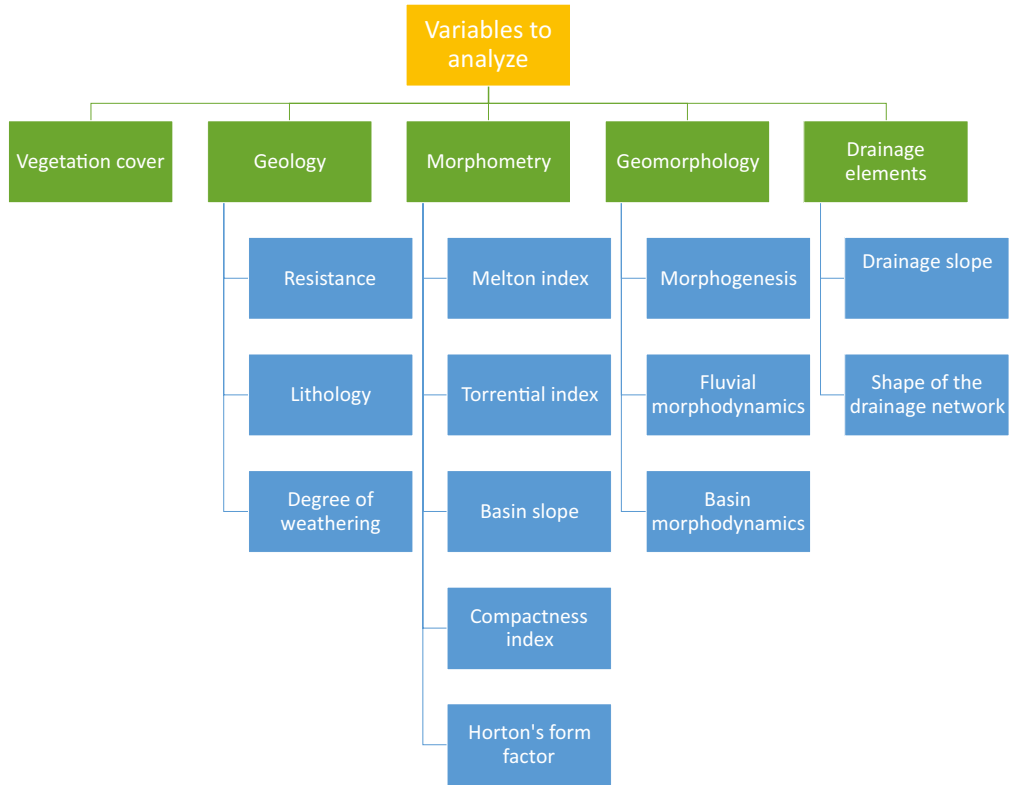
Figure 29. Example of a hierarchy level for variable analysis



Source: own elaboration.

The analysis can be carried out using one, two or more levels of hierarchy of the variables, that is, if two levels of hierarchy are used, you can group the variables

Figure 30. Example of two levels of hierarchy for variable analysis



Source: own elaboration.

2.4.1.2 Normalization of variables

Each of the variables to be included in the multivariate analysis has different ranges and there are even qualitative variables such as vegetation cover, which is why it is necessary to normalize the variables in such a way that they are all in the same range and thus can be crossed to form a unique susceptibility map. For this, different transformation or normalization functions are used, which usually handle ranges of 0–1 or -1–1.

For the qualitative variables, a numerical value must be assigned according to the criteria of the evaluator and experts, taking into account what is mentioned in table 20 about the relationships between the variables and the susceptibility to mud and debris flows, in this way it becomes a quantitative variable, which can be normalized as follows:

- **Increasing or decreasing linear normalization**

The simplest normalization function is the linear one, which can be done based on the maximum value for increasing normalizations or based on the minimum value for decreasing normalizations. An increasing normalization is carried out if the higher the value of the variable, the greater the susceptibility to mud and debris flows, that is, if the value of the normalized variable is 0, it means that the susceptibility related to this variable is very low, on the other hand, if the value of the normalized variable is 1 implies that the susceptibility is very high. While decreasing normalization is used in the opposite case, in which the relationship between the value of the variable is inversely proportional to the susceptibility to mud and debris flows. The increasing and decreasing linear normalization equations are presented below.

Increasing linear normalization function

$$Y = \frac{x - \min}{\max - \min}$$

Decreasing linear normalization function

$$Y = \frac{\max - x}{\max - \min}$$

Where:

x = Value of the variable to be normalized

y = Normalized value of the variable **x**

min = Minimum value that the variable takes

max = Maximum value that the variable takes

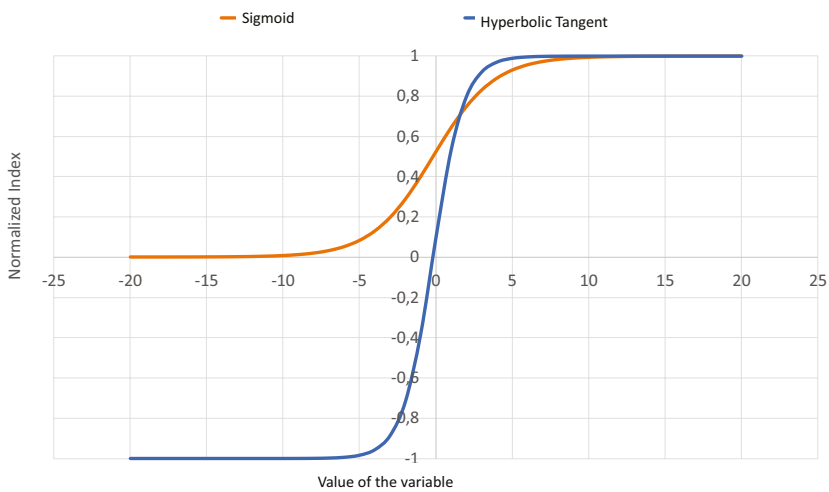
To carry out normalization, the values of each variable must be calculated for all sub-basins or analysis areas and the maximum and minimum values must be calculated.

- **Normalization with sigmoid function and hyperbolic tangent**

The sigmoid and tangent functions are transformation functions that are also used to perform non-linear regressions. These functions allow us to assign upper and lower thresholds and have a more or less linear behavior in the intermediate zone, allowing us to adjust some variables that present clear thresholds for determine the torrentiality.

These functions are S-shaped and allow the variables to be normalized in ranges of 0 – 1 (sigmoid) or -1 – 1 (hyperbolic tangent), as shown in Figure 31. Estas funciones pueden aplicarse después de realizar la normalización lineal descrita anteriormente, de tal forma que la pendiente de la curva a ser de 45° o puede ajustarse la pendiente para representar el comportamiento de las variables.

Figure 31. Comparison of sigmoid and hyperbolic tangent functions



Source: own elaboration.

Sigmoid normalization function

$$Y = \frac{1}{1 + e^{-(ax+b)}}$$

Hyperbolic tangent normalization function:

$$Y = \frac{2}{1 + e^{-2(ax+b)}} - 1$$

x = Value of the variable to be normalized

Y = Normalized value of the variable x

a = curve slope

b = Cutting point

- **Softmax sigmoid normalization function:**

This is a variant of the sigmoid normalization function that takes into account the mean and standard deviation of the variable values.

$$Y = \frac{1}{1 + e^{-\frac{x-\mu}{\sigma}}}$$

Where:

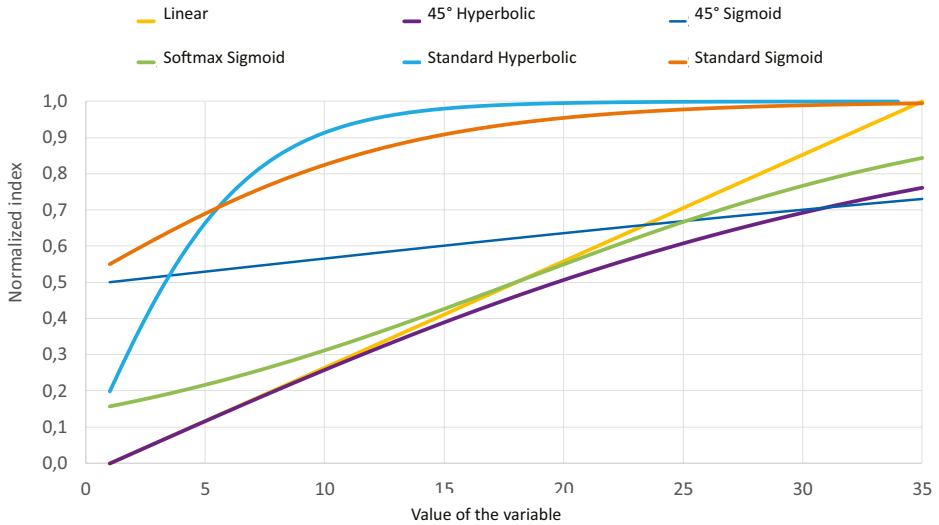
x = Value of the variable to be normalized

Y = Normalized value of the variable x

μ = Mean of the data

σ = Standard deviation

Figure 32 shows the comparison of the functions previously described for positive values of the variables to be normalized, which are the type of values obtained for the physiographic variables. The curves indicated as sigmoid and hyperbolic 45° correspond to the hyperbolic sigmoid functions initially applying a simple linear regression, while those indicated as standard sigmoid and hyperbolic correspond to those to which a different slope was assigned.

Figure 32. Comparison of different normalizations for positive values of variables

Source: own elaboration.

2.4.1.3 Paired comparison

This methodology is based on the fact that human beings are good at making comparisons between two aspects, but not in a complete set or for global comparisons, therefore, a square comparison matrix must be generated in which the level of importance is compared. of one variable with respect to another (Yepes, 2018).

Scores or levels of importance are assigned according to the following:

Table 21. *Saaty Paired Comparison Scale*

Score	Definition	Observations
1	Equal importance	Criterion A is just as important as criterion B
3	Moderate importance	Experience and judgment slightly favor criterion A over criterion B
5	Great importance	Experience and judgment strongly favor criterion A over criterion B
7	Very great importance	Criterion A is much more important than B
9	Extreme importance	The greater importance of criterion A over B is beyond any doubt
2,4,6,8	Intermediate values when it is necessary to refine	

Source: Yepes (2018).

The pairwise comparison matrix has the following properties:

- **Homogeneity:** If two variables are equally important then the comparison $A/B = 1$ and $B/A = 1$.
- **Reciprocity:** If there are 4 variables to analyze, 4 qualifications must be made, since if the comparison of $A/B = 9$, then the comparison B/A is reciprocal with the opposite $B/A = 1/9$.
- **Consistency:** There are no contradictions in the ratings of the matrix. To determine this, the consistency radius is calculated. If this is greater than a threshold, the expert who is making the comparison must reconsider his or her ratings of the variables.

An example of a paired matrix is presented in table 22. It is important to clarify that to make this comparison, a thorough analysis must be carried out, based on previous studies, field observations, among others, to avoid falling into unconsciousness. Additionally, it is recommended to make several matrices changing different variables to compare the sensitivity of the susceptibility to these changes in certain variables.

Table 22. *Ejemplo comparación pareada variables fisiográficas*

Criterion B	Criterion A	Green cover	Melton Index	River Morphodynamics	Basin Morphodynamics	IVET
Coverage vegetable		1/1	1/7	1/1	1/7	1/7
Melton index		7	1/1	5	1/5	1/1
River Morphodynamics		1	1/5	1/1	1/5	1/5
Basin Morphodynamics		7/1	5/1	5/1	1/1	1/1
IVET		7/1	1/1	5/1	1/1	1/1

Source: own elaboration.

2.4.1.4 Calculation of weighted weights and consistency calculation

Once the comparison matrix is made, the weighted weights that will be assigned to each of the variables must be calculated. To calculate the relative weights, the eigenvalues of the matrix are calculated or an approximate simplified calculation can be made by adding each row and dividing it into the total sum of the columns like this (Márquez, 1999):

It is recommended to make several matrices changing different variables to compare the sensitivity of susceptibility to these changes in certain variables.

Table 23. Example calculation of variable weights

Variable	Row total	Weight calculation	Weight
Green cover vegetal	2.4	2.4/53.2	0.05
Melton Index	14.2	14.2/53.2	0.27
River Morphodynamics	2.6	2.6/53.2	0.05
Basin Morphodynamics	19	19/53.2	0.36
IVET	15	15/53.2	0.28
Total in column	53.2		1.00

Source: own elaboration.

Once the calculation of the weights is carried out, the consistency of the matrix must be verified, so that if inconsistency is found, the expert evaluator must reconsider the assigned grades.

First of all, the consistency index CI must be calculated as follows:

$$C.I = \frac{\lambda_{\max} - n}{n - 1}$$

Where:

λ_{\max} = Main eigenvalue of the matrix

n = Number of rows or columns in the matrix (number of variables)

To calculate the value of λ_{\max} These steps must be followed:

- Multiply comparison matrix pair wise **A** TO by the vector of eigen values **W** (weights):

$$V=A * W$$

Table 24. Example lamda calculation

Matrix A					W	V
1.00	0.14	1.00	0.14	0.14	0.05	0.22
7.00	1.00	5.00	0.20	1.00	0.27	1.18
1.00	0.20	1.00	0.20	0.20	0.05	0.28
7.00	5.00	5.00	1.00	1.00	0.36	2.54
7.00	1.00	5.00	1.00	1.00	0.28	1.47

* =

Source: own elaboration.

- Divide the previous resulting vector V in the weights W:

Table 25. Example calculation of lamda max

V/W
4.9
4.4
5.6
7.1
5.2

Source: own elaboration.

- Calculate the average of the resulting vector V/W, this value will be the $\lambda_{\text{máx}}$:

$$\lambda_{\text{máx}} = 5,9$$

- Calculate the CI value

$$C.I = \frac{\lambda_{\max} - n}{n - 1} = \frac{5,5 - 5}{5 - 1} = 0,12$$

- Determine the value of the random index tabulated by Saaty RI according to the number of variables or order of the array.

Table 26. *RI based on matrix order*

n	R.I
1	0
2	0
3	0.58
4	0.90
5	1.12
6	1.24
7	1.32
8	1.41
9	1.45
10	1.49
11	1.51
12	1.48
13	1.56

n	R.I
14	1.57
15	1.59

Source: own elaboration.

- Calculate the consistency ratio RI:

$$R.C = \frac{C.I}{R.I} = \frac{0,12}{1,12} = 0,10$$

Depending on the radius of the matrix, the consistency ratio, the maximum allowed value varies as follows

Table 27. *Thresholds for consistency ratio*

Matrix size	R.C. threshold
3	5 %
4	9 %
5 o más	10 %

Source: Yepes (2018).

According to the above, for the example, the consistency ratio corresponds to 10%, which is why it is within the appropriate consistency range; otherwise the evaluator should reevaluate some of the assignments made in the paired comparison.

2.4.1.5 Maps and assignment of susceptibility categories

Once the weighted weights of each of the variables to be analyzed are determined, map algebra is performed by multiplying the already normalized variables by their

respective weight. The result of this operation gives a number of 0 – 1 (if the variables were normalized in this range) and once this value is obtained, susceptibility categories can be assigned. A minimum of 3 categories are recommended (low, medium-high) or 5 categories. (very low, low, medium, high, very high), this distribution of the ranges is at the discretion of the evaluator. As mentioned above, it is advisable to perform this exercise with various combinations of variables to determine if there are really certain variables that are very decisive.

2.4.1.6 Assignment of susceptibility categories to a basin as a whole

When the multivariate analysis exercise is performed, susceptibility can be determined for very small drainage areas. This analysis can be expressed individually for each drainage or for an entire basin with multiple tributaries. In this last case, what happens when you want to determine the susceptibility for complete basins that have several tributaries? That is, if, for example, basin A has two subbasins A1 and A2, of which A1 is highly susceptible and A2 is moderately susceptible. susceptible, what will be the categorization of A as a complete basin? To carry out this assignment of categories to basins composed of other sub-basins or drainages, the following options are proposed; however, it is up to the expert evaluator to decide whether or not to use any of these criteria.

- Weighting by area: thus, basins with larger areas will have a greater weight in the joint susceptibility index for the higher order basin
- Weighting by the average slope of the subbasins: thus the subbasins with greater slopes will have a greater weight in the joint susceptibility index for the higher order basin, since it is assumed that an area with a greater slope or steeper will have a greater sediment contribution and shorter concentration times than a low area close to the outlet of the higher order basin.
- Weighting by the average elevation of the subbasins: Thus, the subbasins with higher elevations will have a greater weight in the joint susceptibility index for the higher order basin, since it is assumed that an area with a higher elevation will be steeper and therefore It will have a greater contribution of sediments and shorter concentration times than a low area close to the outlet of the higher order basin.

Note: This analysis is relative to the level of segregation of the subbasins or drainages, it is recommended that a single susceptibility value be assigned to an entire basin, subbasin or micro basin and not to individual drainage areas, since this allows the map to be a tool easier-to-use decision-making.

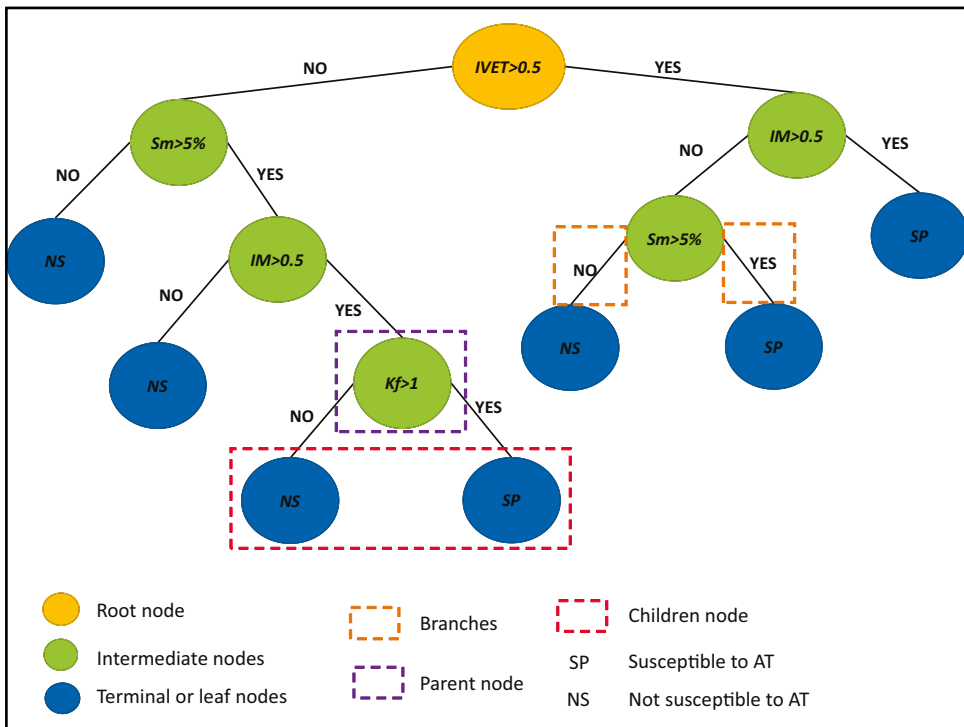
2.4.2 CLASSIFICATION TREES

Decision trees are supervised learning algorithms, which are trained with a set of data, to subsequently produce predictions for different data; They are widely used to represent non-linear behaviors. There are two types, regression trees, which are used to provide quantitative predictions, and classification trees, which produce qualitative predictions that are generally binary (yes/no, reactive/non-reactive, produces events/does not produce events).

This method can be used if you have a good inventory of historical events and is recommended for large basins, in which there are several micro-basins with historical events. The above, because these historical data are required for the training algorithm, so that a tree can be built that represents the characteristics of the basins and their relationship with the occurrence of mud and debris flows events.

Decision trees are made up of the following parts (A simple example for mud and debris flows is presented in Figure 33):

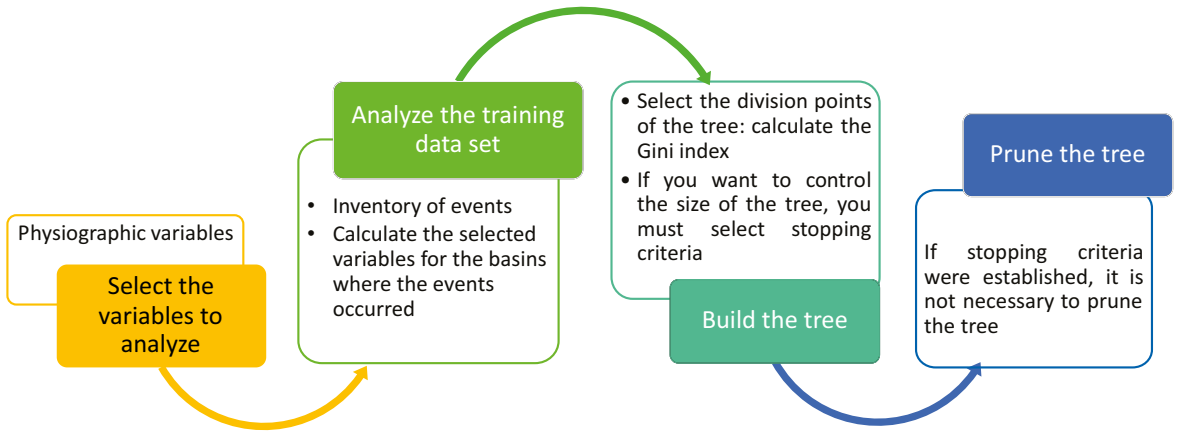
- **Root node:** This is the node where the tree begins to branch. If you have several variables, the most important one will be in the root node.
- **Intermediate nodes:** Decisions are made in these nodes.
- **Terminal nodes or leaves:** They are the nodes in which the final prediction is made, these nodes do not have children.
- **Parent node and child nodes:** A node that is divided into subnodes is called the parent node and its respective subnodes are the child nodes
- **Branches:** It is a subsection of the tree

Figure 33. Classification tree structure

Source: own elaboration.

The process for constructing a classification tree is presented in Figure 34. The first step is to select the variables that are going to be included in the tree. In this case, there is no need to normalize them. Subsequently, the training data set (historical events) must be analyzed, that is, those variables must be calculated for the basins that are going to be analyzed, including those that have and have not had events. Finally, the tree is built, for this there are two options, one selecting stopping criteria that limit the growth of the tree and the other generating a very large tree and then pruning the branches; The construction process is presented below.

Figure 34. Methodology for construction of classification trees for mud and debris flows



Note: is important to clarify and emphasize that this method only allows defining whether a basin tends to be reactive or not, that is, whether it will produce events or not, but does not include susceptibility levels. To include these levels, one must choose to complement the methodology by including magnitude-frequency relationships or with a frequency analysis of the events or conditioning factors, as explained later in the threat analysis.

Source: own elaboration.

2.4.2.1 Tree construction

The key points for building a classification tree are:

- Select where to partition the tree: That is, the threshold for which the YES/NO decision will be made. Example: Should the node be divided into basins whose Melton index (MI) is >0.5 or should it be divided into basins whose $MI > 0.65$? The partition point is decisive if we want to achieve a tree that is correct and that makes correct predictions about which basins will or will not present mud and debris flows events.

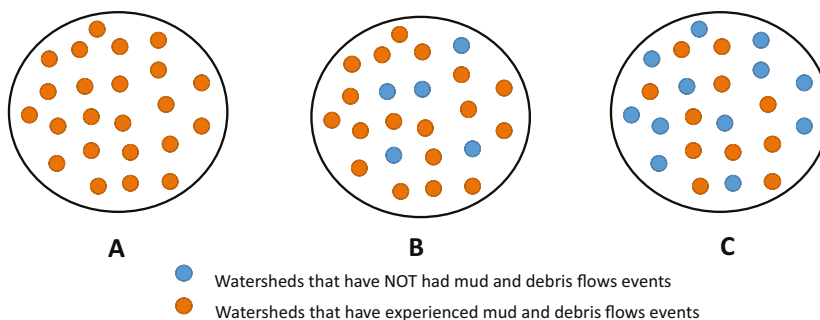
- Limit the size of the tree: determine how many branches the tree will have, when it should stop and reach terminal nodes. To do this, you can select predefined stopping criteria or very large trees can be generated that must then be pruned.

To select how to partition the tree and each of its nodes, there are several criteria, among them the most used are the information gain and the Gini index, both criteria measure the homogeneity in the classification, that is, the more homogeneous the tree. It will best represent the training data, which in this case are the basins with historical events.

Example:

Node A is completely homogeneous, which is why it is a pure node, since it completely represents the basins where mud and debris flows events have occurred. B is a slightly less homogeneous node, since it includes basins that have not had events, however, C is a node that is not homogeneous and therefore impure, since it includes a very similar number of basins that have presented and that have not. They have presented events. The purity of the node defines whether the partition is being performed correctly or not (if it is impure it will not correctly represent the behavior of the basins).

Figure 35. *Example homogeneity/purity of a node*



Source: own elaboration.

Information gain is calculated with entropy,
entropy is a measure of disorder.

- **Information gain**
-

$$\text{Information gain} = \text{Entropy}_{\text{parent node}} - \text{Entropy}_{\text{weighted of the child nodes}}$$

$$\text{Entropy} = - \sum_{i=1}^n P_i * \log_2(P_i)$$

The information gain is calculated with entropy, entropy is a measure of disorder, in this case the disordered combination of basins that have and have not presented events.

Where is the probability that the basin belongs to class i (that produces events or that does not produce them).

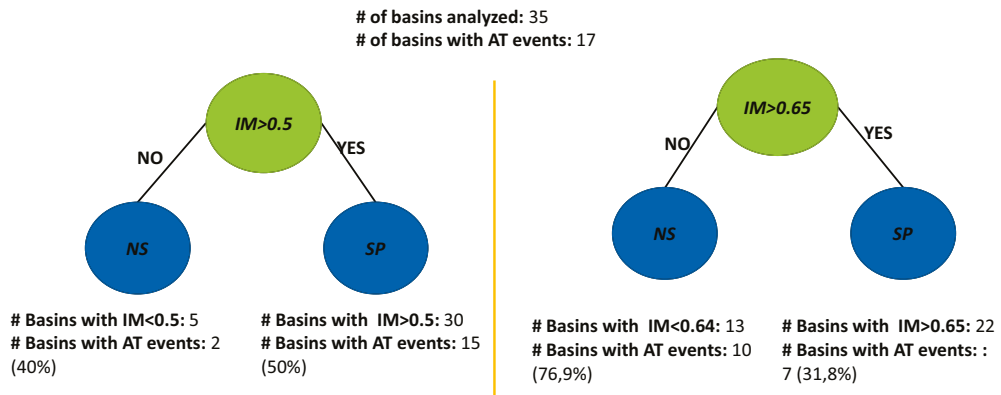
- **Gini index:**

The Gini index measures the purity of a node, that is, if the number of classes represented in a node is small, the better the model or the node is more homogeneous. The closer the Gini index is to zero (0), the purer the node is and therefore the better the partition.

$$GINI = 1 - \sum_{i=1}^n (P_i)^2$$

Note: The Gini index can also be used to select which variable is more important and to select the best one among several tree options, for this the Gini index is weighted for all nodes.

Below is an example of how to use these two criteria to select the best partition for a node.

Figure 36. Example of selecting the partition point of a node

Source: own elaboration.

- **Information gain calculation example:**

» For $IM > 0.5$

Entropy of the parent node:

$$Entropy_{NP} = \left(-\frac{17}{35} * \log_2 \left(\frac{17}{35} \right) \right) - \left(\frac{18}{35} * \log_2 \left(\frac{18}{35} \right) \right) = 0,99$$

Entropy of child nodes:

$$Entropy_{IM < 0,5} = \left(-\frac{2}{5} * \log_2 \left(\frac{2}{5} \right) \right) - \left(\frac{3}{5} * \log_2 \left(\frac{3}{5} \right) \right) = 0,97$$

$$Entropy_{IM > 0,5} = \left(-\frac{15}{30} * \log_2 \left(\frac{15}{30} \right) \right) - \left(\frac{15}{30} * \log_2 \left(\frac{15}{30} \right) \right) = 1$$

$$Entropy_{total} = \left(\frac{5}{35} * 0,97 \right) + \left(\frac{30}{35} * 1 \right) = 0,99$$

$$Information\ gain_{IM > 0,5} = 0,99 - 0,99 = 0$$

» For $MI > 0.65$

$$Entropy_{IM < 0.65} = \left(-\frac{10}{13} * \log_2 \left(\frac{10}{12} \right) \right) - \left(\frac{3}{13} * \log_2 \left(\frac{3}{13} \right) \right) = 0,78$$

$$Entropy_{IM > 0.65} = \left(-\frac{7}{22} * \log_2 \left(\frac{7}{22} \right) \right) - \left(\frac{15}{22} * \log_2 \left(\frac{15}{22} \right) \right) = 0,90$$

$$Entropy_{total} = \left(\frac{13}{35} * 0,78 \right) + \left(\frac{22}{35} * 0,90 \right) = 0,85$$

$$Information\ gain_{IM > 0,65} = 0,99 - 0,85 = 0,14$$

Conclusion: Partition with $IM > 0.65$ should be used since it produces a greater information gain, that is, its entropy is lower, since the sets obtained with this partition are more homogeneous, which is why they better represent the observed data.

- **Gini index calculation example:**

$$GINI = 1 - PP$$

» For $MI > 0.5$

$$PP_{IM < 0,5} = \left(\frac{2}{5} \right)^2 + \left(\frac{3}{5} \right)^2 = 0,52$$

$$PP_{IM > 0,5} = \left(\frac{15}{30} \right)^2 + \left(\frac{15}{30} \right)^2 = 0,50$$

$$PP_{weighted} = \left(\frac{5}{35} * 0,52 \right) + \left(\frac{30}{35} * 0,5 \right) = 0,50$$

$$GINI = 1 - 0,50 = 0,50$$

» For $MI > 0.65$

$$PP_{IM < 0,5} = \left(\frac{10}{13}\right)^2 + \left(\frac{3}{13}\right)^2 = 0,64$$

$$PP_{IM > 0,5} = \left(\frac{7}{22}\right)^2 + \left(\frac{15}{22}\right)^2 = 0,57$$

$$PP_{weighted} = \left(\frac{5}{35} * 0,64\right) + \left(\frac{30}{35} * 0,57\right) = 0,58$$

$$GINI = 1 - 0,58 = 0,42$$

Conclusión: The partition with $IM > 0.65$ should be used since this partition is purer, this is because the GINI value gave a lower value (the closer to zero the purer the node), which indicates that The sets obtained with this partition are more homogeneous, which is why they better represent the observed data.

2.4.2.2 Pruning the tree or limiting its size

When very large trees are made, overfitting can occur, which implies that there are so many possibilities within the tree that it will represent the training data too well, in such a way that it has a leaf or terminal node for each of them. basins with events, but may have a bias when evaluating a new basin. To avoid this overfitting, stopping criteria must be included so that the tree does not grow too much or the maximum possible tree can be generated and then pruned branches Amat (2017).

The criteria for detention can be:

- Count of the minimum number of basins that present events assigned to each terminal node.
- Determine the depth of the tree, that is, the maximum number of branches.
- Maximum number of terminal nodes.

If you want to do a pruning process, it is best to eliminate each leaf node and see the effect it has using a set of test basins or you can use a function to guide the pruning process, which is called error rate. classification (Em), which is used for the terminal nodes (Amat, 2017).

$$E_m = 1 - \max_i(p_{mi})$$

P_{mi} = Proportion of basins within node m that belong to class i

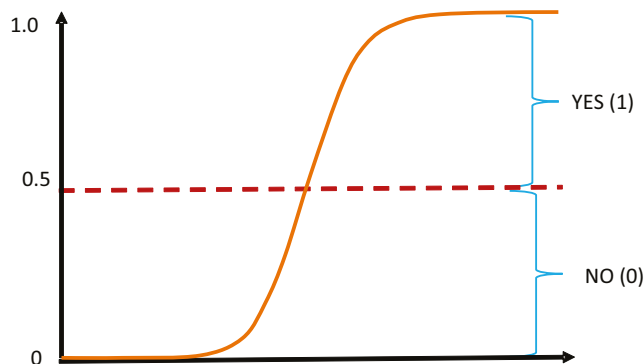
Note: An example of the use of classification trees applied to mud and debris flows can be found in Chevalier (2013).

2.4.3 LOGISTIC REGRESSIONS

Previously, the sigmoid function was described which can be used to normalize variables, however, this function is more used for logistic regressions than in other terms, we could call it in general terms as a “binary multiple nonlinear regression”, that is that based on more than one variable (physiographic) a binary solution of 0 or 1 is obtained; In this case, 0 would correspond to basins that do not tend to present mud and debris flows events, while 1 corresponds to basins that do present events. Like classification trees, this method can only be used if there is a good database of historical events and preferably for large basins with micro-basins that have presented events.

Logistic regression uses the sigmoid function to classify the results into two values 0 and 1, in terms of probability of occurrence, as seen in Figure 37, values close to 1 imply a greater probability of occurrence. The partition point for which the regression takes values of 0 or 1 can vary according to the behavior of the variables included in the regression.

Figure 37. Logistic regression



Source: own elaboration.

The general logistic regression equation is presented below:

$$P(y) = \frac{1}{1 + e^{-(b_0 + b_1X_1 + b_2X_2 + b_3X_3 + \dots)}}$$

Where:

$P(y)$ = Probability that y occurs (that a basin generates AT events)

X_1, X_2, X_3 = Variables included in the regression (Physiographic variables)

b_0, b_1, b_2, \dots = Coefficients analogous to those of a multiple linear regression

Note: When using this type of regressions, several attempts can be made including different variables and choosing the one that presents the best behavior.

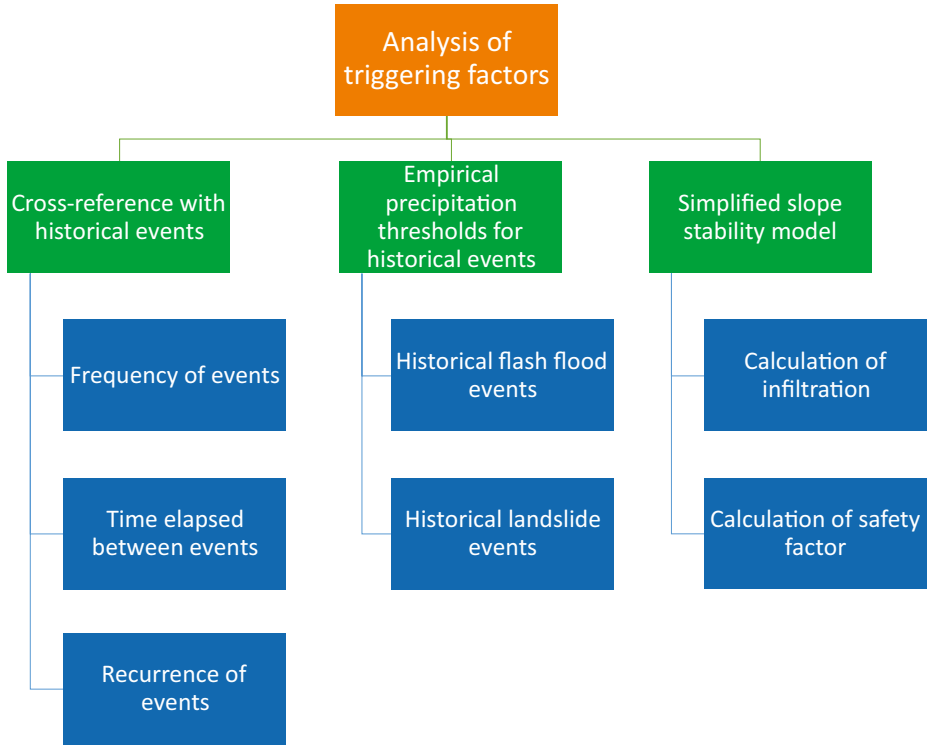
To adjust logistic regressions, statistical software is used with which a multiple linear regression can be transformed into a logistic regression using its logarithmic form.

$$\ln\left(\frac{P(y)}{1 - P(y)}\right) = b_0 + b_1X_1 + b_2X_2 + b_3X_3 + \dots$$

Note: An example of the use of logistic regressions applied to mud and debris flows can be found in Chevalier (2013).

2.5 METHODOLOGIES FOR THE ANALYSIS OF TRIGGER FACTORS AND PROBABILITY OF OCCURRENCE

Once the susceptibility analysis has been carried out, the analysis of conditioning factors must be carried out so that together the threat map is constructed. There are different ways to evaluate the conditioning factors; this analysis depends on the methodology applied for the susceptibility analysis and the level of detail that is desired in the threat study. Next, 3 different approaches are proposed, which will be described later.

Figure 38. Methodologies for the analysis of conditioning factors

Source: own elaboration.

Note: The analysis of conditioning factors can be related to the probability of occurrence of events.

2.5.1 CROSSING WITH HISTORICAL EVENTS

If historical elements were not taken into account in the susceptibility analysis, or if several events have occurred in the study basins, an analysis of the frequency or recurrence of the events can be carried out, assigning a scale according to: 1. The number of historical events recorded in the basin, 2. The recurrence of the events, that is, the time elapsed between events, 3. The time elapsed since the last recorded event. Below is an example:

Table 28. *Example classification of historical events for threat analysis*

Classification/ probability of occurrence	No. Registered historical events	Time since last event	Time between events
Low	0	>50 years	>50 años
Half	1 - 2	20 – 50 years	20 – 50 years
High	>2	<20 years	<20 years

Source: own elaboration.

Note: It is recommended to perform this analysis only at the micro basin or basin scale, not for very small drainage areas.

2.5.2 EMPIRICAL PRECIPITATION THRESHOLDS FOR HISTORICAL EVENTS

This method can be used if there are historical records of events, as well as precipitation information of the time, for this the precipitation preceding the event is analyzed in such a way that a relationship is found between the accumulated precipitation, the preceding days and the event generation.

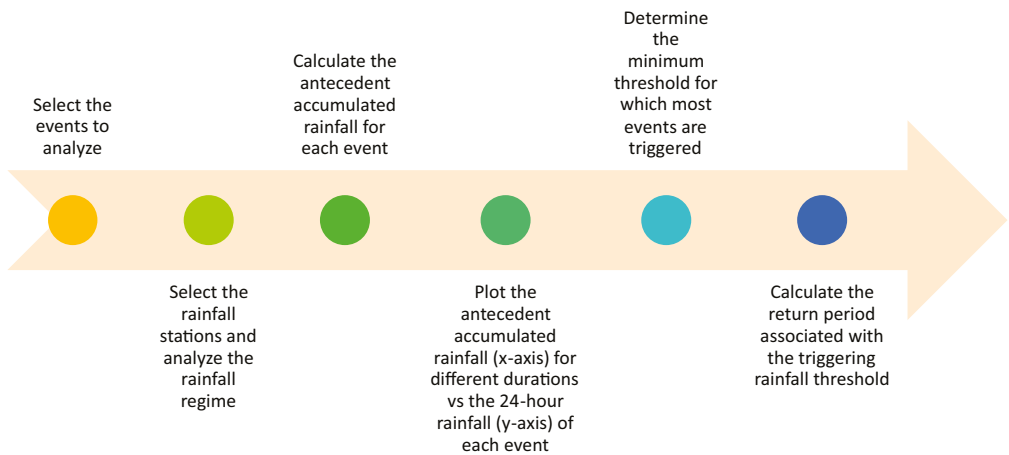
Precipitation thresholds are defined as the minimum or maximum levels for an event to occur. In the case of landslides and mud and debris flows, the minimum threshold represents the amount of rain above which the probability of the event occurring increases drastically (Aristizábal et al., 2011). The method that will be described below is an empirical method, based on historical records, however, there are physically based models with different levels of complexity that will be described later.

Likewise, there are different variations of empirical methods to determine rainfall thresholds, only 2 of them are described here in a simplified manner, however, examples of different applications and variations of these methods can be found in Mayorga (2003), Castellanos (1996), Castellanos and González (1997), Sepúlveda and Patiño (2016) and Aristizábal et al. (2011).

2.5.2.1 Determination of precipitation thresholds that trigger historical landslides

This method consists of analyzing the rainfall preceding the different landslide events, both short-term rain and long-term rain, in such a way that a minimum threshold is identified by which the majority of landslides are triggered, if they occur. If you want, a probability analysis can be carried out, however, the method presented here is simplified, in such a way that the identification of the threshold is carried out graphically. To do this, the following steps must be carried out:

Figure 39. Methodology to determine empirical thresholds of rainfall triggering landslides

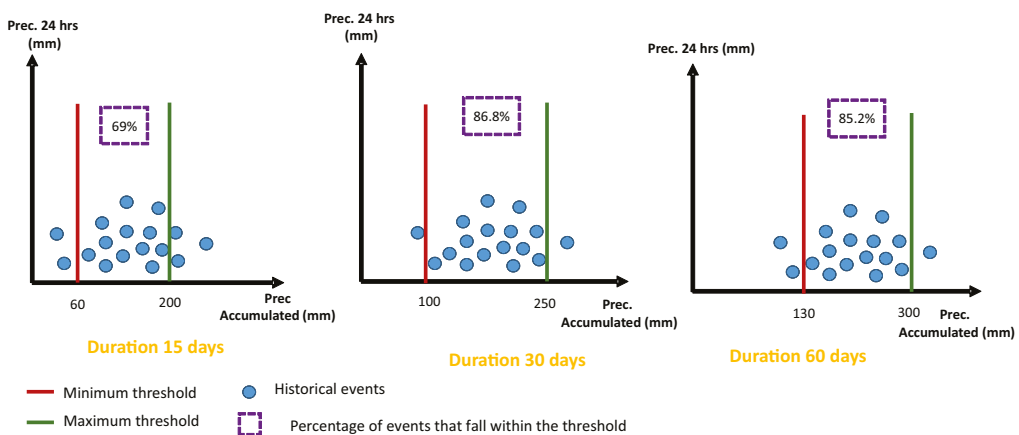


Source: adapted from SGC (2017) and Aristizábal et al. (2011).

- **Select events:** Landslide events that are associated with rain and for which the location and date are known must be selected.
- **Select the seasons and analyze the rainfall regime:** Pluviometric or pluviographic stations must be selected that have daily data from the study area and characterize the precipitation in the area.
- **Calculate the antecedent accumulated rainfall:** the accumulated rainfall must be calculated for different durations, according to some studies it is recommended minimum rain of 15 previous days (SGC, 2017), since for minor rains it is not possible to identify a minimum threshold, however, the ideal is to carry out the analysis with various durations to identify what the duration is most appropriate that adjusts to the conditions of the basin.

- Plot the antecedent accumulated rainfall vs. the 24-hour rainfall on the day of the event and graphically determine the rainfall threshold for which landslides detonate:** The antecedent accumulated rainfall must be graphed for different durations versus the rainfall of the 24 hours of the day of the event. For each event, the threshold is determined by observing in which ranges the majority of the registered landslides are found, as seen in the example of figure 40.

Figure 40. Example identification of thresholds of precipitation triggering landslides



Source: own elaboration.

- Calculate the return period associated with the rain threshold:** taking into account that several studies have identified that the effect of antecedent rain of several days is much more determining for the triggering of landslide events than an intense rain of short duration, it is recommended that, once the accumulated rain has been found, and its duration, its return period is determined.
- However, if we talk about mud and debris flows events specifically, the 24-hour rain return period can be determined, since the triggering of the event (even if previous landslides have occurred due to long-duration rains) is better associated with short-duration and high-intensity events.

To determine the return period of the 24-hour threshold rain, it must be compared with the IDF curves of the study area, while to determine the return period of the accumulated rain, a similar process is carried out in which the following are developed. steps:

- Calculate the accumulated rainfall for the selected duration for the entire available recording period (it must be the mobile accumulation, that is, moving one day at a time and calculating the accumulated for the previous days, days without rain can be skipped).
- Select the maximum accumulated rainfall for each year.
- Carry out a frequency analysis adjusting the maximum values of accumulated rainfall to a probability distribution (same process that is carried out with the maximum rainfall in 24 hours, see section 2.3.1).
- Calculate the accumulated rainfall for different return periods and interpolate the accumulated rainfall threshold to determine the return period to which it belongs.

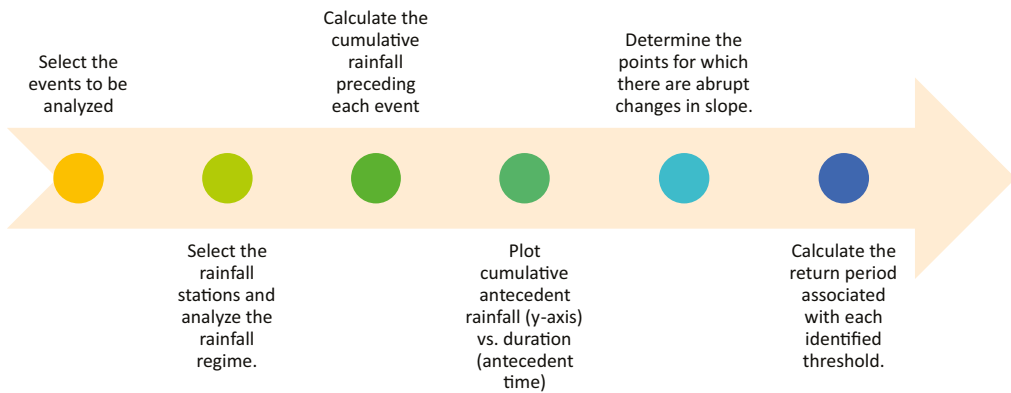
Note: If you do not want to directly select a duration, you can perform the return period analysis for all the durations analyzed, thus obtaining a curve of duration vs accumulated precipitation for each return period and crossing the threshold for each duration.

2.5.2.2 Determination of precipitation thresholds triggering historical mud and debris flows

If you have a robust inventory of historical events with several events, it is possible to carry out the same methodology used for landslides applied to mud and debris flows. However, if you have a few historical mud and debris flows events, you can perform the analysis as follows: according to the methodology of Castellanos (1996).

If you have a robust inventory of historical events with several events, it is possible to carry out the same methodology used for landslides applied to mud and debris flows

Figure 41. *Methodology to determine empirical thresholds of rain triggering mud and debris flows*

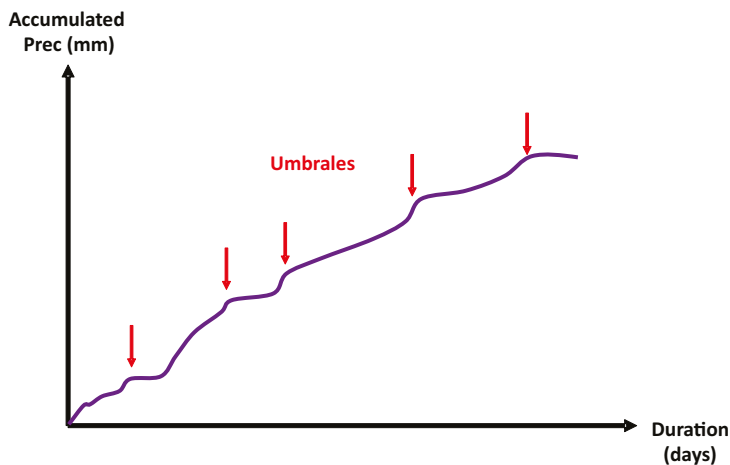


Source: own elaboration.

- **Select events:** The mud and debris flows events to be analyzed must be selected, preferably intense events.
- **Select the seasons and analyze the rainfall regime:** Pluviometric or pluviographic stations must be selected that have daily data from the study area and characterize the precipitation in the area.
- **Calculate the antecedent accumulated rainfall:** the annual rainfall must be calculated mulated for different durations from 15 to 180 days.
- **Plot the antecedent accumulated rainfall vs. antecedent duration and determine abrupt changes in slope:** must be graphed Antecedent accumulated rainfall vs. duration or preceding days, the graph shows if there are abrupt changes in slope, these will be the thresholds for different durations (example of this in figure 42).
- **Calculate the return period associated with the rainfall threshold: T**
 - » Calculate the accumulated rainfall for each threshold and its duration for the entire available recording period (days without rain can be skipped).
 - » Select the maximum accumulated rainfall for each year.

- » Perform a frequency analysis adjusting the maximum rainfall values accumulated to a probability distribution (same process that is carried out with the maximum precipitation in 24 hours, see section 2.3.1).
 - » Calculate the accumulated rainfall for different return periods and interpolate the accumulated rainfall threshold to determine the return period to which it belongs.
- **Select the critical threshold:** Depending on how this threshold is going to be used, the critical threshold may be the one with the longest or the shortest return period. In general terms, the one with the longest return period will have a lower frequency of occurrence, which implies that it will be more intense. However, if we take into account that the greater the probability of occurrence, the greater the threat, the critical threshold would be the one with the shortest return period, since, although it is less intense, it still generates events.

Figure 42. *Example of thresholds of rain triggering mud and debris flows*



Note: Once the return periods are available for the precipitation thresholds that trigger landslides and mud and debris flows, categories of low, medium, and high can be assigned, understanding that at a low return period the probability of occurrence will be higher, which is why the categorization should be higher.

Source: own elaboration.

2.5.3 SIMPLIFIED SLOPE STABILITY MODEL

According to the Colombian Geological Service, the instability of slopes that generates landslides occurs due to an increase in the pore pressure generated by an increase in the water table or in the subsurface flow, therefore, to evaluate the generation of landslides, You must calculate the depth of the sheet of water in the subsoil that accumulates over long periods of time.

If you want to develop a simplified calculation, you can calculate the depth of the water table in relation to the volume of precipitation, for this it is possible to use the equation of the Soil Conservation Service (SCS) of the United States Department of Agriculture to calculate direct runoff and subsequently its complement, which would be infiltration (SGC, 2016). The general procedure for the development of this methodology is presented in figure 43 and is described below.

- **Determine URH and its curve number:** First of all, the vegetation cover and soil type of the study area must be characterized and URH hydrological response units that have the same cover and soil type must be generated in order to determine for each of them the CN curve number. for a normal antecedent humidity condition.
- **Calculate the maximum water retention in the soil S:** S corresponds to the retention of water in the soil, we could also describe it as the threshold for which runoff begins to be generated, this depends on the conditions of the soil and the coverage, which is why it depends on the curve number:

$$S = \frac{25400}{CN} - 254$$

According to the Colombian Geological Service, the instability of slopes that generates landslides occurs due to an increase in pore pressure generated by an increase in the water table or in the subsurface flow

Figure 43. Methodology for determining the threat of landslides due to an increase in the water table



Source: adapted from SGC (2016).

- **Characterize daily precipitation and calculate daily infiltration:** The climatological analysis of precipitation must be carried out (isohyets, Thiessen polygons, etc.) and the direct runoff must be calculated to subsequently calculate the daily infiltration, as indicated below:

$$P_e = \frac{(P - 0.2S)^2}{P + 0.8S}$$

$$P_i = P - P_e$$

Where:

P_e = Direct runoff (mm)

S = Soil water retention capacity (mm)

P = Daily precipitation (mm)

P_i = Infiltrated precipitation (mm)

- **Calculate the annual accumulated infiltrated precipitation, mean, standard deviation and coefficient of variation (CV_{pf}):** For each year of precipitation registration, the accumulated infiltrated precipitation must be calculated; later, with the annual values, the mean value, its standard deviation and coefficient of variation are calculated.
- **Estimate the average depth of the water table (P_f):** This depth must be determined by field exploration and if piezometers are available, if it is not possible to measure it it can be considered that it coincides with the failure depth (SGC, 2016).
- **Calculate the IDF curves and select a rainfall with a return period of 20 years and a duration of 24 hours, calculate the associated infiltrated precipitation gives (P_{i20}):** The IDF curves are made with an analysis of the frequency of maximum precipitation in 24 hours and a distribution of that

precipitation throughout the day. Some IDEAM stations already have these curves or they can be constructed based on precipitation records and potential regressions. Infiltrated precipitation is calculated in the same way as described above, however, since the IDF curve value is in intensity (mm/h) the value of infiltrated precipitation will also be in mm/h.

- **Calculate the depth of the water table associated with a 20-year return period:** This is a simplified estimate of the depth of the water table, which is calculated taking into account the variation of long-term infiltration and rainfall intensity, as follows (SGC, 2016):

$$N_{f20} = (\bar{P}_f - 1.65CV_{pf}) - (P_{i20} * 24)$$

Where:

N_{f20} = Depth of the water table associated with $T = 20$ years (mm)

\bar{P}_f = Mean depth of the water table level measured in the field (mm)

CV_{pf} = Variation coefficient of annual infiltrated precipitation (mm)

P_{i20} = Precipitation/infiltrated intensity associated with $T = 20$ years (mm/h)

- **Determine the geotechnical parameters for each UAG:** Although there are already HRUs that have homogeneous coverage and soil conditions, there may be some variations in geotechnical conditions within these HRUs, which is why geotechnical analysis units (UAG) must be determined and their characteristics such as depth of failure, angle of internal friction, cohesion, slope, soil depth, among others.
- **Calculate the safety factor for each UAG:** The safety factor will determine the stability of the terrain, it is calculated as follows (SGC, 2016):

$$FS = \frac{(c' b \sec \alpha + (\gamma b h \cos \alpha - k \gamma b h \sin \alpha - \gamma_w h_w \cos^2 \alpha) \tan \phi')}{\gamma b h \sin \alpha + k \gamma b h \cos \alpha}$$

Where:

c' = Cohesion

ϕ' = Internal friction

γ = Soil unit weight

b = Width of the slice or cell

h = Height of the ground above the potential slip surface

γ_w = Unit weight of water

h_w = Height of the associated water sheet $T = 20$ years (N_{f20})

α = Failure surface inclination angle

k = Horizontal acceleration coefficient for $T=100$ years

- Classify the threat/probability of occurrence according to the safety factor:** According to the safety factor, a high, medium or low probability of occurrence is associated for the generation of TRIGGERING landslides, according to the following:

Table 29. Threat categorization according to the FS

Threat level	Safety factor
High	<1.1
Average	1.1 – 1.5
Low	>1.5

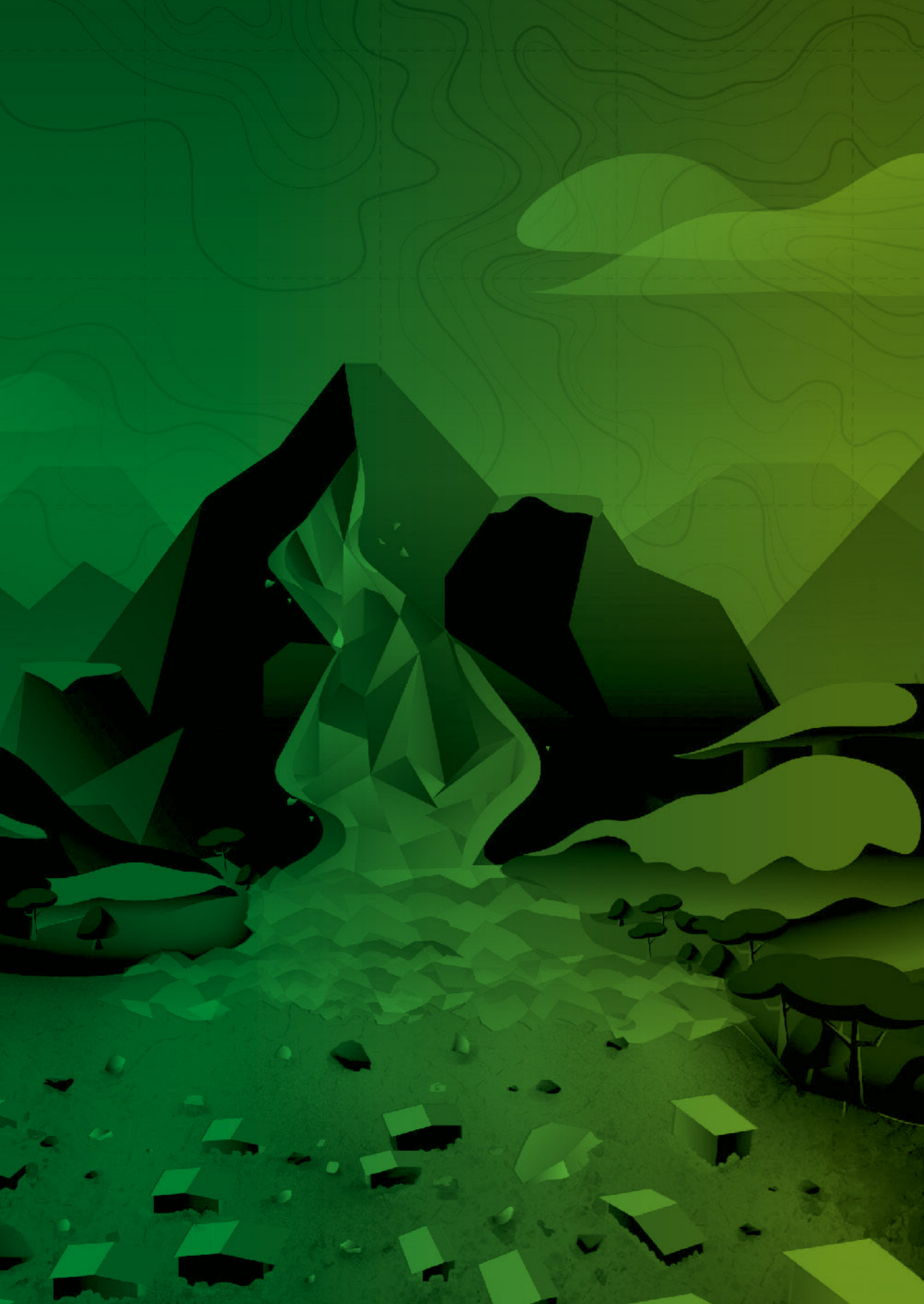
Source: SGC (2016).

2.6 THREAT ANALYSIS

The threat analysis is carried out taking into account the susceptibility together with the probability of occurrence, which in this case is represented by the analysis of conditioning factors. Each of these two variables must be assigned a value of low, medium and high (or intermediate categories can be assigned at the discretion of the evaluator) and the threat will be calculated as follows::

$$\textit{Threat} = \textit{Susceptibility} * \textit{Probability of occurrence}$$

Note: This threat must also be categorized into high, medium and low levels. It should be noted that during the analysis of susceptibility and probability of occurrence, the work scale and level of aggregation may vary from small drainage areas to basins or micro- basins, which is at the discretion of the evaluator and in accordance with the need of the study.



**MODELING SUSCEPTIBILITY
AND THREAT DUE TO
TORRENTIAL FLOODS**

The modeling of susceptibility and threat from mud and debris flows is a very detailed analysis that requires a large amount of information and the integration of several models. This chapter aims to present a generic methodology that can be used for any type of basin, however, there may be variations in the models to be used and their integration depending on the information available and the particular circumstances of the basin.

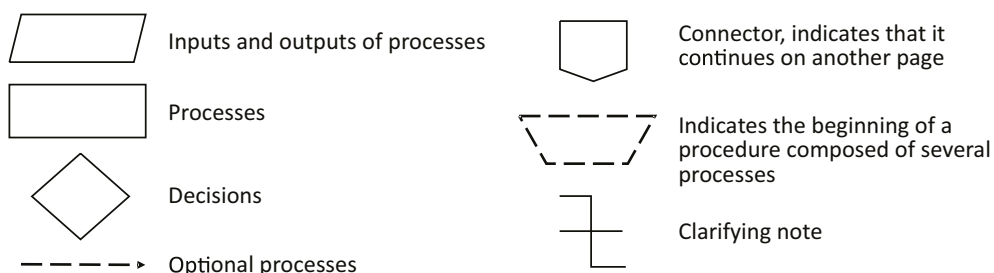
Likewise, the theoretical foundations of some hydrological, hydraulic and landslide models that can be used in the analysis are presented. The general steps for the development of susceptibility and threat modeling due to mud and debris flows are presented in figure 45 and figure 46.

On the other hand, in figure 47 to figure 50 the flow diagrams of the general methodology are presented, including all the various modeling that can be applied according to the characteristics of the basin and the available information, likewise this methodology will be explained in detail later. The explanation of the flowchart symbology is presented in figure 44.

It is worth clarifying that the ideal when modeling mud and debris flows is to use a historical event with sufficient information to calibrate the models and subsequently simulate scenarios for different conditions, such as different rain return periods.

Finally, a calibration example developed by Páez (2016) is presented for the mud and debris flows event generated in the La Negra stream, Útica, Cundinamarca on November 17, 1988.

Figure 44. *Flowchart symbology explanation*



Source: own elaboration.

Figure 45. Steps to follow for modeling susceptibility and threat from mud and debris flows torrenciales

1	<p>Selection of the study basin</p> <ul style="list-style-type: none"> • Local analysis should be performed for riverized basins of special interest. • Basin selection can be made based on the results of the regional risk assessment or for basins in which recent events or several historical events have occurred.
2	<p>Characterization of triggering mechanisms</p> <ul style="list-style-type: none"> • The most recurrent triggering mechanisms must be identified; historical events can be analyzed. • Subbasins or areas of the basin that have greater susceptibility must be identified, for example areas of high mass removal or channels that can easily represent
3	<p>Rain-runoff hydrological modeling</p> <p>If there is information on historical events, if possible, an event should be simulated to calibrate the rheology.</p> <p>Hydrological modeling will be used for modeling the triggering mechanisms as well as for modeling the propagation of the flood in the channel or the Minuscule deposition zone after the two points.</p> <ul style="list-style-type: none"> • Historical event modeling or calibration: Continuous time rainfall-runoff model that represents the conditions of the event. • Risk scenario modeling: Continuous time model that represents average and maximum conditions of the basin or flood transit model associated with a return period.
4	<p>If an event is being calibrated, the triggering mechanisms must be investigated; if scenarios are being simulated, triggering scenarios must be selected:</p> <ul style="list-style-type: none"> • Landslides caused by intense or prolonged rain. • Representations of channels and failure of natural dams • In-channel processes

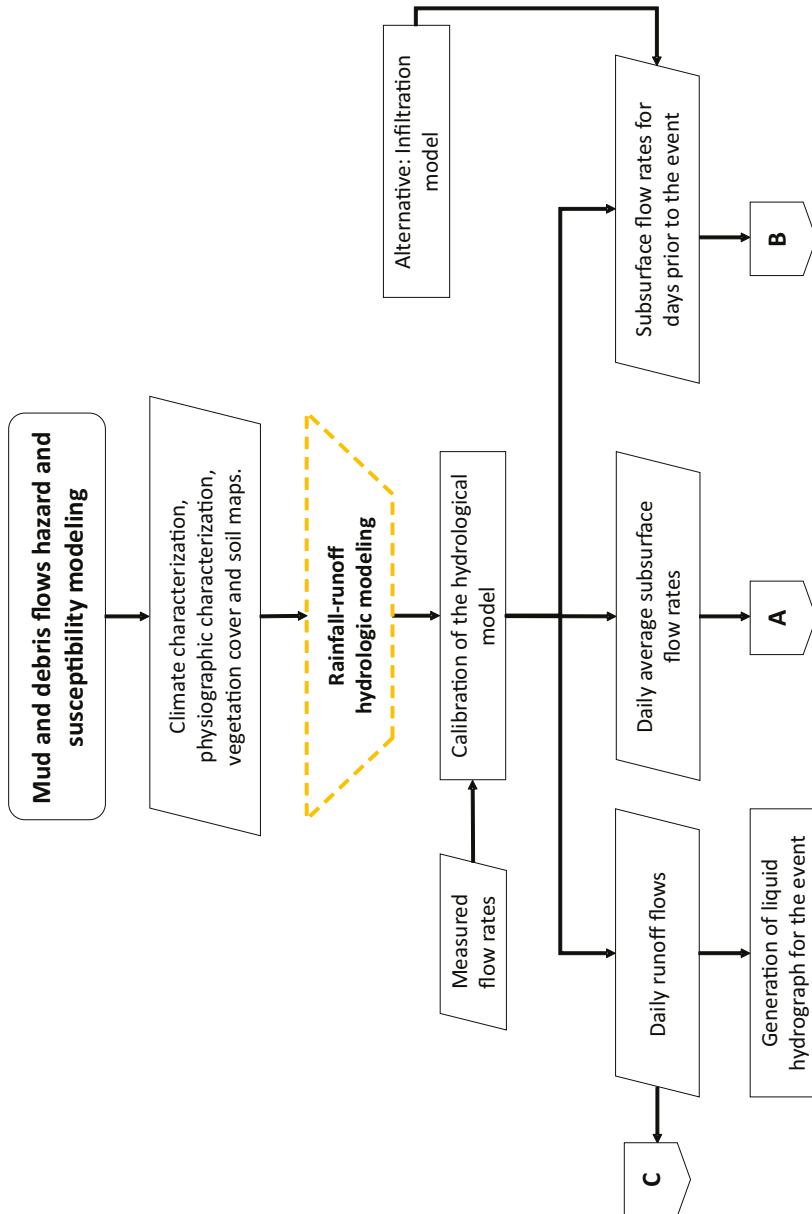
Source: own elaboration.

Figure 46. Steps to follow for modeling susceptibility and threat from mud and debris flows

5	<p>Determination of sediment concentration and flow type</p> <p>From the modeling of the triggering mechanisms and the geological characterization of the basin, an initial estimate of the sediment concentration of a given event can be made, as well as the type of flow.</p>
6	<p>Selection of rheology and hydraulic model</p> <ul style="list-style-type: none"> • Based on the concentration and the type of flow, one or more rheological models must be chosen that can be adjusted to the type of flow. • Taking into account the rheological model(s) to be used, the hydraulic model must be selected, since each hydraulic model has different rheological models incorporated.
7	<p>Hydraulic modeling of Torrencial Flood</p> <ul style="list-style-type: none"> • A flood hydrograph must be constructed that combines solid and liquid flows. One-dimensional or two-dimensional models can be used to simulate the behavior of the mud and debris flows in transit through the channel, as well as the deposition in the alluvial fan. If possible, a historical event should be simulated to later simulate risk scenarios.
8	<p>Rheology Calibration</p> <ul style="list-style-type: none"> • If possible, the rheological model should be calibrated with a historical event, this will allow the rheological parameters to be used for future simulations, the calibration can be carried out with depths (marks left by the historical flood) and flooded areas.
9	<p>Scenario simulation</p> <ul style="list-style-type: none"> • Select the simulation scenarios (rain scenarios and TRIGGERING events). To do this, once the rheology has been calibrated, steps 3, 4 and 7 must be performed again for each scenario.
10	<p>Threat map generation</p> <ul style="list-style-type: none"> • Threat categories are determined according to the depth and speed of the flow, as well as possible flooded areas. • A threat map can be generated for different return periods (selected scenarios)

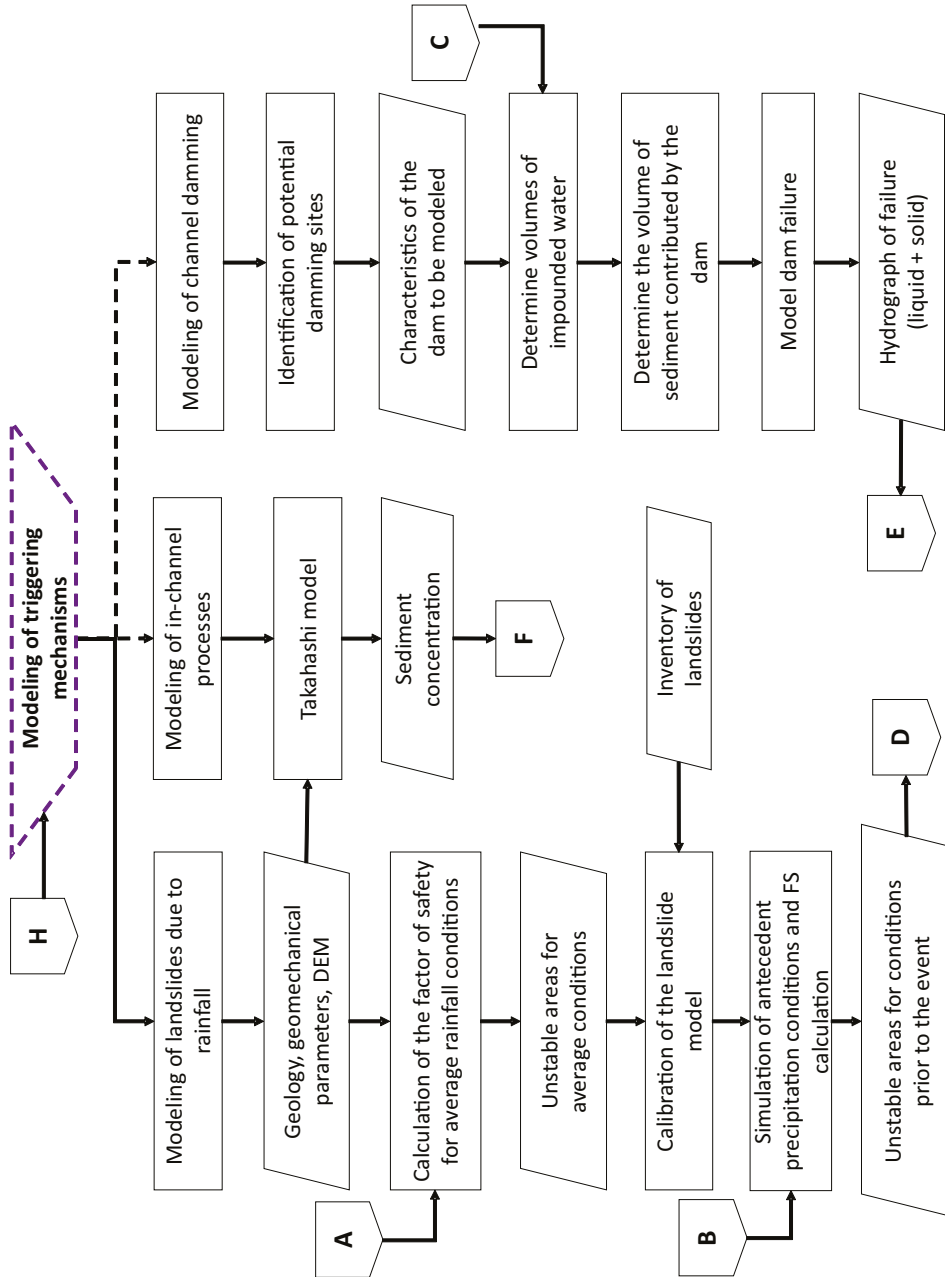
Source: own elaboration.

Figure 47. General flowchart modeling susceptibility and threat from mud and debris flows – Hydrological modeling



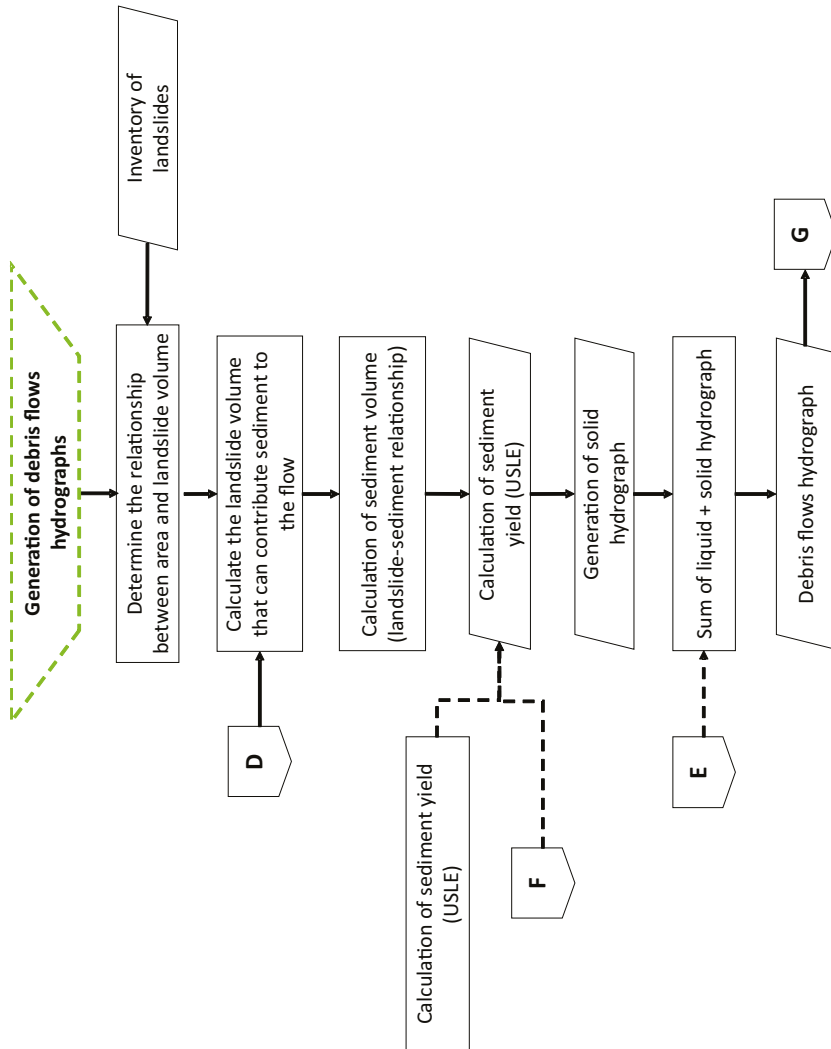
Source: own elaboration.

Figure 48. General flowchart modeling susceptibility and threat from mud and debris flows – Modeling of triggering mechanisms



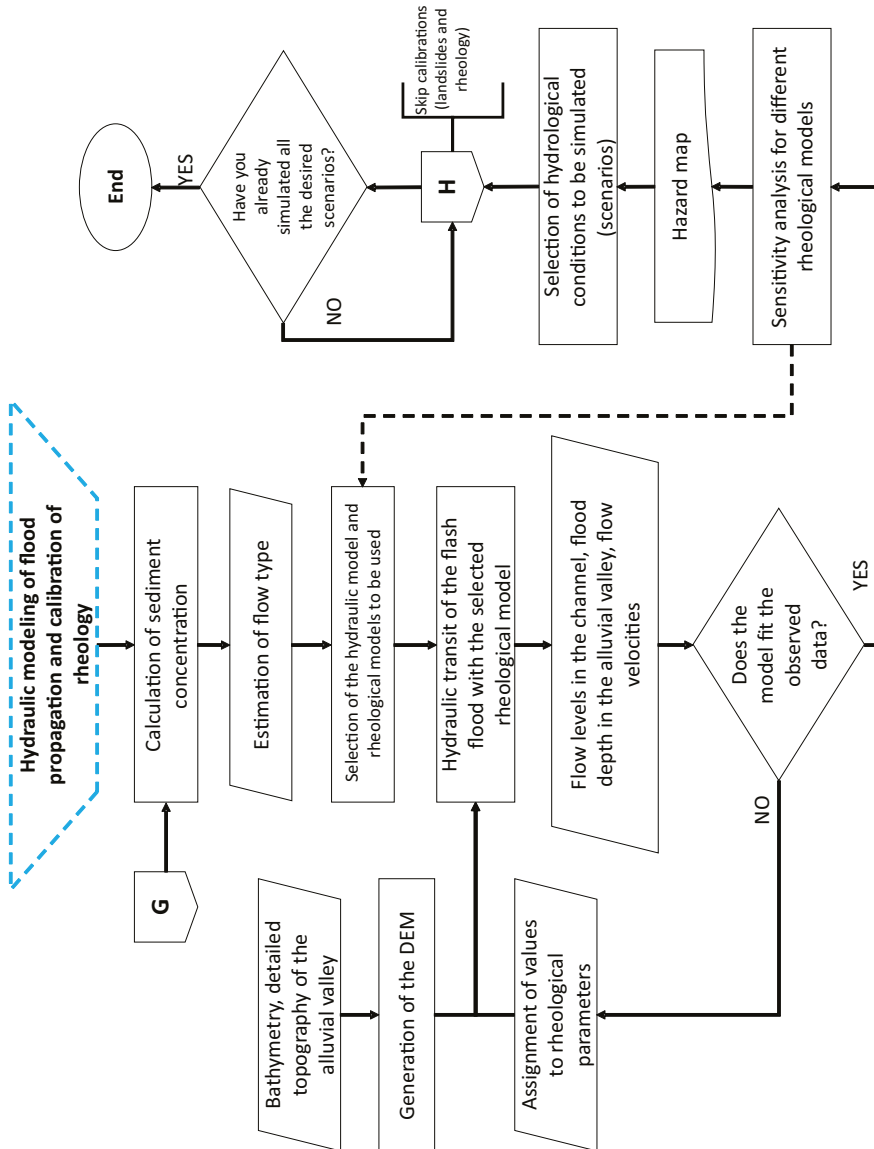
Source: own elaboration.

Figure 49. General flow diagram modeling susceptibility and threat from mud and debris flows – Generation of mud and debris flows hydrographs



Source: own elaboration.

Figure 50. General flow diagram modeling susceptibility and threat from mud and debris flows – Hydraulic modeling of flood propagation and rheology calibration



Source: own elaboration.

In accordance with what is presented in figure 47 to figure 50, some general clarifications are presented regarding the methodology for modeling susceptibility and threat from mud and debris flows:

- Since landslides are generally produced by long periods of time with relatively moderate rainfall, it is recommended to use continuous- time hydrological models, that is, they allow simulating average daily conditions and not specific flood events.
- Although all hydrological models perform the water balance internally, not all of them generate results of subsurface flows or infiltration explicitly, therefore, if a hydrological model that does not generate these results explicitly is used as an alternative for landslide modeling, models can be used. horizontal or vertical infiltration with different levels of complexity, some landslide models even already include infiltration modules internally.
- The most common triggering mechanism for mud and debris flows corresponds to mass removal phenomena; however, in some cases, channel damming or erosive phenomena may occur within the channel, so it is possible to choose which triggering mechanism(s) are included in the list. modeling.
- It is important to calibrate the landslide model for average conditions or a specific period for which landslide inventory information is available, especially for parameters related to subsurface flow. However, if you have good field data on geomechanical parameters, you can skip this step.
- For the final calculation of sediment concentration, the washing load may or may not be included if it is considered relevant. When basins tend to generate sludge flows, this load may be relevant.
- As has been mentioned in other sections of this document, it is very important to carry out a characterization of the geology and soils to determine what type of materials are transported by the channel and also determine the type of flows that the basin tends to generate, since this will determine the rheology to be used. A sensitivity analysis can be performed for different reology, which is recommended when the sediment concentration is at the transition limit between two types of sludge-hyperconcentrated or hyperconcentrated-debris flows, since the results can vary substantially.
- It is recommended to simulate several scenarios for different hydrological conditions, since these various scenarios can generate different depths,

velocities and flooded areas, therefore, with the simulation of several scenarios a very complete threat map can be built.

- When the scenario simulation is carried out, the simulation of triggering mechanisms and hydraulic modeling must be carried out again, however, it is important to emphasize that at this point a calibration of the models should not be carried out again.

3.1 HYDROLOGICAL RAINFALL– RUNOFF MODELING

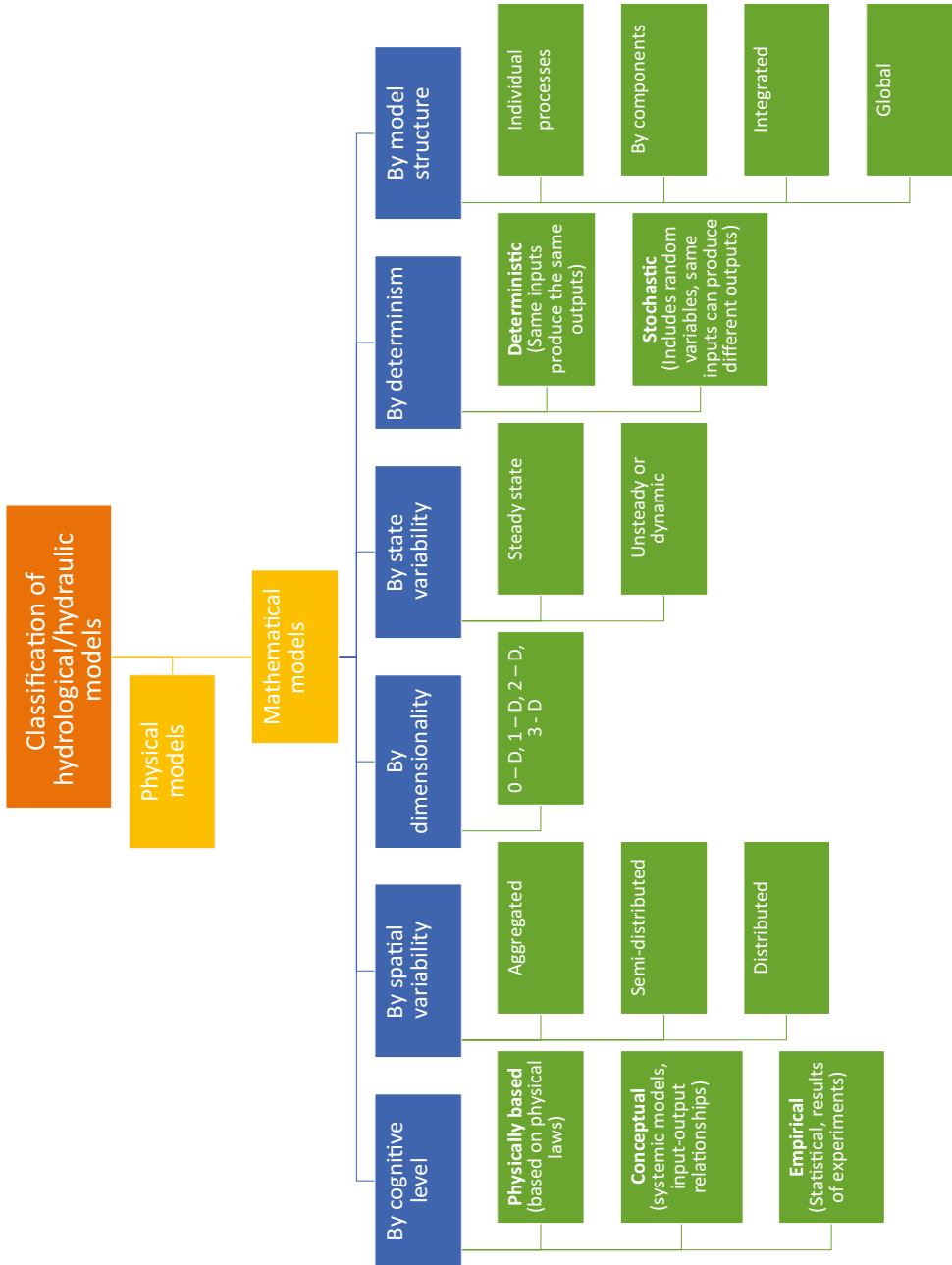
3.1.1 TYPES OF HYDROLOGICAL MODELS

Hydrological rainfall-runoff modeling allows determining runoff flows, base flow, infiltration, among others, through a water balance in the study basin or input and output relationships; either deterministic or stochastic (probabilities). The complexity of hydrological models is very varied, as is their usefulness, level of detail and type of results.

Figure 51 presents a general classification of hydrological models that can also be applied to hydraulic models. For the modeling of mud and debris flows, it is recommended to use physically based models, since these can correctly represent the complex conditions that occur in basins with mud and debris flows. Additionally, these models explicitly present results for most of the water balance variables, such as subsurface flow, base flow, interception, evapotranspiration, among others. However, conceptual models can be used as long as you have very good information for its calibration.

On the other hand, it is also recommended to use semi-distributed or distributed models, since these allow representing the variable conditions of soils, slopes and vegetation cover of the high mountain basins where mud and debris flows occur. Likewise, these models will be deterministic as they are rainfall-runoff models and integrated models since they integrate various processes of the hydrological cycle.

Figure 51. Classification of hydrological/hydraulic models



Source: adapted from Díaz-Granados (2016).

3.1.2 RAINFALL–RUNOFF MODELING PROCESS

Figure 52 presents the procedure for the development of a rainfall-runoff hydrological modeling; Depending on the model used, some steps may vary a little. It is important to emphasize that, prior to the development of the modeling, the climatological data must be analyzed in terms of consistency, homogeneity, anomalous data, and missing data must be completed.

Some hydrological models have built-in evapotranspiration models, while others take it as input. It is suggested to calculate evapotranspiration with the Penman Monteith equation as long as there is sufficient climatic information: wind speed, solar brightness or solar radiation, average, maximum and minimum temperature, relative humidity; However, if this information is not available, simpler equations that depend on temperature or measured evaporation data can be used.

On the other hand, it is very important that the model be calibrated with measured flow data in the channel, preferably data from limnimetric or limnigraphic stations. However, if this information is not available, gauging can be used that must be carried out in several hydrological conditions (dry and humid season).

Once this information is available, an objective function must be assigned that allows the model results to be compared with the measured data. One of the most used objective functions is the Nash Sutcliffe coefficient (NSE), which has values between $-\infty$ and 1, where 1 represents a perfect fit of what is modeled vs. what is observed, the NSE equation is presented below.

$$NSE = 1 - \frac{\sum_{t=1}^T (Q_m - Q_o)^2}{\sum_{t=1}^T (Q_m - \bar{Q}_o)^2}$$

Where:

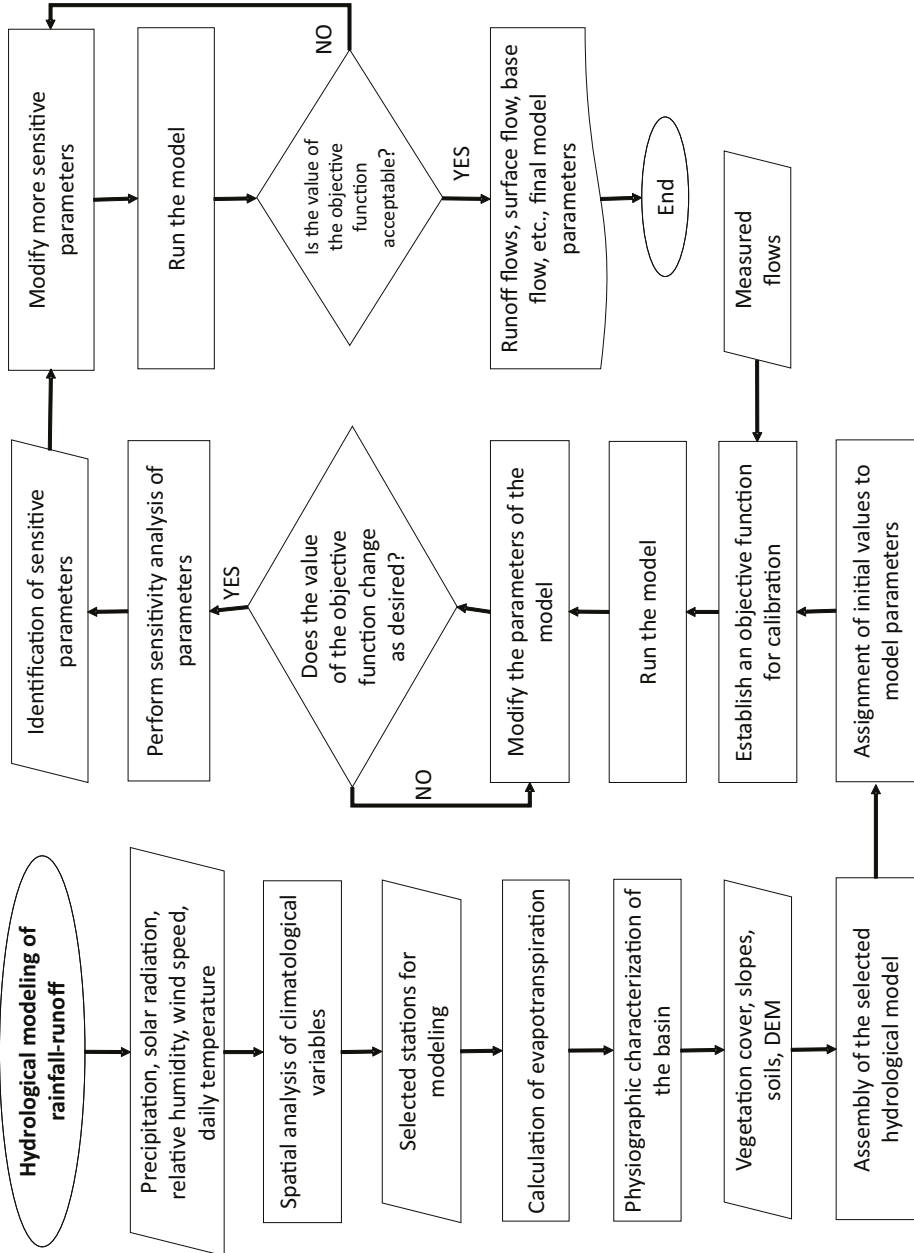
Q_m = Modeled flow

Q_o = Observed flow

\bar{Q}_o = Average of observed flows

Finally, it is advisable to perform a sensitivity analysis to determine which parameters are most sensitive and identifiable, that is, those that most affect the results of the model, in order to achieve optimal calibration by correctly modifying the parameters.

Figure 52. Rainfall–runoff modeling flowchart



Source: own elaboration.

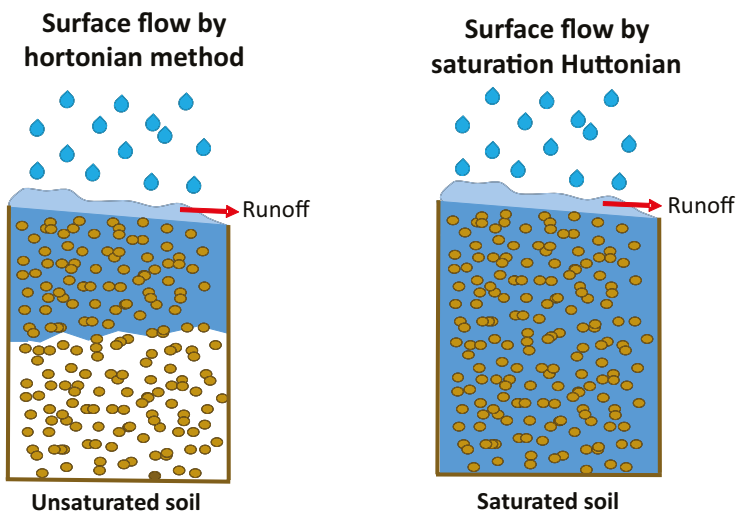
3.1.3 TOPMODEL MODEL

TOPMODEL is a semi-distributed rainfall–runoff model that is based on the topographic humidity index, which represents the tendency of a point in the basin to develop saturation conditions. For areas with a similar topographic humidity index, it could be assumed that they are hydrologically homogeneous or behave hydrologically in a similar way (Tarboton, 2003).

The model explicitly calculates the following flows: surface runoff flow $q(it)$, surface runoff by Hortonian mechanism, surface runoff due to excess saturation qof , vertical flow towards the water table $q(uz)$, subsurface flow q , base flow. This model calculates the runoff flow through the following methods:

- Hortonian mechanism: this mechanism acts when the intensity of precipitation exceeds the infiltration capacity of the soil or when the duration of precipitation is greater than the waterlogging time in small depressions in the ground.
- Surface flow due to excess saturation: occurs when the subsurface zone is completely saturated.

Figure 53. *Graphic Representation of runoff generation methods*



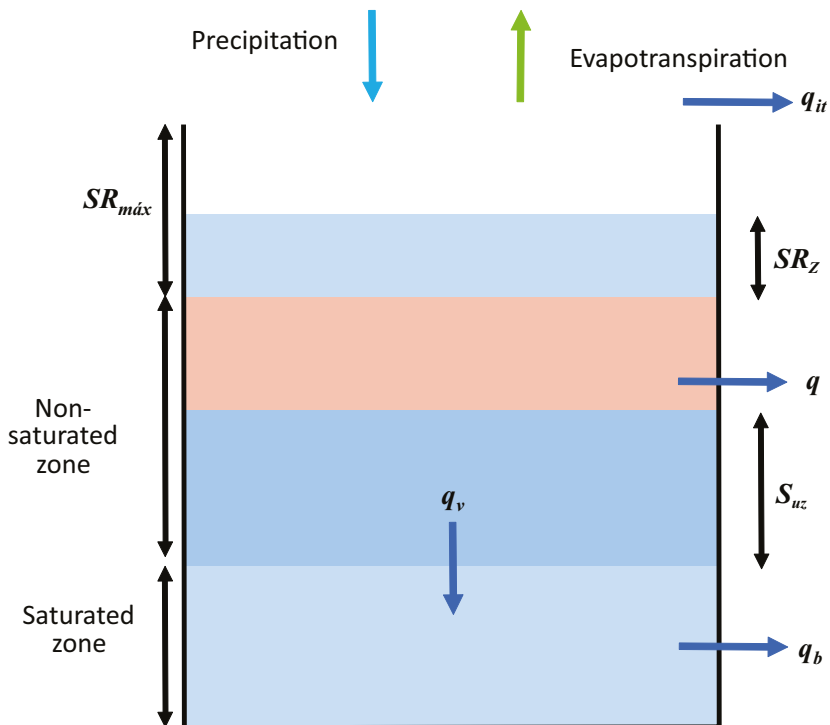
Source: own elaboration.

TOPMODEL performs the soil water balance under the following assumptions (Tarboton, 2003):

- The dynamics of the saturated zone can be approximated to successive steady states.
- The recharge R (m/h) that enters the water table is spatially homogeneous.
- The effective hydraulic gradient of the saturated zone approximates the topographic slope of the surface ($\tan \beta$).
- The effective transmissivity T of a soil profile at a given point is a function of the moisture deficit at that point. Hydraulic conductivity decreases exponentially with depth.

Figure 54 schematically presents the balance carried out by the model on the ground, as well as the areas and variables it takes into account.

Figure 54. TOPMODEL soil water balance diagram



Source: adapted from Nawarathna et al. (2002).

Assuming steady state and a recharge R homogeneous, the subsurface flow in the direction of the slope per unit of contour “ q ” is expressed as

$$q = R * a$$

The simulation of the moisture deficit is carried out based on the depth and storage of water in the soil, as follows:

$$D = \theta_c z_w$$

θ_c = Effective porosity

z_w = Depth of water table

The transmissivity can be expressed as a function of the humidity deficit in the following way, where f = Parameter that determines how quickly the transmissivity decreases (constant).

$$T(D) = T_o e^{-f z_w} = T_o e^{-D/m}$$

$$m = \frac{\theta_c}{f}$$

The maximum subsurface flow can be expressed as follows:

$$q = T_o e^{-D/m} S$$

$$R * a = T_o e^{-\frac{D}{m}} S$$

$$D = -m \ln \left(\frac{R * a}{T_o * S} \right)$$

This can be expressed in terms of the topographic humidity index:

$$\lambda = \ln \left(\frac{a}{S} \right)$$

Yeah is less than zero means that the soil is completely saturated and all water that continues to fall in this area will become runoff (Tarboton, 2003).

The vertical drainage of the unsaturated zone towards the water table can be expressed as follows:

$$q_v = \frac{S_{uz}}{D * t_d}$$

Where:

q_v = Vertical flow from the unsaturated zone

S_{uz} = Storage in the unsaturated zone

D = Soil moisture deficit

t_d = Unsaturated zone delay time

On the other hand, in the root zone there may be water losses due to evapotranspiration, so the actual evapotranspiration is calculated as a function of the potential evapotranspiration and the maximum storage deficit in the root zone, according to the following (Muhammed , 2012):

$$ET_a = ET_p \left(1 - \frac{SR_z}{SR_{m\acute{a}x}} \right)$$

Where:

ET_a = actual evapotranspiration

ET_p = Potential evapotranspiration

SR_z = Storage deficit in the root zone

$SR_{m\acute{a}x}$ = Maximum storage deficit in the root zone

Below are the model parameters, as well as their description:

Table 30. *TOPMODEL parameters*

Parameter	Description
m (m/m)	Parameter that describes the exponential decrease in transmissivity with depth.
To [$\ln(m^2/h)$]	Natural logarithm of the hydraulic transmissivity of the soil when it is saturated.
SRmáx (m)	Maximum storage capacity in the root zone.
SRinit (m)	The initial storage deficit in the soil.
CHV (m/h)	Flow speed in the channel outside the main stream
VR (m/h)	Flow speed in the main channel
Td (h/m)	Delay time in the unsaturated zone per unit of storage deficit
Qo (m/day)	Initial subsurface flow
d θ (-)	Change of water content across suction point
XKmín (m/h)	Minimum hydraulic conductivity
XKmáx (m/h)	Maximum hydraulic conductivity
Porosity (-)	Soil porosity

Source: Muhammed (2012).

3.1.4 HEC-HMS MODEL

The HEC-HMS was developed by the United States Army Corps of Engineers, it is a semi-distributed model that can simulate both flood events and continuous flow (daily flows). This model has separate submodels to represent runoff volume, direct runoff, base flow, and channel flow (US Army Corps of Engineers, 2000).

The HEC-HMS includes the submodels presented below, the most commonly used is the SCS model.

- Runoff volume calculation
 - » Initial and constant rate
 - » SCS curve number (event model)
 - » Green and Ampt(event model)
 - » Deficit and constant rate
 - » Soil moisture accounting(SMA) (continuous time model)
- Base flow calculation:
 - » Monthly cash
 - » Exponential recession
 - » Linear reservoir
- Transit models:
 - » Kinematic wave
 - » Delay
 - » Modified pulses
 - » Muskingum
 - » Muskingum-Cunge
 - » Confluence
 - » Fork
- **Model of the Soil Conservation Service (SCS) –curve number**

This model estimates excess precipitation based on accumulated precipitation, soil type, land use and antecedent humidity, using the following equation:

$$P_e = \frac{(P - I_a)^2}{P - I_a + S}$$

Where:

P_e = Excess accumulated precipitation

P = Accumulated precipitation

I_a = Initial abstraction (losses)

S = Storage\potential

Through experiments it has been determined that $I_a = 0.2S$, so the equation would be of the form:

$$P_e = \frac{(P - 0.2S)^2}{P - 0.8S}$$

While S can calculate based on the curve number (CN):

$$S = \frac{25400 - 254CN}{CN}$$

Curve number values can be taken from tables provided by US Army Corps of Engineers (2000).

- **Green and Ampt Model**

The model of Green and Ampt combines the Richards infiltration capacity equations and the flow in the Darcy unsaturated zone, the model calculates the precipitation losses (infiltration) in the permeable zones in a certain period of time as follows (US Army Corps of Engineers, 2000):

$$f_t = K \left[\frac{(1 + (\phi - \theta_i)S_f)}{F_t} \right]$$

Where:

f_t = Infiltration losses during the period of time

K = Saturated hydraulic conductivity

$(\phi - \theta)$ = Moisture deficit volume Pore suction (function of porosity)

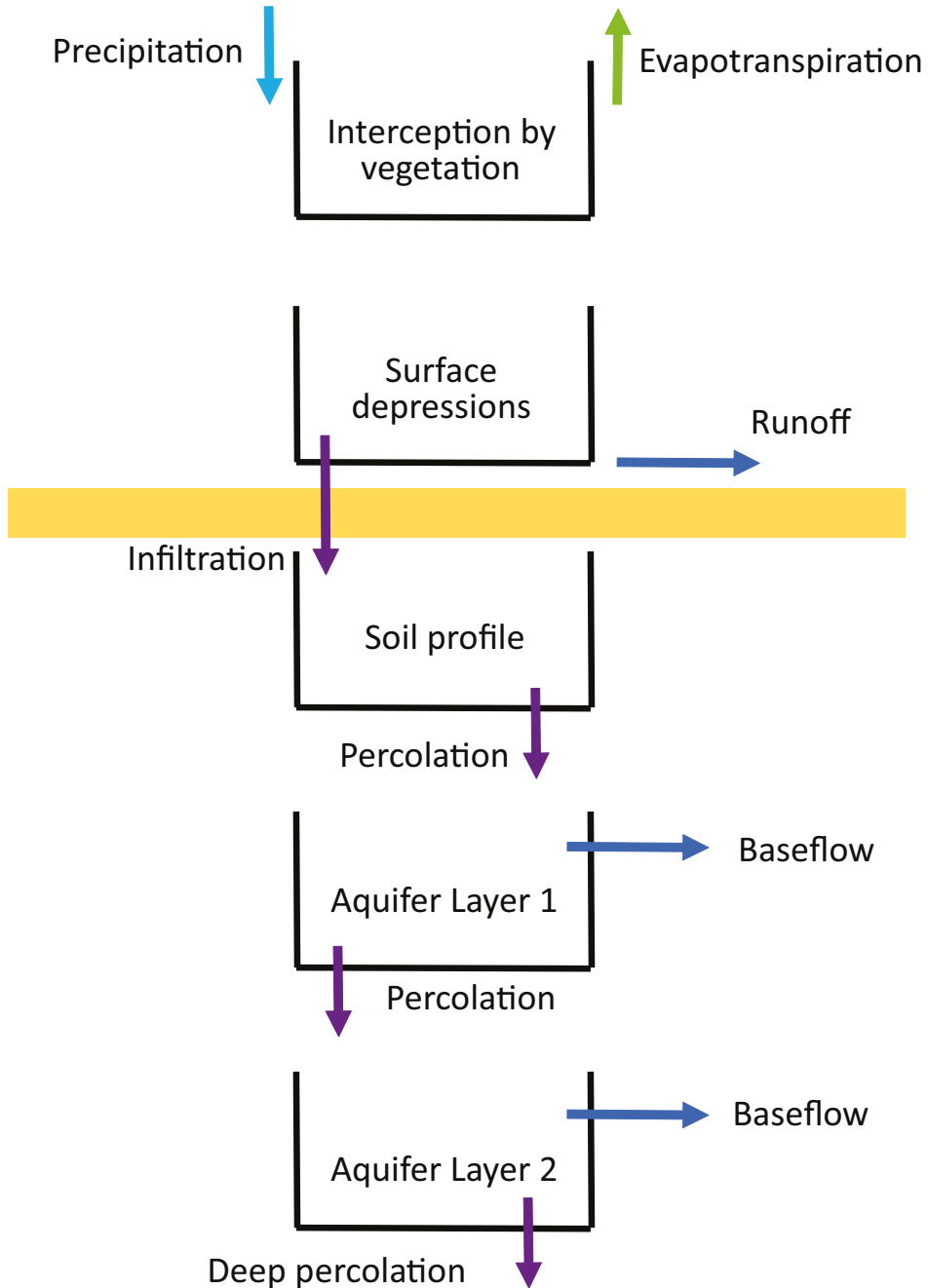
S_f = Pore suction (function of porosity)

F_t = Losses accumulated over time t

- **Soil moisture accounting model (SMA)**

This is the model used by HEC-HMS to simulate continuous conditions, rather than spike precipitation events. This model simulates the movement of water in 5 tanks that represent water in the vegetation, on the soil surface, in the soil profile and underground. Figure 55 schematically presents the operation of the model.

This model simulates the movement of water in 5 tanks that represent water in the vegetation, on the soil surface, in the soil und underground profile.

Figure 55. SMA model tank diagram

Source: adapted from US Army Corps of Engineers (2000).

- **Canopy Interception:** It represents the precipitation that is captured by trees, shrubs and grass and that does not reach the soil surface. Only after this storage is filled does precipitation go to the following storages. The water in this area evaporates (US Army Corps of Engineers, 2000).
- **Depressions in the ground:** The precipitation that reaches this storage is that which is not captured by the vegetation and that exceeds the infiltration rate, hence the water can evapotranspire or infiltrate, when this storage is filled, runoff is generated (US Army Corps of Engineers, 2000).
- **Soil profile:** The soil profile is divided into two zones, the upper zone and the tension zone. The upper zone is the portion of soil where water is lost through evapotranspiration or percolation, while the retention zone is the one where water is only lost through evapotranspiration. The upper zone is the one that contains the water in the pores of the soil, while the tension zone is the one where the water is attached to the soil particles (US Army Corps of Engineers, 2000).
- **Aquifer:** It is represented by horizontal flow processes, this zone includes two layers, water enters by percolation, it can pass from the first layer to the second and from the second to deep percolation, the latter is considered losses of the system (US Army Corps of Engineers , 2000).
- **Infiltration process:** The volume of infiltrated water during a time interval is a function of the volume of available water, the storage capacity of the soil and the maximum infiltration rate and is modeled as follows (US Army Corps of Engineers, 2000):

$$P_{Sinf} = Max_{Sinf} - \frac{Cur_{SS}}{Max_{SS}} Max_{Sinf}$$

Where:

P_{Sinf} = Potential infiltration volume

Max_{Sinf} = Maximum infiltration rate

Cur_{SS} = Volume of water stored in the soil at the beginning of time t

Max_{SS} = Maximum water storage capacity in the soil

- **Percolation process:** The percolation rate is greater when the upper layer is full and the receiving layer is empty and is calculated as follows, taking into account that the amount of water available for percolation is equal to the initial storage of the soil plus infiltration (US Army Corps of Engineers, 2000).

For layer 1

$$P_{SP} = \text{Max}_{SP} \left(\frac{\text{Cur}_{SS}}{\text{Max}_{SS}} \right) \left(1 - \frac{\text{Cur}_{SGW}}{\text{Max}_{SGW}} \right)$$

For layer 2

$$P_{GWP} = \text{Max}_{PGW} \left(\frac{\text{Cur}_{SGW}}{\text{Max}_{SGW}} \right) \left(1 - \frac{\text{Cur}_{SGW2}}{\text{Max}_{SGW2}} \right)$$

Where:

P_{SP} = Potential percolation volume

Max_{SP} = Maximum percolation rate

Cur_{SS} = Volume of water stored in the soil at the beginning of time t

Max_{SS} = Maximum water storage capacity in the soil

Cur_{SGW} = Volume of water stored in layer 1 at the beginning of time t

Max_{SGW} = Maximum storage capacity in layer 1

Max_{PGW} = Maximum storage capacity in layer 2

Cur_{SGW2} = Volume of water stored in layer 2 at the beginning of time t

Max_{SGW2} = Maximum storage capacity at layer 2

P_{GWP} = Potential percolation

- **Runoff generation process and base flow:** Runoff corresponds to water that exceeds the infiltration capacity and leaves the surface storage, this volume is direct runoff. The base flow is the volume of groundwater that leaves the aquifer layers and is calculated as follows (US Army Corps of Engineers, 2000):

$$Gwflow_{t+1} = \frac{Act_{SP} + Cur_{SGWi} - P_{GWPi} - \frac{1}{2}Gwflow_t * t}{Rout_{SGWi} + \frac{1}{2}t}$$

Where:

$Gwflow_t$ y $Gwflow_{t+1}$ = Base flow over time t and $t+1$

Act_{SP} = Current percolation of soil to aquifer layer

P_{GWPi} = Potential percolation of layer i

$Rout_{SGWi}$ = Groundwater routing coefficient

t = Simulation time interval

Cur_{SGWi} = Volume of water stored in layer i

$$Gwvolume = \frac{1}{2} (Gwflow_{t+1} + Gwflow) * t$$

3.1.5 SWAT MODEL

The SWAT (Soil & Water Assessment Tool) is a semi-distributed model by HRU or hydrological response units, which have homogeneous characteristics of coverage, soils and slopes. SWAT carries out simulations taking into account two phases:

- **Terrestrial phase of the hydrological cycle**

The model performs the water balance of water in the soil in one day, taking into account the initial water content in the soil ($SW0$), precipitation ($Rday$), runoff ($Qsurf$), evaporation (Ea), percolation ($Wseep$), and the return flow or base flow (Qgw), which is calculated as the lateral flow (subsurface flow) and the return flow through groundwater, as follows (Netsch et al., 2011).

$$SWt = SW0 + \sum_{i=1}^t (Rday - Qsurf - Ea - Wseep - Qgw)$$

The model includes the calculation of evapotranspiration through the Penman-Monteith equation, additionally taking into account infiltration, storage in the tree canopy and accumulation in reservoirs. Next, it is described how the model takes into account all the variables described above.

- **Infiltration:** It refers to the amount of water that enters directly into the soil profiles. It is determined by the initial moisture content of the soil in addition to the saturated hydraulic conductivity. To calculate it, it requires the saturated hydraulic conductivity and the water retention capacity in the profile. from the ground.
- **Surface runoff:** It is directly related to infiltration, since it is assumed
- that water that does not infiltrate becomes runoff on the land surface. It includes two models, among them the SCS curve number.
- **Storage in the tree canopy:** This parameter refers to the amount of water that does not reach the soil, since it is taken up by plant surfaces that retain it to later be transpired through the leaves of the plants. To do this, the model uses the numerical curve method, considering canopy storage within surface runoff.
- **Evapotranspiration:** The model estimates potential evapotranspiration through the Penman-Monteith equation. Which includes parameters of latent flux density, evaporation, net radiation, air density, slope of the vapor pressure saturation curve, specific heat and heat flux density.

$$\lambda E = \frac{\Delta * (H_{net} - G) + \rho_{air} * c_p * [e_z^0 - e_z] / r_a}{\Delta + \gamma * (1 + r_c / r_a)}$$

- **Reservoirs or ponds:** This parameter allows the SWAT model to include the volumes of water that are stored within a subbasin. For its modeling, characteristics such as the capacity of the pond, tributaries and drains measured on a daily scale, in addition to infiltration and evaporation, must be taken into account. . Ponds affect supply since water storage is generated that will not be available downstream.
- **Redistribution:** the redistribution of water occurs at the underground level after precipitation or irrigation events that give way to the entry of water into the soil; Redistribution refers to the movement of water from a point close to the soil surface to more distant areas. This depends on the water content in the different soil profiles and is affected by the saturated conductivity of the medium and the temperature.

- **Lateral flows:** The simulation of subsurface flows is developed through a kinematic storage model. Lateral flows are related to redistribution since both processes develop below the soil surface. However, these do not occur within the same profile, but, similar to surface runoff, they are generated horizontally.
- **Base flow:** Return flows are calculated by SWAT based on the establishment of two aquifer systems, the first is related to flows within the basin, while the second contributes to the return flow of streams that are outside the basin.
- **Routing phase of the hydrological cycle**

This phase considers the losses due to evaporation while the water flows within the basin and the channel, for its modeling SWAT determines the frequency and speed of the flow in the HRU through the Manning equation, likewise, it uses the hydrological transit method. of Muskingum to model the volumes that are stored along the length of the channel.

The SWAT model considers that the channels that make up the basins have a trapezoidal shape, in this way it simplifies the calculation of flows by requiring as input data the depth of water in the channel, the width of the channel and the length of the main channel.

$$q_{ch} = \frac{A_{ch} * R_{ch}^{\frac{2}{3}} * slp_{ch}^{1/2}}{n}$$

$$v_c = \frac{R_{ch}^{2/3} * slp_{ch}^{1/2}}{n}.$$

Where

A_{ch} = Cross-sectional area of flow in the channel

q_{ch} = Flow rate in the channel

R_{ch} = Radiohydraulic

slp_{ch} = Longitudinal inclination of the channel

n = Manning's coefficient

v_c = Flow Speed

From the flow and speed index, calculated with the Manning equation, the Muskingum method is used to calculate the storage volumes of the channels. This method develops the simulation by considering several segments within the channel that are affected. due to the entry and exit of water from each one, in addition to the storage that occurs in cases where the entry of water is greater than the exit.

This method assumes that the cross-flow area is directly proportional to the water discharge for a channel segment, as assumed by applying the Manning equation. Based on the above, the storage volume can be calculated based on the discharge on a time scale, which in turn is determined by the storage ratio, the flow stored in a segment of the channel is calculated through the following equation::

$$V_{stored} = K * q_{out} + K * X * (q_{in} - q_{out})$$

Where

V_{stored} = Volume stored in the segment

q_{in} = Segment inlet flow

q_{out} = Segment outlet or discharge flow K

K = Storage time in segment

X = Factor that relates relative importance of inflow and outflow

3.1.6 TETIS MODEL

TETIS is a physically based and distributed model that represents the hydrological cycle through five tanks that are perfectly interconnected (interception, static storage, surface, gravitational storage, aquifer), the flow between the tanks is a function of the water stored in them. The water balance represented by the tanks is carried out for each cell and is presented in figure 56 (Universitat Politècnica de València, 2014).

- **Interception:** It represents the water intercepted by the plant cover and

only leaves it by evaporation of the leaves. Until this tank is filled, water is not allowed to pass to the following tanks. The amount of water that enters this tank is calculated as follows (Universitat Politècnica de València, 2014):

$$D_6 = X_1 - X_6$$

$$X_6 = \text{Max}(0, X_1 - \lambda_v * I_{m\acute{a}x} + H_6)$$

Where:

D_6 = Amount of precipitation entering the interception tank x

X_6 = Shallow rain

X_1 = Direct precipitation

$I_{m\acute{a}x}$ = Interception tank max. storage (depends on vegetation type)

λ_v = Vegetation factor that modifies the $I_{m\acute{a}x}$ (one value for each month)

Current amount of water in the tank:

$$H_6 = H_6 + X_1 - X_6$$

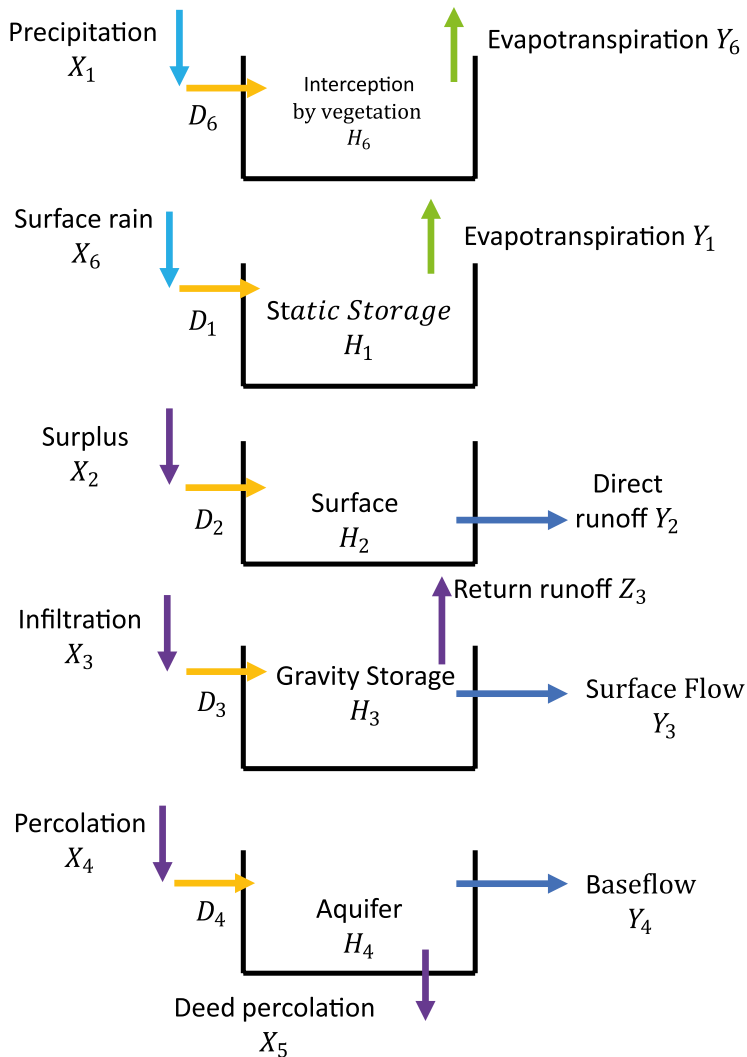
The direct evaporation that occurs in the interception tank is calculated as

$$Y_6 = \text{Min}(ETP * \lambda_v * FC_2, H_6)$$

Where

FC_2 = Correcting factor close to one

ETP = Potential evapotranspiration

Figure 56. *TETIS model tank diagram*

Source: adapted from Universitat Politècnica de València (2014).

- Static storage and evapotranspiration:** This tank represents the water that passes through the basin and leaves it by evapotranspiration, it is not part of the runoff (detention of water in puddles), this water is retained in the soil by capillary forces. The amount of water that enters this tank depends on the moisture content, the characteristics of the soil and the surface rainfall, as follows (Universitat Politècnica de València, 2014):

$$D_1 = \text{Min}[(X_6 + Y_0) \left(1 - \frac{H_1}{H_u * FC_1}\right)^{p_1}, H_u * FC_1 - H_1]$$

Where:

Y_0 = Snow melting contribution

H_1 = Water content in static storage tank

p_1 = Exponent that determines when there begins to be a surplus (X_2)

FC_1 = Correcting factor close to one

H_u = Maximum storage capacity in the static tank

Note: for a $p_1=0$ It means that for there to be a surplus, the tank must be full. If this exponent is greater than 0, it implies that there is a surplus before the tank is full. FC_1 It means that it increases the storage capacity and vice versa, the water in this tank does not enter the infiltration process.

The excess rain that passes to the surface is expressed as

$$X_2 = \text{Max}(0, X_6 + Y_0 - D_1)$$

The evapotranspiration in this tank is expressed as

$$Y_1 = \text{Min}((ETP * FC_2 - Y_6)\lambda_v * f(\theta), H_1)$$

Where:

$f(\theta)$ = Moisture content based on three thresholds

Note: Potential evapotranspiration must be calculated separately, TETIS does not internally include evapotranspiration models, it is recommended to calculate it using the Penman- Monteith method.

- **Surface storage and direct runoff:** This tank represents water that is susceptible to moving across the surface or infiltrating to the lower level. The flow entering the upper tank to the surface storage tank is calculated as follows (Universitat Politècnica de València, 2014):

$$X_3 = \text{Min}(X_2, \Delta t * k_s * FC_3)$$

$$D_2 = X_2 - X_3$$

$$H_2 = H_2 + X_2 - X_3 + Z_3$$

Where:

X_3 = Gravitational infiltration

k_s = Field capacity

FC_3 = Correction factor for spatial and temporal scale ($\approx 0,2$)

D_2 = Water entering the surface storage tank

H_2 = Storage in the surface tank

Z_3 = Gravity Tank Return Runoff

Note: an increase in the F.C.3 indicates that the hydraulic conductivity of the soil or the infiltration rate is increased, so that a greater part of the flow infiltrates deeper strata.

The direct runoff that travels along the slopes is estimated taking into account the speed with which it travels through the terrain, as follows:

$$Y_2 = H_2 * \alpha_1$$

$$\alpha_1 = 1 - \frac{\Delta x}{v_t * FC_4 * \Delta t + \Delta x}$$

$$v_t = 1,4141 * S_o^{0,5}$$

Where:

α_1 = Direct runoff discharge coefficient

v_t = Vel. of flow (it can be assumed between **0.01 - 1 m/s** 1m/s or calculate it with S_o)

S_o = Slope

FC_4 = Correction factor can vary between **0.01 - 10**

- **Gravitational storage and subsurface flow:** Gravity storage is understood as water stored in the soil, a part of which passes into the aquifer by percolation, another becomes subsurface flow and another can become return runoff. Subsurface flow is that which flows horizontally across the slopes and concentrates in small cracks or conduits in a thin layer of soil (it is what produces landslides) until it exits into the drainage network. Return runoff flow occurs when soil storage exceeds its maximum capacity.

$$X_4 = \text{Min}(X_3, \Delta t * k_p * FC_5)$$

$$D_3 = X_3 - X_4$$

$$H_3 = \text{Min}(H_3 + X_3 - X_4, H_{3\text{máx}})$$

$$Z_3 = \text{Max}(0, H_3 + X_3 - X_4 - H_{3\text{máx}})$$

Where:

D_3 = Amount of water entering the gravity storage tank

X_4 = Percolation

k_p = Percolation capacity-Hydraulic conductivity

FC_4 = Correction factor ($\approx 0,2$)

H_3 = Storage in the gravity tank

H_{3max} = Maximum storage capacity in the gravity tank

Z_3 = Return runoff

The subsurface flow is expressed in terms not only of volume, but also takes into account the transit within the soil, as follows:

$$Y_3 = H_3 * \alpha_2$$

$$\alpha_2 = 1 - \frac{\Delta x}{FC_6 * k_{ss} * \Delta t + \Delta x}$$

Where:

FC_6 = Saturated hydraulic conductivity corrector (0.001-100000)

k_{ss} = Saturated hydraulic conductivity

- **Underground storage and base flow:** This corresponds to the storage in the aquifer, from there comes the base flow that will return to the channel and the deep percolation, which is considered losses of the system. This deep percolation can be estimated in the following way, although it can be assumed to be 0:

$$X_5 = \text{Min}(X_4, \Delta t * k_{PS} * FC_6)$$

$$D_4 = X_4 - X_5$$

Where:

X_5 = Deep percolation

k_{ps} = Percolation rate in the deep soil zone

D_4 = Water entering underground storage

The base flow is also expressed based on the hydraulic conductivity or speed with which water moves in the subsoil as follows:

$$Y_4 = H_4 * \alpha_3$$

$$\alpha_3 = 1 - \frac{\Delta x}{FC_8 * k_{sa} * \Delta t + \Delta x}$$

Where:

Y_4 = Base flow

α_3 = Groundwater discharge coefficient (base flow)

k_{sa} = Saturated horizontal hydraulic conductivity of the substrate

FC_8 = Correction factor (0.001-100000)

3.1.7 COMPARISON OF HYDROLOGICAL MODELS

Below is a brief comparison between the hydrological models described above and some other models that can be evaluated for use in this type of analysis.

Table 31. Comparison of hydrological models

Model	Classification by spatial variability	Classification by Cognitive degree	Interface	General Characteristics
TOPMODEL	Semi-distributed by topographic index of humidity	Physically based	Fortran/R	Model explicitly interactions between surface water, subsurface and underground. Performs water balance in the soil and depends on the topographic humidity index (Tarboton, 2003).
HEC-HMS	Semi-distributed by subbasins	Physically based	Own	Designed for modeling processes in basins dendritic, can model transit of floods and continuous time. The continuous time model is based on a tank model (SMA) (US Army Corps of Engineers, 2000).
S.W.A.T.	Semi-distributed by hydrological response units	Physically based	CHALK	Developed for predict the impact of soil management practices on the generation of water, sediments and chemicals agricultural in basins complex. Includes the curve number model, plus a complete water balance in the soil (Netsch et al., 2011).

Model	Classification by spatial variability	Classification by Cognitive degree	Interface	General Characteristics
TETIS	Distributed by rectangular cells	Physically based	Own	Results can be obtained at any two points in the basin, improving the representation of spatial variability. Time intervals ranging from 10 minutes to 1 day can be modeled. The water balance is calculated using 5 interconnected tanks (Universitat Politècnica de Valencia, 2014).
GR4J	Aggregate	Conceptual	Own - RS-MINERVE	It is an aggressive model, although it can become demigod tributed if modeled several sub-basins connected. Make a simple water balance including only 4 parameters: maximum tank capacity of production, coefficient exchange client of groundwater, maximum capacity of transit in canals and hydro base time UH1 grass (Carvajal and Roldán, 2006).

Model	Classification by spatial variability	Classification by Cognitive degree	Interface	General Characteristics
MIKE SHE	Semi-distributed	Physically based	Own	Use MIKE Hydro River to simulate flow in the channel. Includes the Richards equation for infiltration and the Darcy equation for groundwater flow, Additionally, it performs wave modeling diffusive for surface runoff (DHI, 2017).
TOPKAPI	Distributed by cells square	Physically based	CHALK	TOPographic Kinematic Approximation and Integration has in account equations kinematic wave in combination with topography, parameter values are assigned physical to each cell and movement is generated in cells with a difference scheme finite (Todini and Mazzetti, 2008).
USGS-PRMS-IV	Semi-distributed by HRU	Physically based	Fortran	The hydrological cycle is simulated by 17 processes and 39 modules (Markstrom et al., 2015)

Source: own elaboration.

3.2 MODELING EXAMPLE HYDROLOGICAL – LA NEGRA CREEK, ÚTICA, CUNDINAMARCA

3.3 DESCRIPTION OF THE CASE STUDY – EXAMPLE

The La Negra stream is located in the municipalities of Útica (lower basin) and Quebradanegra (Upper basin), Cundinamarca, it originates in Alto el Palmar on the border between the municipalities of Villeta and Quebradanegra with the name of El Naranjal stream; Its basin is located between levels 2,065 and 497 meters above sea level. The municipality of Útica is located on the right bank of the La Negra stream at its mouth with the Negro River (Institute for Research in Geosciences, Mining and Chemistry and National University of Colombia , 2009).

Deforestation processes have been consistently generated in the basin, which has increased the detonation of landslides, which are already common due to the intrinsic instability of the geological materials, which are mainly composed of silt and clay. This, added to the high slopes and constant rains, has triggered several mud and debris flows events that have affected the urban area of the municipality of Útica.

The example case study, for which the modeling and calibration of the models was carried out, was that of November 17, 1988, a mud and debris flows event that affected the urban area of the municipality of Útica, Cundinamarca, causing the loss of 3 lives. human injuries, floods, damage to the railway bridge, the cemetery and other town facilities.

It was identified that during the 30 days prior to the event, 470 mm of precipitation fell in the basin, an estimated rainfall value with a return period of 50 years. These heavy rains generated the damming of the La Papaya stream, a tributary of the La Negra stream. This natural dam broke, generating a sludge flow that added to the flow generated by multiple landslides in the upper basin of the La Negra stream. This sludge flow caused the flooding of the municipality of Útica with depths of 0.2 – 1.5 m and the dragging of large rock blocks (Institute for Research in Geosciences Mining and Chemistry and National University of Colombia, 2009).

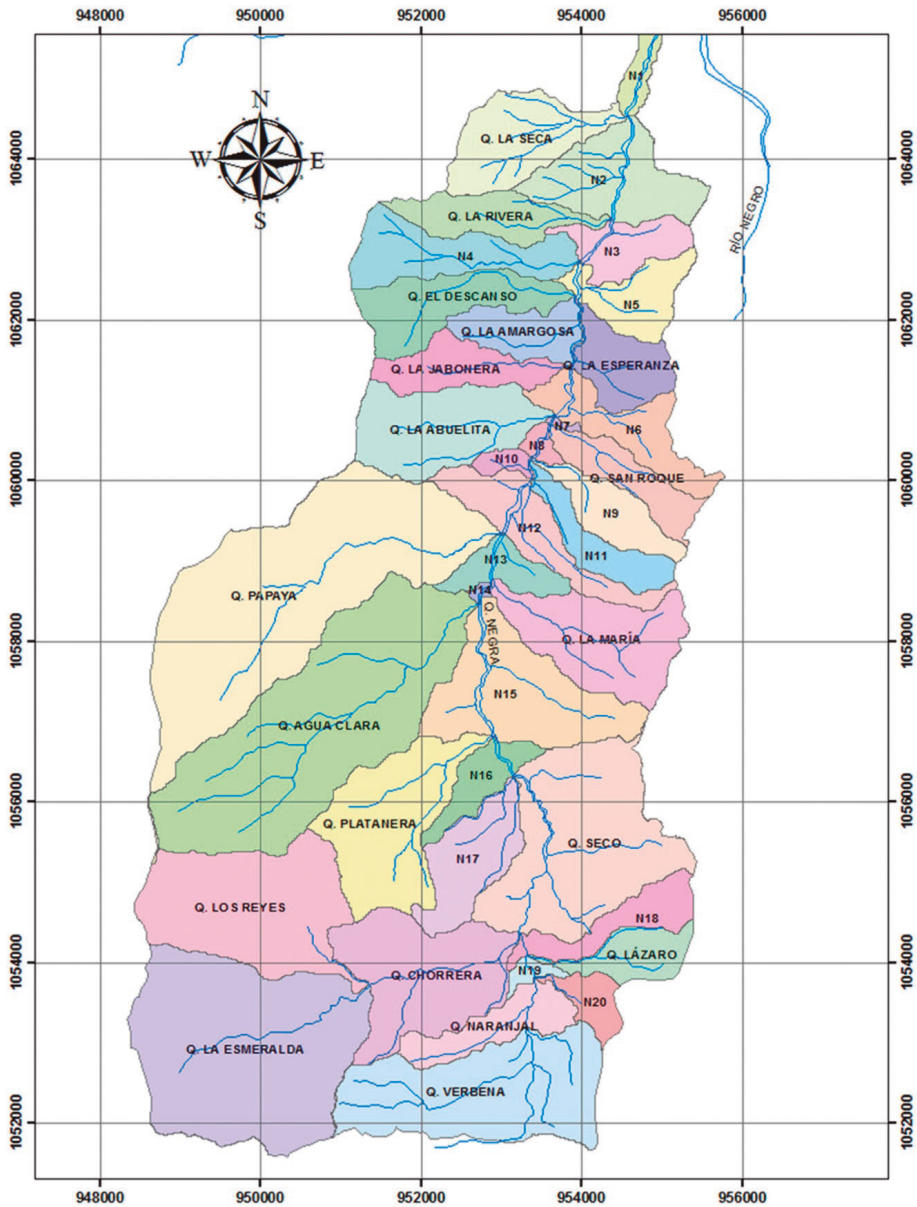
This modeling example was taken from one of the authors of this book and can be found in detail in (Páez, 2016); Although it presents some small differences with the methodology presented here, it generally follows the same methodological steps proposed in this document. Figure 57 shows the satellite image with the main tributaries of the La Negra stream, while figure 58 shows each of the sub-basins into which the basin was divided.

Deforestation processes have been consistently generated in the basin, which has increased the triggering of landslides which are already common due to intrinsic instability of geological materials, which are mainly composed of silt and clay. This, added to the high slopes and constant rains, has triggered several mud and debris flows events that have affected the urban area of the municipality of Utica

Figure 57. *Main drainages of La Negra stream*



Source: Páez (2016).

Figure 58. *La Negra creek sub-basins*

Source: Páez (2016).

3.2.2 TOPMODEL IMPLEMENTATION OF QUEBRADA LA NEGRA, ÚTICA, CUNDINAMARCA

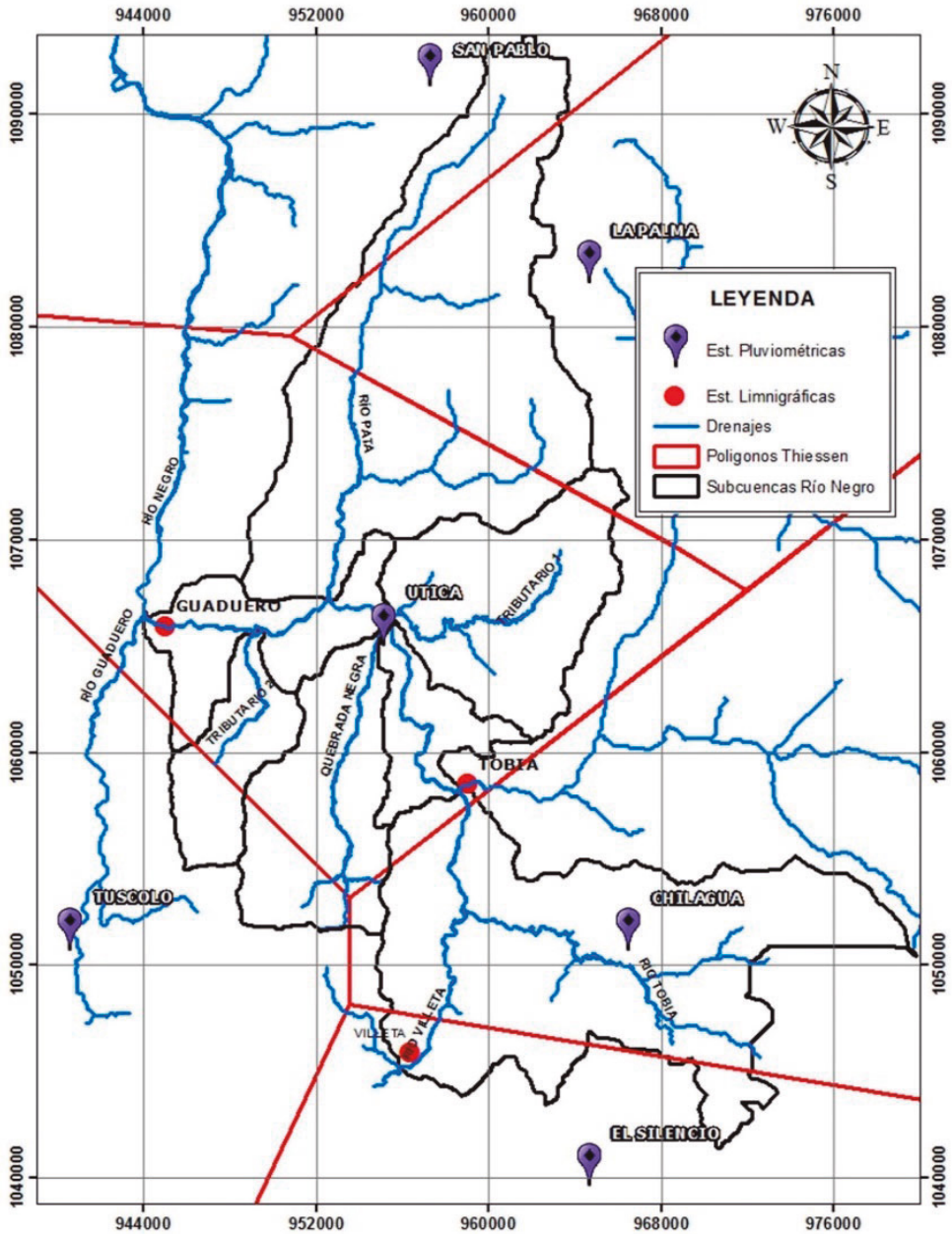
The hydrological model implemented in this case study corresponds to the TOPMODEL, its implementation is described below.

- **Precipitation analysis**

For the precipitation analysis, 3 rainfall stations located in the Negro River basin and the La Negra stream sub-basin were used. Thiessen polygons were made (see figure 59) to determine the area afferent to each of the stations; these have daily information (Páez, 2016).

For the precipitation analysis, 3 rainfall stations located in the river basin were used. Negro River and sub-basin of La Negra creek.

Figure 59. Thiessen polygons Black River subbasins



Source: Páez (2016).

- **Evaporation analysis**

Because there was no climatological information to calculate evapotranspiration, an approximation was made with the evaporation of the tank from the station closest to the La Esperanza basin (23025020). The evaporation of the tank was corrected with the FAO coefficients (see table 32) taking into account that the average relative humidity of the area was 75.1% and in accordance with the Colombia Wind Atlas 1.5 – 2 m/s (Institute of Hydrology, Meteorology and Environmental Studies [IDEAM] and Mining and Energy Planning Unit [UPME], 2006).

$$Ev_{QN} = Ev_{es} * C$$

Where:

Ev_{QN} = Daily evaporation in the La Negra stream basin

Ev_{es} = Daily evaporation at La Esperanza station

C = Evaporimeter tank coefficient

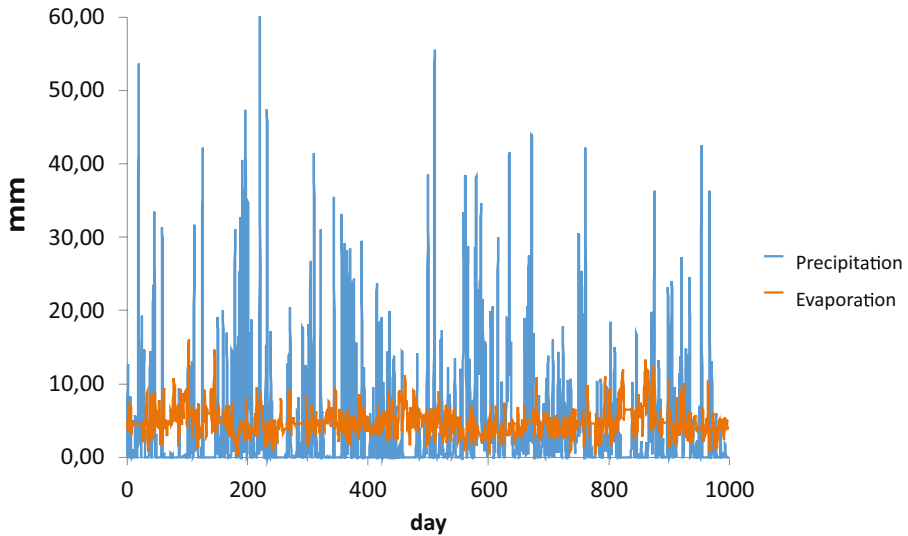
Table 32. *Evaporimeter tank coefficient type A*

Average HR		Low <40%	Average 40 %-70 %	High > 70 %
Wind speed (m/s)	Distance from the cul-windward (m)			
Low < 2	1	0.55	0.65	0.75
	10	0.65	0.75	0.85
	100	0.7	0.8	0.85
	1000	0.75	0.85	0.85

Average HR		Low <40%	Average 40 %-70 %	High > 70 %
Wind speed (m/s)	Distance from the cul-windward (m)			
Moderate 2 - 5	1	0.5	0.6	0.65
	10	0.6	0.7	0.75
	100	0.65	0.75	0.8
	1000	0.7	0.8	0.8
High 5 - 8	1	0.45	0.5	0.6
	10	0.55	0.6	0.65
	100	0.6	0.65	0.7
	1000	0.65	0.7	0.75
Very high > 8	1	0.4	0.45	0.5
	10	0.45	0.55	0.6
	100	0.5	0.6	0.65
	1000	0.55	0.6	0.65

Source: Allen et al. (2006).

Figure 60. *Precipitation and evaporation La Negra creek basin (April 8, 1987 – December 31, 1989)*



Source: Páez (2016).

- **Flow rates for calibration**

Because on the date of the event there was no information on measured flows or levels, it was necessary to calculate an approximate flow based on the difference in flows measured at 2 stations on the Negro River, upstream Tobia (2306706) and downstream. Guaduro (2306705) and taking into account the areas of the tributary drainages to the Negro River in that section, according to the following (Páez, 2016):

$$Q_G - Q_T = Q_v + Q_n + Q_{t1} + Q_p + Q_{t2}$$

Where:

Q_G = Guaduro station flow

Q_T = Tobia station flow

Q_v = Villeta River flow

Q_n = La Negra creek flow

Q_{t1} =Tax flow 1

Q_p =Patá river flow

Q_{t2} =Tax flow 2

Since there are no measured flows for each of the tributaries, a percentage of the flow of the section was assigned ($Q_G - Q_T$) according to the precipitation of each one of the subbasins and its potential runoff according to the following formula, obtaining the flows presented in figure 61.

$$C_n = \frac{V_n}{\sum V_i} * 100$$

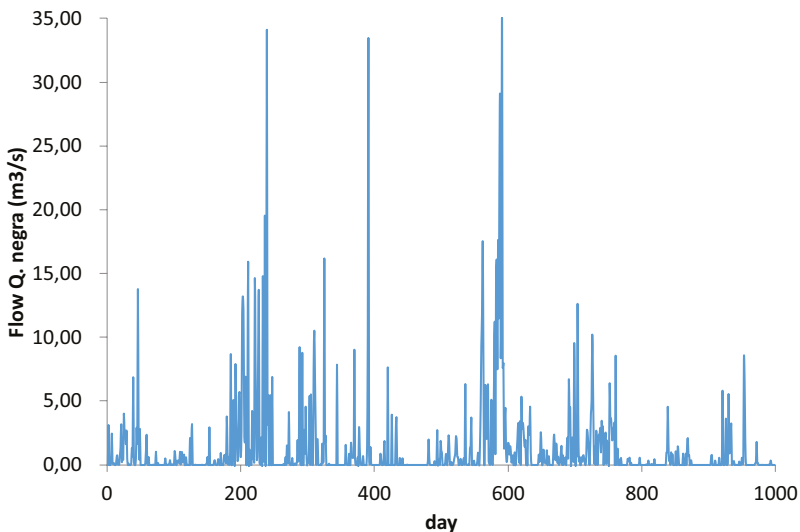
Where:

C_n = Percentage of the flow of the section ($Q_G - Q_T$) corresponding to Q. La Negra

V_n = Daily precipitation volume Q. La Negra

V_i = Daily precipitation volume in each of the sub-basins of the section

Figure 61. *Estimated flows for La Negra creek calibration (April 8, 1987 - December 31, 1989)*



Source: Páez (2016).

- **Calculation of the topographic humidity index**

The topographic humidity index was calculated using the following expression:

$$ITH = \ln\left(\frac{a}{\tan \beta}\right) \text{ (Ec. 32)}$$

Where:

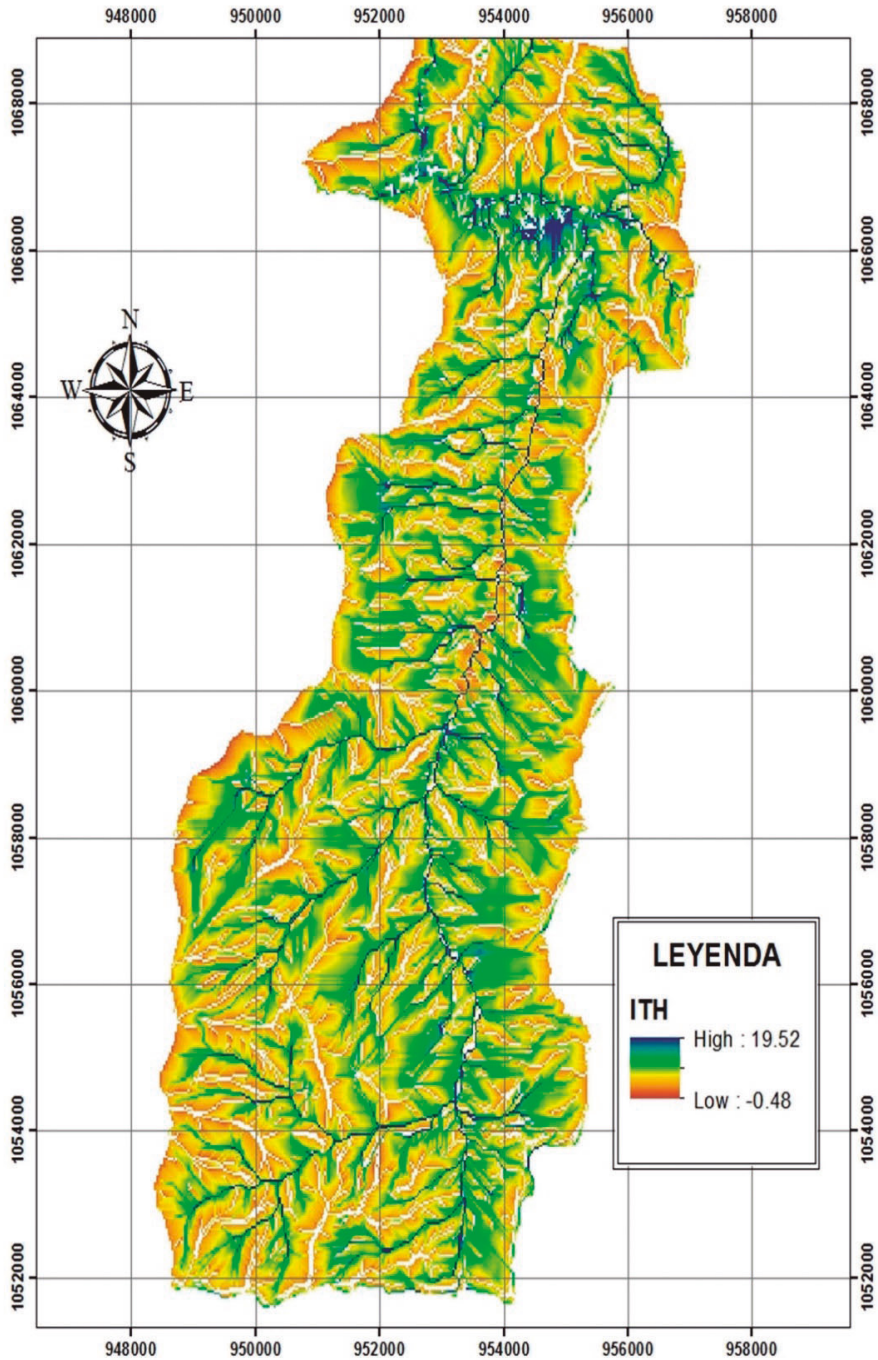
ITH = Topographic humidity index

a = Local area draining to each calculation point (flow accumulation)

β = Terrain inclination angle

Figure 62 shows the map of the topographic humidity index for the La Negra stream basin. A high value of the ITH indicates areas with a higher concentration of runoff and therefore more prone to saturation.

Figure 62 shows the map of the topographic humidity index for La Negra stream basin. high value of the ITH indicates areas of greater concentration of runoff and therefore more prone to saturation

Figure 62. *La Negra creek humidity topographic index*

Source: Páez (2016).

- **Model Calibration**

For the calibration of the TOPMODEL, the base flow of the stream was first taken into account, for which 4 gauges were used with tracers on the La Negra stream carried out on July 26, 2006 in a very dry season by the Research Institute in Geosciences Mining and Chemistry (INGEOMINAS), resulting in an approximate base flow of 178.7 L/s.

The calibration of the model was carried out through Monte-Carlo simulations, giving random values to the model parameters in the initial ranges suggested by Beven and Kirkby (1979) and subsequently taking into account the results of a first calibration, the ranges were modified. in order to obtain a more satisfactory calibration (Páez, 2016).

Table 33. TOPMODEL parameter calibration ranges

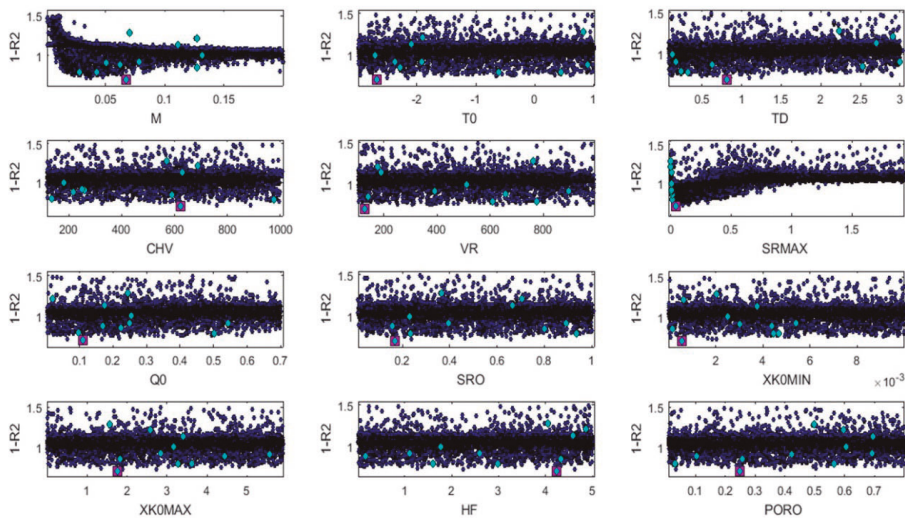
Parameter	Starting rank	Modified range
m (m/m)	0.0001 – 0.2	0.0001 – 0.15
To (ln(m ² /h))	-2 – 1.0	- 3 – 1.0
SRmáx (m)	0.1 – 3.0	0.0005 – 1.0
SRO (m)	0.01 – 2.0	0.01 – 1.0
CHV (m/h)	100 - 2500	100 - 1000
VR (m/h)	100 - 2500	100 - 1000
Td (h/m)	0.01 – 3.0	0.005 – 3.0
Qo (m/day)	0.001 – 1.0	0.001 – 0.7
dθ(-)	0 – 5.0	0 – 5.0

Parameter	Starting rank	Modified range
XK _{mín} (m/h)	0 – 0.01	0 – 0.01
XK _{máx} (m/h)	0.1 – 5.0	0.1 – 6.0
Poro (-)	0.01 – 0.6	0.01 – 0.8

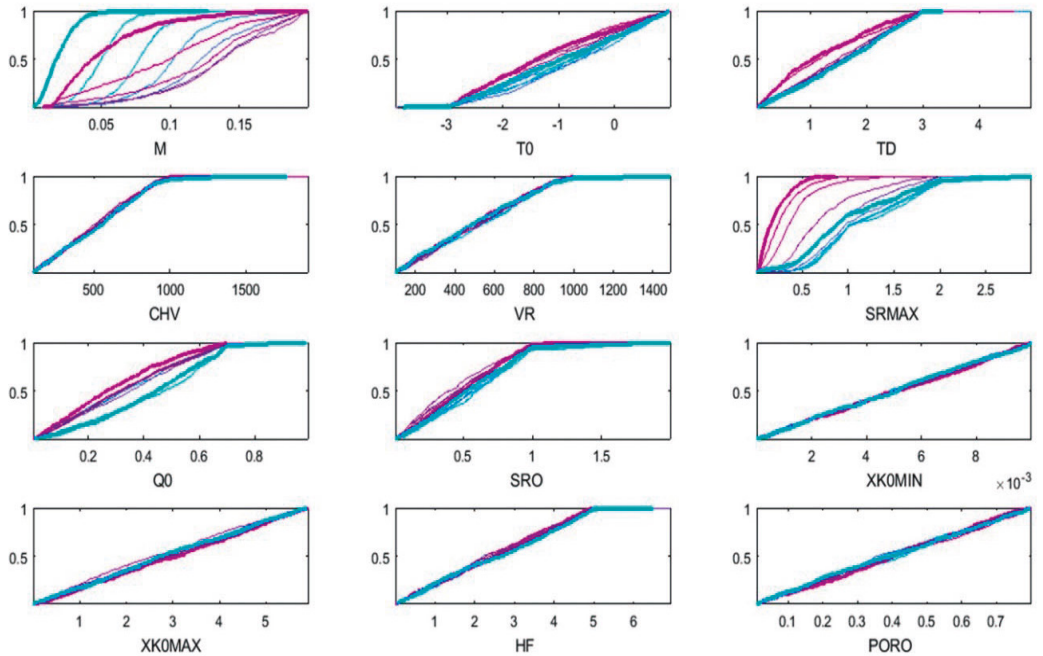
Source: Beven and Kirkby (1979).

A sensitivity analysis of the parameters was carried out using the GLU methodology, which is presented in Figure 63, where the light blue points correspond to the 10 best simulations for each parameter. Additionally, Figure 64 presents the sensitivity of the parameters, where it is observed that most of the parameters are poorly identifiable and have optimal values throughout the calibration range. However, the parameter m is quite identifiable with optimal values between 0.025 and 0.05 and SRMAX which has optimal values that have zero. It is also observed that it is possible that there is some parametric interaction between T_0 and M ; Because T_0 is poorly identifiable for optimal values of m , it may not result in satisfactory simulations. The parameters CHV, VR, XK₀MIN, XK₀MAX, HF and PORO are completely insensitive, so any value within the calibration range could give both good and bad Nash coefficients (Páez, 2016).

Figure 63. Fit to the objective function for each TOPMODEL parameter



Source: Páez (2016).

Figure 64. Regional sensitivity of TOPMODEL parameters

Source: Páez (2016).

Finally, Table 34 presents the results of direct runoff $q(i)$, subsurface flow q and excess saturation flow for the 5 best runs of the TOPMODEL for the day of the analyzed mud and debris flows event.

Table 34. Results November 17, 1988 for the top 5 simulations

Nash coef.	$q(i)$ (m/day)	qof (m/day)	q (m/day)
0.304	1.31E-02	5.77E-03	3.71E-03
0.258	1.62E-02	2.93E-03	5.10E-03
0.275	1.36E-02	5.77E-03	2.87E-03

Coef. Nash	q(i) (m/day)	qof (m/day)	q (m/day)
0.287	1.64E-02	5.77E-03	5.39E-03
0.286	1.48E-02	5.77E-03	4.65E-03
Promedio	1.48E-02	5.20E-03	4.34E-03

Source: Páez (2016).

3.3 MODELING OF TRIGGERING MECHANISMS – LANDSLIDES GENERATED BY RAINS

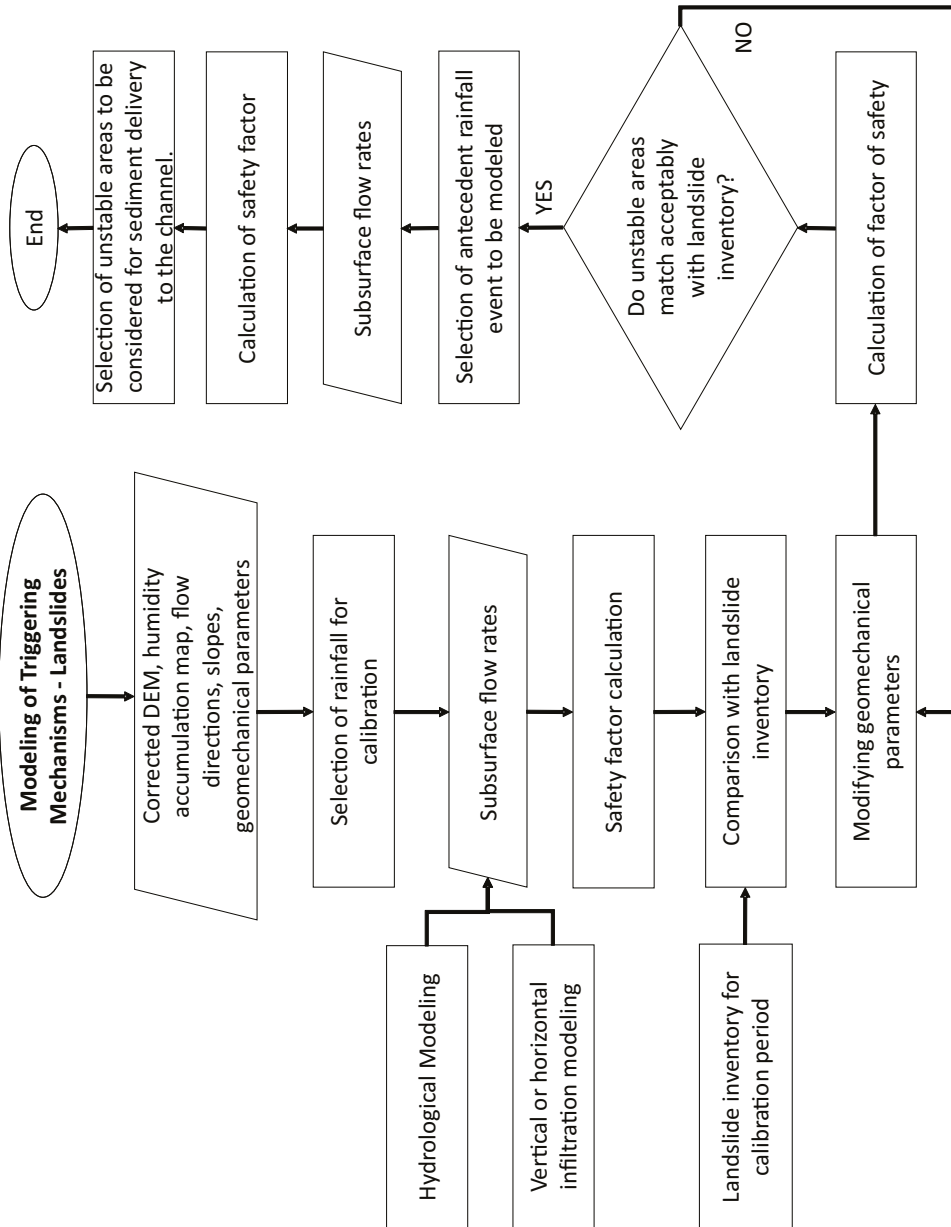
As mentioned in the first section of this document, the causes of mud and debris flows are multiple, however, the most common of them are landslides generated by rain. It is important to emphasize that the trigger is not only a very high intensity rain, but moderate to high intensity rains that occur for several days generate saturation of the soil and instability of the terrain. When a very intense rain is generated, the event is triggered, causing landslides and transport of this along the channel at high speeds; Therefore, the modeling of the landslides must be carried out for the antecedent rain, while the modeling of the propagation of the flood is carried out for the rain triggering the event.

There are various approaches for modeling slope stability, some more complex than others, most models take into account an approximation to the flow of water in the soil, modeling the flow horizontally, while other more complex models carry out the vertical flow modeling, model selection will depend on the amount of information available and the purpose of the study. The limitation of these models is that they allow the calculation of unstable areas but not the probability of occurrence, which would be necessary for a complete threat analysis. However, these unstable areas can be taken as those that provide sediments to carry out the propagation of the mud and debris flows.

Some models such as SHALSTAB produce less detailed results, however, if you have a good landslide inventory and properly calibrate the model it can be a useful and low-cost tool, in combination with qualitative propagation models. While if you want to carry out a very detailed analysis you can use the USGS TRIGRS model, which uses the Richards model to calculate vertical infiltration. Now, this document presents an intermediate point with a good level of detail corresponding to the infinite slope model, with which it is possible to calculate the safety factor.

Figure 65 presents the flow diagram of the general process to develop slope stability modeling using quantitative models (infinite slope or TRIGRS, among others).

There are various approaches for modeling slope stability, some more complex than others, most models take into account an approximation to the flow of water in the soil, modeling the flow horizontally, while other more complex models perform vertical flow modeling, model selection will depend on the amount of information available and the purpose of the study.

Figure 65. Modeling of triggering mechanisms - landslides generated by rain

Source: own elaboration.

- Susceptibility is determined by modeling the conditioning factors, while the threat is determined by hydraulic modeling of flood propagation.
- As mentioned in previous sections, if there is a hydrological model that explicitly calculates the subsurface flow rates, these flows can be used to model landslides. Otherwise, simplified infiltration models can be used or, in some cases, the landslide model includes the infiltration model; as is the case of the TRIGRS model that includes the Richards model of vertical infiltration.
- The calibration of the landslide model can be carried out both for the study event (calibration event of the joint mud and debris flows model) if there is sufficient landslide inventory information from previous months, and for a selected time period with good inventory information. of landslides or for the average rainy condition; clarifying that this last scenario will generate high uncertainty, since the landslide inventory used will be the one generated for multiple hydrological conditions and not necessarily for the average condition.
- Landslide models include geomechanical parameters that are the subject of calibration, such as cohesion, the angle of internal friction and the density of the soil, which depend on the slipped soil, here it must be taken into account that it not only depends on the geology. but also of the superficial soils since this last layer is the one that will slide to a greater or lesser extent.
- It is important to consider that these models include water movement parameters in the soil, such as hydraulic transmissivity or hydraulic conductivity, which is why it is important to have field measurements of these parameters, as well as the geomechanical parameters, so that the passage could be avoided. calibration or, failing that, achieve a more satisfactory calibration.
- Once the selected rain event has been simulated, it is necessary to consider the areas with safety factors less than 1. It is possible to take all these areas to simulate the worst possible condition. However, of the unstable areas, it is necessary to evaluate which ones could really contribute sediments to the area. channel according to the proximity to it and its tributaries.

Below, the theoretical foundations of some slope stability models that can be used for the analysis of mud and debris flows are presented.

3.3.1 SHALSTAB MODEL

This is a simple model that can be used if you have little information, however, if you use this model you should also use a qualitative propagation model, since it does not generate enough information to use a quantitative propagation model such as FLO2D, FLATModel or RIVERFLOW2D, unless there is a very good inventory of landslides with which the model can be optimally calibrated (Bateman and Medina, 2019).

The SHALSTAB model is based on the Mohr-Coulomb failure law, in which the shear stress required for the slope to fail is equal to the resistance generated by soil cohesion and the friction resistance due to normal stress. Based on the above, the model assumes that the resistance along the sides and ends is not significant.

Another simplification of the model is that it can assume cohesion as zero or with a spatially constant value, in this way it is possible to carry out the analysis for large areas very quickly. There are other versions of the model in which it is possible to vary the depth and cohesion of the soil spatially and the hydraulic conductivity vertically. According to the above, the expression used by the model corresponds to the following and can be simplified according to the behavior of the parameters of cohesion, depth and hydraulic transmissivity (Dietrich and Montgomery, 1998).

$$\frac{q}{T} = \frac{\sin \theta}{\frac{\alpha}{b}} \left(\left(\frac{C}{\rho_w g z \cos^2 \alpha \tan \phi} \right) + \left(\frac{\rho_s}{\rho_w} \right) \left(1 - \frac{\tan \alpha}{\tan \phi} \right) \right)$$

Where:

q = Subsurface flow (**m/day**)

T = Soil hydraulic transmissivity (**m²/day**)

α = Slope

α/b = Cumulative drainage area per unit flow width (*m*)

C = Soil cohesion (**Pa**)

φ = Internal friction angle

$$P_s = \text{Soil density}$$

$$P_w = \text{Density of water}$$

$$z = \text{Soil thickness (m)}$$

According to the above, the model does not directly calculate the safety factor but rather the saturation necessary for the soil to fail. From the values of this q/T relationship, a stability classification is generated in accordance with what is presented in table 35, taking into account that unconditionally stable implies that no storm can cause it to fail and on the other hand unconditionally unstable indicates that the area is unstable even when completely dry, in both cases it could be rock outcrops (Dietrich and Montgomery, 1998).

Table 35. *Stability classification in the SHALSTAB model*

Stability rating	Condition
Unconditionally stable, saturated	$\tan \alpha < \tan \phi \left(1 - \frac{\rho_w}{\rho_s} \right)$ $\frac{a}{b} > \frac{T}{q} \sin \alpha$
Unconditionally stable, not saturated	$\tan \alpha < \tan \phi \left(1 - \frac{\rho_w}{\rho_s} \right)$ $\frac{a}{b} < \frac{T}{q} \sin \alpha$
Unstable, saturated	$\frac{a}{b} \geq \frac{\rho_s}{\rho_w} \left(1 - \frac{\tan \alpha}{\tan \phi} \right) \left(\frac{T}{q} \right) \sin \alpha$ $\frac{a}{b} > \frac{T}{q} \sin \alpha$ $\tan \phi > \tan \alpha \tan \phi \left(1 - \frac{\rho_w}{\rho_s} \right)$

Stability rating	Condition
Unstable, not saturated	$\frac{a}{b} \geq \frac{\rho_s}{\rho_w} \left(1 - \frac{\tan \alpha}{\tan \phi}\right) \left(\frac{T}{q}\right) \sin \alpha$ $\frac{a}{b} < \frac{T}{q} \sin \alpha$ $\tan \phi > \tan \alpha \tan \phi \left(1 - \frac{\rho_w}{\rho_s}\right)$
Stable, not saturated	$\frac{a}{b} < \frac{\rho_s}{\rho_w} \left(1 - \frac{\tan \alpha}{\tan \phi}\right) \left(\frac{T}{q}\right) \sin \alpha$ $\frac{a}{b} < \frac{T}{q} \sin \alpha$ $\tan \phi > \tan \alpha \tan \phi \left(1 - \frac{\rho_w}{\rho_s}\right)$
Unconditionally unstable, saturated	$\tan \phi > \tan \alpha$ $\frac{a}{b} > \frac{T}{q} \sin \alpha$
Unconditionally unstable, unsaturated	$\tan \phi > \tan \alpha$ $\frac{a}{b} < \frac{T}{q} \sin \alpha$

Source: Dietrich and Montgomery (1998).

Susceptibility in terms of $\log(q/T)$ can be classified according to what is presented in table 36.

Table 36. *Susceptibility classification with SHALSTAB model*

Susceptibility	Log (q/T)
High	<-2,9
Average	<-2,4 y ≥-2,9
Low	≥-2,4

Source: Bateman and Medina (2019).

3.3.2 INFINITE SLOPE MODEL

The infinite slope model is valid for granular soil and initial dry soil conditions, it combines the Mohr-Coulomb failure mechanism with steady-state horizontal flow taking into account the accumulated drainage area and the local slope (Beven and Kirkby, 1979). The model allows calculating the safety factor according to the following expression:

$$FS = \frac{C_r + C_s + \cos^2\theta[\rho_s g(z - D_w) + (\rho_s g - \rho_w g)D_w] \tan\phi}{z\rho_s g \sin\theta \cos\theta}$$

Where:

$$C_r = \text{Root cohesion } \left(\frac{N}{m^2}\right)$$

C_s = Soil cohesion (N/m^2)

θ = Angle of inclination of the terrain (slope)

P_s = Moist soil density (kg/m^3)

P_w = Density of water (kg/m^3)

z = Vertical Soil Depth

D_w = Water table height

ϕ = Internal friction angle

However, since hydrological models provide discharge values from subsurface flow and not from the water table directly, the expression can be simplified to be in terms of subsurface flow according to the following:

$$h = z \cos\theta$$

$$w = \frac{D_w}{z} = \frac{h_w}{h}$$

$$C = \frac{C_r + C_s}{h\rho_s g}$$

$$FS = \frac{C + \cos\theta [1 - wr] \tan\phi}{\sin\theta}$$

Where:

h = Depth in the direction of the slope (**m**)

r = P_w/P_s relative density

The subsurface flow “ q ” per unit length (**m²/h**) corresponds to

$$q = R * a$$

$$a = \frac{A}{b} = \frac{\text{Contributing area (m}^2\text{)}}{\text{Width of the contributing area (m)}} = \frac{\text{m}^2}{\text{m}}$$

Assuming that the hydraulic transmissivity is constant and homogeneous and does not decrease with depth, we have the following expression for w .

$$w = \text{Min}\left(\frac{R * a}{T \sin\theta}, 1\right)$$

The model yields different stability conditions according to the safety factor value as presented in table 37. Like the SHALSTAB model, the unconditionally unstable condition refers to unstable areas in dry conditions, these areas are related to areas very steep that in practice are rocky outcrops that should not be taken into account because they are not going to slide as they are rocks (Bateman and Medina, 2019).

Table 37. *Infinite slope model stability classification*

FS	Stability rating
$FS > 1,5$	Unconditionally stable
$1,5 > FS > 1,25$	Moderately stable
$1,25 > FS > 1,0$	Quasi stable
$1 > FS > 0,5$	Unstable - Lower limit
$0,5 > FS > 0$	Unstable - Upper limit
$0 > FS$	Unconditionally unstable

Source: Pack et al. (2005).

Note: It is possible to develop a susceptibility map for different rain return periods considering that unstable areas for low return periods have a very high susceptibility and vice versa.

3.3.3 STEP TRAMM MODEL

The STEP TRAM model is specially designed for modeling mud and debris flows since it allows modeling the chain reaction of small faults that trigger landslides and also allows modeling the mobilization of material to the main drainages. The model is divided into 3 modules: 1. Landslides, 2. Fault progression, 3. Flow mobilization (ETH Zürich, 2020).

- **Slide module**

This module calculates the average amount of water in the soil column, which progressively affects the mechanical resistance of the soil. The model takes into account that for a slide to be generated there must be an imbalance of the forces exerted on the ground (driving forces and resistance forces), the driving force is composed of the weight of the soil column and the force exerted by neighboring soil columns, while resistance forces include cohesion and friction (ETH Zürich, 2020).

The tensile resistance generated by the failure and which is also transferred to the neighboring soil columns is based on the Mohr-Coulomb criterion and is calculated using the following expression:

$$\tau_t = \frac{2 \sin \phi}{1 + \sin \phi} \rho_w g h \chi + \frac{2 C_s \cos \phi}{1 + \sin \phi} + C_r$$

Where:

ϕ = Internal friction angle

h = capillary pressure

C_s = Soil cohesion

C_r = Root cohesion

X = Coefficient that defines the relationship between capillary force and capillary pressure

While the compressive strength is calculated using the following expression:

$$\tau_c = \frac{2 \sin \phi}{1 - \sin \phi} \rho_w g h \chi + \frac{2 C_s \cos \phi}{1 - \sin \phi}$$

- **Failure progression module**

The model represents the mechanical interactions of the soil through conceptual mechanical links in which it interconnects the neighboring soil columns and the soil-rock interface with well-defined resistance thresholds, in such a way that each link is represented by an FBM or “package of fiber” that breaks at the predefined threshold, however, local failures are generated first that trigger a general failure of the entire column (ETH Zürich, 2020).

The FBM are numerous mechanical elements that are called fibers, when the weakest fibers break, their respective loads are redistributed in the other fibers that can also subsequently break, which triggers a chain reaction of fiber breakage, thus generating the failure of the entire the soil column, also taking into account the neighboring floor columns. The resistance of each fiber is chosen randomly from a Weibull distribution defined as follows (ETH Zürich, 2020):

$$p(\sigma_{th}) = \frac{m}{k} \left(\frac{\sigma_{th}}{k} \right)^{m-1} \exp \left(- \frac{(\sigma_{th})^m}{k} \right)$$

- **Flow Mobilization Module**

The model is coupled with simple estimates of landslide flow distances and trajectories, very similar to empirical models. STEP TRAMM implements the empirical model proposed by Rickenmann in 1999 which relates the landslide volume () with the difference in elevation between the liberation of the mass and the deposition () and finally the length between both points () as follows (ETH Zürich, 2020):

$$L = 1.9V^{0.16}H^{0.83}$$

$$L = 15V^{\frac{1}{3}}$$

The module must be calibrated with observed landslide and earth flow data.

3.3.4 TRIGRS MODEL – USGS

The Transient Rainfall Infiltration and Grid-Bases Regional Slope – Stability Model (TRIGRS) is a model developed by the USGS in Fortran and designed to model shallow landslides triggered by rainfall. This model calculates progressive changes in pore pressure and changes in factor of safety due to rainfall infiltration, including its own one-dimensional vertical infiltration model for saturated and unsaturated conditions.

It is a more complex version of the infinite slope model since in addition to the subsurface flow it includes the flow in the unsaturated zone above the water table or the subsurface flow level through the Richards model of vertical infiltration.

- **Infiltration model for wet initial conditions**

This model is based on the linearized Inversion solution of the Richards equation, in which infiltration depends on the initial depth of the water table and a constant infiltration rate. While the vertical hydraulic gradient is constant and the initial infiltration rate and saturated hydraulic conductivity are a function of the slope. The solution to the vertical infiltration equation using TRIGRS is presented below:

$$\begin{aligned} \psi(Z, t) = & (Z - d)\beta \\ & + 2 \sum_{n=1}^N \frac{I_{nz}}{K_s} \left(H(t - t_n) [D_1(t - t_n)]^{\frac{1}{2}} \operatorname{ierfc} \left[\frac{Z}{2[D_1(t - t_n)]^{\frac{1}{2}}} \right] \right) \\ & - 2 \sum_{n=1}^N \frac{I_{nz}}{K_s} \left(H(t - t_{n+1}) [D_1(t - t_{n+1})]^{\frac{1}{2}} \operatorname{ierfc} \left[\frac{Z}{2[D_1(t - t_{n+1})]^{\frac{1}{2}}} \right] \right) \end{aligned}$$

Where:

Ψ = Groundwater pressure head

t = Time

$Z = z/\cos\delta$: vertical soil depth

d = Depth of water table for steady state in vertical direction

δ = Slope angle

$$\beta = \cos^2 \delta - \left(\frac{I_{zLT}}{K_s} \right)$$

K_s = Saturated hydraulic conductivity in the direction Z

I_{zLT} = Initial surface flow

I_{nz} = Flux on the surface given by an intensity for a time interval

$D_1 = \frac{D_o}{\cos^2 \delta}$; D_o = is the diffusivity of the saturated hydraulic

$D_o = \frac{K_s}{S_s}$; S_s = is the specific storage

$H(t - t_n)$ = Heaviside function for time flow

The **ierfc** function corresponds to:

$$\operatorname{ierfc}(\eta) = \frac{1}{\sqrt{\pi}} \exp(-\eta^2) - \eta \operatorname{erfc}(\eta)$$

$\operatorname{erfc}(\eta)$ is another complementary error function

Note: This model is very sensitive to initial conditions, so if you do not have reliable field measurements, it is not advisable to use it since it is a very complex model that could lose reliability due to the absence of quality information.

- **Infiltration model for unsaturated initial conditions**

This model treats the soil as a two-layer system, joining the saturated zone with a capillary strip above the water table, superimposed by an unsaturated layer that extends to the soil surface. The unsaturated zone absorbs part of the water that infiltrates and another part passes and accumulates at the base of this zone above the initial water table and therefore raises the water table. This water load propagates downwards as pressure waves. Diffusive by increasing the pore pressure, this process is also described with a one-dimensional form of the Richards equation as follows:

$$\frac{\partial \theta}{\partial t} = \frac{\partial}{\partial Z} \left[K(\psi) \left(\frac{1}{\cos^2 \delta} \frac{\partial \psi}{\partial Z} - 1 \right) \right]$$

$$K(\psi) = K_s \exp(\alpha \psi^*)$$

$$\theta = \theta_r + (\theta_s - \theta_r) \exp(\alpha \psi^*)$$

$$\psi^* = \psi - \psi_o$$

Where:

Ψ = pressure head

Θ = Volumetric water content

Θ_r = Residual water content

Θ_s = Saturation water content

3.4 MODELING OF TRIGGERING MECHANISMS – DAM BREAK

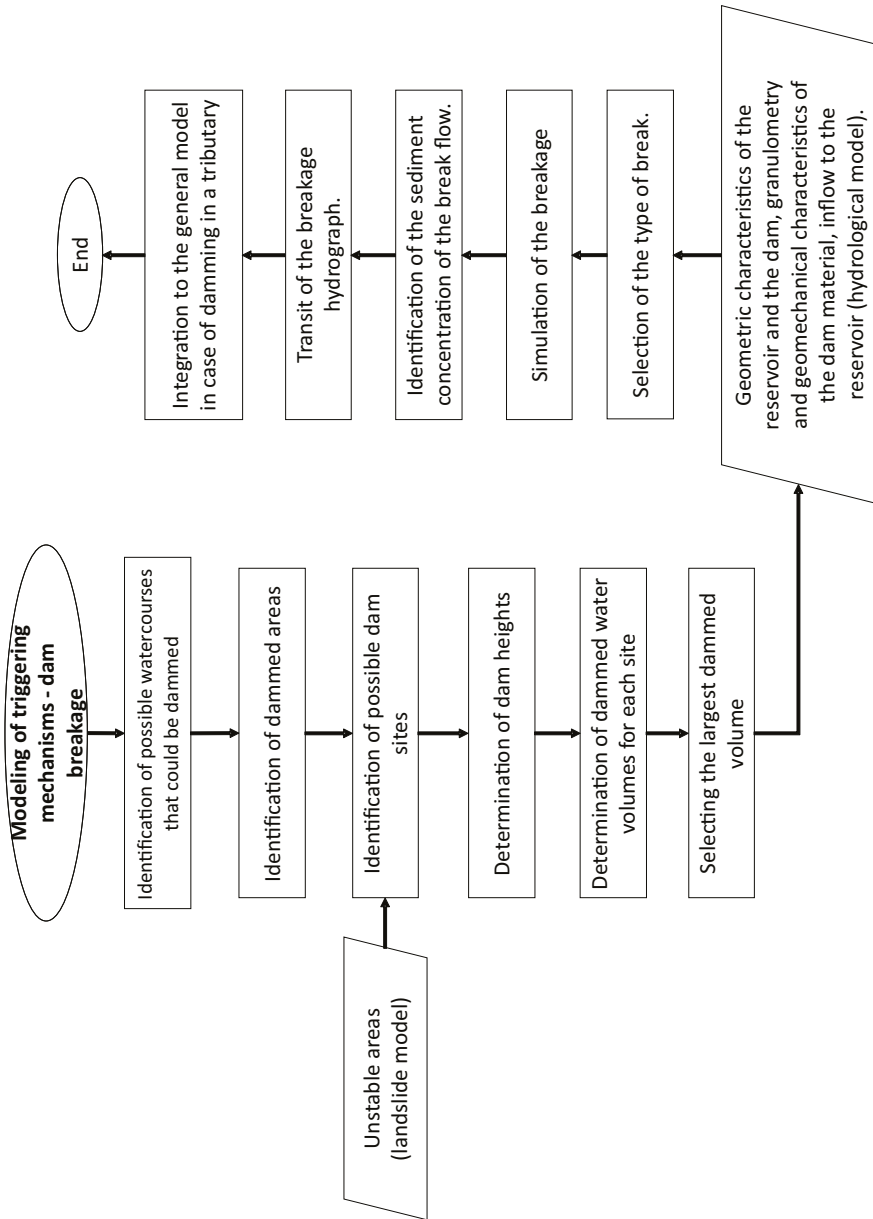
Modeling of natural dams can be carried out independently or jointly with slope stability modeling, since it is not necessarily the landslides themselves that generate the mud and debris flows but the dam itself.

According to the above, the sediments contributed by landslides can be included throughout the basin as explained in the previous section or only the stability analysis is carried out for the areas vulnerable to damming and only the sediments contributed by the damming are included.

Figure 66 presents the general procedure for modeling the failure of natural dams as a trigger mechanism for mud and debris flows and some clarifications regarding this modeling are presented below:

- Natural dams can be generated by landslides in any part of the basin, however, to generate a damming of a sufficient amount of water to detonate a mud and debris flows, relatively large heights are required and in areas where the channel narrows enough for is completely clogged.
- Dam modeling can be subject to calibration, however, it is not usual to have information in this regard, however, the landslide inventory can be taken as a reference and find some large landslides that may be candidates to be the damming generators.
- The landslide generated by the dam can occur many days before the event, so as indicated above, these landslides take into account the antecedent rain; however, the dam breaks when a triggering rain event is generated that generates a flood. of great magnitude that exceeds the dam and erodes it or that generates excess pore pressure and begins to erode due to piping.
- It is important when modeling dam failure to select the failure mechanism, with tubing being one of the most common for natural dams.
- Natural dam failure models take into account the characteristics of the dam material, which is why it is very important to have field information on the geomechanical characteristics of the soil in the area that may possibly slide.
- Dam failure models take into account the area of the reservoir generated by the damming, which is why it is essential to have a DEM of good resolution to make an estimate of the volume and area impounded at a certain point in the channel.

Figure 66. Flowchart modeling triggering mechanisms–dam break



Source: own elaboration.

3.4.1 BREACH DAM BREAK MODEL

There are various physically based and empirical dam failure models, among the most notable are the NWS-DAMBRK, BOSS-DAMBRK and some hydraulic models that include failure moduli. This document describes the BREACH model, which is a physically based model and is designed to model the breaking of natural dams, whether built or generated naturally by landslides; Therefore, it is a good tool for modeling dams that generate mud and debris flows.

The BREACH model models the erosion of the dam and not only its overflow, it also includes a rupture model due to tubing, which is a great advantage over other models that only include rupture due to overflow, which requires very specific conditions for failure, which is why this model can more accurately represent the failure conditions of a dam generated by landslides.

The dam can be made of homogeneous material or two materials: 1) External zone; 2) Inner core, each with different values of cohesion, friction angle, D50 and unit weight. The water face below the dam can have 3 different conditions:

1) Grass cover of specified length of good or fair support; 2) Material identical to the outside of the dam; 3) Material of grain size larger than the outside of the dam.

- **Breakage due to overflow**

To model the failure due to overflow, the model assumes that when erosion begins in the dam, a channel 1 ft deep by 2 ft wide is formed. The flow in this channel is calculated as

$$Q_b = 3 B_o (H - H_c)^{1.5}$$

Where:

Q_b = Flow in the gap channel

B_o = Instant width of initial rectangular channel

H = Water surface elevation

H_c = Gap Bottom Elevation

Once the breakage begins, the speed of the water on the downstream side is calculated with the following expression; however, if the downstream side of the dam contains grass, the flow speed is calculated with the Manning equation.

$$q = 3(H - H_c)^{1,5}$$

$$y = \frac{qn'}{1,49 \left(\frac{1}{ZD}\right)^{0,5}}$$

$$n' = aq^b$$

$$v = \frac{q}{y}$$

Where:

q = Overflow flowftcrest length

$H-H_c$ = Hydrostatic head on the crest in **ft**

n' = Manning coefficient for grassy channels

b = Coefficient given by Chow

ZD = Represents the slope of the downstream face

- **Pipe breakage**

If a pipe break is simulated, the model assumes that the pipe erodes at the same speed up and down, the flow through the pipe can be represented with the orifice equation:

$$Q_b = A \left(\frac{2g(H - H_p)}{1 + \frac{fL}{D}} \right)^{0,5}$$

Where:

Q_b = Flow rate passing through the orifice (**cfs**)

g = Gravity

A = Hole area (ft^2)

$H-H_p$ = Hydrostatic head in the hole (ft)

l = Hole length (ft)

D = Hole diameter (ft)

f = Darcy friction factor

When the dam has eroded sufficiently upwards, the flow begins to be a spillway type, so from that moment on the flow is calculated using the overflow breakage equation, assuming that the gap has a rectangular shape.

$$Q_b = A \left(\frac{2g(H - H_p)}{1 + \frac{fl}{D}} \right)^{0.5}$$

Where:

B_o = Orifice diameter at the moment of transition from piping to landfill

B_r = Factor based on hydraulically optimal section

y = Depth of flow in the gap

However, the gap changes to be trapezoidal when the sides collapse, for which a critical depth is reached that is calculated in the following way, in such a way that the flow can be simulated as uniform with the Manning equation, clarifying that the Manning's should be calculated based on the average diameter of the dam material.

$$H'_k = \frac{4 C \cos \phi \sin \theta'_{k-1}}{\gamma(1 - \cos(\theta'_{k-1} - \phi))} \text{ Para } k = 1,2,3$$

$$a = \cos \theta (1 - 1,54 \tan \theta)$$

$$\theta = \text{Tan}^{-1} S$$

$$R^* = 1524 D_{50} (DS)^{0,5}$$

$$\tau'_c = \frac{0,122}{R^{*0,97}} \text{ Para } R^* < 3$$

$$\tau'_c = \frac{0,056}{R^{*0,266}} \text{ Para } 3 \leq R^* \leq 10$$

$$\tau'_c = \frac{0,0205}{R^{*0,173}} \text{ Para } R^* > 10$$

Where:

H'_k = Critical depth

ϕ = Internal friction angle

k = Successive conditions of collapse

θ = Angle that the gap wall forms with the horizontal

C = Soil cohesion

γ = Unit weight

$$n = 0,013 D_{50}^{0,67}$$

D_{50} = Average grain diameter

- **Sediment transport in the break flow**

The erosion rate of the gap depends on the sediment transport capacity of the breakwater flow. To calculate this solid flow, the model uses the Meyer-Peter and Müller equation for steep channels:

$$Q_s = 3,64 \left(\frac{D_{90}}{D_{30}} \right)^{0,2} P \frac{D^{\frac{2}{3}}}{n} S^{1,1} (DS - \Omega)$$

Where:

Q_s = Sediment flow (**cfs**)

D = Hydraulic depth (**ft**)

$$S = \frac{1}{ZD}$$

$\Omega = 0.0054 \tau_c D_{50}$ no cohesive

$$\Omega = \frac{b'}{62,4} (PI)^{c'} \text{ cohesive}$$

PI = Plasticity index for cohesive soils

b', c' = Empirical coefficients

3.5 MODELING OF TRIGGER MECHANISMS –IN-CHANNEL PROCESSES

The in-channel processes correspond to events in which a large-magnitude flow can generate channel erosion and transport of material, generating sediment concentrations above 20%, although these processes do not generate large-magnitude events, they can be included in channels where erosive processes are evident in the channel. To model this mechanism, the Takahashi equation (19991) is taken into account, the shear stress of the mobilized flow:

$$\tau_m = [(zC + hC)(\rho_s - \rho_w) + (z + h)\rho]g * \cos\alpha * \sin\alpha$$

Where:

z = Thickness of the saturated soil layer

C = Sediment concentration

h = water depth

P_s = Soil density

P_w = Water density

α = Slope

This method allows calculating the equilibrium or maximum limit concentration of sediments that the flow will transport, according to the following:

$$C_{\infty} = \frac{\tan \alpha}{(\rho_s - \rho_w)(\tan \phi - \tan \alpha)}$$

Where:

C_{∞} = Equilibrium sediment concentration

ϕ = Debris flow angle of internal friction

s = Depth\ eroded

Note: It is worth clarifying that the internal friction angle included in the Takahashi equilibrium sediment concentration equation does not necessarily correspond to the angle of repose of the bed material, but to the friction angle of the flow (combination of water and sediment). which generally corresponds to the angle at which the flow stops and begins to deposit, this angle can be measured in the field by observing the deposits of historical flows or can be subject to calibration.

3.6 MODELING OF TRIGGERING MECHANISMS-INCORPORATION OF WASHING LOAD

The washing load corresponds to the sediments contributed by the water erosion of the soil of the basin that is transported with the runoff, this is not as such a triggering mechanism, however, it can contribute sediments, which, added to the landslides, generate a high concentration, generating a non-Newtonian behavior load, especially

when we refer to sludge flows, so this load can be included to carry out a more complete and realistic analysis of the sediment concentration of the flow. The most recommended method for calculating the washing load corresponds to the Universal Soil Loss Equation (USLE), which is described below:

$$E = R * K * LS * C * P$$

Where:

E = Potential soil loss

R = Rain erosivity

K = Erodability factor

LS = Slope length factor

C = Plant cover factor

P = Factor for soil conservation practices

- **Rain erosivity (R)**

Rain can break up soil particles when they fall and these particles are transported by runoff to the channel. This impact of the drops depends on the kinetic energy of the drop, which will therefore depend on the magnitude of the precipitation. To calculate this factor there are various approaches, which are presented below (Díaz-Granados, 2014).

For a precipitation event:

$$E = \sum_{j=1}^n (916 + 331 \log_{10} * I_j) \Delta P_j$$

ΔP_j = Precipitation depth in the interval inches j

I_j = Rain intensity in the interval j (*pulgadas/hora*)

n = Total number of hyetogram discretization intervals

$$R = 0.01 \sum_{i=1}^N (EI_{30})_i$$

N = Number of storms per year

Pérez and Mesa equation (2002) applicable to Colombia::

$$R = 0.00001193P_{ma}^{1,70148}$$

R = Average annual rainfall erosivity factor (KJ/m^2) (mm/h)

PMA = Average annual precipitation (mm/h)

General Diaz-Granados equation:

$$R = 3,49N - 0,1375H_m + 0,1631P_{ma} - 140$$

N = Number of days with average annual rainfall

H_m = Average height of the basin ($msnm$)

P_{ma} = Average annual precipitation (mm)

- **Soil erodibility (K)**

Erodibility is a measure of the susceptibility of soil particles to detachment by rain and transport by runoff. This parameter depends on the following factors (Díaz-Granados, 2014):

- Texture: fine clay-type particles are more resistant due to the formation of cohesive aggregates, while silt and fine sand are less resistant.
- Content of minerals and organic materials that allow the formation of aggregates through chemical bonds.
- Pore size and soil moisture content.

According to the above, the factor can be calculated in the following way:

$$100K = 0,00021M^{1,14}(12 - a) + 3,25(b - 2) + 2,5(c - 3)$$

Where:

$M = \% \text{ particles (0.002 a 0.1 mm)} * (100 - \% \text{ particles (>0.002 mm)})$

a = Organic content

b = Structure index

c = Permeability index

Factors b and c can be determined by literature according to what is indicated in table 38 or the value of the factor can be taken directly from the literature according to what is indicated in table 39.

Table 38. *Structure and permeability indices by texture*

Texture	Structure index	Permeability index
Clayey	1	1
Clay-silty	1	1
Clay-sandy	1	2
Slimy	1	2
Clay loam	2	3
Clay-silt loam	2	3
Clay-sandy loam	2	3
Loamy loam	2	4
Frank	2	4
sandy loam	3	5

Texture	Structure index	Permeability index
Sandy-loam	3	6
Sandy	3	6

Source: Díaz-Granados (2014).

Table 39. *USLE K factor in ton/ha*

Texture	% MO <2 %	% MO >2 %
Clay	0.54	0.47
Clay loam	0.74	0.63
Coarse Sandy loam		0.16
Fine sand	0.20	0.13
Fine sand loam	0.49	0.38
Heavy clay	0.43	0.34
Loam	0.76	0.58
Loamy fine sand	0.34	0.20
Loamy sand	0.11	0.09
Loamy very fine sand	0.99	0.56
Sand	0.07	0.02
Sandy clay loam		0.45
Sandy loam	0.31	0.27

Texture	% MO <2 %	% MO >2 %
Silt loam	0.92	0.83
Silty clay	0.61	0.58
Silty clay loam	0.79	0.67
Very fine sand	1.03	0.83
Very fine Sandy loam	0.92	0.74

Source: Stone y Hilborn (2001).

- **Slope length factor (*LS*)**

The *LS* factor represents the relationship of soil loss for certain standard conditions (9% slope and 22.13 meters of slope length), with respect to the conditions of the basin; The greater and longer the slope, the greater the risk of erosion (Díaz-Granados, 2014). The *LS* factor can be calculated using some of the equations presented below or taken and/or interpolated directly from table 41.

According to Stone and Hilborn (2001):

$$LS = (0,065 + 0,0456S + 0,006541S^2) \left(\frac{L}{22,1} \right)^{NN}$$

Table 40. *NN* factor

S (%)	<1	1 ≤ S < 3	3 ≤ S < 5	≥5
NN	0.2	0.3	0.4	0.5

Source: Stone y Hilborn (2001).

Table 41. *LS factor for different slopes and slope lengths*

Slope length (m)	Slope (%)	LS factor
30.5	10	1.38
	8	1.00
	6	0.67
	5	0.54
	4	0.40
	3	0.30
	2	0.20
	1	0.13
	0	0.07
	61	10
8		1.41
6		0.95
5		0.76
4		0.53
3		0.39
2		0.25
1		0.16
0		0.08

Slope length (m)	Slope (%)	LS factor
122	10	2.76
	8	1.99
	6	1.35
	5	1.07
	4	0.70
	3	0.52
	2	0.30
	1	0.20
	0	0.09
	244	10
8		2.82
6		1.91
5		1.52
4		0.92
3		0.68
2		0.37
1		0.24
0		0.11

Slope length (m)	Slope (%)	LS factor
488	10	5.52
	8	3.99
	6	2.70
	5	2.15
	4	1.21
	3	0.90
	2	0.46
	1	0.30
	0	0.12
	975	10
8		5.64
6		3.81
5		3.03
4		1.60
3		1.19
2		0.57
1		0.36
0		0.14

Source: Stone and Hilborn (2001).

- **Factor C of vegetal cover**

Vegetative cover includes soil loss since it is a protective layer against erosion; additionally, it can absorb part of the energy of rain and thus reduce the erodibility of the soil and the transport of particles. However, this applies to a greater extent for low-lying vegetation cover. The factor C can be calculated using the following expression (Díaz-Granados, 2014):

$$C = C_1 * C_2 * C_3$$

$$C_1 = 1 - \exp(-0,339H * FC)$$

$$C_2 = \exp\left(-b * S_p \left(\frac{0,61}{R_s}\right)^{0,08}\right)$$

Where:

C_1 = Leaf protection that reduces the speed of rain

C_2 = Plant residue in the soil that reduces the rate of runoff

C_3 = Residual effects of land use-organic matter

H = Drop height

FC = Fraction of forest cover

S_p = % covering plant waste

b = 0.05 to 0.07

R_s = Surface roughness (cm)

Table 42. *Vegetation cover factor C_3*

Organic matter content	% MO	C_3 Grass	C_3 Scrub
Very low	10	0.44	0.40
Low	25	0.41	0.32
Medium to low	35	0.40	0.27
Medium	50	0.37	0.21
Medium to high	65	0.36	0.15
High	75	0.35	0.12
Very high	85	0.34	0.11

Source: Díaz-Granados (2014).

The C factor for crops can be taken directly from table 43 and table 44 and multiply both values.

Table 43. *Factor C by type of crop*

Crop type	C-Factor
Corn in grain	0.40
Corn in silo, beans and canola	0.50
Cereals	0.35
Vegetable crops	0.50
Fruit trees	0.10
Hay and grass	0.02

Source: Stone y Hilborn (2001).

Table 44. *Factor type of Tillage*

Ploughing type	C-Factor
Tillage in autumn	1.0
Tillage in spring	0.90
Mulch tillage	0.60
Ridge tillage	0.35
Zone tillage	0.25
No - till	0.25

Source: Stone y Hilborn (2001).

The model used was the infinite slope model implemented within the SINMAP platform compatible with GIS. This model has the advantage that it accepts ranges for geomechanical

- **P Factor of soil conservation practices**

This factor represents the practices used to reduce erosion, this ranges from 0 – 1 where 1 indicates that no conservation practice is used. These practices are related to the type of tillage or cultivation technique (Díaz-Granados, 2014). To determine this factor, literature must be used; some values are presented in Table 45 to Table 47.

Table 45. *P factor for crops at level*

Slope (%)	P factor
1 – 2	0.4
2 – 7	0.5
7 -12	0.6
Slope (%)	P factor
12 – 18	0.8
18 – 24	0.9

Source: Díaz-Granados (2014).

Table 46. *P factor for strip crops*

Slope (%)	P factor
1 – 2	0.45
3 – 5	0.38
6 – 8	0.38
9 – 12	0.45

Slope (%)	P factor
13 – 16	0.52
17 – 20	0.60

Source: Díaz-Granados (2014).

Table 47. *P factor for different agricultural practices*

Practice	P factor
Cross slope	0.75
Contour agriculture	0.50
Cultivation in strips and transverse slope	0.37
Cultivation in strips and contour	0.25

Source: Stone y Hilborn (2001).

3.7 EXAMPLE MODELING OF TRIGGERING MECHANISMS – LA NEGRA CREEK, ÚTICA, CUNDINAMARCA

For the case study of the La Negra stream, Páez (2016) implemented a model of infinite silt conjunction with a dam failure model, this because multiple landslides were generated in the upper basin of the La Negra stream and its Once it is presumed, according to the reports of the risk management entities, that a damming of one of the tributaries corresponding to the La Papaya stream was generated, the implementation of both initiation or trigger models is described below.

3.7.1 INFINITE SLOPE MODEL – SINMAP

The model used was the infinite slope model implemented within the SINMAP platform compatible with GIS. This model has the advantage that it accepts ranges for the geomechanical parameters (friction and cohesion angle) and not a single value, which allows generating a higher threshold. and lower to represent the probability of instability above and below 50% (Pack et al., 2005).

The implementation of the model in GIS requires the following steps: 1. Correction of the DEM, 2. Calculation of the slopes, 3. Calculation of the flow direction with the Tarboton method, 4. Calculation of the catchment area or Flow accumulation, 5. Calculation of moisture accumulation in the basin, 6. Calculation of the stability index and calibration of the geomechanical parameters.

- **SINMAP model calibration**

Because there was no landslide inventory for the flood event to be simulated, the model calibration was carried out for the average rainfall conditions and taking 383 landslides from an inventory carried out by INGEOMINAS (figure 68), however, as shown indicated in previous paragraphs, a certain period of recording time can be selected in which landslide information is available to perform the calibration (Páez, 2016).

In accordance with the above, to include the average rainfall conditions, values of α (where α is the hydraulic transmissivity and the subsurface flow of the TOPMODEL model) between 2000 and 3000. For the calibration of the geomechanical parameters of friction angle, cohesion and soil density, different ranges were assigned for each of the geological units of the basins based on their lithological characteristics and the analysis of the landslide inventory of each unit (Páez, 2016).

Most of the geological units of the basin correspond to fine materials such as siltstones, shales, claystones, sedimentary rocks, d clayey and silty fluvio-torrential deposits, as seen in figure 67 and described in table 48 (INGEOMINAS and National University of Colombia, 2009).

Once the characteristics of the geological units were identified, calibration ranges were established for the geomechanical parameters according to the literature and the analysis of the landslide inventory, as seen in table 49.

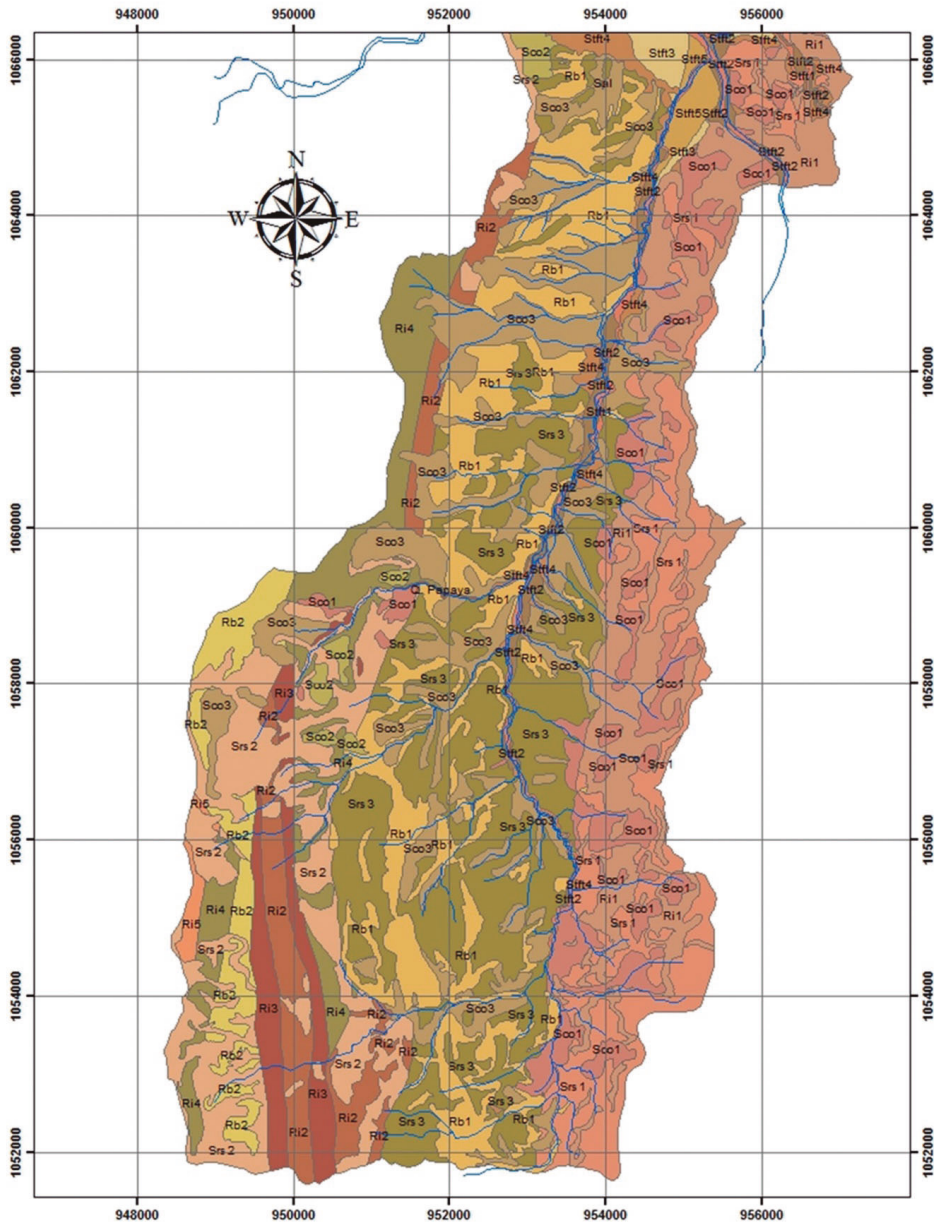
Table 48. *Characterization geological units of La Negra creek basin*

Symbol	Guy	UGS Type
Ri1	Rock Units	Interstratified sequence of occasionally calcareous siliceous claystones and siltstones.
Ri2		Interstratified sequence of calcareous, sometimes siliceous shales and siliceous siltstones.
Ri3		Very thin layers of chert, lydite and siliceous siltstone.
Ri4		Interstratified sequence of siliceous siltstones and occasionally siliceous calcareous mudstones, interbedded with fine to medium quartz sandstones.
Ri5		Black shales, occasionally siliceous and calcareous with sporadic intercalations of limestone and sandstone.
Rb1		Black calcareous shales, with calcareous concretions and intercalations of siliceous limonite occasionally chert and Sandy limestones.
Rb2		Parent rock with fine to medium grain size, predominantly sandy. Sandy with clays and silts in lesser proportion.
Srs1		Rock floor sedimentary
Srs2	From fine-grained parent rock, predominantly silty. Silty with clays and sands in lesser proportion.	
Srs3	Parent rock with fine to very fine grain size, predominantly clayey. Clay with silt and sand in lesser proportion.	

Symbol	Guy	UGS Type
Sco1	Colluvial Floor	Sandy matrix, derived from the rock massifs of the Útica formation. Sandy with silt and clay in a lesser proportion.
Sco2		Silty matrix, derived from the rock masses of the Socotá, Capotes, Hiló, Lidi-ta Interior, Shale and Sandstone Formation and Guaguaqui Group. Silty with sand and clay in a smaller proportion.
Soc3		Clay matrix, derived from the rock masses of the Trincheras formation. Clay with sand and silt in lesser proportion.
Stft1	Torrential fluvial soil	Recent alluvial fans, current main drainage channels. Clay, silty and sandy in different proportions.
Stft2		Alluvial terraces. Clay, silty and sandy in different proportions.
Stft3		Alluvial fans. Fine gravel, silt sand and clay.
Stft4		Dejection cones, sandy, silty or clayey matrix. Matrix of sands, silts and clays in different proportions.
Stft5		Debris flows. Sand-silt and clay-silt matrix.

Source: INGEOMINAS and National University of Colombia (2009).

Figure 67. Geological map of La Negra creek basin



Source: INGEOMINAS and National University of Colombia (2009).

Table 49. SINMAP calibrated parameters

Unit geological	Parámetro	Rango/valor	Referencias bibliográficas utilizadas	Unidad geológica	Parámetro	Rango /valor	Referencias bibliográficas utilizadas
Ri1	ϕ	35 – 45	(Suárez, 1998)	Srs3	ϕ	25 – 35	(Wyllie y Mah, 2004) (Instituto Geológico y Minero de España, 1986)
	C	0,05 – 0,15	(Navarro, 2008) (Instituto Geológico y Minero de España, 1986)		C	0 – 0.13	
	ρ_s	2 150			ρ_s	1 729	
Ri2	ϕ	25 – 35	(Suárez, 1998)	Sco1	ϕ	25 - 35	(Bañon y Bevia, 2000) (Wyllie y Mah, 2004) (Hoek y Bray, 1981)
	C	0,12 – 0,58	(Wyllie y Mah, 2004) (Instituto Geológico y Minero de España, 1986)		C	0 – 0.12	
	ρ_s	2 249			ρ_s	1 878	
Ri3	ϕ	25 – 35	(Suárez, 1998)	Sco2	ϕ	25 - 35	(Bañon y Bevia, 2000) (Wyllie y Mah, 2004) (Instituto Geológico y Minero de España, 1986)
	C	0,12 – 0,58	(Wyllie y Mah, 2004) (Instituto Geológico y Minero de España, 1986)		C	0.12 – 0.58	
		2 249				1 729	
Ri4	ϕ	30 – 40	(Suárez, 1998)	Sco3	ϕ	25 – 35	(Bañon y Bevia, 2000) (Wyllie y Mah, 2004) (Instituto Geológico y Minero de España, 1986)
	C	0,05 – 0,15	(Wyllie y Mah, 2004) (Instituto Geológico y Minero de España, 1986)		C	0 – 0,01	
	ρ_s	2 700			ρ_s	1729	
Ri5	ϕ	25 – 35	(Suárez, 1998) (Wyllie y Mah, 2004) (Instituto Geológico y Minero de España, 1986)	Stft1	ϕ	30 – 40	(Suárez, 1998) (Bañon y Bevia, 2000) (Wyllie y Mah, 2004) (Instituto Geológico y Minero de España, 1986)
	C	0,12 – 0,58			C	0 – 0.01	
	ρ_s	2 249			ρ_s	2 134	

Unit geological	Parámetro	Rango/valor	Referencias bibliográficas utilizadas	Unidad geológica	Parámetro	Rango /valor	Referencias bibliográficas utilizadas
Rb1	ϕ	25 – 35	(Suárez, 1998) (Wyllie y Mah, 2004) (Instituto Geológico y Minero de España, 1986)	Stft2	ϕ	30 – 40	(Suárez, 1998) (Bañon y Bevia, 2000) (Wyllie y Mah, 2004) (Instituto Geológico y Minero de España, 1986)
	C	0,12 – 0,58			C	0 – 0.01	
	ρ_s	1 937			ρ_s	2 163	
Rb2	ϕ	25 – 35	(Suárez, 1998) (Wyllie y Mah, 2004) (Instituto Geológico y Minero de España, 1986)	Stft3	ϕ	30 – 40	(Suárez, 1998) (Bañon y Bevia, 2000) (Wyllie y Mah, 2004) (Instituto Geológico y Minero de España, 1986)
	C	0,12 – 0,58			C	0 – 0.01	
	ρ_s	1 937			ρ_s	2 134	
Srs1	ϕ	30 – 35	(Wyllie y Mah, 2004) (Hoek y Bray, 1981)	Stft4	ϕ	30 – 40	(Suárez, 1998) (Bañon y Bevia, 2000) (Wyllie y Mah, 2004) (Instituto Geológico y Minero de España, 1986)
	C	0,05 – 0,15			C	0 – 0.01	
	ρ_s	1 755			ρ_s	2 134	
Srs2	ϕ	25 – 35	(Bañon y Bevia, 2000) (Wyllie y Mah, 2004) (Instituto Geológico y Minero de España, 1986)	Stft5	ϕ	25 – 30	(Bañon y Bevia, 2000) (Wyllie y Mah, 2004) (Instituto Geológico y Minero de España, 1986)
	C	0 – 0,13			C	0.09 – 0.44	
	ρ_s	1 729			ρ_s	1 729	

Source: Páez (2016).

With the calibration of the model, it was possible to identify that cohesion is a sensitive parameter and that its reduction reduces the stability index, while soil density is the least sensitive parameter, the change in stability in relation to the modification of this. The internal friction angle is the most sensitive parameter of the model, substantially modifying the stability of the slope (Páez, 2016).

According to the above, it is most advisable to carry out field measurements of this type of parameters to achieve simulations with lower uncertainty.

Regarding the parameter / A limit is observed in its sensitivity for values greater than 2,000, while for values less than 1,000 there are substantial changes in the stability of the model (Páez, 2016), this could indicate certain thresholds of precipitation - subsurface flow that generate the instability processes.

Once the model parameters were calibrated with the observed landslides, the stability of the basin was reclassified into 4 categories, according to its safety factor value as presented in table 50 and in this way the stability map was obtained for the average conditions, presented in figure 69.

Table 50. *SINMAP model stability classification*

Stability Classification	Safety factor
Completely unstable	0 – 0,01
Instability lower limit	0,01 – 0,5
Upper limit instability	0,5 – 1
Stable	>1

Source: adapted from Pack et al. (2005).

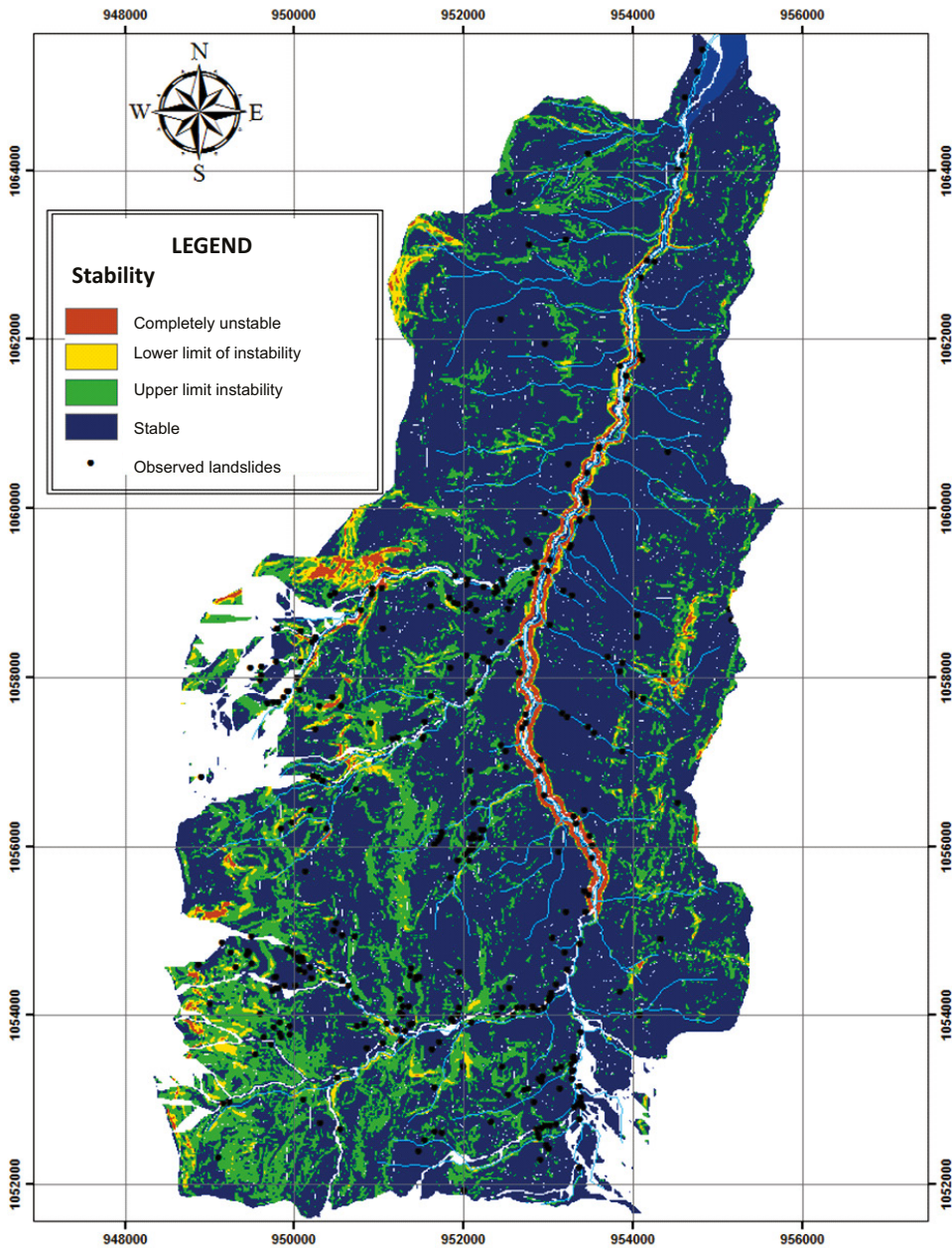
- **Simulation of the conditions preceding the mud and debris flows event of November 17, 1988**

Once the model was calibrated, the subsurface flow conditions of the 30 days prior to the mud and debris flows event of November 17, 1988 were simulated. For this purpose, the subsurface flow values from the TOPMODEL model were taken (R), taking values of T/R between 400 – 550 and obtaining the stability map presented in figure 70.

It is observed that the instability conditions for the days preceding the mud and debris flows event are very different from the average conditions and that the antecedent rain plays a fundamental role in the landslide generation process since many stable areas became unstable, generating the majority of the basin values the safety factor below 1. Subsequently, it will be described which unstable areas were taken as sediment contribution zones to the mud and debris flows flow (Páez, 2016).

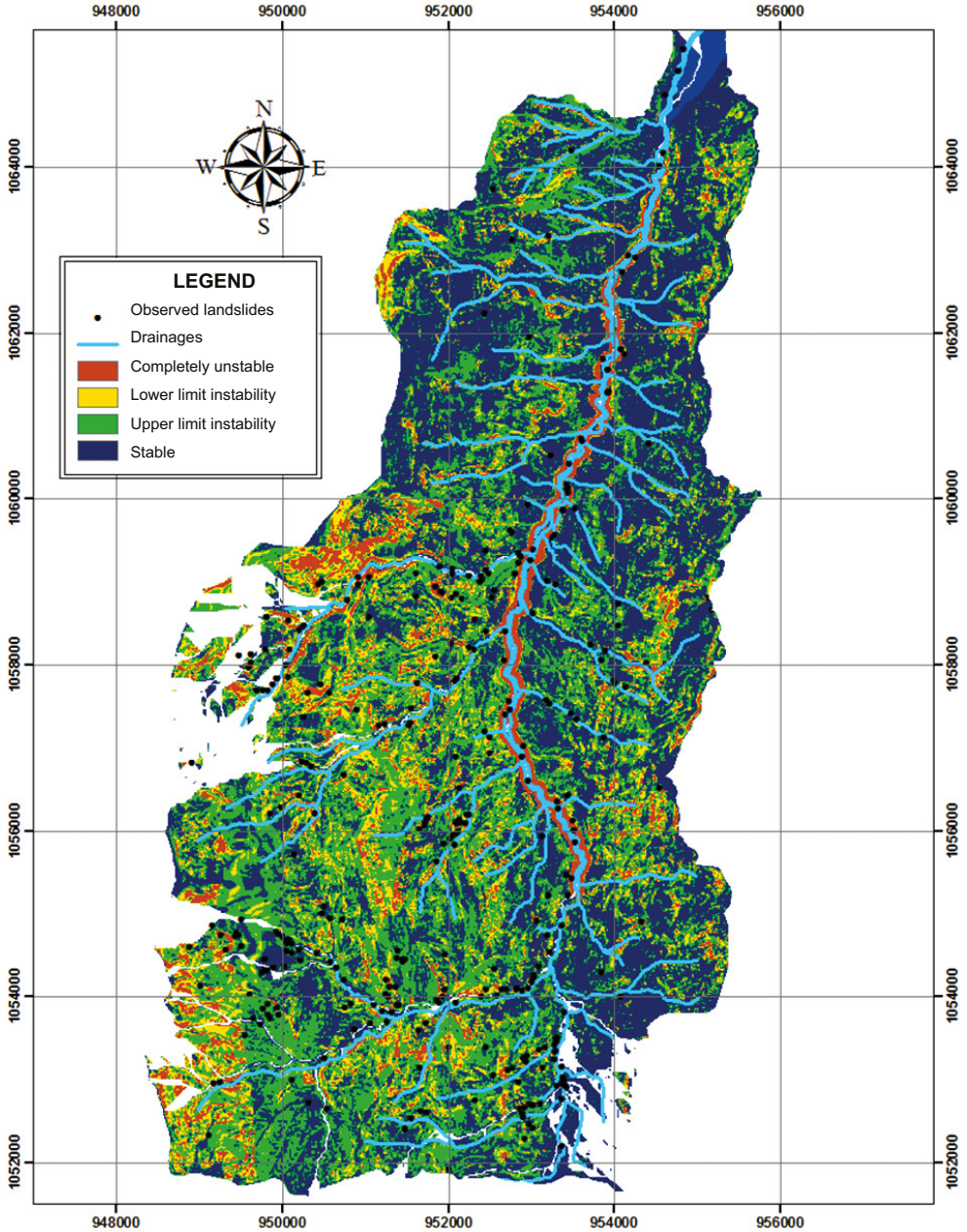
Regarding the parameter λ / A limit is observed in its sensitivity for values greater than 2,000, while for values less than 1,000 there are substantial changes in the stability of the model (Páez, 2016), this could indicate certain thresholds of precipitation - subsurface flow that generate the instability processes.

Figure 69. Stability map for medium humidity conditions of the La Negra creek basin



Source: Páez (2016).

Figure 70. Stability map for humidity conditions preceding the mud and debris flows event of November 17, 1988, La Negra stream basin



Source: Páez (2016).

3.7.2 DAM BREAK MODEL

To model the breakage of the presumed dam generated in the La Papaya stream, a tributary of the La Negra stream, the BREACH model was used and the pipe breakage method was applied, since this breakage is gradual and leads to the removal of almost total of the dam structure (Estudios y Asesorías Ingenieros Consultores Ltda., 2012).

- **Identification of dam sites and heights**

Taking into account that there was no information on the location of the dam for the mud and debris flows event of November 17, 1988, it was necessary to identify, from the landslide model, areas with large landslides in order to determine the possible sites of damming. Once the possible landslide sites were identified, the landslide volume was calculated using a relationship to area vs volume generated from the INGEOMINAS landslide database for each of the geological units (Páez, 2016).

This relationship was calculated in the following way (Suárez, 2009), resulting in the area-volume relationships for each geological unit presented in table 51.

$$\text{Área} = W_r * L_r$$

$$\text{Volumen} = \left(\frac{1}{6} \pi * D_r * W_r * L_r \right) F_{ex}$$

Once the possible landslide sites were identified, the landslide volume was calculated using a relationship between area and volume generated based on the INGEOMINAS landslide database for each geological unit.

Where:

W_r = Width of fault surface (m)

L_r = Fault surface length (m)

D_r = Depth of fault surface (m)

F_{ex} = Soil expansion factor

Table 51. Area-volume relationships for each geological unit

Geological unit	Area (x) vs volume (y) ratio
Ri1	$y = 0.9491x - 148.53$ $R^2 = 0.9992$
Ri2	$y = 0.4227x + 1.0691$ $R^2 = 0.8431$
Ri3	$y = 0.2404x + 1.1677$ $R^2 = 0.8015$
Ri4	$y = 5.5347x - 1208.2$ $R^2 = 0.988$
Ri5	No slipping observed
Rb1	$y = 0.4869x + 1.1838$ $R^2 = 0.784$
Rb2	No slipping observed
Srs1	$y = 14.934x + 0.6939$ $R^2 = 0.6201$
Srs2	$y = 3.0245x - 599.4$ $R^2 = 0.8359$

Geological unit	Area (x) vs volume (y) ratio
Srs3	$y = 0.5222x1.1747$ $R^2 = 0.8314$
Sco1	$y = 0.5026x1.2244$ $R^2 = 0.7572$
Sco2	No slipping observed
Sco3	$y = 0.2477x1.2573$ $R^2 = 0.8903$
Stft1	$y = 2.5876x - 243.91$ $R^2 = 0.9051$
Stft2	$y = 0.1221x1.437$ $R^2 = 0.9857$
Stft3	No slipping observed
Stft4	$y = 0.4784x1.2918$ $R^2 = 0.9168$
Stft5	No slipping observed

Source: Páez (2016).

Finally, from the slid volume, the height of each possible prey was calculated, according to what is indicated below and represented in figure 71.

$$V_d = \left(\left(\frac{(H_p * L/2)}{2} \right) * 2 \right) * B$$

$$\frac{L}{2} = \frac{H_p}{\tan \phi}$$

$$H_p = \sqrt{\frac{V_d * \tan \phi}{B}}$$

Where:

H_p = Dam height (m)

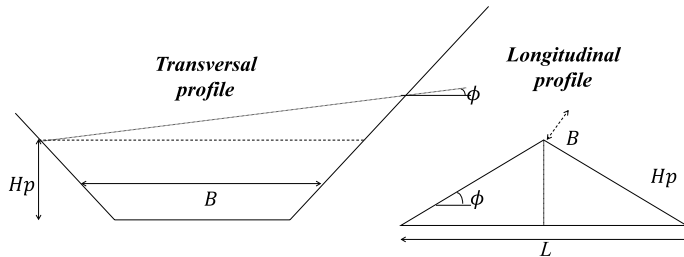
V_d = Slide volume (m³)

L = Dam base length (m)

B = Average width of the cross section of the channel (m)

ϕ = Internal friction angle (degrees)

Figure 71. *Geometry for calculating the depth of dams*



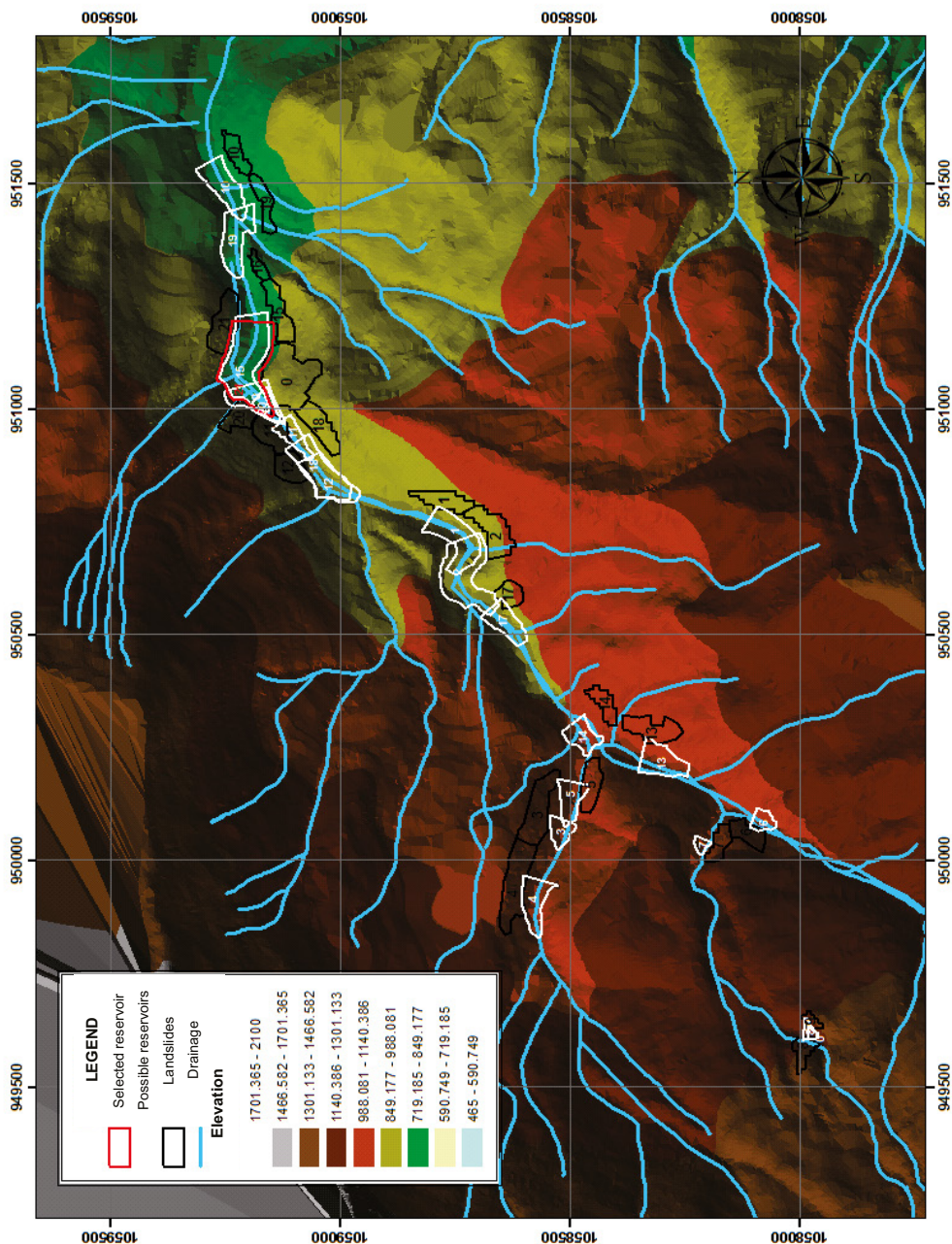
Source: Páez (2016).

- **Selection of dam to model**

Once the damming depths were calculated, the impounded areas and volumes were determined for each case, based on a digital terrain model (see figure 72). Finally, reservoir number 21 was selected, which generates the largest reservoir volume and damming height of 28 meters (Páez, 2016).

It is worth clarifying that the dam was not chosen for its height since depending on the site where the landslide is generated, the volume of impounded water will be different due to the topo- bathymetry of the channel.

Figure 72. Location of possible reservoirs generated in the La Papaya stream



Source: Páez (2016).

- **Implementation of the BREACH model**

For the implementation of the BREACH model, the data presented in table 52 was taken. Additionally, the dam material was calculated through the analysis of the landslide inventory for the geological unit Ri4. While the Manning of the channel was calculated with the Strickler equation, using as 1.9 mm taken from the granulometric curve of the La Papaya stream (Páez, 2016).

Table 52. *Description BREACH parameters*

Parameter	Description	Selected Reservoir value
HI	Initial elevation of water surface in the reservoir (ft)	92.17
HU	Dam elevation (ft)	92.17
HL	Dam bottom elevation (usually river bed elevation) (ft)	0
HPI	Elevation at which tubing failure begins (if there is no tubing, leave blank) (ft)	90
HSP	Elevation of crest of overflow (if there is no overflow, leave blank space) (ft)	-
PI	Clay plasticity index for dams with predominantly clay material	-
CA	Coefficient for critical shear stress of clay	-
CB	Coefficient for critical shear stress of clay	-
QIN(I)	Inlet flow to the reservoir (hydrograph)	-
TIN(I)	Time associated with the inlet flow to the reservoir	-
RSA	Reservoir area (acres)	See Table 53
HSA	Elevation (ft) associated with reservoir area	See Table 53

Parameter	Description	Selected Reservoir value
HSTW(l)	Elevation associated with top of cross section	See Table 53
BSTW(l)	Cross section widths associated with HSTW elevation	See Table 53
CMTW	Manning coefficient associated with each width of the cross section	0.017
ZU	Slope of upstream face of dam (1:ZU)	1.43
ZD	Slope of upstream face of dam (1:ZD)	1.43
ZC	Average slope of the upstream and downstream faces of the internal core of the dam (if there is no core, it is left empty)	-
GL	Average length of grass (in) (if there is no Grass it is left empty)	-
GS	Grass condition 1: good, 2: bad or non-existent	-
VMP	Maximum allowable speed (ft/s) for channels covered with grass or grass (if there is no grass, leave empty)	-
SEDCON	Maximum sediment concentration of 0.4 – 0.5 (if left blank it will be assumed as 0.5)	0.5
D50C	D_{50} (mm) of the core. If there is no core, leave empty	-
PORC	Core porosity. If there is no core, leave empty	-
UWC	Specific weight of core material. If there is no core, leave empty (lb/ft ³)	-
CNC	n Manning's core. If there is no core, leave empty	-
AFRC	Angle of internal friction of the core (degrees). If there is no core, leave empty	-
COHC	Cohesion (lb/ft ²) of the core. If there is no core, leave empty	-
UNFCC	Quotient between D_{50} and the core D_{30} here is no core, leave empty	-

Parameter	Description	Selected Re- servoir value
D50S	D_{50} (mm) of the outer material of the dam	7.0
PORS	Porosity of the outer material of the dam	0.25
UWS	Specific weight of outer dam material (lb/ft ³)	168.5
CNS	n Manning's n exterior dam material	0.034
AFRS	Angle of internal friction of the outer material of the dam (degrees)	35
COHS	Cohesion (lb/ft ²) of the outer material of the dam	208.71
UNFCS	Quotient between d_{90} and d_{30} of the outer material of the dam. If you leave $D_{90}D_{30}$ empty is assumed to be 10	10
BR	Relationship between flow width and depth for the initial rectangular gap. Usually 2 is used for gaps due to overflow and 1 for gaps due to tubing.	1
WC	Ridge Width (ft)	0
CRL	Ridge length (ft)	293.5
SM	Downstream river slope (ft/miles)	262.3
D50DF	D_{50} (mm) of the first ft of the top of the downstream face of the dam. If left blank, D50S is assumed to be the same.	7.0
UNFCDF	Ratio between D_{90} and D_{30} of the downstream face of the dam	10
BMX	Maximum width for bottom of gap, constrained by valley cross section (ft)	93.6
BTMX	Maximum width for top of gap, constrained by valley cross section (f)	293.5
DTH	Model run time delta (hr)	0.01

Parameter	Description	Selected Reservoir value
DBG	Indicates which results you want to display in the output file	0.0
H	Initial gap depth (ft). If left empty it is assumed as 0.1	-
TEH	Simulation duration (hrs)	2
ERR	Error tolerance for iterations	0.01
FTP	Time interval for which the output flow will be graphed	0.01
SPQ(l)	Overflow flow (cfs)	-
SPH(l)	Depth of flow over the overflow corresponding to the overflow flow SPQ(l) (ft)	-

Source: Fread (1988) y Páez (2016).

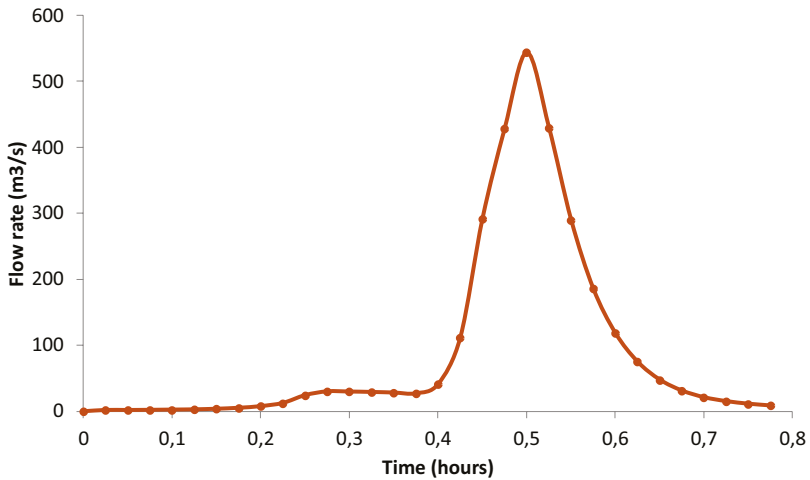
Table 53. Reservoir area and width vs height

RSA (acres)	4.20	3.79	3.40	2.99	2.30	1.22	0.44	0
HSA (ft)	92.2	79.0	65.8	52.6	39.4	26.2	13.0	0.0
HSA elevation (masl)	905.2	892.0	878.8	865.6	852.4	839.2	826.0	813.0
HSTW (m)	0.0	13.4	26.6	39.7	52.8	65.9	79.0	92.2
BSTW (m)	0.0	93.6	126.3	151.5	197.7	238.1	267.8	293.5

Source: Páez (2016).

Finally, a rupture hydrograph was obtained with a rupture duration of 46.5 minutes and a peak flow rate of 543 m³/s that was achieved after 3 minutes, as seen in Figure 73.

Figure 73. *La Papaya creek dam failure hydrograph*

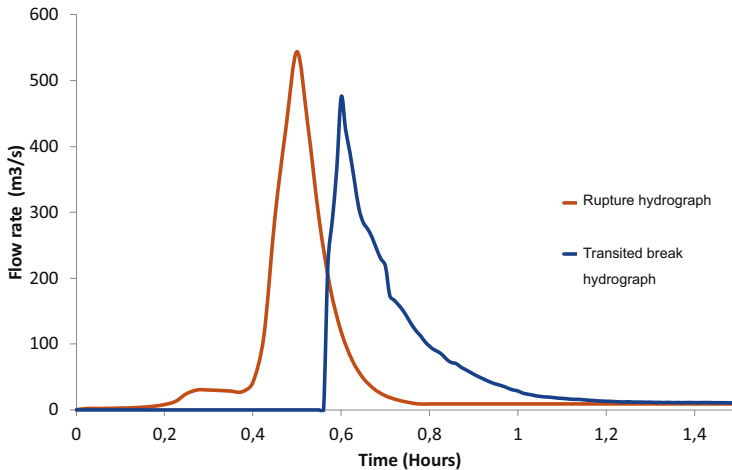


Source: Páez (2016).

- **Transit break hydrograph**

Taking into account that the failure of the dam in the La Papaya stream occurred 2 km upstream from the mouth of this tributary with the La Negra stream, it was necessary to transit the hydrograph to the mouth using a hydraulic model (RIVERFLOW 2D), a process that will be described in detail in the hydraulic modeling section. In such a way that the transited hydrograph that is presented in figure 74 was obtained.

Figure 74. *La Papaya stream dam break hydrograph traveled to the mouth with La Negra stream*



Source: Páez (2016).

3.8 EXAMPLE GENERATION OF LIQUID HYDROGRAMS AND SOLIDS—LA NEGRA CREEK, ÚTICA, CUNDINAMARCA

Once the liquid flows of the hydrological model and the unstable areas of the landslide model are available, together with the failure hydrograph of the La Papaya stream dam, hydrographs must be generated for each of the sub-basins in such a way that can be entered into the hydraulic model to be transported to the flood valley area where the urban area of the municipality of Útica is located.

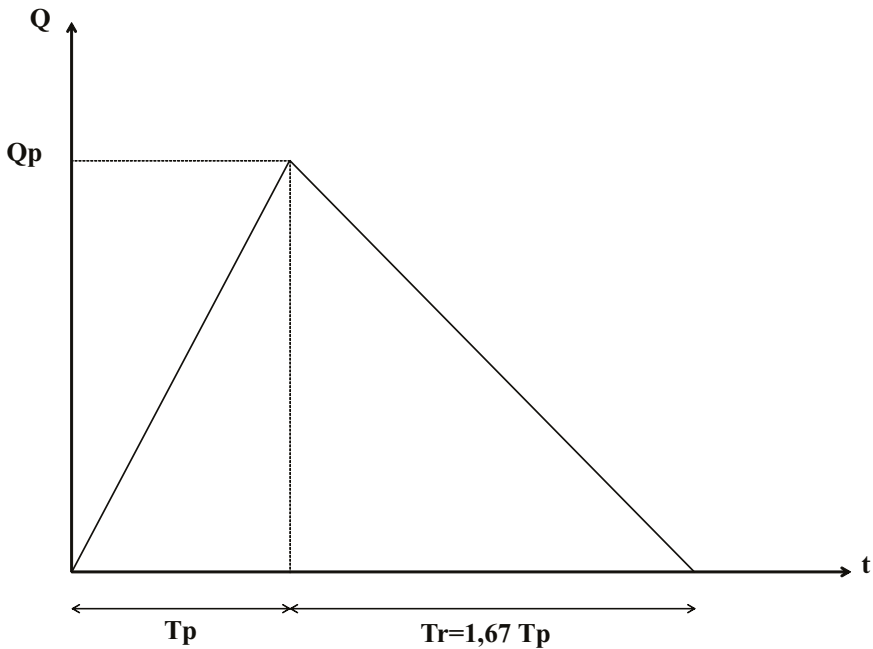
- **Liquid hydrographs**

Taking into account that there is daily information and that there is no information on the duration of the event, synthetic flood hydrographs were generated for each of the 37 sub-basins of the La Negra stream, through the triangular hydrograph of the SCS, which was subsequently smoothed with a gamma function (Páez, 2016).

It is worth clarifying that there are other methodologies that can be applied to generate synthetic hydrographs and if there is some knowledge of the duration of the event, the analysis can be complemented with this information.

The triangular hydrograph of the *Soil Conservation Service* (SCS) of the United States estimates the peak flow based on the total volume of runoff, which in this case corresponds to the daily volume and the time to peak and the duration of the hydrograph based on the time of concentration, as seen in the figure 75. The concentration time was calculated as the average of the equations of Témez, Kirpich and Giandiotti (Páez, 2016).

Figure 75. *Triangular hydrograph of the SCS*



Source: Páez (2016).

$$Q_p = \frac{2Q}{T_p + T_r}$$

$$T_p = 0,7 T_c$$

$$T_r = 1,67 T_p$$

Where:

Q_p = Peak flow

Q = Runoff volume (m3)

T_p = Time to peak(s)

T_r = Recession time (s)

T_c = Concentration time (s)

- **Solid hydrographs**

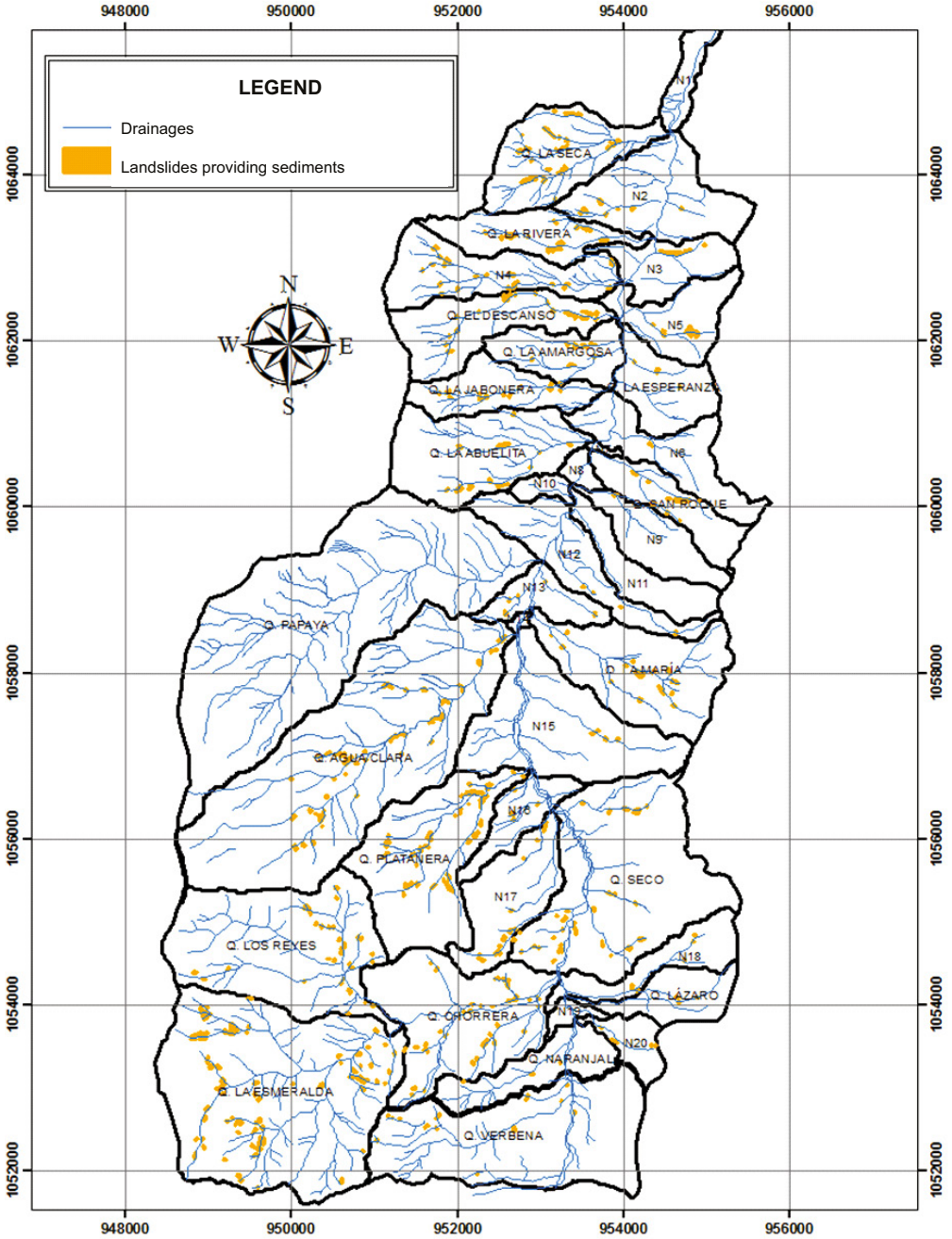
To generate solid hydrographs, first the landslides of the infinite slope model that could potentially contribute sediments to the channel were selected, which are presented in figure 76.

The slid volume was calculated using the area-volume relationships for each geological unit, found through the analysis of the landslide inventory as previously mentioned. Finally, the sediment volume was calculated taking into account the porosity, as follows (Páez, 2016)::

$$Volumen\ sedimentos = Volumen\ deslizado (1 - Porosidad)$$

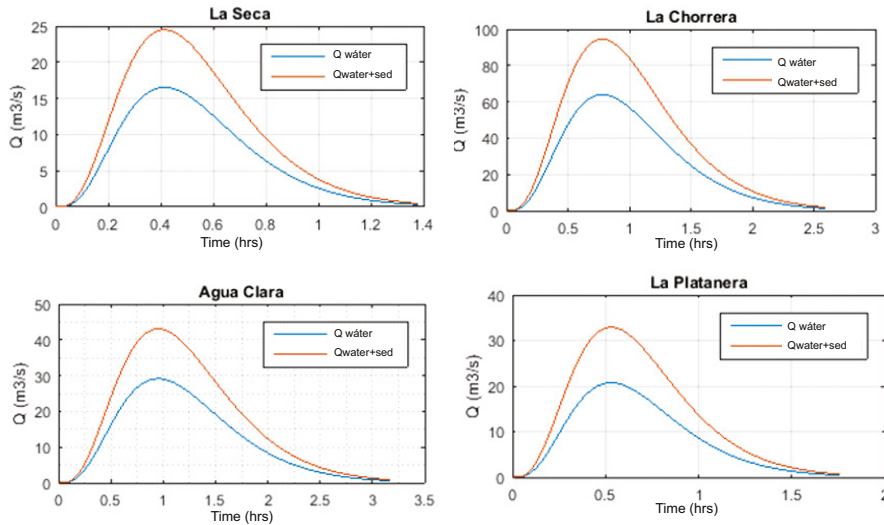
A constant sediment concentration was assumed throughout the entire hydrograph such that solid hydrographs with the same shape as the liquid hydrographs were generated. Figure 77 shows the water and mud and debris flows hydrographs (water and sediments) of some of the sub-basins of the upper part of the La Negra stream.

Figure 76. Landslides that potentially contribute sediment to the flow



Source: Páez (2016).

Figure 77. Synthetic hydrographs of water and mud and debris flows sub-basins of La Negra creek



Source: Páez (2016).

3.9 HYDRAULIC MODELING OF FLOOD PROPAGATION AND RHEOLOGY CALIBRATION

Once the flood hydrographs are available for each of the tributaries, it is necessary to transit these flows through the main channel to the flood valley. To do this, a hydraulic model that includes rheological models must be used. Although, for certain cases it is possible to use the Newtonian fluid model, that is, simulate it as water with sediment transport and a of Manning, it is advisable to use a hydraulic model that includes non-Newtonian fluid models that can better represent the flow behavior in the flood valley. Likewise, depending on the purpose and level of detail of the study, it is recommended to use two-dimensional models, since these adequately represent the spatial and temporal flow behavior.

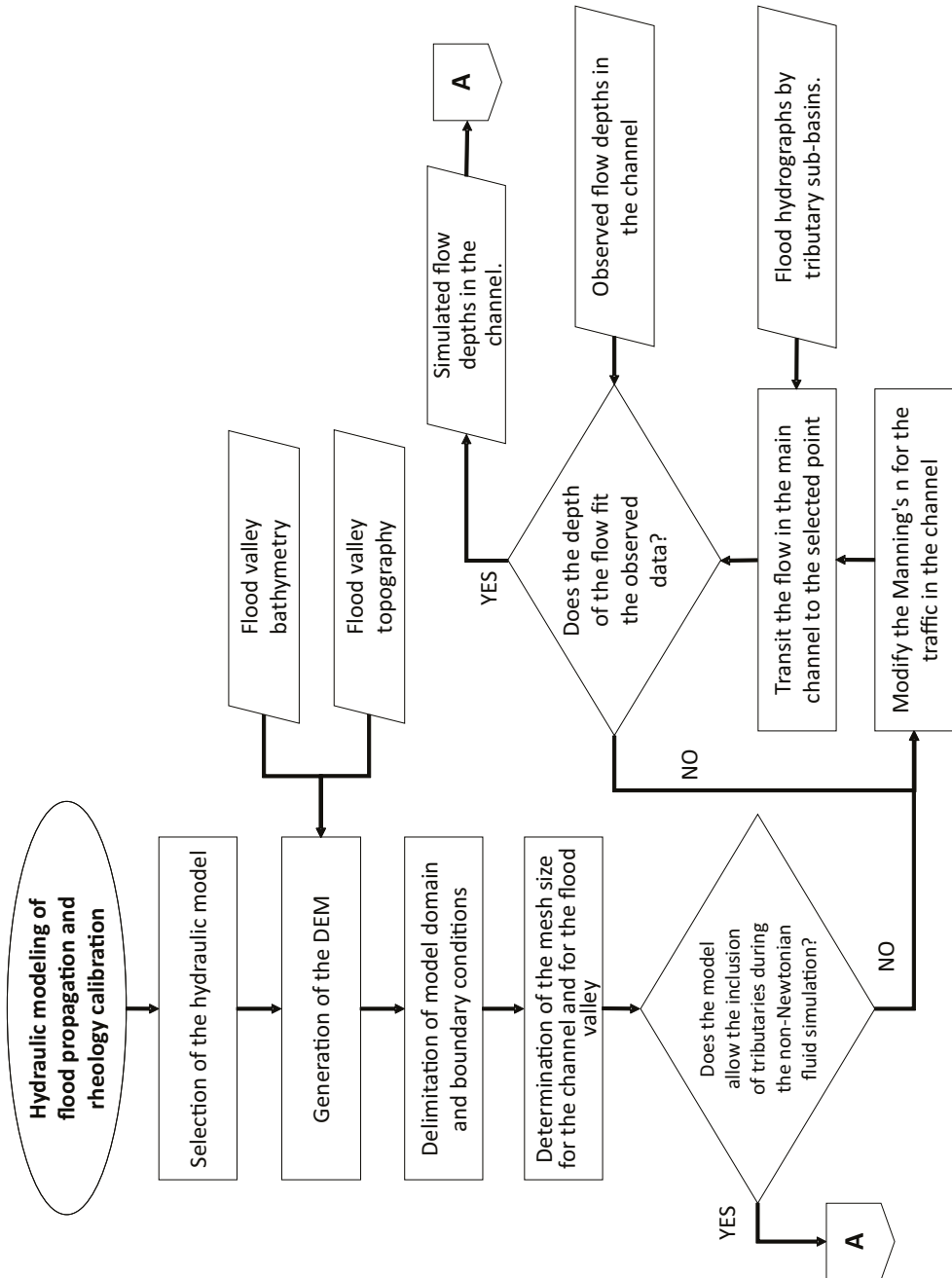
In figure 78 and figure 79, the flow diagram is presented for the development of a hydraulic modeling of the propagation of the mud and debris flows through the main channel and the flood valley, however, the following clarifications are presented:

- Some models can represent the erosion of the channel at the same time that the flood hydrograph is transited, which can more adequately represent reality, however, there are very few models that have this capacity, so this aspect is not essential for a adequate modeling.
- It is very important to have a very good resolution of the topography of the flood valley, in such a way that the uncertainty of the model in this area is minimized, since being such flat areas the model can fall into instabilities or substantial errors due to the resolution of the mesh.
- If the hydraulic model allows the application of a rheological model while the tributaries enter, the transit can be carried out in this way from the head of the basin, however, generally the models assume that at the beginning of the section the entire flow is found. which is not possible to model the tributaries while modeling the rheology. Additionally, it is possible that the rheology changes along the channel due to contributions from the tributaries and hydraulic models do not have the capacity to model these rheology changes.
- In accordance with the above, it is recommended to model the traffic in the main channel with the contribution of the tributaries as water with sediment transport up to a certain point of the main channel, where a change in slope is evident or where the contribution of tributaries is not very relevant and from there a new transit must be made with the selected rheological model to the flood valley.
- It is recommended to perform a sensitivity analysis with two or more rheological models in order to determine the flow rheology with greater certainty, especially in flows that are at the transition limit from sludge flow to hyperconcentrated flow and hyperconcentrated flow. to debris flow, as rheology plays a fundamental role in flooding times, velocities and depths, which can make a difference in the level of threat. However, if a good calibration is achieved and there is some certainty about the type of flow that occurs in the channel, this step can be skipped.

- Rheological parameters are always subject to calibration, however, if possible, field information and descriptions of the event should be obtained to achieve a more satisfactory calibration.
- Once the rheology calibration has been carried out, it is possible to generate threat scenarios for different hydrological conditions, taking into account that the flow behavior is determined by the concentration and type of sediments, so a basin will tend to generate events with always similar rheological behavior (Bateman and Medina, 2019).
- To generate a complete threat analysis, scenarios must be simulated
- for different return periods, since hydraulic modeling allows determining the intensity of the event, but the probability of occurrence is given by the return period, so together the threat.

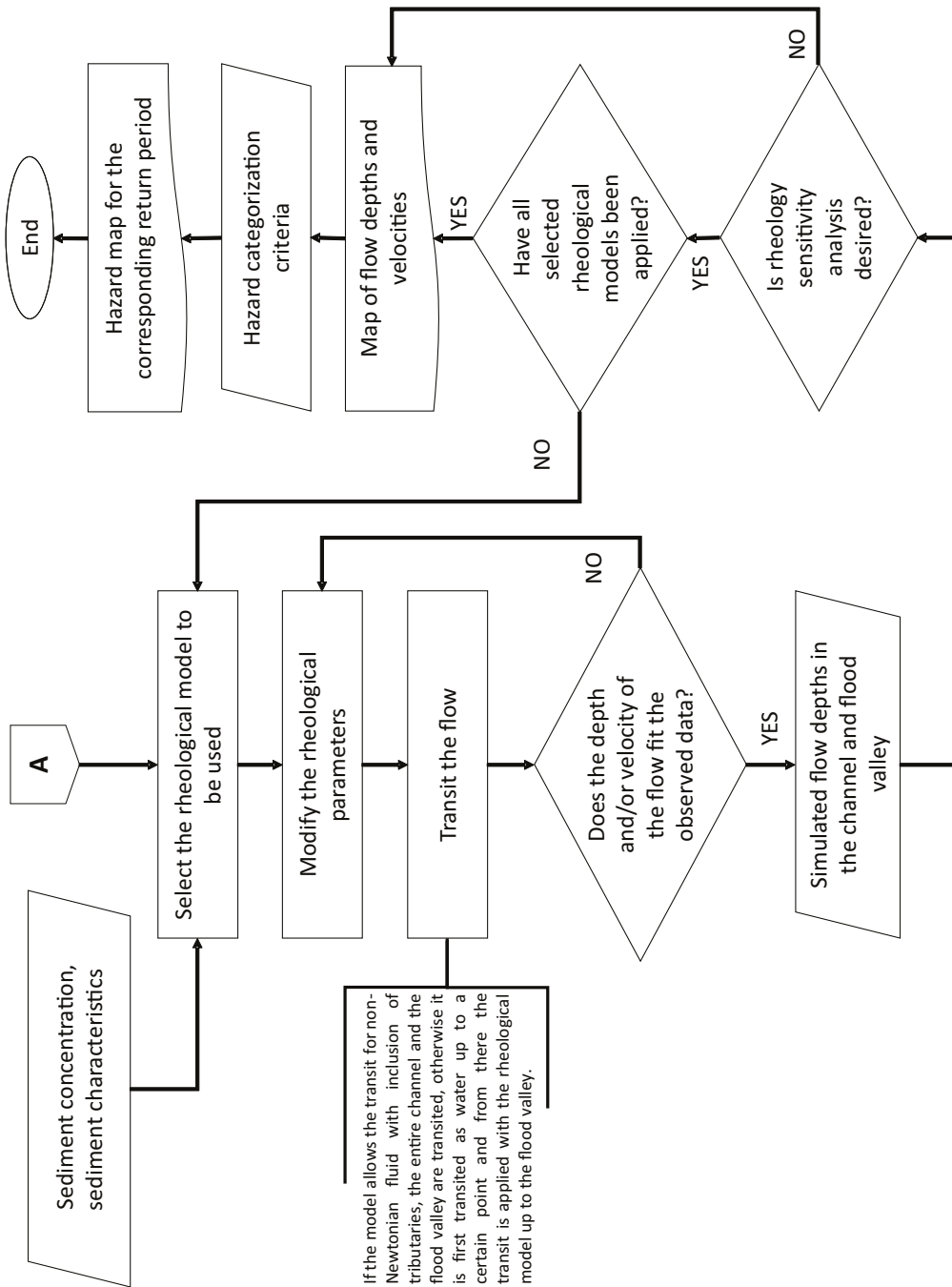
Some models can represent the erosion of the channel at the same time that the flood hydrograph is transited, which can more adequately represent reality, however, there are very few models that have this capacity, so this aspect is not essential for a adequate modeling.

Figure 78. Flowchart for hydraulic modeling and rheology calibration



Source: own elaboration.

Figure 79. Flowchart for hydraulic modeling and rheology calibration



Source: own elaboration.

3.9.1 HYDRAULIC MODELS

The hydraulic traffic models used for modeling mud and debris flows are two-dimensional and solve the Navier-Stokes equations in a finite volume scheme, calculated for a triangular or rectangular mesh that can be of variable size for different areas of the channel. The shallow water equations are described by the momentum and mass conservation equations expressed as follows (Hydroina, 2014):

$$\frac{\partial U}{\partial t} + \frac{\partial F(U)}{\partial x} + \frac{\partial G(U)}{\partial y} = S(U, x, y)$$

$$U = (h, q_x, q_y)^T, q_x = uh, q_y = vh$$

$$F = \left(q_x, \frac{q_y^2}{h} + \frac{1}{2}gh^2, \frac{q_x q_y}{h} \right)^T$$

$$G = \left(q_y, \frac{q_x q_y}{h}, \frac{q_x^2}{h} + \frac{1}{2}gh^2 \right)^T$$

$$S = \left(0, gh(S_{ox} - S_{fx}), gh(S_{oy} - S_{fy}) \right)^T$$

$$S_{ox} = -\frac{\partial z_b}{\partial x}, S_{oy} = -\frac{\partial z_b}{\partial y}$$

$$S_{fx} = \frac{n^2 u \sqrt{u^2 + v^2}}{h^{4/3}}, S_{fy} = \frac{n^2 v \sqrt{u^2 + v^2}}{h^{4/3}}$$

Where:

u, v = Components of velocity in coordinates x, y

$\frac{1}{2}gh^2$ = Term obtained from a hydrostatic pressure distribution

n = Manning roughness coefficient

On the other hand, some models include sediment transport expressed in the following way (Hydroina, 2014):

$$\frac{\partial(h\phi_p)}{\partial t} + \frac{\partial(hu\phi_p)}{\partial x} + \frac{\partial(hv\phi_p)}{\partial x} = R_p$$

Change in bed elevation:

$$\frac{\delta z(1 - p_p)}{\delta t} = - \sum_{p=1}^{N_p} w_{sp} (\phi_{*p} - \phi_p)$$

Where:

ϕ_{*p} = Sediment concentration in equilibrium volume

ϕ_p = Suspended sediment concentration

w_{sp} = Sedimentation rate

Table 54 presents a comparison of some of the most useful hydraulic models for modeling mud and debris flows.

Taking into account that the RIVERFLOW2D model used does not allow transit with tributaries and at the same time applying rheological models of non-Newtonian fluids, the transit was divided into two sections

Table 54. Comparison of hydraulic models for mud and debris flows

Model	Does it include processes in-channel or trans-sediment load?	Interface	Free?	Rheological models included	Recommended for types of flow
Debris Dices	None	GNU coupled to GIS	Yes	N/A	Any whenever calibration data is available
RIVERFLOW2D	Transportation of sedi-bottom and suspension ments	Own attached to QGIS and ArgusOne	No / Version free limited	Manning Full Bingham Bingham simplified Manning and Coulomb Manning with es-force of yield Coulomb with yield force Quadratic Granular	Mud flows Hypercon-focused Flows of detritos
FLO2D	Transportation of sediments from bottom and suspension	Own Attached to QGIS	YES / Version Pro-Paid	Manning Quadratic	Ludge flows Hypercon-centrated

Model	Does it include processes in-channel or trans-sediment load?	Interface	Free?	Rheological models included	Recommended for types of flow
FLATModel	In-channel processes	Fortran	Yes	Bingham Herschel Bulkey Voellmy	Sludge flows Hyperconcentrated Flows of detritus
RAMMS	None	Own	Yes	Voellmy	Hyperconcentrated Flujos de detritos
AVAFLOW	Two phase flow In-channel processes	Attached to QGIS	Yes	N/A	Hyperconcentrated Flows of detritos
TELEMAC MASCARET	Transportation of sediments at bottom and suspensionents	Fortran	Yes	Manning	Hyperconcentrated

Source: own elaboration.

3.10 EXAMPLE HYDRAULIC MODELING – LA NEGRA CREEK, ÚTICA, CUNDINAMARCA

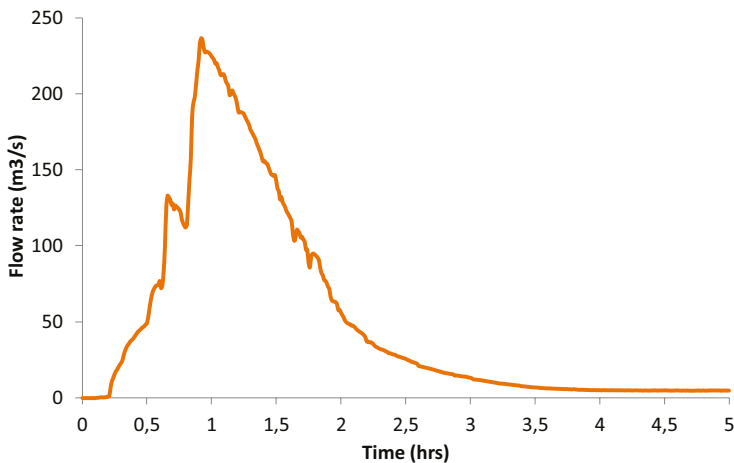
Taking into account that the model used RIVERFLOW2D does not allow transit with tributaries and at the same time applying rheological models of non-Newtonian fluids

the traffic was divided into two sections. The first from the head of the La Negra stream to just before the mouth of the La Papaya stream and the second from the mouth of the La Papaya stream to the flood valley. In this last section, the different rheological models that will be implemented were implemented. mentioned later (Páez, 2016).

- **Transit of the first section (headwater–mouth of La Papaya creek)**

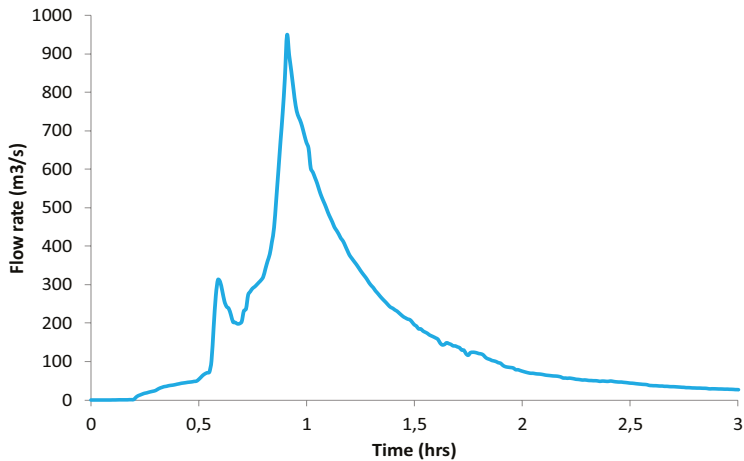
In the first section, the flood flow was traversed with the Manning model including all the synthetic hydrographs of the tributaries found upstream of the La Papaya stream. He of Manning was calculated with the Strickler and Meyer- Peter and Müller equations, for the 2 available bed granulometries, obtaining a Manning average for the channel of 0.021 (Páez, 2016). Figure 80 shows the hydrograph traveled over the La Negra stream until just before the mouth of the La Papaya creek.

Figure 80. *Hydrograph traveled until the end of section 1*



Source: Páez (2016).

To the hydrograph traveled for section 1, the dam break hydrographs and the synthetic hydrographs of the tributaries downstream of La Papaya stream were added, obtaining the mud and debris flows hydrograph that is presented in figure 81, which was traveled with different reology up to the flood valley.

Figure 81. Hydrograph of mud and debris flows to be traveled in section 2

Source: Páez (2016).

- **Transit of the second section (mouth of La Papaya creek to flood valley), calibration and comparison of rheological models**

According to the previously calculated hydrographs, it was determined that the average sediment concentration is 32% by volume with a large amount of fine sediments, so the flow is between sludge flow and granular hyperconcentrated flow, for which the transit of section 2 to the flood valley with the following rheological models (Páez, 2016).

- Manning without sediment transport
- Manning with sediment transport
- Full Bingham
- Quadratic model

Table 55 presents the calibrated rheological parameters for each of the models, where it is observed that in order to simulate mud and debris flows conditions of the hyperconcentrated flow type with Newtonian fluid, one must resort to Manning much higher than the usual ones for water with values between 0.08 and 0.12.

Table 55. *Results of calibration of rheological parameters*

Rheological model	Parameter	Worth
Manning without sediment transport	n by Manning	0.08
Manning with sediment transport	n by Manning	0.12
	Average diameter of sediments (mm)	0.01
Full Bingham	Yield shear stress (N/m ²)	320
	Bingham viscosity(Pa*s)	5
	Density (kg/m ³)	2 200
Quadratic model	Yield shear stress(N/m ²)	320
	Viscosity (Pa*s)	5
	Density (kg/m ³)	2 200
	n by Manning	0.035

Source: Páez (2016).

On the other hand, Table 56 presents the measured depths in the flood valley vs. the maximum simulated depths for each rheological model, where it is observed that all the selected models adjust relatively well to reality, however, in table 57 presents the root mean square error (RSME) which goes from 0 to infinity, where it is observed that all models have small errors, but the one that best fits is the Manning model with sediment transport, which would confirm that It is a hyperconcentrated flow with a high load of fine sediments.

Table 56. *Measured vs simulated depths in the floodplain*

Measured depth (m)	Simulated maximum depth			
	Manning without transportation of sediments	Manning with transportation of sediments	Full Bingham	Quadratic model
0.7	0.716	0.808	0.563	0.455
0.8	0.541	0.604	0.428	0.427
0.9	0.624	0.697	0.488	0.443
0.9	0.482	0.859	0.360	0.31
0.3	0.488	0.538	0.607	0.526
1.5	0.357	0.532	0.349	0.35
0.3	0.671	0.426	0.885	1.082
0.5	0.605	0.669	0.930	0.715
1.0	0.769	0.752	0.392	0.715
1.5	0.642	0.904	0.689	0.638
1.0	0.181	0.727	0.492	0.421
0.4	0.831	0.137	0.657	0.528
0.5	0.268	0.452	0.434	0.403
1.0	0.441	0.264	1.082	1.303
0.3	0.670	0.496	0.340	0.26
0.2	0.713	0.773	0.801	1.179
0.5	0.785	0.769	0.581	0.472

Measured depth (m)	Simulated maximum depth			
	Manning without transportation of sediments	Manning with transportation of sediments	Full Bingham	Quadratic model
1.0	0.482	0.114	0.155	0.113
0.5	0.697	0.826	0.509	0.501

Source: Páez (2016).

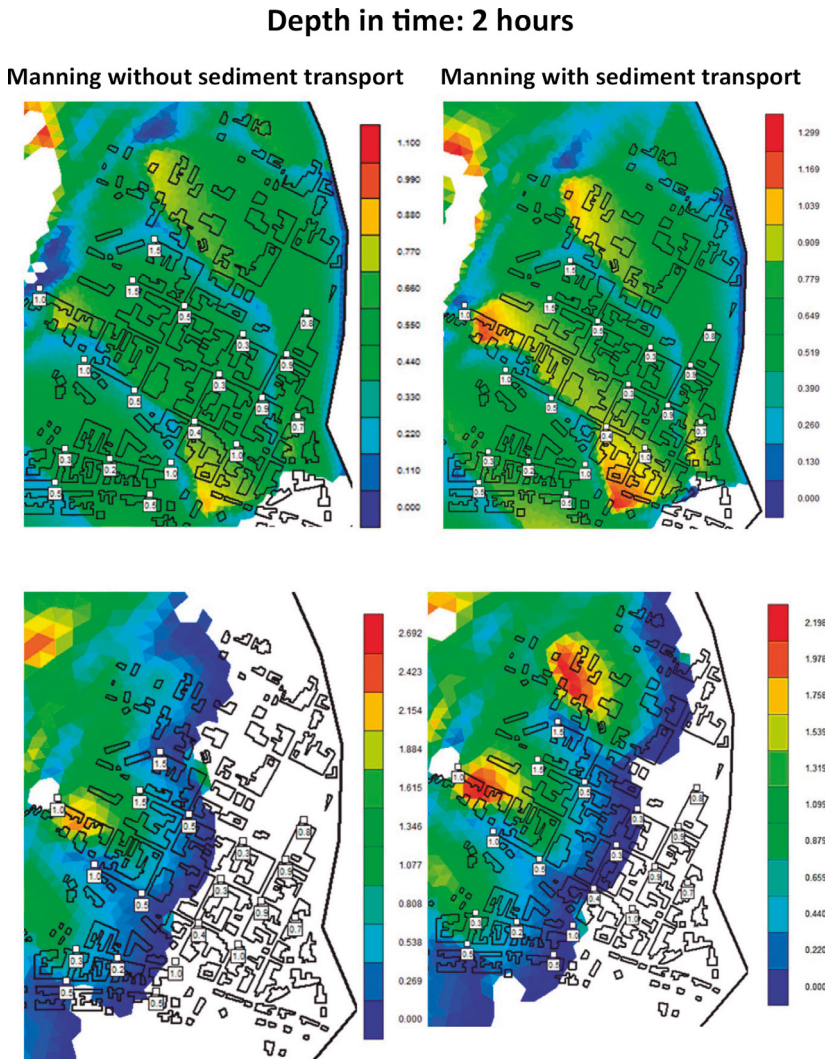
Table 57. *RSME for selected rheological models*

Rheological model	RSME
Manning without sediment transport	0.113
Manning with sediment transport Full	0.099
Full Bingham	0.118
Quadratic model	0.127

Source: adapted from Páez (2016).

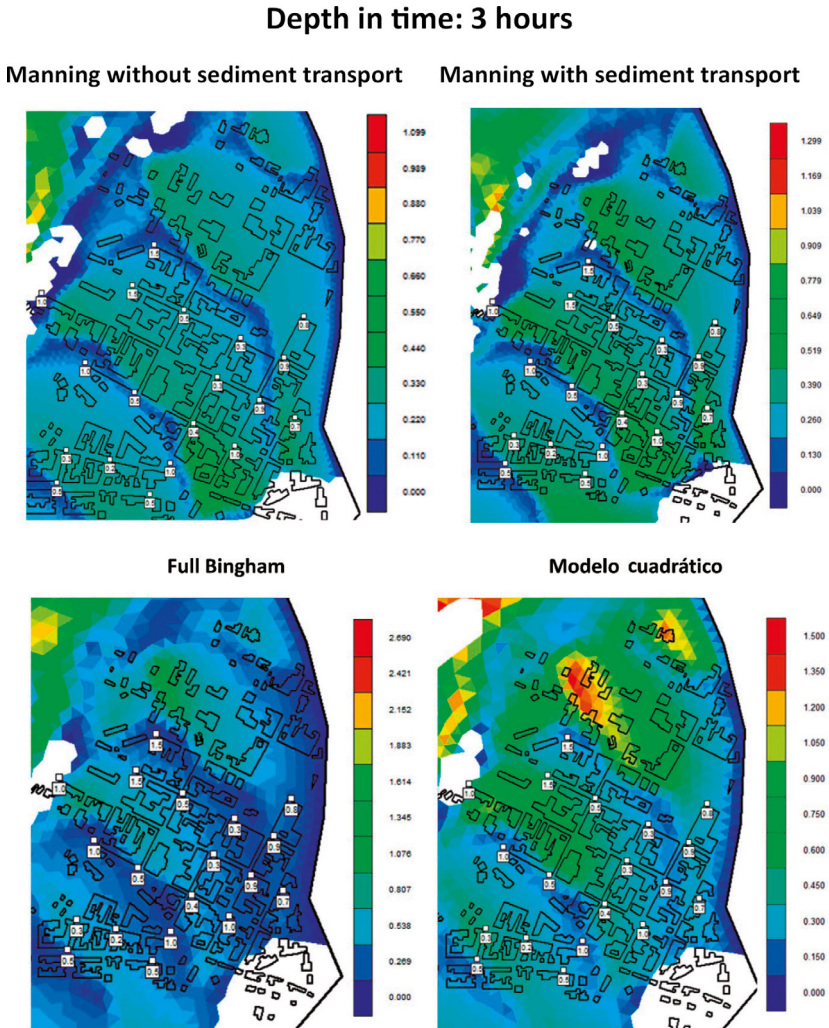
As mentioned above, all models adequately represented the maximum depths, however, there are substantial differences in the duration of the event and the distribution of velocities as seen in figure 82 to figure 85.

It is observed that viscous flow models such as Bingham and quadratic generate greater depths, but lower velocities and, in turn, longer transit times. While Manning models generate lower depths and higher flow velocities.

Figure 82. Comparison of simulated depths for each rheological model at $t = 2$ hours

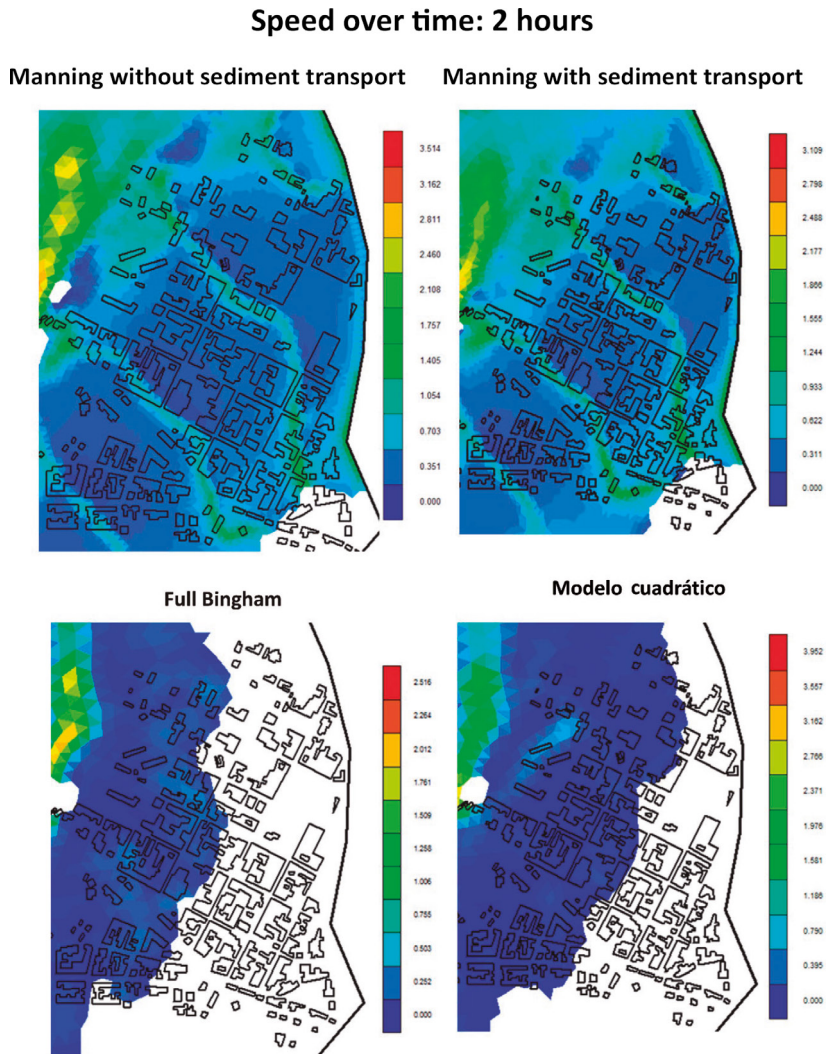
Source: Páez (2016).

Figure 83. Comparison of simulated depths for each rheological model at $t = 3$ hours



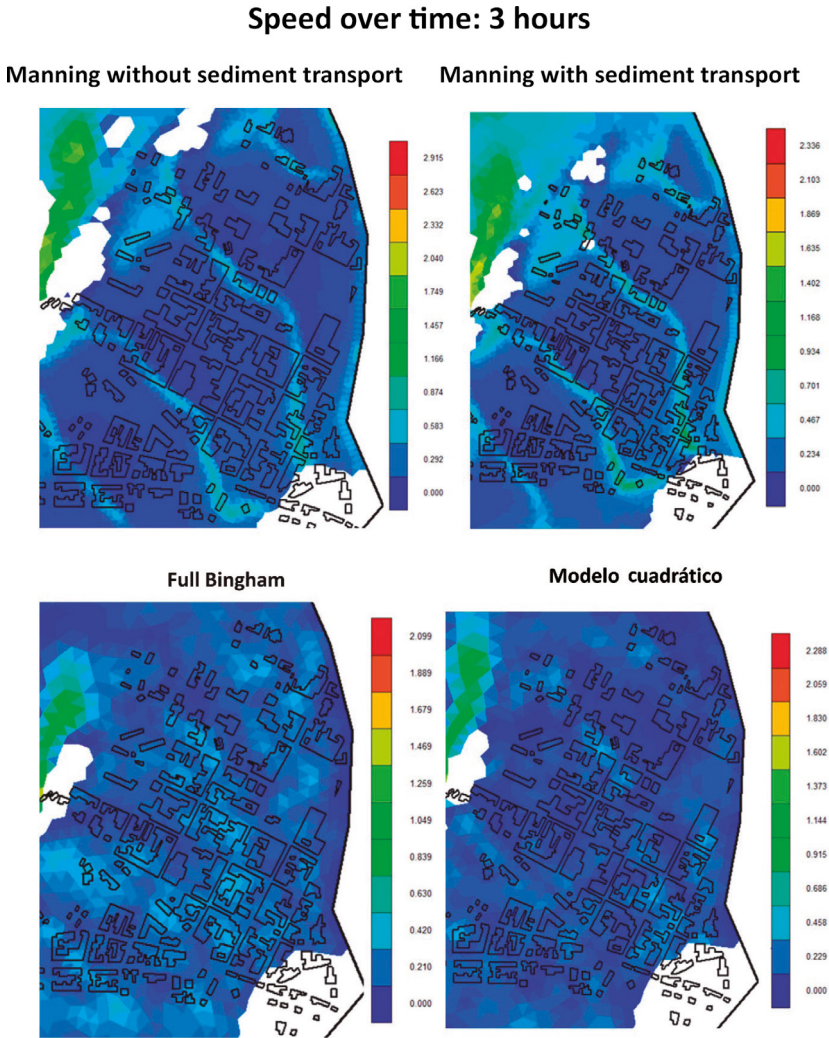
Source: Páez (2016).

Figure 84. Comparison of simulated depths for each rheological model at $t = 3$ hours



Source: Páez (2016).

Figure 85. Comparison of simulated velocities for each rheological model at $t = 3$ hours



Source: Páez (2016).

3.11 GENERATION OF THE THREAT MAP

As mentioned above, to generate a robust threat map, both the intensity calculated through modeling and the probability represented as each of the return periods must be included, taking into account the following::

$$\textit{Threat} = \textit{Intensity} * \textit{Probability of occurrence}$$

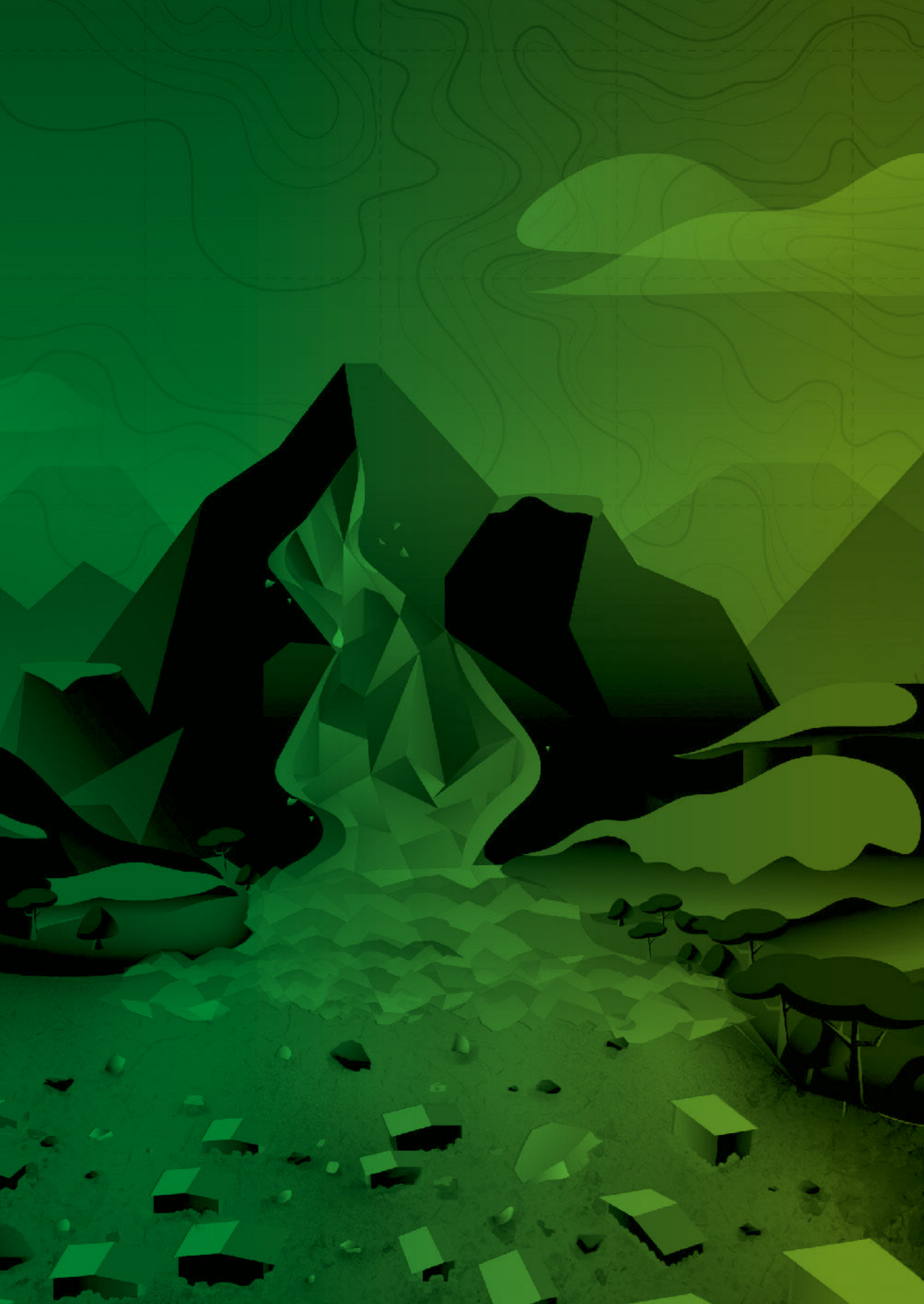
Rickenmenn (2005) and Loat and Petrascheck (1997) classify the intensity of the event depending on the depth and speed of the flow and finally the threat according to the probability of occurrence according to the return periods, taking into account high probability as the return period. return of 10 years, average of 100 years and decline of 500 years (Bateman and Medina, 2019); as seen in table 58.

However, these return periods can be variable according to the evaluator's criteria. Following some recommendations from specialists, a threat greater than 100 years of return period should not be accepted, so this categorization could be rescaled with a high probability of occurrence for 10 or 100 years. 20 years return period, average for 50 years and low for 100 years.

Table 58. *Intensity and threat categorization matrix for mud and debris flows*

	Loat and Petrascheck (1997)		Rickenmenn (2005)	Category intensity	Probability of occurrence (return period)		
					High	Average	Low
Intensity	h>1.0 m		h>1.0 m	High	High	High	Moderate
	y		o				
	v>1.0 m/s		v>1.5 m/s				
	h<1.0 m		h<1.0 m	Average	Moderate	Moderate	Low
	o		y				
	v<1.0 m/s		0.4<v<1.5 m/s				
	No existe		h<0.4 m	Low	Low	Low	Very low
		y	v<0.4 m/s				

Source: *Bateman and Medina (2019).*



ANALYSIS OF VULNERABILITY AND RISK

4.1 VULNERABILITY ANALYSIS

Analyzing the vulnerability of a system is an important step in risk management plans. Although vulnerability has several definitions, in this case it is assumed as

the condition by which a population is exposed or in danger of being affected by a natural or anthropic phenomenon, and also refers to the capacity of this population to recover from the effects of a disaster (Humboldt Center, 2004, p. 10).

Characterizing the vulnerability of a population then implies determining the factors or dimensions that intervene and increase the intrinsic vulnerability condition of the system.

Generally, vulnerability is typified according to the elements exposed to the event, with physical, social, economic and environmental vulnerability being common.

However, depending on the model, these categories may change or be integrated. The main methodologies for the analysis and assessment of vulnerability within the framework of Risk Management Plans are described below.

4.1.1 VULNERABILITY ANALYSIS IN POMCAS BASED ON INDEX AND INDICATOR MODELS

This methodology has been integrated into the Protocol for the incorporation of Risk Management in the Planning and Management Plans of Hydrographic Basins. In this methodology, vulnerability is related to three main elements, which are: the exposure of populations to the threat, the physical susceptibility of the exposed elements to be affected by the occurrence of an event, and the lack of resilience of communities to respond to the threat. a disaster or absorb its impact (Minambiente, 2014).

According to this methodology, each of the aspects mentioned above is evaluated as an index within the vulnerability analysis, so that through the use of indices the vulnerability responds to the following expression:

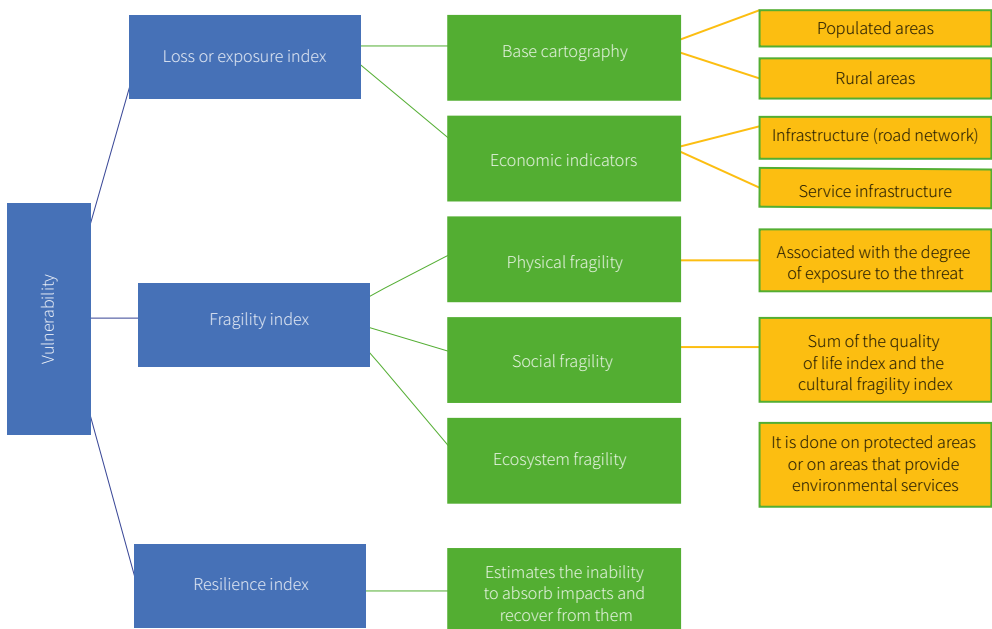
$$\text{Vulnerability} = \frac{\text{Loss index or Exposure index} * \text{Fragility index}}{\text{Resilience index}}$$

The loss or exposure index corresponds to the inventory of natural assets or exposed elements that may be affected by different threatening events and is expressed in terms of assets and population. The model can be evaluated with different levels of resolution and when detailed information is not available, it is necessary to make approximate estimates that approximately represent or account for said inventory of exposed assets.

The fragility index for the POMCAS refers to the degree of fragility of the different elements and sectors (economic, social and environmental) to withstand the onslaught of the events. As seen in figure 86, there are three types of fragility.

Physical fragility refers to the susceptibility condition of human settlements; Social fragility is related to the predisposition that arises as a result of the level of marginality and social segregation of the human settlement and its disadvantaged conditions; and ecosystem fragility, which is mainly related to the level of threat present in protected areas or in areas that provide environmental services.

Figure 86. POMCAS methodology based on index and indicator models



Source: own elaboration.

The resilience index as a vulnerability factor refers to the lack of resilience or, in other words, the lack of capacity to face the impact of threatening phenomena. For this reason, it is related to the level of development and the explicit existence of risk management, so this index can be represented by indicators of governance, financial protection, human capital, technological development, etc. (Minambiente, 2014).

Each index presented is broken down into indicators that allow the factors that may intervene in a threat event to be independently assessed and that facilitate its evaluation in the field. It is important that the indicators for describing the degree of exposure, fragility and resilience are formulated in such a way as to provide reliability to the data collected, therefore, care should be taken to avoid repeated use of the same indicator as this would be giving a greater weight compared to the others.

All the aforementioned indices are valued in a range of 0-1 so that the resulting vulnerability index presents three categories that range between low and high, as detailed in table 59.

Table 59. *Categories of the Vulnerability Index in the methodology used in POMCA*

Worth	Vulnerability index category (IV)	Symbol
0.75 - 1	High	Red
0.30 - 0.75	Average	Yellow
0 - 0.30	Low	Green

Source: Minambiente (2014).

4.1.2 VULNERABILITY ANALYSIS BASED ON DIMENSIONS

Vulnerability in terms of dimensions has been used in the book of *Threat, vulnerability and risk due to mass movements, mud and debris flows and floods in the Aburrá Valley* (National University of Colombia, 2009). In this document, five dimensions are considered::

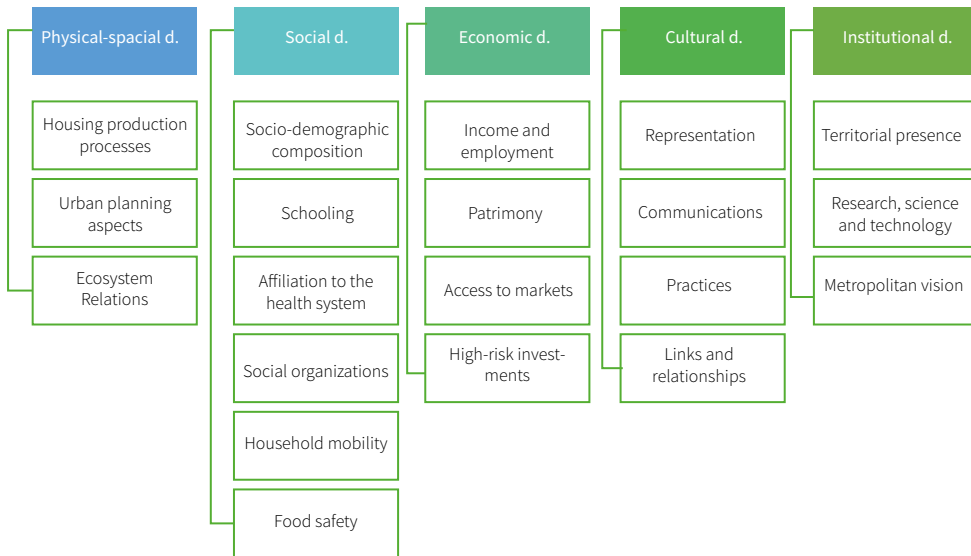
- **Physical-spatial dimension:** related to the issues of buildings and conditions.

- **Social dimension:** related to aspects of demography, migration, education, health, food security and organization.
- **Economic dimension:** that addresses aspects such as employment, income, tenure, among others.
- **Cultural dimension:** It is related to matters of risk Representation, communications and actions in the matter.
- **Institutional dimension:** related to municipal economic, financial and institutional management, is analyzed on a macro scale.

For each dimension, specific indicators are defined, which are detailed in figure 87. For each indicator, the scale of analysis on which the work will be carried out must be defined (micro, meso or macro). According to the aforementioned document, the first four dimensions can be worked on at a micro and meso scale, while the last dimension (institutional) can be worked on at a macro scale (Universidad Nacional de Colombia, 2009).

At the micro scale, all aspects that are analyzed based on the information from the census and the household survey are considered; at the meso-scale, everything that is analyzed at the settlement level in field work or that comes from primary or secondary information about the neighborhoods; and at the macro scale, everything that comes from primary or secondary information obtained at municipal or metropolitan scales.

For each dimension, specific indicators are defined, which are detailed in figure 87. For each indicator, the analysis scale must be defined in which micro, meso, or macro will be developed.

Figure 87. *Dimensions and indicators for vulnerability analysis*

Source: own elaboration.

The proposed indicators lead to the construction of factors called “crossroads” in which aspects can be related; thus, fragility is obtained from the intersections between economic solvency, knowledge, social capabilities, marginalization, migratory dynamics and housing characteristics; exposure depends on the intersections between location and ecosystemic relationships; and the capacity for response and recovery is given by the intersections between economic solvency, social capabilities and opportunities of the territory (Universidad Nacional de Colombia, 2009).

It is important to highlight that the factors are interdependent, just like the intersections, and that they allow for guiding management by relating different aspects of the settlements and understanding the connection between social, physical-spatial, economic and political aspects.

In this methodology, vulnerability ranges from 0 to 10 and are defined as follows::

Table 60. *Vulnerability ranges in the dimension-based methodology*

Range	Classification
0 - 2	Low
2 - 4	Medium low
4 - 6	Medium
6 - 8	Medium high
8 - 10	High

Source: adapted from National University of Colombia (2009).

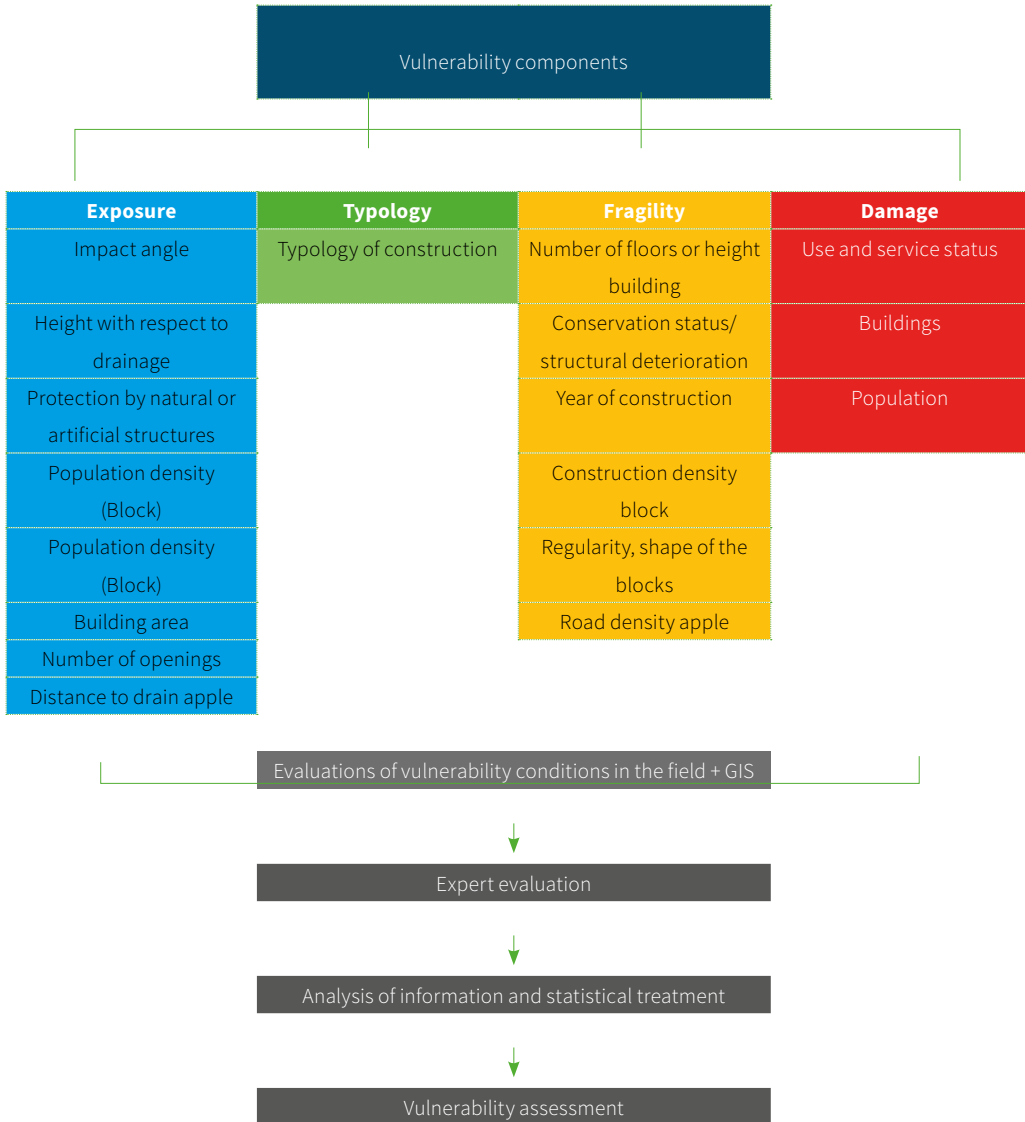
4.1.3 VULNERABILITY EVALUATION: SALGAR ANTIOQUIA CASE

The methodology proposed in the conference titled “Evaluation of physical vulnerability to mud and debris flows. Case study: urban capital of the municipality of Salgar (Antioquia)” by Cañas-Gómez et al. (2017) mentions exposure, typology, fragility and damage as components of vulnerability.

The exhibition includes aspects related to population density at different scales: building, block, building area, protection by natural or artificial structures, among others. For its part, the typology refers to the characterization of the constructions in the area of interest, including types of material, reinforcement and quality.

The third component, fragility, takes into account the number of floors of the buildings, the state of conservation (deterioration), age of the buildings, road density and density of buildings per block.

Finally, the damage component includes three indicators, the state of use and service, the buildings and the inhabitants (figure 88).

Figure 88. *Vulnerability assessment in the Salgar case*

Source: own elaboration.

Vulnerability conditions must be evaluated in the field in order to build cartographic models that make visible degrees of vulnerability in the area of interest. Likewise, the field evaluation should help identify the factors that they can play a predominant role in the vulnerability of an area to threat events.

4.1.4 METHODOLOGY FOR VULNERABILITY ANALYSIS IN URBAN CENTERS (PERU)

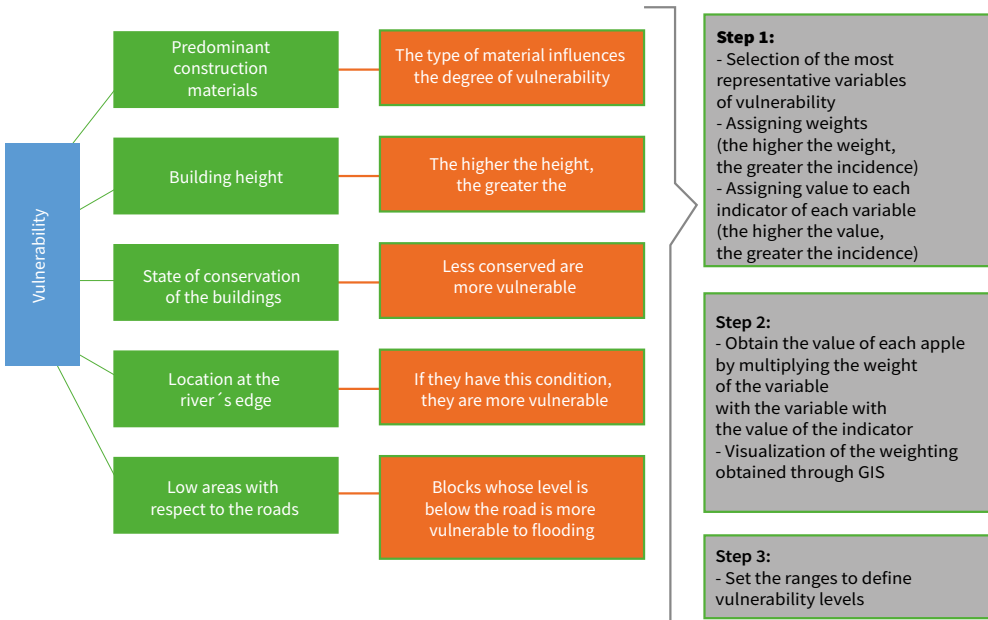
The methodology for the analysis of vulnerability and risk to floods and earthquakes, of buildings in urban centers, is the methodology proposed by the Center for Disaster Studies and Prevention of Peru (Lozano-Cortijo, 2008). This methodology requires an evaluation of threats and a physical diagnosis of the urban center under study in order to be applied. Although the vulnerability analysis methodology focuses on floods, it can be applied in the case of mud and debris flows.

The analysis proposed in this document includes the use of two complementary methodologies. On the one hand, a qualitative methodology through which blocks or lots with critical indicators of the variables selected for the analysis are identified, comparing them with the threat areas; so that levels of vulnerability and risk are obtained at the same time (Lozano-Cortijo, 2008).

The second methodology is heuristic, in which a weight is assigned to each selected variable, according to its importance in the event of floods (or mud and debris flows), as well as the assignment of a value to each indicator of each variable, according to its level of criticality. . Finally, the vulnerability levels of each block are established through ranges (Lozano-Cortijo, 2008).

In figure 89, the proposed variables and indicators are defined. Among the variables, construction materials, height of buildings, state of conservation of buildings, relationship of the area with respect to rivers or bodies of water and height of the area of interest with respect to roads stand out.

The relationship of the variables with respect to vulnerability establishes a directly proportional relationship between the height of the buildings and the state of conservation with the level of vulnerability. On the other hand, the height of buildings with respect to roads presents an inverse relationship with respect to vulnerability (Lozano-Cortijo, 2008); The vulnerability will be greater to the extent that the buildings are at lower levels than the roads.

Figure 89. *Vulnerability Analysis in Urban Centers – PREDES*

Source: own elaboration.

It is recommended to carry out the analysis in graphic form, dividing the city by sectors and comparing the thematic maps. The methodology is defined as simple and easy to implement, especially for small urban centers, where it is possible to specifically identify block fronts and lots that are vulnerable and at risk.

4.1.5 INGEOMINAS METHODOLOGY: PRADERA VALLE CASE STUDY

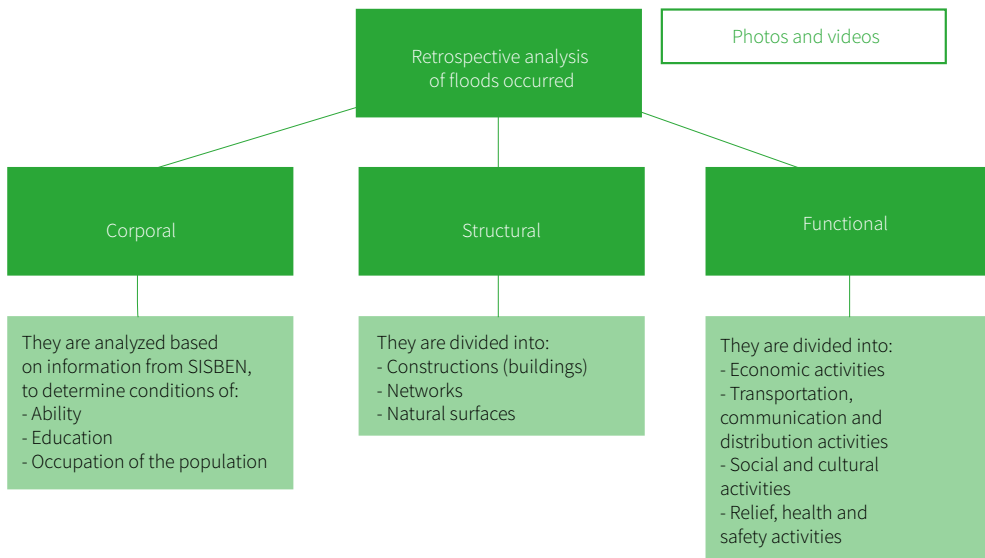
The methodology for vulnerability analysis used by INGEOMINAS in the Pradera Valle case is based on floods, but its theoretical basis can be used in mud and debris flows. This analysis is retrospective and uses photographs and videos to identify the modes of damage to elements exposed to threat events.

The exposed elements can be classified as: corporal, structural and functional (Montaño et al., 2015). The body elements correspond to data on habitability, education and occupation of the population, which can be obtained through censuses of the Identification System of Potential Beneficiaries of Social Programs (Sisbén). The structural elements are divided into buildings (according to the type of construction), networks (which includes roads, lines, ditches) and natural surfaces or types of ground cover.

Finally, the functional elements are grouped by types of activities, among which are:

- Economic activities: which refers to areas of commercial and agricultural activity, and aspects related to employment generation and types of cultivation are also established.
- Transportation, communication and distribution activities: characterizing the degree of importance of communication routes, telephone communication and energy distribution systems (estimating the number of beneficiaries) and important sites for the supply of basic services.
- Social, cultural and educational activities: the active educational population and its location are characterized there; location of administrative and cultural entities, recreation sites, among others.
- Relief, health and safety activities: which refers to the location of institutions related to the health sector, disaster response since these institutions are important in the stage after the possible materialization of the phenomenon, if it were to occur (Montaño et al., 2015).

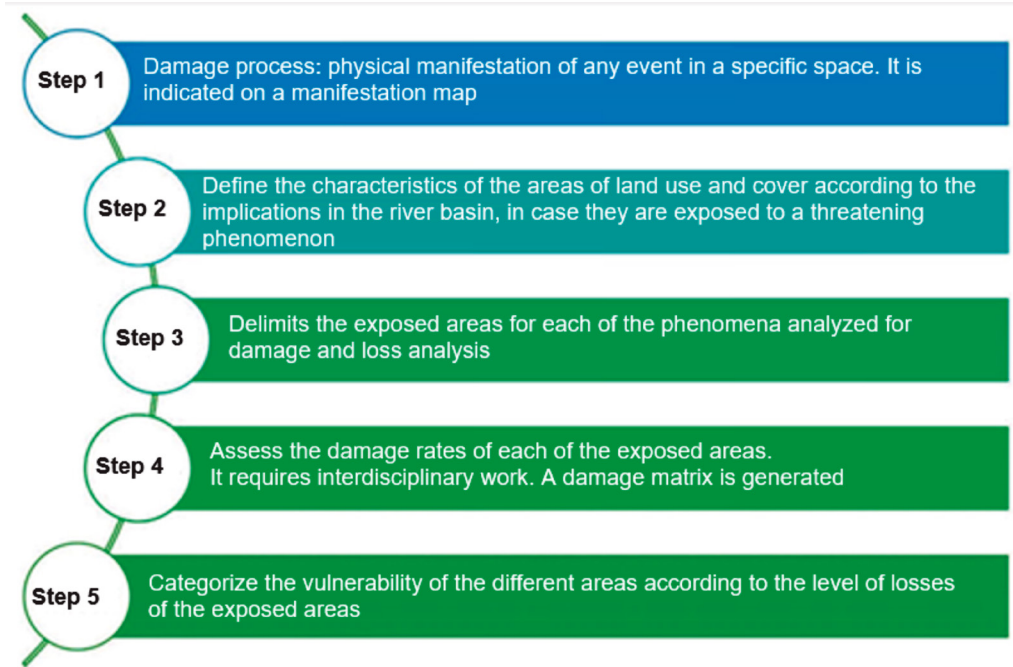
The methodology for vulnerability analysis used by INGEOMINAS in the Pradera Valle case is based on floods, but its theoretical basis can be used in mud and debris flows.

Figure 90. *Retrospective analysis of floods that occurred*

Source: own elaboration.

4.1.6 VULNERABILITY EVALUATION IN THE POMCAS-MINAMBIENTE

The vulnerability assessment methodology used in the POMCAS is oriented to determine the “level of damage and losses that occur with the manifestation of a specific event, which can affect environmental sustainability, safe location, economic sustainability and strategic infrastructure.” (Montaño et al., 2015, p.7.7). The methodology involves five steps as seen in figure 91.

Figure 91. *Vulnerability assessment for POMCAS*

Source: own elaboration.

In step 1, the evaluation of the damage associated with threat phenomena within the territory is contemplated. In step 2, the characteristics of the use areas are defined based on the Corine Land Cover methodology. An attribute is assigned to each of the categories of areas to be evaluated taking into account their importance as a conservation area or in the provision of environmental services, among others.

In step 3, the areas exposed to damage are delimited and in step 4, the damage rates are established, which implies interdisciplinary work in which the aim is to obtain a damage matrix for the different areas. The damage index is the indicator of the vulnerability of each of the exposed areas evaluated. Finally, in step 5, the vulnerability of each area is categorized (Montaño et al., 2015).

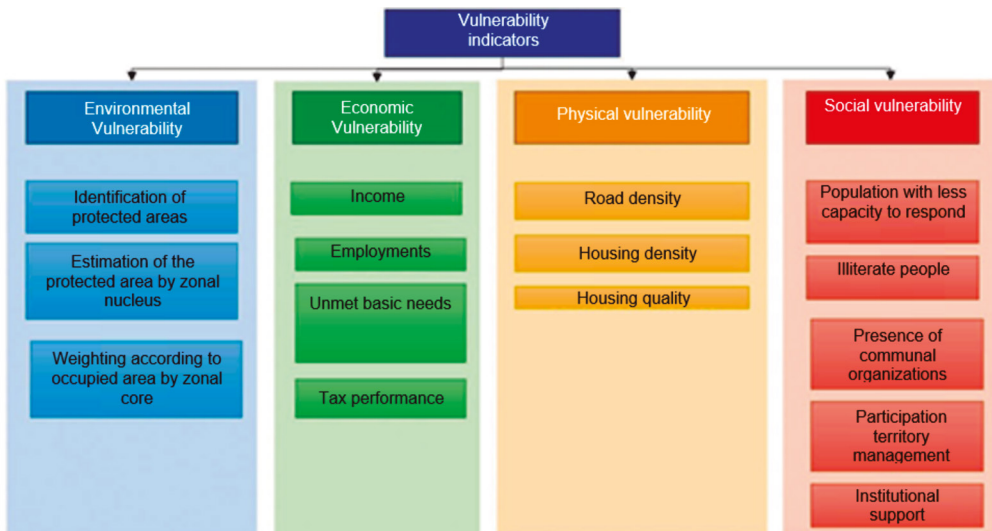
4.1.7 ANALYSIS OF VULNERABILITY IN THE CONARE JURISDICTION

In this methodology, the analysis is carried out based on four vulnerability indicators: environmental, economic, physical and social vulnerability (figure 92).

The environmental vulnerability indicator includes aspects related to protected areas in the territory, and the weighting of this indicator is based on the extent of the protected area within the zone and the level of vulnerability it may present.

Economic vulnerability refers to aspects related to employment (relationship between employment, unemployment and underemployment within the territory under analysis), income per family unit, coverage of basic needs and the fiscal performance of the municipalities.

Figure 92. *Vulnerability indicators in the CONARE jurisdiction*



Source: own elaboration.

Physical vulnerability is related to the state of the general infrastructure (density of roads and housing) and particular infrastructure (quality of buildings and location). Social vulnerability is determined from the social fabric and the presence of community organizations, as well as the participation and institutional support they receive. Social organizations include entities such as the Red Cross, Civil Defense, Firefighters, as well as Community or Local Action Boards.

In this study, the level of weighting given to vulnerability as a factor within risk analysis is 30%, taking into account that the information comes from secondary sources such as censuses, surveys and other reports generated previously and for others finnish.

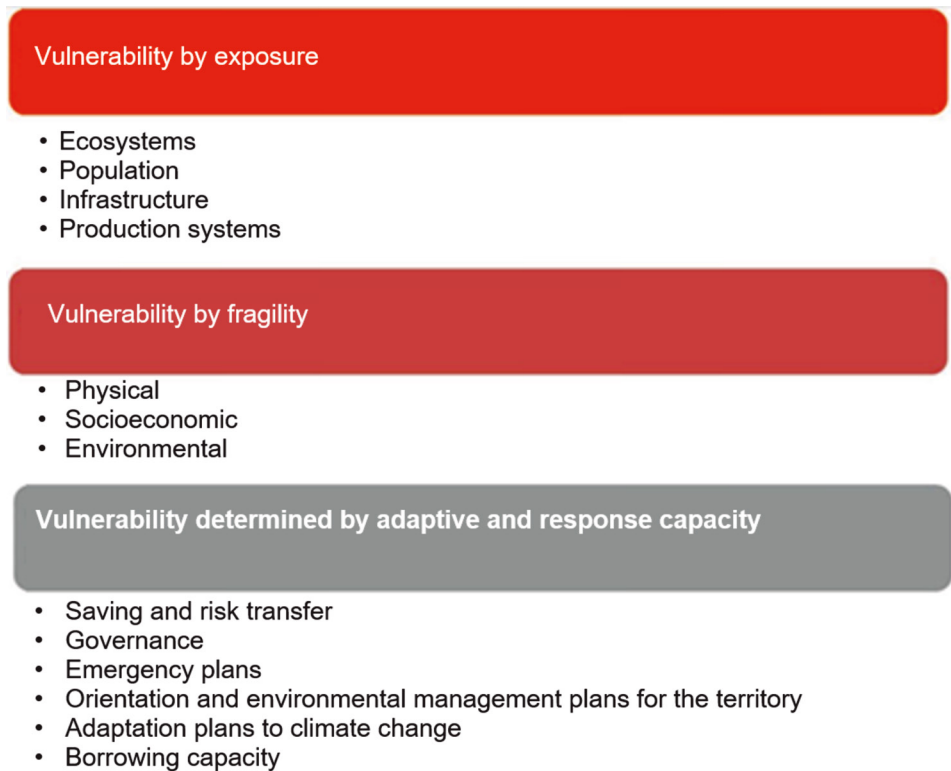
4.1.8 METHODOLOGY FOR THE ANALYSIS OF VULNERABILITY TO THE THREATS OF FLOODING, MASS REMOVAL AND MUD FLOWS IN HYDROGRAPHIC BASINS

This methodology analyzes vulnerability based on three factors: exposure, fragility, and the capacity to adapt and respond, therefore, this methodology aims to estimate global vulnerability based on these three factors (figure 93).

The exhibition aims to estimate the level of potential incidence that would occur on ecosystems, population, infrastructure and production systems. For its part, fragility is related to the level of intrinsic susceptibility of the elements exposed to a potential threat. Finally, the response and adaptation capacity has to do with the response that communities could have to attend to and recover from threat events, if they occur, and therefore is closely related to the institutional capacity of the territory (Vera- Rodríguez and Albarracín-Calderón, 2017).

This methodology analyzes vulnerability based on three factors: exposure, fragility, and the capacity to adapt and respond.

Figure 93. *Factors and components of vulnerability*



Source: own elaboration.

For each component mentioned in Figure 93, measurement variables and assessment criteria are established, which are based on the information analyzed to comply with the variable and the corresponding component. The criteria are defined in three categories, high, medium and low; which finally allows the information to be crossed and obtain a global analysis of the vulnerability for each component.

4.1.9 VULNERABILITY ANALYSIS AT ORGANIZATIONAL LEVEL

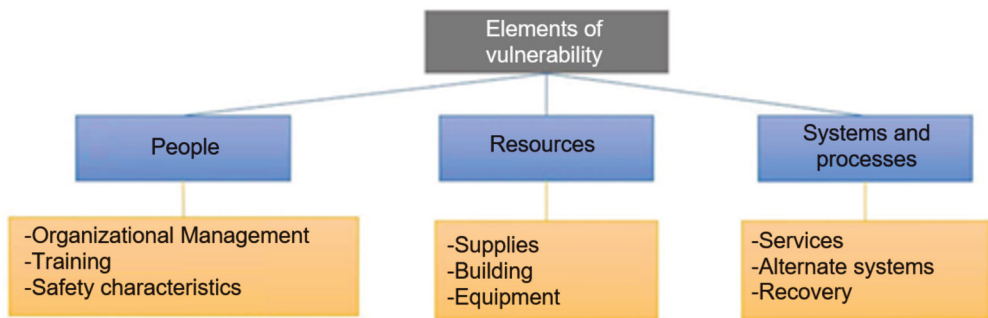
The vulnerability analysis at the organizational level has adjustments with respect to the previously analyzed methodologies since its purpose is to guide the design of plans with a limited scope to organizations that make up the District System for the

Prevention and Attention of Emergencies (SDPAE), as well as all public and private sector organizations.

At this scale, the elements associated with vulnerability analysis are divided into three categories: people, resources, and systems and processes. For each of the aspects::

Formats are developed that, through questions, qualitatively seek to provide a general overview that allows the evaluator to classify as bad, regular or good, the vulnerability of the people, resources and systems and processes of their organization to each of the threats described (Emergency Prevention and Attention Fund, 2012, p. 11).

Figure 94. *Elements of vulnerability in organizations*



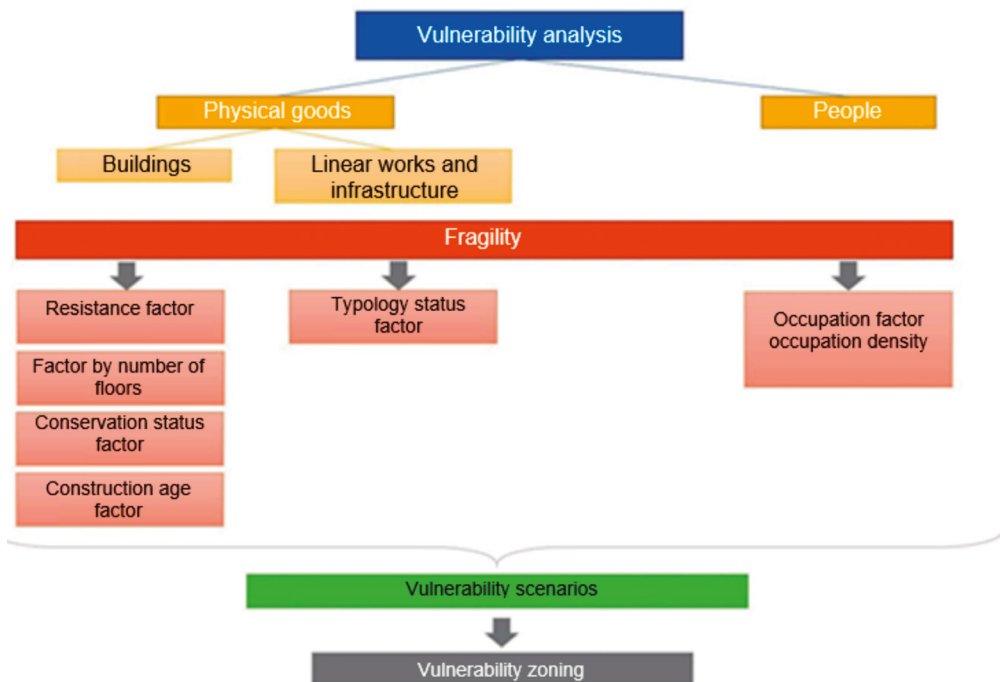
Source: own elaboration.

4.1.10 METHODOLOGICAL GUIDE FOR STUDIES OF THREAT, VULNERABILITY AND RISK DUE TO MASS MOVEMENTS (SGC, 2016)

This guide proposes a specific methodology for urban environments so it does not contemplate risk assessment in rural areas. The vulnerability analysis is based on two large categories: physical assets (which include buildings, linear works and infrastructure) and people. In all cases the objective is to identify and characterize the elements exposed to possible threats. The analysis of the information is done based on the fragility represented by different factors associated with each element; which are detailed in figure 95.

Subsequently, the analysis of the fragility of factors is carried out in the event of the occurrence of various types of vulnerability scenarios that are defined from the threat analysis and the possible damages that would be caused if the event occurs. Finally, vulnerability is classified into three categories (high, medium and low) for the elements and factors addressed, in this way a zoning of vulnerability in the territory is generated.

Figure 95. *Vulnerability analysis for urban sector*



Source: own elaboration.

4.2 RISK ANALYSIS

As mentioned in previous sections, the risk is made up of the vulnerability of the exposed elements and the threat generated by the event or natural phenomenon. In this case, the vulnerability is determined for the population exposed to the mud and debris flows, while the threat is determined by hydrological, hydraulic and geotechnical modeling of the basin for different return periods, for which the total risk would be calculated by means of the following expression:

$$\text{Risk} = \text{Threat} * \text{Vulnerability}$$

In accordance with the above, a modified risk classification is proposed below based on the recommendations of Bateman and Medina (2019), however, this classification is subject to the criteria of the evaluator and consultation with the actors involved.

Table 61. Risk classification proposal

		Vulnerability		
		High	Medium	Low
Threat	High	High	High	Med
	Medium	High	Med	Low
	Baja	Medio	Low	Low

Source: adapted from Bateman and Medina (2019).

It is necessary to clarify that the risk analysis must be carried out for different hydrological conditions, since the magnitude of the event varies according to these and therefore also the possible impact generated on the population, in addition, the incorporation of high-risk areas must be considered. from other processes such as channel erosion, which also generates contributions of material and can increase the magnitude of the event.

On the other hand, as has been mentioned throughout the different chapters, the risk assessment process must be a methodical process with different levels of detail. A large number of basins in our country are located in high mountain or foothill areas, which implies a great technical and economic effort to be able to cover the entire territory at possible risk, so the analysis by less detailed to more detailed phases allows prioritization. areas that require high-detail technical studies.

Finally, it is important that risk analyzes do not remain on paper and become territorial planning tools and are integrated into Territorial Planning Plans and other planning instruments, so that they are truly useful in risk management. in such a way that tragedies such as those that are becoming more frequent in Colombia are avoided.

It is necessary to clarify that the risk analysis must be carried out for different hydrological conditions, since the magnitude of the event varies according to these and therefore, also the possible impact generated on the population, it must also be considered for high-risk areas, the incorporation of other processes such as channel erosion, which also generates contributions of material and can increase the magnitude of the event.

REFERENCES

- Allen, R., Pereira, L., Raes, D. y Smith, M. (2006). *Evaporación del cultivo. Guías para la determinación de los requerimientos de agua de los cultivos*. FAO. <http://www.fao.org/3/x0490s/x0490s.pdf>
- Amat, J. (2017, febrero). Árboles de decisión, random forest, gradient boosting y C5.0. *Cienciadedatos.net*. https://www.cienciadedatos.net/documentos/33_arboles_de_prediccion_bagging_random_forest_boosting
- Aristizábal, E., González, T., Montoya, J. D., Vélez, J. I., Martínez, H. y Guerra, A. (2011). Análisis de umbrales empíricos de lluvia para el pronóstico de movimientos en masa en el Valle de Aburrá, Colombia. *Revista EIA*, (15), 95- 111. <https://revista.eia.edu.co/index.php/reveia/article/view/249/244>
- Bagnold, R. (1954). Experiments on a gravity-free dispersion of large solid spheres in a Newtonian fluid under shear. *Proceedings of the Royal Society of London*, 225(1160), 49 - 63. <https://doi.org/10.1098/rspa.1954.0186>
- Bañon, L. y Bevíá, J. (2000). *Manual de carreteras*. Ortiz e Hijos, Contratista de Obras, S.A.
- Bateman, A. y Medina, V. (2019, junio). *Flujos de avalancha - Valoración del riesgo* [material de clase]. Escuela Colombiana de Ingeniería Julio Garavito.
- Beven, K. J. y Kirkby, M. J. (1979). A physically based, variable contributing area model of basin hydrology. *Hydrological Sciences Bulletin*, 24(1), 43 - 69. <https://doi.org/10.1080/02626667909491834>
- Bingham, E. C. y Green, H. (1919). Paint, a plastic material and not a viscous liquid; the measurement of its mobility and yield value. *Proceedings of the American Society for Testing and Materials*, 19, 640 - 664.
- Budyko, M. I. (Ed.). (1974). *Climate and Life* (Vol. 18). Academic Press.

- Campos, D. F. (1978). *Cálculo de las curvas IDF a partir de registros de lluvia máxima en 24 horas y relaciones duración lluvia promedio*. Subdirección Regional Noreste de Obras Hidráulicas e Ingeniería Agrícola para el Desarrollo Rural.
- Cañas-Gómez, J., Estrada-Maya, M., Jiménez-Galvis, C., Márquez-Jaramillo, J., Mejía-Hernández, V., Ochoa-Osorio, S., Rodríguez-Gaviria, E. y Builes-Jaramillo, L. (2017). *Evaluación de la vulnerabilidad física ante avenidas torrenciales. Caso de estudio: cabecera urbana del municipio de Salgar (Antioquia)* [sesión de conferencia]. IX Seminario La sostenibilidad un punto de encuentro. Medellín, Colombia.
- Carvajal, L. y Roldán, E. (2006). Calibración del modelo lluvia-escorrentía agregado GR4J. Aplicación: Cuenca del Río Aburrá. DYNA, 74(152), 73 - 87. <https://revistas.unal.edu.co/index.php/dyna/article/view/912>
- Castellanos, R. (1996). *Lluvias críticas en la evaluación de amenazas de eventos de remoción en masa* [tesis de maestría]. Universidad Nacional de Colombia.
- Castellanos, R. y González, A. (1997, 10-14 de noviembre). *Algunas relaciones de precipitación crítica - duración de lluvias que disparan movimientos en masa en Colombia*. 2nd Panamerican Symposium on Landslides - ABMS, Río de Janeiro.
- Chevalier, G. (2013). *Assessing Debris flow hazard focusing on statistical morpho-fluvial susceptibility models and magnitude-frequency relationships: application to the central-eastern Pyrenees* [tesis doctoral]. Universitat Politècnica de Catalunya. <http://hdl.handle.net/2117/95041>
- Chien, N. y Wan, Z. (1999). *Mechanics of Sediment Transport*. American Society of Civil Engineers. <https://doi.org/10.1061/9780784404003>
- Chorley, R. (1957). Illustrating the laws of morphometry. *Geological magazine*, 94(2), 140-150. <https://doi.org/10.1017/S0016756800068412>
- Centro Humboldt. (2004). *El ABC de la Gestión del Riesgo*. Oxfam y Consejería en Proyectos. <https://humboldt.org.ni/el-abc-de-la-gestion-de-riesgos/>

- Congreso de Colombia. (2012, 24 de abril). Por la cual se adopta la política nacional de gestión del riesgo de desastres y se establece el Sistema Nacional de Gestión del Riesgo de Desastres y se dictan otras disposiciones. [Ley 1523 de 2012]. DO: 48.411.
- Cousot, P. y Meunier, M. (1996). Recognition, classification and mechanical description of *debris flow*. *Earth Sciences Reviews*, 40(3-4), 209 - 227. [https://doi.org/10.1016/0012-8252\(95\)00065-8](https://doi.org/10.1016/0012-8252(95)00065-8)
- Crece los afectados por avalancha en Salgar. (2015, 20 de mayo). *El Mundo*. <https://n9.cl/n79j5>
- Cruden, D. M. y Varnes, D. J. (1996). Landslides types and processes. En R. L. Schuster y A. K. Turner (Eds.), *Landslides Investigation and Mitigation* (pp. 36 – 75). National academy Press. <https://onlinepubs.trb.org/Onlinepubs/sr/sr247/sr247-003.pdf>
- DHI. (2017). MIKE SHE. DHI Water & Environment. https://manuals.mikepoweredbydhi.help/2017/Water_Resources/MIKE_SHE_printed_V1.pdf
- Díaz-Granados, M. (2014). Hidráulica de ríos [material de clase]. Universidad de los Andes.
- Díaz-Granados, M. (2016). Modelación de hidrosistemas [material de clase]. Universidad de los Andes.
- Dietrich, W. E. y Montgomery, D. R. (1998, 1 de febrero). SHALSTAB. *A digital terrain model for mapping shallow landslide potential*. <http://calm.geo.berkeley.edu/geomorph/shalstab/index.htm>
- Díez-Herrero, A., Lain-Huerta, L. y Llorente-Isidro, M. (2008). *Mapas de peligrosidad por avenidas e inundaciones. Guía metodológica para su elaboración*. Instituto Geológico y Minero de España. <https://n9.cl/rg46u>
- Estudios y Asesorías Ingenieros Consultores Ltda. (2012). *Informe de avance Estudio de Rompimiento de la Ataguia de la presa RCC de la Central Hidroeléctrica San Pedro - República de Chile*.
- ETH Zürich. (2020). STEP-TRAMM. Soil and Terrestrial Environmental Physics (Emeritus). <https://step.ethz.ch/step-tramm.html>

- Fondo de Prevención y Atención de Emergencias. (2012). *Metodologías de análisis de riesgo. Guía para elaborar planes de emergencia y contingencia*. FOPAE, Alcaldía de Bogotá. <http://www.ridsso.com/documentos/muro/fe6dd4f800e4ed-2467827680f51e2ae8.pdf>
- Fread, D. (1988). *BREACH: An erosion model for earthen dam failures*. Hydrologic Research Laboratory, National Weather Service, NOAA.
- Gómez-Blanco, J. A. y Cadena, M. C. (2017). *Validación de las fórmulas de evapotranspiración de referencia ET_o para Colombia*. IDEAM. <https://n9.cl/19c99>
- Grupo de Estándares para Movimientos en Masa. (2007). *Movimientos en Masa en la Región Andina: Una guía para la evaluación de amenazas*. Proyecto Multinacional Andino: Geociencias para las Comunidades Andinas, PMA.
- Grupo de investigación OSSO y LA RED. (2009). *DesInventar. Sistema de Inventario de Desastres. Guía metodológica*. <https://n9.cl/ltuf9>
- Hermelin, M. (1985). Suelos, rocas y formaciones superficiales. *DYNA*, (106), 25 - 29.
- Herschel, W. M. y Bulkley, R. (1926). Measurement of consistency as applied to rubber benzene solutions. *Proceedings of the American Society for Testing and Materials*, 26(2), 621 - 633.
- Hoek, E. y Bray, J. (1981). *Rock slope engineering*. Institution of Mining and Metallurgy.
- Hungr, O., Evans, S. G., Bovis, M. J. y Hutchinson, J. N. (2001). A review of the classification of landslides of the flow type. *Environmental and Engineering Geoscience*, 7(3), 221 - 238.
- Hydronia. (2014). *Riverflow 2D Plus User's Guide*. Pembroke Pines.
- Ibarrola, E. (2015). *Introducción a los fluidos no newtonianos*. <https://n9.cl/kepod>
- Instituto de Hidrología, Meteorología y Estudios Ambientales. (2010). *Leyenda Nacional de coberturas de la tierra: metodología CORINE Land Cover Adaptada para Colombia. Escala 1:100.00*. IDEAM.

- Instituto de Hidrología, Meteorología y Estudios Ambientales. (2013). *Lineamientos conceptuales y metodológicos para la Evaluación Regional del Agua - ERA*. IDEAM. <http://www.invemar.org.co/documents/10182/14487/JC-249.pdf/051c4f2d-81f1-4acb-99ed-97e2e169cd3f>
- Instituto de Hidrología, Meteorología y Estudios Ambientales. (2015). *Glosario*. <http://www.ideam.gov.co/web/atencion-y-participacion-ciudadana/glosario>
- Instituto de Hidrología Meteorología y Estudios Ambientales y Unidad de Planeación Minero Energética. (2006). *Atlas de viento y energía eólica de Colombia*. Ministerio de Minas y Energía.
- Instituto Distrital de Gestión de Riesgos y Cambio Climático. (2016). *Caracterización general de escenario de riesgo por avenidas torrenciales*. <https://www.idiger.gov.co/riesgo-por-avenidas-torrenciales>
- Instituto de Investigaciones en Geociencias Minería y Química y Ministerio de Minas y Energía. (1994). *El sismo de Páez, Cauca 6 de junio de 1994: Evaluación de emergencia. Informe presentado al sistema nacional para la prevención y atención de desastres en Colombia*. Ingeominas.
- Instituto de Investigaciones en Geociencias Minería y Química y Universidad Nacional de Colombia. (2009). *Formulación de una guía metodológica para la evaluación de la amenaza por movimientos en masa tipo flujo: caso piloto quebrada La Negra, Útica, Cundinamarca*.
- Instituto Geológico y Minero de España. (1986). *Manual de taludes*. IGME.
- Johnson, A. M. (1970). *Physical Processes in Geology*. Freeman.
- Johnson, A. M. y Rodine, J. R. (1984). Debris flow. En D. Brunsten y D. B. Prior (eds.), *Slope Instability* (pp. 257-360). Jhon Wiley & Sons.
- Körner, H. (1976). Reichweite und Geschwindigkeit von Bergstürzen und FlieBschnelawinen. *Rock Mechanics*, 8, 225 - 256.
- Loat, R. y Petrascheck, A. (1997). Berücksichtigung der Hochwassergefahren bei raumwirksamen Tätigkeiten. Bundesamt für Umwelt BAFU.

- Lozano-Cortijo, O. (2008). *Metodología para el análisis de vulnerabilidad y riesgo ante inundaciones y sismos, de las edificaciones en centros urbanos*. Centro de Estudios y Prevención de Desastres (PREDES).
- Markstrom, S., Regan, R., Hay, L., Viger, R., Webb, R., Payn, R. y LaFontaine, J. (2015). *PRMS-IV, the Precipitation-Runoff Modeling System, Versión 4* (Techniques and Methods, 6-B7). United States Geological Survey. <https://doi.org/10.3133/tm-6B7USGS>.
- Márquez, H. (1999). Métodos matemáticos de evaluación de factores de riesgo para el patrimonio arqueológico: una aplicación GIS del método de Jerarquías Analíticas de T.L Saaty. *SPAL*, 8, 21 - 37. <https://doi.org/10.12795/spal.1999.i8.02>
- Mayorga, R. (2003). Determinación de umbrales de lluvia detonante de deslizamientos en Colombia. *Meteorología Colombiana*, (7), 157-168. <https://n9.cl/crll>
- Melton, M. A. (1965). The geomorphic and paleoclimatic significance of alluvial deposits in Souther Arizona. *Journal of Geology*, 73(1), 1 - 38. <https://doi.org/10.1086/627044>
- Ministerio de Ambiente y Desarrollo Sostenible. (2014). *Protocolo para la incorporación de la gestión del riesgo en los Planes de Ordenación y Manejo de Cuencas Hidrográficas*. Minambiente. <https://n9.cl/yu66>
- Montaño, M., Maca, X., Torres, W., Iragorri, R., Agredo, E. y Rengifo, A. (2015). Estudio de vulnerabilidad a inundaciones para las principales corrientes del municipio de Popayán. Popayán. En A. Gallardo, M. E. Guevara, L. J. González, R. A. Lemos, M. P. Torres, M. E. Montaño, E. L. Agredo, C. A. Chilito y E. Quijano. *Estudio preliminar (afectación y daños) asociados a fenómenos de inundación lenta y súbita (avenidas torrenciales) en la zona urbana y rural del municipio de Popayán*. Alcaldía de Popayán y Universidad del Cauca.
- Mott, R. (2015). *Mecánica de fluidos*. Pearson Educación.
- Muhammed, A. H. (2012). *Satellite based evapotranspiration estimation and runoff simulation: A topmodel application to the Gilgel Abay catchment, Ethiopia* [tesis de maestría]. University of Twente. <http://essay.utwente.nl/84858/1/ahmed.pdf>
- Navarro, S. (2008). *Estabilidad de taludes*. <https://sjnavarro.files.wordpress.com/2008/09/estabilidad-de-taludes.pdf>

- Nawarathna, N.M.N.S., Kazama, S. y Sawamoto, M. (2002). Improvement of calibration procedure of the block wise topmodel with muskingum-cunge routing method using sub basins simulated results: application to part of the lower mekong river basin. En J. Guo (Ed.), *Advances in Hydraulics and Water* (pp. 540 – 545). World Scientific Publishing.
- Netsch, S. L., Arnold, J. G., Kiniry, J. R. y Williams-Grassland, J. R. (2011). *Soil and Water Assessment Tool Theoretical Documentation* Version 2009. Texas Water Resources Institute. <https://swat.tamu.edu/media/99192/swat2009-theory.pdf>
- Noticias Caracol. (2018, 18 de mayo). *Crónica de una tragedia anunciada: el day que una avalancha sepultó a Armero* [video]. YouTube. <https://youtu.be/MEFuyFYeo4c>
- O'Brien, J. S. y Julien, P. Y. (1985). Physical properties and mechanics of hyperconcentrated sediment flows. En D. S. Bowles (Ed.), *Delineation of Landslides, Flash Flood and Debris flow Hazards in Utah. Proceedings of Specialty Conference* (pp. 260 - 279). Utah Water Research Laboratory, Utah State University.
- O'Brien, J. S. y Julien, P. Y. (1997). On the importance of mudflow routing. En C. L. Chen (Ed.), *Debris-Flow Hazards Mitigation: Mechanics, Prediction, and Assessment* (pp. 667 - 686). American Society of Civil Engineers.
- Pack, R. T., Tarboton, D. G. y Goodwin, C. N. (2005). SINMAP 2.0 for ArcGIS - *A stability index approach to terrain stability hazard mapping, User's Manual*. Utah State University.
- Páez, J. (2016). *Modelación matemática de flujos de avalancha* [tesis de maestría]. Universidad de los Andes. <https://repositorio.uniandes.edu.co/handle/1992/13751?s-how=full>
- Pérez, J. (1979). *Fundamentos del ciclo hidrológico*. Universidad Central de Venezuela.
- Pérez J. y Mesa O. (2002, 29 de agosto). *Estimación del factor de erosividad de la lluvia en Colombia* [ponencia]. XV Seminario Nacional de Hidráulica e Hidrología, Medellín, Colombia. <https://repositorio.unal.edu.co/handle/unal/7823>
- Real Academia Española. (2020). Alud. En *Diccionario de la lengua española* (edición de tricentenario). <https://dle.rae.es/alud#0x80msV>
- Rickenmann, D. (2005). *Hangmuren und Gefahrenbeurteilung. Kurzbericht für das Bundesamt für Wasser und Geologie. Universität für Bodenkultur*.

- Rickenmann, D. (2016). *Methods for the Quantitative Assessment of Channel Processes in Torrents (Steep Streams)*. CRC Press.
- Rivas, M., Ovalles de Cabezas, Y., Soto, A. C., Ramírez, G., Ripanti, F. y González, J. L. (2009). Determinación de niveles de potencialidad torrencial de la cuenca del río Mocotíes, Mérida, Venezuela. *Revista Forestal Venezolana*, 53(1), 33-34.
- Romero, A. y López, F. (1987). Morfometría de redes fluviales: revisión crítica de los parámetros más utilizados y aplicación al alto Guadalquivir. *Papeles de Geografía*, (12), 47-62.
- Ruiz, R. y Torres, H. (2008) *Manual de Procedimientos para la delimitación y codificación de cuencas hidrográficas -Caso América del Sur*. Unión Internacional para la Conservación de la Naturaleza (UICN).
- Hsu, S. M., Chiou, L. B., Lin, G. F., Chao, C. H., Wen, H. Y. y Ku, C. Y. (2010). Applications of simulation technique on debris-flow hazard zone delineation: a case study in Hualien County, Taiwan. *Natural Hazards and Earth System Sciences*, 10(3), 535-545. <https://doi.org/10.5194/nhess-10-535-2010>
- Saaty, T. (1980). *The Analytic Hierarchy Process: Planning, Priority Setting, Resource Allocation*. McGraw-Hill.
- Sepúlveda, A. y Patiño, J. (2016). *Metodología para la evaluación de riesgo por flujo de detritos detonados por lluvia [tesis de maestría]*. Pontificia Universidad Javeriana. <http://hdl.handle.net/10554/18828>
- Servicio Geológico Colombiano. (2016). *Guía metodológica para estudios de amenaza, vulnerabilidad y riesgo por movimientos en masa*. SGC. <https://n9.cl/uwyy>
- Servicio Geológico Colombiano. (2017). *Guía metodológica para la zonificación de amenaza por movimientos en masa escala 1:25.000*. SGC. <http://bit.ly/2kB3Z7e>
- Stone, R. P. y Hilborn, D. (2001). *Universal soil loss equation*. Ministry of Agriculture, Food and Rural Affairs.
- Suárez J. (1998). *Deslizamientos y estabilidad de taludes en zonas tropicales*. Instituto de Investigaciones sobre Erosión y Deslizamientos.
- Suárez, J. (2009). *Deslizamientos*. Universidad Industrial de Santander.

- Suárez J. (2001). *Control de erosión en zonas tropicales*. Instituto de Investigaciones sobre Erosión y Deslizamientos.
- Takahashi, T. (1978). Mechanical characteristics of *debris flow*. *Journal of the Hydraulics Division*, 104(8),1153-1169.
- Takahashi, T. (1991). *Debris flow*. International Association for Hydraulic Research.
- Tarboton, D. (2003). Simulation of runoff generation in hidrologic models. En *Rainfall-Runoff Processes Utah* (pp. 127-145). Utah State University.
- Todini, E. y Mazzetti, C. (2008). TOPKAPI - TOPographic Kinematic AProximation and Integration - user manual and references. Protezione e Gestione Ambientale.
- Comité Nacional para el Conocimiento del Riesgo. (2017). *Terminología sobre Gestión del Riesgo de Desastres y Fenómenos Amenazantes*. UNGRD.
- Universidad Nacional de Colombia. (2009). *Amenaza, vulnerabilidad y riesgo por movimientos en masa, avenidas torrenciales e inundaciones en el Valle de Aburrá. Formulación de propuestas de gestión*. Municipio de Medellín, Área Metropolitana del Valle de Aburrá. <http://hdl.handle.net/20.500.11762/19864>
- Universitat Politècnica de València. (2014). *Descripción del modelo conceptual distribuido de simulación hidrológica TETIS v.8*. Grupo de Investigación de Modelación Hidrológica y Ambiental (GIMHA). <http://lluvia.dihma.upv.es/ES/software/software.html>
- U.S. Army Corps of Engineers. (2000). *Hydrologic Modeling System HEC*. Hydrologic Engineering Center. <https://n9.cl/y104>
- Velásquez, A. y Rosales, C. (1999). *Escudriñando en los desastres a todas las escalas*. Red de Estudios Sociales en Prevención de Desastres en América Latina – LA RED. <https://www.osso.org.co/docu/publicac/1999/escudrinhando/completo.pdf>
- Vera-Rodríguez, J. y Albarracín-Calderón, A. (2017). Metodología para el análisis de la vulnerabilidad ante amenazas de inundación, remoción en masa y flujos torrenciales en cuencas hidrográficas. *Ciencia e Ingeniería Neogranadina*, 27(2), 109-136. <http://dx.doi.org/10.18359/rcin.2309>

Voellmy, A. (1955). Über die Zerstörungskraft von Lawinen. *Schweizerische Bauzeitung*, 73(12),159–162; 73(15), 212-217; 73(17), 246-249; 73(19), 280-285.

Wyllie, D. y Mah, C. (2004). *Rock slope engineering: civil and mining*. Spon Press

Yepes, V. (2018, 27 de noviembre). Proceso analítico Jerárquico AHP. *Universidad Politécnica de Valencia*. <https://victoryepes.blogs.upv.es/2018/11/27/proceso-analitico-jerarquico-ahp/>



Sello Editorial

Universidad Nacional
Abierta y a Distancia

UNAD University Press

National Open and Distance University
Calle 14 sur No. 14-23
Bogota, DC

www.unad.edu.co

ISBN 628778619-1



9 786287 786196